MULTIPLE STAGES OF SENSORIMOTOR PROCESSING IN THE PRIMATE BASAL GANGLIA

by

Alice Weaver Flaherty
A. B., Biology, Harvard College
(1985)

Submitted to the Department of
Brain and Cognitive Sciences
in partial fulfillment of
the requirements for the degree of

DOCTOR OF PHILOSOPHY
in Neuroscience
at the

MASSACHUSETTS INSTITUTE OF TECHNOLOGY

September 1992

Signature of Author _____
Department of Brain and Cognitive Sciences
July 31, 1992

Certified by _____
Professor Ann M. Graybiel
Thesis Advisor

Accepted by _____
Professor Emilio Bizzi
Chairman, Department of Brain and Cognitive Sciences

ABSTRACT

Multiple Stages of Sensorimotor Processing in the Primate Basal Ganglia
by
Alice Weaver Flaherty

Submitted to the Department of Brain and Cognitive Sciences in partial fulfillment of the requirements for the degree of Doctor of Philosophy in Neuroscience

To study the organization of movement-related inputs at successive stages of basal ganglia processing, motor and somatosensory cortex in 34 squirrel monkeys were mapped with microstimulation and multiunit recording, and injected with multiple anterograde tracers in identified sites in the cortical maps. Multiple retrograde tracers were injected in the external and internal segments of globus pallidus (GPe and GPi) and substantia nigra. A single sensorimotor cortical region, such as the hand region, innervated multiple regions in the matrix of the putamen, regions which we have termed matrisomes. A matrisome that received inputs from a body part representation in one cortical map also received convergent inputs from the same representations in other cortical maps. Such a matrisome did not receive strong inputs from other body part representations. Inputs from contralateral motor cortex formed a second sensorimotor input system, innervating matrisomes which are near, but largely separate from, those innervated by ipsilateral sensorimotor cortex. Contralateral motor and ipsilateral sensorimotor inputs did not uniformly innervate the matrix, indicating that there are other, as yet unidentified, matrix input systems in this region.

Output neurons in the striatal matrix were also organized into sets of discrete matrisomes. Different output matrisomes did not project to different target nuclei: neurons projecting to GPe and GPi were extensively intermingled, not segregated into different clusters. However, GPe- and GPi-projecting neurons formed separate classes. The number of neurons sending collaterals to both GPe and GPi was not significantly different from zero, and neurons projecting to GPe were much more likely to express enkephalin than were neurons projecting to GPi. Sets of input and output matrisomes were systematically related, and a set of matrisomes which shared a cortical input could also share pallidal outputs. The multiple matrisomes innervated by a single cortical representation, such as the foot area, sent outputs that could reconverge on small regions in both GPe and GPi. Regions of GPe and GPi formed small modules, some of which received inputs from sensorimotor matrisomes, whereas other nearby ones did not. Overall, the existence of multiple sets of matrisomes whose inputs and outputs are functionally related indicates that modularity may be a general principle of striatal organization. The purpose of this modularity may be to increase the lateral interactions between different matrix input systems, as well as to channel inputs to specific regions of target nuclei.

Thesis Supervisor: Dr. Ann M. Graybiel, Professor of Neuroanatomy

JOURNAL SUBMISSIONS

Chapter 1 will be published as

Flaherty, A. W., A. M. Graybiel. The anatomy of the basal ganglia. In *Movement Disorders, III*, C. D. Marsden and S. Fahn, eds. Butterworths, London. *In press.*

Chapter 2 was published as

Flaherty, A. W., A. M. Graybiel (1991). Corticostriatal transformations in the primate somatosensory system: I. Projections from physiologically-mapped body-part representations. *J. Neurophys.* 66:1249-1263.

Chapter 3 has been submitted to the Journal of Neuroscience.

Chapters 4 and 5 will be submitted to journals in August.

Two chapters described and approved in my thesis proposal, "Relative magnifications of body part representations in the corticostriatal projection," and "Functional topography of cortical and pallidal projections to the subthalamic nucleus," are not included in this Ph.D. thesis but instead will be submitted in my M.D. thesis to Harvard Medical School, to meet the requirements of the M.D.-Ph.D. program in the Harvard-M.I.T. Division of Health Sciences and Technology.

ACKNOWLEDGEMENTS

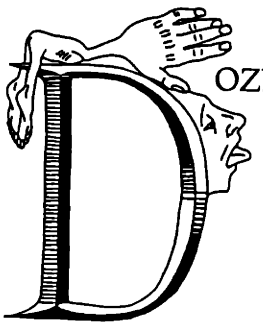 OZENS OF PEOPLE have helped me since I came to M.I.T. I would like to thank Mriganka Sur for teaching me how to use our electrophysiology set-up, Nikos Logothetis, now of Baylor University, for teaching me how to fix it, and Robert P. Marini for his invaluable advice on the veterinary care of my monkeys -- I learned a great deal of medicine from him that I didn't learn in medical school. At Harvard Medical School, Farish A. Jenkins, Jr.'s legendary course made me realize that anatomy can be as fascinating as physiology, and William S. Beck, for whom I did some editorial work, showed me how good scientific writing can be. Edward Tufte's *Envisioning Information* shaped many of my figures, and Wendell Krieg's classic *Functional Neuroanatomy* was the model that the typography and decorated initials of this thesis pallidly imitate. In Ann Graybiel's lab I am indebted to Henry Hall, who did most of the photography, always kept me on my toes, and had elegant solutions to every practical problem; to Diane Major, for histology tips and lovely afternoon teas; and to Hemai Parthasarathy, a most stimulating person to bounce ideas off, and a great friend. Finally, I am very grateful to Ann Graybiel for her tolerance, her insight into science and non-science, excited conversations about Jaques Brel and other important subjects, and many happy hours in surgery together; and to Andrew Hrycyna for work on some of the figures, for helping me move 37 human brains across campus on a rickety cart during a thunderstorm, and for a thousand, thousand other things.

INDEX

If you don't find it in the Index, look very carefully through the entire catalog.

– Sears, Roebuck, Co., *Consumer's Guide* (1897)

Some men pretend to understand a Book
by scouting thro' the Index:
as if a Traveller should go about to describe a Palace
when he had seen nothing but the Privy.

– Jonathan Swift, *Mechanical Operation of the Spirit* (1784)

CHAPTER 1. CIRCUITRY OF THE BASAL GANGLIA

> However painful may be the objects with which the Anatomist's knowledge is connected, he feels that his knowledge is pleasure; and where he has no pleasure he has no knowledge.
>
> – Wordsworth, Preface, Second edition of *Lyrical Ballads* (1800)

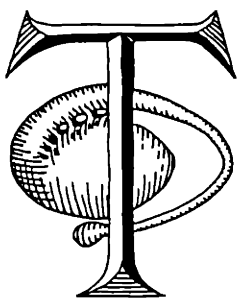

HE FUNCTIONAL ORGANIZATION of the basal ganglia has long interested neurologists studying extrapyramidal movement disorders. Nonetheless, links between structure and function in the basal ganglia are less well understood than are those in the cerebral cortex -- in part because the basal ganglia and their allied nuclei, buried deep in the forebrain, are less accessible than the cortex, and because the basal ganglia are not as clearly linked to sensation and behavior as are sensory and motor areas of the cortex. However, four technical innovations have recently advanced basal ganglia neurobiology. First, axon transport methods with markers such as horseradish peroxidase, lectins, and radiolabeled and fluorescent molecules have clarified the connections of the basal ganglia. Second, chemoanatomical methods such as immunohistochemistry, receptor binding, microdialysis, and *in situ* hybridization have allowed study of neurotransmitters in the basal ganglia. Third, CT, MRI, and PET scanning methods have permitted observation of the living human brain. Fourth, the methods of molecular biology and genetics have illuminated cellular mechanisms in both normal and dysfunctional basal ganglia.

Studies with these four methods have helped confirm and extend the classic hypothesis that many movement disorders are associated with highly specific damage to particular nuclei -- or specific groups of neurons within particular nuclei -- in the basal ganglia and allied regions. They have also provided

unexpected evidence for a role of the basal ganglia in neuropsychiatric disorders such as depression, obsessive–compulsive disorder, and schizophrenia (Carlsson and Carlsson, 1990; Sedvall, 1990). We will review some of the recent discoveries in basal ganglia neuroanatomy, emphasizing functional and neurochemical subdivisions of the basal ganglia and their allied nuclei. We will focus on the parts of the basal ganglia most clearly identified with movement disorders, although there are also provocative findings about the ventral part of the basal ganglia, a region thought to be related to motivation and limbic functions (Alheid and Heimer, 1988).

The chief nuclei of the basal ganglia are the striatum and the pallidum (globus pallidus). Each nucleus is itself divided into parts. The term "striatum", especially in clinical discussions, often connotes the caudate nucleus and putamen, together called the dorsal striatum. However, the striatum also includes the ventral striatum: the region at the base of the caudate–putamen complex that lies mainly anterior to the anterior commissure. The ventral striatum contains the ventral continuations of the caudate nucleus and putamen, the nucleus accumbens septi, and parts of the olfactory tubercle. The globus pallidus has an external segment (GPe), an internal segment (GPi), and a region known as the ventral pallidum. Strictly speaking, the amygdala is part of the basal ganglia. It is now generally discussed separately, but it does have direct connections with the striatum, especially with the ventral striatum.

Two other nuclei, the subthalamic nucleus and the substantia nigra, are closely allied to the basal ganglia. The substantia nigra has two main parts: the dopamine–rich pars compacta (SNpc), and the non–dopaminergic pars reticulata (SNpr). In many respects, the SNpr can be considered a caudal extension of the GPi. But it differs from the GPi in having a special link with the dopamine–rich SNpc: many dopamine–containing dendrites, and some dopamine–containing cell bodies, extend from the SNpc into the SNpr. Other regions that are important for basal ganglia function include cortical motor, somatosensory, and premotor areas; thalamic ventral anterior (VA), ventral lateral (VL), and centre

median-parafascicular (CM-PF) nuclei; midbrain monoamine-containing cell groups near the SNpc (including the ventral tegmental area, retrorubral area, and dorsal raphe nuclei); and the tegmental pedunculopontine nucleus.

Basal ganglia circuitry is notoriously complicated (Fig. 1-1), but the current model of basal ganglia function simplifies it by focusing on only two of the pathways. Both of them, the "direct pathway" through GPi and SNpr, and the "indirect pathway" through GPe and the subthalamic nucleus, can be interpreted as cortical feedback loops in which information from the entire neocortex is sent in sequence through the dorsal striatum, pallidum, and thalamus, and then back from the thalamus to the cortex, especially the frontal cortex. A related circuit goes through the ventral basal ganglia: the hippocampal formation and related allocortex project to the ventral striatum, then the ventral pallidum and substantia nigra, thalamus, and cortex.

In this model, a series of inhibitory projections in the direct pathway create a double inhibition that results in a net positive feedback loop: the cortex sends excitatory inputs to the striatum, the striatum sends inhibitory inputs to the pallidum, the pallidum inhibits the thalamus, and the thalamus sends excitatory inputs to the frontal cortex. The net effect of cortical activity via these pathways is to trigger the striatum to release the thalamus from pallidal inhibition, thus allowing thalamic outputs to excite the cortex (Fig. 1-2). This double inhibition is not simply the result of taking the negative of a negative to make a positive; the two successive stages of inhibition in these output pathways need not necessarily have added up to net excitation. For instance, the striatum can "release" the thalamus from pallidal inhibition only because the pallidal neurons are tonically active. If pallidal neurons normally had low firing rates -- as do those in the striatum -- then inhibition from the striatum might not change the firing rate of pallidal outputs to the thalamus. In other words, whether double inhibition adds up to net release empirically depends on the exact neuronal connections and physiological characteristics of each stage of the circuit.

Moreover, net effects of the direct pathway are influenced by alternate

pathways through the basal ganglia. Some of these, notably the GPe–subthalamic loop discussed below, may result in triple, rather than double, inhibition. If the influence of such other pathways is dominant, then the net effect of the basal ganglia on the thalamus and cortex will be negative feedback, not release. There is an interesting possibility, however, that basal ganglia inhibition of cortical activity might not inhibit movement, but facilitate it, by selectively inhibiting muscles antagonistic to the desired movement (Mink and Thach, 1991b; Mink and Thach, 1991a). Thus the direct and indirect pathways through the basal ganglia may not be working in opposition, but in tandem.

This model has been effective in integrating anatomy and electrophysiology with the symptoms of basal ganglia disorders (Albin et al., 1989), but it is not without drawbacks. For instance, although it is convenient to think of basal ganglia processing as a sequence of inhibitory stages, it may also be misleading: electrophysiological studies of movement-related activity in the motor cortex and the striatum suggests that the two regions may control movement in parallel, rather than creating a strict hierarchy (Crutcher and Alexander, 1990). Moreover, although the main sources and ultimate targets of the basal ganglia are cortical, there are other important inputs from within and without the extended basal ganglia system. Activity in the direct pathway may be modulated by side-loops that connect the striatal and pallidal stages of the primary circuit to the substantia nigra, the subthalamic nucleus, the CM-PF thalamic nuclei, and the tegmental pedunculopontine nucleus. The debilitating movement disorders that result from damage to the substantia nigra and the subthalamic nucleus demonstrate the important influence these accessory loop nuclei can have on basal ganglia processing. Indeed, it is a problem for the current model of basal ganglia processing that lesions of the modulatory side-loops seem to do more damage to behavior than do lesions in the direct pathway.

I. INPUTS TO THE BASAL GANGLIA

Inputs to the striatum and the pallidum differ greatly. The striatum is the region in the basal ganglia loop that receives the majority of cortical inputs, and it receives most of the non-cortical inputs as well. The pallidum, by contrast, receives most of its inputs from two sources: the striatum, and the subthalamic nucleus. The striatum is much larger than the pallidum; it is the largest subcortical cell mass in the forebrain. But both the pallidum and the striatum, like the neocortex, are proportionally very large in primates, especially humans. It is tempting to suppose that the large size of the primate basal ganglia reflects the primate specialization for fine motor control. As well as differing in size, the basal ganglia of primates differ from non-primates in morphology, connectivity, and regional specialization. It is important to keep in mind these species differences when attempting to make inferences about human diseases from observations of other species. In the rat, for instance, the caudate nucleus and putamen are not distinct nuclei, and the apparent homologues of the two segments of the primate pallidum are split into two nuclei: the "globus pallidus," homologous to the primate GPe, and the "entopeduncular nucleus," homologous to the primate GPi.

A. Inputs to the striatum

Inputs to the striatum are summarized in Table 1-1. Besides receiving cortical afferents, the striatum receives robust inputs from the CM-PF complex of the thalamus and from the amygdala. It also receives fiber projections from three monoaminergic regions of the brainstem: (1) the dopamine-containing midbrain nuclei, including the substantia nigra pars compacta (SNpc, roughly equivalent to cell group A9), its caudal extension in the retrorubral region (cell group A8), and the ventral tegmental area (cell group A10); (2) the serotonin-containing dorsal raphe nucleus, and (3) the norepinephrine-containing locus coeruleus, which projects mainly to the ventral striatum. Dopamine, serotonin, and

norepinephrine make up only a small subset of the many neurotransmitters found in the striatum, which is noted for its high concentration and diversity of neurotransmitters (Graybiel, 1990).

Long lists of interconnections are a frustrating aspect of basal ganglia neurobiology, in part because they give no information about the relative strengths of the different fiber projections. But anatomical strength may not be the best index of functional relevance. For instance, studies of Parkinson's disease demonstrate that the dopamine-containing nigrostriatal pathway is crucial functionally, yet nigrostriatal synapses are thought to make up only a small percent of all striatal afferent synapses. Thus, it is possible that the sparse inputs to the striatum from the subthalamic nucleus, pallidum, and tegmental pedunculopontine nucleus are more important than their numbers suggest.

1. Corticostriatal Inputs

Given the plentiful subcortical inputs to the striatum, what justifies the traditional emphasis on the cortical inputs to the striatum? First, in the context of motor processing, the cerebral cortex -- and especially the sensorimotor cortex, which has a massive fiber projection to the striatum -- is the one region projecting to the striatum that is known to have an executive role in the control of movement. Second, because the entire cortex projects to the striatum, fiber projections from cortex carry as a whole a broader array of information to the striatum than do those from non-cortical regions. Third, functional domains in the striatum seem to be strongly influenced by the types of cortical input they receive. Behavioral experiments have shown that lesions within a particular striatal zone produce deficits similar to the deficits produced by lesions in the cortical area projecting to that zone (Dunnett and Iversen, 1980; Dunnett and Iversen, 1982).

The dopamine-, serotonin-, and norepinephrine-containing inputs seem to have a different role in striatal processing than the "informational inputs" that the

striatum receives from the neocortex. The current best guess at the function of these monoaminergic inputs is that they are modulators of corticostriatal processing, rather than themselves carrying detailed information about the sensorimotor periphery. Clues to the nature of this "modulation" will be discussed below. The functions of inputs from the thalamus and amygdala to the striatum are unclear. The CM-PF nuclei of the thalamus may be important in feedback or even feedforward motor control, for they receive dense inputs from motor cortex (to CM) and premotor cortex (to PF). These nuclei project to the same regions of the striatum as do the motor and premotor cortices themselves. A more "limbic" function, related to affect and memory, is proposed for the amygdala's projection to the ventral striatum and to the striosomes within the dorsal striatum (see below).

Corticostriatal fibers use glutamate or aspartate as their neurotransmitter, and are thought to excite striatal output neurons. It is not certain whether the other forebrain inputs to the striatum are excitatory as well; nor have their neurotransmitters been identified. All of these inputs are thought to terminate, at least in part, directly on the output neurons of the striatum. Excitatory amino acids such as glutamate may play a role in the striatal cell death of Huntington's disease (DiFiglia, 1990), and the interactions of glutamate and dopamine effects on striatal neurons may have implications for Parkinson's disease; for instance, the substantia nigra is protected by antagonists to the glutamate NMDA receptor in one model of drug-induced parkinsonism (Turski et al., 1991).

The corticostriatal projection is highly ordered topographically. The neocortex primarily innervates the dorsal striatum, whereas the allocortex (especially the hippocampal formation) innervates the ventral striatum. Within the striatum, the neocortical projection is broadly systematic, with the zones of densest input following a front-to-front and back-to-back topography. Frontal cortex projects most strongly to the head of the caudate nucleus, sensorimotor and parietal cortex to the putamen, temporal cortex to the medial and caudal putamen and caudate nucleus, and occipital cortex to the tail of the caudate nucleus. However, any

given cortical area projects not only to such a single circumscribed striatal region, but to an elongated, patchy zone that can extend nearly the entire length of the striatum. Because of this divergent projection, any particular part of the striatum receives inputs from multiple discrete regions of cortex.

Projections from different cortical regions diverge or converge in the striatum depending on their areas of origin. This suggests that the striatum processes certain inputs along independent, parallel channels while integrating other cortical inputs. Determining the topography and interaction of corticostriatal projections is important because of the roles cortical inputs play in determining the function of their striatal targets.

(A) Sensorimotor Inputs from the Cortex to the Striatum. One of the strongest cortical inputs to the striatum comes from the sensorimotor cortex (cortical areas 1, 2, 3 and 4). The location of fiber projections from these areas defines the sensorimotor–recipient striatum. The striatal zone that receives inputs from motor and somatosensory cortex is almost entirely within the putamen, supporting the view that the putamen is the "motor nucleus" of the striatum. Physiological evidence supports a role of the putamen in motor function: neurons that fire during limb movement are more common in the putamen than in the caudate nucleus, and electrical stimulation of discrete zones of the putamen produces limb movement (Alexander and DeLong, 1985a). By contrast, the caudate nucleus receives dense projections from the prefrontal cortex. It is thought to have fewer direct ties to movement execution and a greater role in the planning, memory–based, and psychological aspects of basal ganglia function.

The sensorimotor–recipient zone of the putamen is somatotopically organized. The body maps of motor cortex and somatosensory cortex all are projected in register onto the lateral putamen (Künzle, 1975; Künzle, 1977; Jones et al., 1977; Flaherty and Graybiel, 1991a; Fotuhi et al., 1989). Cortical regions with representations of the foot project most dorsally, and cortical regions representing trunk, arm, hand, and face project successively more ventrally. This somatotopic

organization may account for focal extrapyramidal movement disorders, such as parkinsonian tremors restricted to a single body part, and focal dystonias.

There is a major exception to the generalization that the putamen is the "sensorimotor" part of the striatum: oculomotor functions are prominently represented in the caudate nucleus. Eye movement–related regions in the frontal lobes -- notably the frontal eye fields and medial (supplementary) eye fields -- project mainly to the caudate nucleus (Stanton et al., 1988; Huerta and Kaas, 1990; Parthasarathy et al., 1992), and many neurons firing in relation to saccadic eye movements are found there (Hikosaka and Sakamoto, 1986). This striatal region appears to influence the midbrain's control of eye movements, as we will discuss below.

There is evidence that functional deficits in disorders of the basal ganglia reflect these corticostriatal projection patterns. In the early stages of idiopathic Parkinson's disease, more dopamine is lost from the putamen than from the caudate nucleus (Kish et al., 1988). This differential loss may help account for the early appearance in Parkinson's disease of its characteristic motor deficits. In Huntington's disease, early degeneration is prominent in the caudate nucleus (Vonsattel et al., 1985), and cognitive and eye movement abnormalities are common (Kennard and Lueck, 1989).

(B) Local Compartmentalization of Corticostriatal Inputs. The striatum has local modules within it, much as the cortex has layers and columns. The most extensively studied modules in the striatum are the neurochemically–specialized striosomes ("striatal bodies") that form branched three–dimensional labyrinths in the striatum. These regions have attracted interest because their boundaries govern the distribution of nearly every neurotransmitter–related compound in the striatum, and because of their connections with the limbic system. In tissue sections striosomes appear as differentially–stained ellipses and rings, about 0.5 mm wide, having a higher or lower level of a given transmitter–related compound than does the surrounding extrastriosomal matrix. For instance,

neurons in striosomes have higher levels of mu opiate receptors, D_1 dopamine receptors, and neuropeptides such as dynorphin and substance P. The extrastriosomal matrix is enriched in D_2 dopamine receptors, cholinergic markers such as acetylcholinesterase, and enkephalin-containing neuropil. Striosomes are not distributed uniformly: they are especially evident in the head of the caudate nucleus and rostral putamen, and also in the most caudal sectors of these nuclei. The sensorimotor-recipient region of the putamen apparently has few striosomes, at least as detected with current methods.

Striosomes and matrix have different inputs and outputs. Striosomes receive inputs from much of the prefrontal, insular, and temporal cortex. By contrast, the extrastriosomal matrix receives inputs from the sensorimotor cortex, from much of the parietal-temporal-occipital association cortex, and from the cingulate gyrus. Most subcortical inputs are governed by striosomal boundaries as well: the CM-PF complex of the thalamus projects to the matrix, whereas the midline nuclei of the thalamus and basolateral amygdala project to striosomes. Striosomes in different regions of the striatum receive different inputs, just as the matrix does, and these regional differences in corticostriatal projections are anatomically "rule-driven." For instance, cortical association areas in the cat can be placed in a simple hierarchy according to their patterns of striosome-matrix projections (Ragsdale and Graybiel, 1990), and, in the rat, cells in different cortical layers project preferentially to striosomes or to matrix (Gerfen, 1989). Such patterns have not yet been studied in primates.

It is thought that motor signals in the striatum are processed primarily in the matrix: projections from both motor and somatosensory cortex innervate the extrastriosomal matrix and avoid striosomes, and indirect evidence indicates that physiologically identified movement-related neurons are also in the matrix. Moreover, the matrix projects strongly to the pallidum and the SNpr, sites thought to be the main outputs of the basal ganglia motor system. Striosomes, by contrast, project primarily to the SNpc or to the immediately adjacent part of SNpr.

Because striosomes interdigitate with the surrounding matrix, matrix/striosome borders may serve as interfaces where the sensorimotor systems of the matrix interact with the processing of prefrontal and other inputs that occurs within striosomes. Some striatal cell types send dendrites across striatal boundaries, and could presumably mediate striosome–matrix interactions, but it is interesting that the dendrites of certain other striatal cell types obey striosomal boundaries, and do not cross them (Bolam et al., 1988; Penny et al., 1988; Kawaguchi et al., 1990). In humans and other primates, but not in non–primates, these border regions are distinguished by rings of neurochemically–distinct tissue (Graybiel, 1984; Dragunow et al., 1990a). The neurochemical differences between striosomes and matrix make it possible that new drugs could selectively target either striosomal or matrix neurons. Disease processes, too, might have such selective targets. In the striatal degeneration seen in Huntington's disease, for instance, there are reports that striosomes and matrix are differentially affected (Ferrante and Kowall, 1987; Seto–Ohshima et al., 1988; Hedreen, 1990).

It has only recently become evident that the matrix is not merely a homogeneous tissue surrounding striosomes, but itself contains discrete input and output zones -- matrisomes -- within it (Graybiel et al., 1991). For instance, sensorimotor cortical fiber projections do not innervate all of the matrix, but only isolated zones within it (Malach and Graybiel, 1986; Flaherty and Graybiel, 1991a). Thus the entire striatum, and not just the striosomal system, appears to have a modular organization. Such modularity is reminiscent of the layers and columns of the cerebral cortex.

In functional terms, this patchwork may allow individual inputs to the striatal matrix to be parcelled among different striatal subsystems. The degree of convergence and divergence of inputs to the striatum, and the degree to which they select different output modules, influences information processing in the striatum.

B. Other inputs to the basal ganglia

1. Direct and Indirect Cortical Inputs

Two of the loop nuclei linked to the striatum and pallidum, the CM–PF complex of the thalamus and the subthalamic nucleus, receive inputs directly from the motor cortex. There are also projections from motor cortex to other sites in the basal ganglia circuit (e.g. to the tegmental pedunculopontine nucleus), but they are apparently not strong. The motor cortex projects to the CM nucleus, and the premotor cortex innervates the PF nucleus. CM and PF in turn project to the striatum, so the striatum receives indirect as well as direct information from the motor and premotor cortical areas. The fiber projection from the motor cortex to the subthalamic nucleus, which is dense and somatotopic, is accompanied by a weaker fiber projection from neighboring cortical areas. The subthalamic nucleus projects to both segments of the pallidum and to the SNpr, thus providing a route by which signals from sensorimotor cortex can reach these nuclei without passing through the striatum. The subthalamic nucleus is now considered a pivotal modulator of basal ganglia circuitry (see below).

2. Inputs from the Brainstem

Except for the well-known nigrostriatal pathway and a small nigropallidal pathway, direct brainstem inputs to the basal ganglia are sparse. Serotonin-containing fibers from the dorsal raphe nucleus reach the striatum, pallidum, and the substantia nigra. The norepinephrine-containing locus coeruleus projects to the ventral striatum, but not strongly to the dorsal striatum or the pallidum. Besides these direct brainstem inputs, the pallidum and the striatum receive information indirectly, via the CM–PF complex, from the reticular formation (including the tegmental pedunculopontine region) and from the spinothalamic tracts. The brainstem inputs to the SNpc, discussed further

below, include projections from parts of the subcortical limbic system, but the SNpr, like the pallidum, receives few non-striatal inputs. In general, nuclei in the basal ganglia circuit -- except the striatum -- receive most of their subcortical inputs from each other, not from other nuclei.

This limited access to the nuclei of the basal ganglia circuit, combined with the rich interconnections of these nuclei, is one of the best pieces of evidence that the basal ganglia circuit is a functional unit. Strong internal connectivity does not imply, however, that the extrinsic inputs to these nuclei are not important. For example, it may be that the input to the subthalamic nucleus from the motor cortex provides the main excitatory drive for this key nucleus, and limbic inputs to the SNpc may condition dopaminergic actions on the entire system.

II. PROJECTIONS FROM THE STRIATUM TO GP AND SNpr

Compared to the cortex, the striatum is unusual in that most of its neurons are output neurons rather than interneurons. And nearly all of its outputs are directed towards the substantially smaller pallidum and substantia nigra (see Tables 1-2 and 1-3). These two nuclei are thus, in a sense, bottle-necks in the primary basal ganglia circuit, a fact that may account for the devastating motor disturbances that damage to them can produce. Two subdivisions of these nuclei, the GPi and SNpr, play similar roles in relaying information from the striatum to thalamocortical circuits, and the GPi and SNpr share many other connections and neurochemical characteristics. Indeed, GPi and SNpr are in some ways more similar to each other than are GPe and GPi or SNpr and SNpc.

Striatal output neurons are classified as medium spiny neurons by their size and their abundance of dendritic spines. They release gamma-aminobutyric acid (GABA) as their neurotransmitter, and generally contain one or more neuropeptide co-transmitters as well. Because GABA hyperpolarizes active and resting neurons, when striatal neurons fire, they inhibit the normally high tonic activity of the pallidum and substantia nigra (Chevalier and Deniau, 1990). Striatal

neurons probably also inhibit each other through their rich local axon collaterals. This may account for the characteristic very low firing rates of striatal neurons (Groves, 1983).

Despite occasional reports to the contrary, it is clear that both the caudate nucleus and the putamen project to all four striatal targets: GPe, GPi, SNpc, and SNpr. The fiber bundles that form the striatopallidal and striatonigral pathways set up a roughly radial projection topography. The putamen -- including the sensorimotor zone -- projects more strongly to GPe and GPi, and less strongly to the SNpr, whereas the caudate nucleus -- including the eye movement zone -- projects more strongly to the SNpr. The SNpc apparently receives most of its striatal inputs from the ventral striatum and from striosomes, which are more abundant in the caudate nucleus than in the putamen. The ventral striatum also has its own projection target in the ventral pallidum, a region that lies below the anterior commissure within the substantia innominata, near the nucleus basalis of Meynert.

Until recently, it was believed that striatal outputs were all collaterals of each other. In the rat, single striatal neurons do indeed project to both segments of the pallidum and to the substantia nigra (Staines and Fibiger, 1984; Loopuijt and van der Kooy, 1985). But in higher mammals, neurons projecting to a given striatal target nucleus apparently send few collaterals to other target nuclei (Feger and Crossman, 1984; Beckstead and Cruz, 1986). This target restriction could provide a neural mechanism by which the striatum can control the activity of different parts of the pallidum and nigra independently. Selective output channeling is now thought to be of great importance for movement control.

Striatal neurons projecting to the GPe, GPi and substantia nigra differ neurochemically. Although each set of neurons contains GABA as a transmitter, they appear to have predominantly different co-transmitters: striatal fibers projecting to GPe contain enkephalin, whereas those projecting to GPi and SNpr are more likely to contain substance P and dynorphin. This difference in co-transmitters suggests that pharmacological manipulations could target individual

striatal output systems independently. However, pharmacological differences between the pathways are unlikely to be absolute. For instance, some neurons coexpress enkephalin, dynorphin, and substance P (Penny et al., 1986; Besson et al., 1990); and enkephalin-containing projections are not entirely restricted to the GPe; the inner part of GPi also has considerable enkephalin levels.

Striatal projection systems are segregated not only at the level of single neurons, but also at the level of macroscopic clusters of neurons. As mentioned above, the outputs to GPe, GPi, and SNpr all arise primarily from the matrix, whereas striosomes project mainly to the SNpc or to the immediately surrounding SNpr. Within the matrix there appear to be distinct patches and bands of neurons projecting to GPe, GPi, and SNpr (Jiménez-Castellanos and Graybiel, 1989c; Desban et al., 1989; Giménez-Amaya and Graybiel, 1990; Selemon and Goldman-Rakic, 1990), each set of clusters forming a branching three-dimensional network of matrisomes. It is not yet known how these matrix output modules are distributed with respect to the matrix input modules described above, but the relationship may be key to understanding basal ganglia processing. It could turn out, for instance, that the matrisomes that project to GPe preferentially receive input from the sensorimotor cortex. This would make possible a specialized path from sensorimotor striatum to GPe and then to the subthalamic nucleus.

Despite the predominance of striatal output neurons, there are also several types of striatal interneurons. The cholinergic and somatostatin-containing interneurons have received the most attention recently. Cholinergic interneurons are large, aspiny cells that interact directly with medium spiny output neurons. Interactions between acetylcholine and dopamine have long been assumed because of the opposing effects dopaminergic and cholinergic drugs have on movement disorders, but ultrastructural studies show little direct dopaminergic input to the cholinergic interneurons. The striatal matrix, especially the sensorimotor part of the putamen, is richer in cholinergic cell bodies, neuropil, and uptake sites than are striosomes. However, striosomes have denser

muscarinic M1 binding than the matrix (Nastuk and Graybiel, 1988). Somatostatin-containing interneurons are medium-sized aspiny cells that, like the cholinergic neurons, are sprinkled through the striatum. Both cholinergic and somatostatin-containing neuropil are more dense in the matrix than in striosomes. In Huntington's disease, the somatostatin-containing and cholinergic interneurons are selectively spared (Nemeroff et al., 1983; Ferrante et al., 1987) -- in dramatic contrast to the degeneration of nearby medium spiny projection neurons.

III. LOOP PATHWAYS OF THE BASAL GANGLIA

Inputs from the striatum to the pallidum and substantia nigra influence two sorts of pathways: those leading out of the basal ganglia, and loop pathways that project back to the basal ganglia. Output pathways will be discussed in the last section. The main loop pathways are the following:

A. Striatum → SNpc → Striatum

B. Pallidum → subthalamic nucleus → Pallidum.

C. Striatum → GPi → CM-PF thalamus → Striatum.

A. Mesostriatal Pathways

Because the degeneration of nigrostriatal dopamine-containing fibers is pathognomonic of Parkinson's disease, this pathway has received much attention. Dopamine released in the striatum is made both in the cell bodies of SNpc neurons and in their striatal axon terminals. In the striatum, dopamine release is thought to be multiply controlled by the inputs and intrinsic circuitry of the SNpc, by "autoreceptors" for dopamine on the nigrostriatal axon terminals, and possibly by local circuits in the striatum itself.

The SNpc and striatum are often said to be reciprocally interconnected, but this may be true only for neurons in striosomes. Most striatonigral neurons are in the matrix, however, and project not to the SNpc but to the SNpr -- which is

not known to project back to the striatum. Nevertheless, the dendrites (and some cell bodies) of dopamine-containing neurons of the SNpc extend into SNpr. These may mediate interactions between the SNpc and SNpr.

Work to date suggests that there are four main groups of inputs to the SNpc (see Table 1-3): (a) striatal input from striosomes and the ventral striatum; (b) limbic input from the central nucleus of the amygdala, the lateral preoptic area of the hypothalamus, and the dorsal raphe nucleus; (c) cortical input from the frontal cortex, including the supplementary motor cortex; and (d) some fibers from the pallidum and subthalamic nucleus. The SNpc thus provides a means for a number of nuclei -- many of them related to the limbic system -- to exert an influence on striatal activity. The diversity of inputs to the SNpc is in sharp contrast to the restricted inputs to the SNpr.

The striatum, besides receiving input from the SNpc, receives projections from the other major midbrain dopaminergic cell groups: the retrorubral region (cell group A8), and the ventral tegmental area (A10 cell group). Different dopaminergic cell groups project selectively to either striosomes or matrix in the dorsal striatum (Jiménez-Castellanos and Graybiel, 1987; Langer and Graybiel, 1989). The ventral tegmental area is the primary source of dopamine for the ventral striatum, prefrontal cortex, and limbic targets, but some dopamine-containing fibers from the medial SNpc also innervate these regions. These specializations of striatal dopaminergic innervation have implications for disease. For instance, both in Parkinson's disease and following exposure to the neurotoxin MPTP, there is greater cell loss in the SNpc than in the ventral tegmental area (Langston et al., 1984). Thus in parkinsonian disorders the "limbic" functions of the striatum could be spared relative to striatal "sensorimotor" functions. However, it is important to remember that dopaminergic neurons have a much less clear relation to movement than do neurons in the striatum and pallidum. Dopaminergic neurons in the SNpc do not fire in relation to movement or preparation for movement, but to stimuli that are behaviorally relevant (Schultz and Romo, 1990).

Dopamine-containing axon terminals synapse directly on striatal output neurons, as do the excitatory inputs from the cerebral cortex and thalamus. The arrangements of these synapses reflect dopamine's modulatory function. Many of the dopaminergic synapses on striatal neurons are on the necks of dendritic spines, whereas it is the heads of the spines that receive synaptic inputs from cortical fibers (Freund et al., 1984). Dopamine-containing terminals are thus in a position to modulate transmission of cortical inputs selectively, at the level of individual spines, rather than to produce the non-selective modulation that they would produce were they near the axon hillock of the striatal neurons.

There has been a long debate over whether dopamine is excitatory or inhibitory: electrical stimulation of the substantia nigra causes a mixture of excitatory and inhibitory postsynaptic effects in striatal neurons, but application of dopamine directly into the striatum inhibits the already low basal firing rate of its neurons. Whether these effects are monosynaptic or not is not known. Recent evidence from whole-cell voltage clamp study of striatal neurons suggests that the effects of dopamine are mediated at least in part by potassium channels (Freedman and Weight, 1988), and appear to be voltage-dependent (Rutherford et al., 1988; Kitai et al., 1990). If they are voltage-dependent, the results of activity at a dopaminergic synapse will depend on the state of local activity in the recipient neuron. This conditional action fits well with the long-postulated notion that the monoaminergic pathways have a "filtering effect" on their target structures, enhancing the signal-to-noise ratio.

The nature of the postsynaptic dopamine receptor is, of course, crucial to its response to dopamine, and different dopamine receptors have different anatomical distributions in the basal ganglia. In the rat, dopamine D_2-like receptors are found on enkephalin neurons projecting to the globus pallidus (the rat homologue of the primate GPe), whereas D_1-like receptors are found on substance P neurons projecting to the substantia nigra (Gerfen et al., 1990). These differential effects set up the possibility, to be tested, that D_2-active drugs could target the enkephalin-containing GPe pathway, and D_1 drugs target the substance

P-containing GPi-Snpr pathway. Besides the D_1 and D_2 receptor subtypes, three new subtypes, the D_3, D_4, and D_5 receptors, have recently been cloned (Sokoloff et al., 1990; Sunahara et al., 1991; Van Tol et al., 1991). Only the D_1 and D_2 subtypes have had their second-messenger effects characterized. D_1 receptors are positively coupled to adenylate cyclase (Stoof and Kebabian, 1981) and to phosphatidyl inositol turnover (Mahan et al., 1990), whereas D_2 receptors are negatively coupled to adenylate cyclase (Stoof and Kebabian, 1981) and to phosphatidyl inositol turnover (Pizzi et al., 1988). It had long been postulated that D_2 receptors mediate the antipsychotic effects of neuroleptics such as haloperidol, but the discovery of the D_3 and D_4 receptors makes re-evaluation of this hypothesis necessary. In contrast with the D_1 and D_2 receptors, which are found in both the dorsal and ventral striatum, the D_3 receptor is concentrated especially in the ventral striatum, and thus may have a special role in limbic or affective functions. Atypical neuroleptics, such as clozapine, have high affinity for D_4 receptors, and have fewer extrapyramidal side-effects than do the traditional neuroleptics, such as haloperidol, which tend to bind D_2 receptors (Van Tol et al., 1991). Neuroleptics such as haloperidol may also have effects through their binding to sigma sites, which are highly concentrated in the SNpc (Largent et al., 1984; Gundlach et al., 1986) -- especially in the part of the SNpc that projects to striosomes (Graybiel et al., 1989).

D_1 and D_2 receptors, along with nearly all other dopamine-related compounds, are differentially distributed with respect to striosomes and matrix. D_3, D_4, and D_5 receptors have not yet been evaluated for their compartmental affiliations. D_1-like binding sites are denser in striosomes than in matrix (Besson et al., 1990), whereas D_2-like binding sites (and also high-affinity dopamine uptake sites) are denser in matrix than in striosomes (Joyce et al., 1986; Graybiel and Moratalla, 1989). These differences, together with other neurochemical differences between the two compartments, make it possible for dopamine to have different effects on striosomal and matrix neurons. In fact, basal release of newly-synthesized dopamine is higher in matrix-rich regions than in regions that

contain many striosomes, and acetylcholine has different effects on that release in the two compartments (Kemel et al., 1989).

Drugs that bind to dopamine receptors or change dopamine levels in the striatum change gene transcription in striatal neurons. For instance, they stimulate synthesis of enkephalin in enkephalin-containing neurons, most of which project to GPe. By contrast, they produce a decrease in the synthesis and content of substance P in substance P-containing neurons, most of which -- at least in the matrix -- project to GPi and SNpr (Gerfen et al., 1990). Curiously, although the opioid peptide dynorphin coexists with substance P in striatal projection neurons, the effects of dopaminergic drugs on these two peptides are not the same. Because D_1 receptors are richer in the substance P- and dynorphin-rich striosomes, whereas D_2 sites are richer in the enkephalin-rich matrix, D_1- and D_2-mediated effects on striatal output pathways could be significantly different.

The pallidum, although not a major target of the SNpc, is not devoid of dopamine-containing innervation. It is interesting that the two segments of the pallidum themselves, as well as their striatal control pathways, are distinguished by different types of dopamine receptor subtypes: ligands for D_1 receptors mainly bind to GPi, and ligands for D_2 receptors mainly bind to GPe (Richfield et al., 1987; de Keyser et al., 1988; Camps et al., 1989). The GPi also receives a denser dopaminergic input than does the GPe (Parent and Smith, 1987; Besson et al., 1990).

The effects of psychomotor stimulant dopamine agonists such as amphetamine and cocaine may be mediated in striatal neurons by expression of immediate-early genes such as c-*fos* (Graybiel et al., 1990; Young et al., 1991). Curiously, dopamine antagonists such as haloperidol also increase the expression of c-*fos*, but this effect seems to be mediated by D_2-like rather than D_1-like receptors (Dragunow et al., 1990a; Miller, 1990). The products of these immediate-early genes are DNA-binding proteins that influence the transcription of other genes, including the gene for enkephalin (Sonnenberg et al., 1989). It is possible that such immediate-early genes mediate such long-term behavioral

effects of dopaminergic drugs as tardive dyskinesias and addictive syndromes. Determining the patterns within the basal ganglia of postsynaptic changes in gene transcription may help in understanding the pathological changes seen in Parkinson's disease and other basal ganglia disorders, and transcriptional regulation may be important in their treatment as well. For example, the effects of dopamine agonists on striatal c-*fos* can be duplicated in grafts derived from embryonic striatal tissue which have been implanted into damaged striatum (Dragunow et al., 1990b; Liu et al., 1991; Cenci et al., 1990).

B. The GPe-Subthalamic Loop

The subthalamic nucleus is reciprocally interconnected with the pallidum (see Table 1-4). GPe sends a massive projection to the subthalamic nucleus, which projects to GPi and SNpr, and also back to the GPe. The output neurons of the subthalamic nucleus are now thought to use glutamate as a neurotransmitter, and to be excitatory, not inhibitory as was long believed (Nakanishi et al., 1987; Smith and Parent, 1988). This is a pivotal finding, because it helps explain how striatal activity can have remarkably different effects on basal ganglia output, depending on whether it excites neurons projecting to GPi and SNpr -- the direct pathway, or neurons projecting to GPe -- the indirect pathway (see Fig. 1-2). As we will discuss further below, GPi and SNpr both inhibit the VA-VL nuclei of the thalamus. The subthalamic loop, however, could modulate this inhibition. Striatal activity inhibits GPi's and SNpr's tonic inhibition of the thalamus, so cortical activation of striato-GPi and striatonigral neurons should increase thalamocortical activity. But striatal activity also inhibits GPe's inhibition of the subthalamic nucleus, permitting the subthalamic nucleus to excite GPi. GPi should then increase its inhibition of the thalamus and decrease thalamocortical activity (Albin et al., 1989).

Until recently, it was thought that nearly all GPe output was directed towards the subthalamic nucleus; that is, that there was no direct way for the GPe to

influence the output from GPi to the thalamus. There now is evidence, however, that GPe and GPi are reciprocally interconnected (Hazrati et al., 1990; Kincaid et al., 1990; Smith and Bolam, 1990). This resurrects the once-postulated notion of a step-by-step pathway from the striatum through GPe to GPi to the thalamus.The GPe-to-GPi pathway could have the same effects as the subthalamic loop: the striatum, by projecting to GPe, could disinhibit GPi neurons and increase inhibition of the thalamus, decreasing thalamocortical activity.

This simple circuit model has testable and practical implications. For instance, if the presence of the subthalamic loop dampens thalamocortical activity, removal of the loop should increase it, and increase motor activity. This result is seen in hemiballism, long known to follow subthalamic lesions. The effect of subthalamic lesions could have a therapeutic role in Parkinson's disease: in MPTP-treated parkinsonian monkeys, lesions of the subthalamic nucleus produce an immediate, dramatic alleviation of akinesia, tremor, and rigidity (Bergman et al., 1990). Such subthalamic lesions are thought to counteract a pathological increase in subthalamic activity in the parkinsonian monkey, an increase produced by a decrease of GPe activity relative to GPi activity (Miller and DeLong, 1987; Filion et al., 1988).

Observations made on the brains of patients with Huntington's disease suggest a pathological process in which GPe activity increases relative to GPi activity. In early-stage Huntington's disease, there is evidence that enkephalin immunostaining in GPe selectively decreases, whereas substance P immunostaining in GPi is relatively spared (Reiner et al., 1988; Albin et al., 1990), although this has recently become controversial (Ferrante et al., 1990). A specific deficit in GPe enkephalin staining suggests that striatal neurons projecting to GPe are selectively damaged relative to those projecting to GPi. According to the model described above, this would decrease the striatum's inhibition of GPe and hence increase GPe's inhibition of the subthalamic nucleus. The resulting reduction of activity in GPi would decrease inhibition of the thalamus, ultimately leading to increased thalamocortical activity and chorea.

As this circuit model is further developed, several aspects of basal ganglia wiring will need to be added. First, the motor cortex directly excites the subthalamic nucleus, and thus might bypass the cortex-to-striatum-to-GPe-to-subthalamic nucleus projection of the indirect pathway. Second, given the modular organization of inputs from cerebral cortex, and the modular organization of striatal output neurons projecting to GPe and GPi, it may be that different cortical commands are sent into the GPe and GPi pathways. Third, striatal inputs may synapse only on certain pallidal output neurons; certainly not all neurons in the pallidum fire equally following striatal stimulation. Finally, the "plus and minus sign" analysis of the basal ganglia circuit ignores the effects of the neuropeptides coexisting in the striatal pathways. Nevertheless, this model is appealing because of its simplicity and its success in predicting clinical findings.

C. The GPi - CM-PF - Striatum Loop

Outputs from GPi reach not only the ventral anterior (VA) and (VL) nuclei, but also the centre median (CM) and parafascicular (PF) nuclei (see Table 1-5). As with the other basal ganglia paths, the ventral striatum has its own thalamic loop, involving the subparafascicular nucleus. The function of the CM-PF complex is a mystery -- current theories of basal ganglia interactions have nothing substantive to say about it. Yet CM and PF are very large in the primate brain, and they project strongly to the striatum. CM and PF receive significant inputs from motor cortex (to CM), premotor cortex (to PF), and some inputs from the brainstem, and this brings extrinsic signals as well as feedback information to the striatum. Because both CM and PF project to discrete cell clusters within the striatal matrix, they may selectively target particular striatal output modules projecting to GPe, GPi, and SNpr. CM and PF are anatomically, and perhaps functionally, differentiated from each other in that CM projects primarily to the sensorimotor region of the putamen, whereas PF projects to the "associative" regions of both caudate nucleus and putamen. (Sadikot et al., 1990). CM and PF

both send fibers back to the pallidum: CM primarily to GPe, and PF primarily to GPi (Sadikot and Parent, 1989). They project sparsely to cerebral cortex and subcortical regions as well.

D. Other basal ganglia loops

The tegmental pedunculopontine nucleus is part of yet another basal ganglia loop. It receives input from the GPi, SNpr, and motor cortex, inputs that suggest a motor rather than limbic role for the pedunculopontine nucleus. Most of the output of the pedunculopontine nucleus is sent back to the substantia nigra, especially to the SNpc, and also to the pallidum, subthalamic nucleus, and CM–PF thalamus. But there are descending projections from the pedunculopontine nucleus as well. One such is to the reticular formation of the caudal brainstem and apparently includes the inhibitory area of Magoun, a region known to influence activity in the spinal cord. Neurons in the region of the pedunculopontine nucleus are cholinergic, and it is intriguing that they are selectively vulnerable in parkinsonian disorders, especially in progressive supranuclear palsy (Hirsch et al., 1987; Zweig et al., 1987). Cholinergic neurons in this region supply cholinergic input to the SNpc and the superior colliculus (Beninato and Spencer, 1986; Woolf and Butcher, 1986).

IV. OUTPUTS OF THE BASAL GANGLIA

Compared to the tangled loops of interconnections among the basal ganglia and their allied nuclei, their outputs to other parts of the brain are few indeed. GPi and SNpr both send inhibitory input to the nuclei of the VA and VL thalamus, to the tegmental pedunculopontine nucleus, and to the lateral habenular nucleus. The SNpr, but apparently not GPi, also sends a fiber projection directly to the superior colliculus.

A. GPi and SNpr outputs to the thalamus.

The fiber projections to the VA and VL nuclei are the best-known of the GPi and SNpr outputs, because they are by far the strongest outputs, and because VA and VL project to premotor and supplementary motor cortex. The deep cerebellar nuclei project to VL as well, and it was long thought that VL might be a site where the basal ganglia and cerebellum, the two classical extrapyramidal motor systems, could interact. More recent evidence suggests, however, that the basal ganglia and cerebellum project mainly to different subdivisions within the motor-related thalamus. For example, in the VLo subnucleus of VL, GPi projects to cell-dense islands, whereas the cerebellum projects to the cell-sparse regions in between them (Asanuma et al., 1983). The cerebellum innervates other parts of VL, whereas the GPi predominantly innervate VA. SNpr also sends fibers to the adjacent mediodorsal thalamic nucleus.

The gross anatomical segregation of inputs to VA and VL does not rule out the possibility that cerebellar and basal ganglia systems have some interactions in the thalamus. The separation does, however, indicate that different regions of the cerebral cortex are most strongly influenced by the basal ganglia and cerebellum, because the different VA and VL input-fields have outputs to distinct regions of cortex. The cerebellum-recipient region sends fibers primarily to motor cortex and some premotor cortex; the GPi-recipient region sends fibers to non-overlapping parts of premotor cortex and some motor cortex; and the SNpr-recipient regions of VL and the mediodorsal nucleus send fibers yet farther forward to the frontal lobes, including the frontal eye fields and prefrontal cortex (Asanuma et al., 1983; Schell and Strick, 1984; Ilinsky et al., 1985). Curiously, the Vim subnucleus, which apparently does not receive inputs from the basal ganglia, is the thalamic nucleus in which lesions block parkinsonian tremor. Lesions in the VL nucleus relieve parkinsonian rigidity, but not tremor (Narabayashi, 1989).

Because the supplementary motor cortex is thought to play a role in pre-movement cortical activity, in contrast to a more immediate executive function

for motor cortex, the influence of the basal ganglia's path to the cortex is also thought to be mainly at the level of movement "planning." In contrast, the fiber projection from the cerebellum via VL to motor cortex is considered to have more influence on movement execution. The frontal regions to which SNpr projects may have a role in "motor memory" and "working memory" (Fuster, 1989). Such hypotheses, despite their vagueness, have been popular because certain aspects of basal ganglia motor disorders suggest disorders at the level of motor scheme or movement initiation rather than at the level of detailed movement execution. These include the difficulty that parkinsonian patients have in initiating and terminating movements, and the "unwilled" nature of choreic movements. Such functional distinctions are not absolute, however, and the anatomical distinctions are not either. For instance, there is recent evidence that basal ganglia–affiliated areas of the thalamus do project to certain areas of motor cortex (Holsapple et al., 1991). Moreover, electrophysiological studies show that most basal ganglia neurons fire too late during the course of a movement to have much role in movement initiation (Mink and Thach, 1991b; Mink and Thach, 1991a)

B. SNpr outputs to the superior colliculus

The oculomotor connections of the basal ganglia are unique in having a major tectal output in addition to their thalamic output. There is a strong GABAergic fiber projection from the SNpr to the superior colliculus. Fibers from SNpr innervate the middle layers of the superior colliculus, which contain many neurons that fire before saccadic eye movements. This pathway has been intensively studied, and, in the monkey, has been shown to influence whether saccadic eye movements occur or not. When saccadic eye movements are made, the tonic activity of SNpr neurons briefly decreases (Hikosaka and Wurtz, 1983a). Because the output from the SNpr to the superior colliculus is inhibitory, this brief decrease allows a burst of spikes in the cells of the superior colliculus, and

this, in turn, can trigger the initiation of saccades. Saccade-related bursts of activity have been recorded in the part of the caudate nucleus that projects to the SNpr. The path from striatum to SNpr to the superior colliculus, like the path from striatum to thalamus, is a doubly inhibitory one (Deniau and Chevalier, 1985). Injection of GABAergic agonists into SNpr, or of GABAergic antagonists into the superior colliculus mimics the activity of this pathway and facilitates saccades (Hikosaka and Wurtz, 1985a; Hikosaka and Wurtz, 1985b). The path from SNpr to the thalamus may also influence eye movements, because the thalamic target of SNpr fibers projects in part to the frontal eye fields, but little is yet known about this cortically-directed path.

Some of the "eye movement" neurons in the caudate nucleus and in the SNpr show behavioral state dependence (Hikosaka et al., 1989). It may be that this dependence reflects the inputs from the frontal lobes to the caudate nucleus. The activity of some of these eye movement neurons is related to the remembered positions of targets. SNpr's projection to the superior colliculus, and also its projection via the thalamus to frontal cortex, may thus play some role in controlling behaviors contingent on stored as well as externally-generated signals.

C. Other basal ganglia outputs

Hypotheses that explain the function of the basal ganglia exclusively in terms of basal ganglia effects on cortical mechanisms neglect not only the projections to the superior colliculus, but also those to the tegmental pedunculopontine nucleus, and the lateral habenular nucleus. The lateral habenular nucleus is interconnected with sites in the limbic system, tegmental motor region, and especially the dorsal raphe nucleus. Because the dorsal raphe nucleus is, in turn, the major source of serotonergic inputs to several parts of basal ganglia circuitry, the lateral habenular nucleus, too, is to some extent part of a loop system of the basal ganglia. This is one of the many basal ganglia circuits remaining to be explored.

V. SUMMARY

Recent advances in research on the basal ganglia include (1) a large increase in knowledge of the modular design of the striatum and its projections to GPe, GPi, and SNpr; (2) a new view of the mechanisms by which increased or decreased activity in the subthalamic nucleus may lead to akinetic and choreic movement disorders respectively; (3) a new base of information about neurophysiological processing in basal ganglia circuitry, especially in relation to saccadic eye movements, and (4) indications that dopaminergic drugs can selectively interact with different basal ganglia circuits and can alter gene transcription within circuit nuclei. We hope that molecular biologists will soon add to this list of advances the genetic basis of some basal ganglia disorders.

TABLES

Table 1-1. Connections of the striatum.

CAUDATE NUCLEUS AND PUTAMEN

inputs

from neocortex. Glutamate.
- to matrix from sensorimotor cortex.
  - to putamen from primary and supplementary motor cortex, somatosensory cortex.
  - to caudate nucleus from frontal and medial eye fields, posterior association cortex.
- to striosomes from frontal cortex.

from thalamus. Glutamate.
- to matrix from
  - **CM-PF.** CM to sensorimotor putamen, PF to association areas of caudate nucleus and putamen.

from SNpc and ventral tegmental area. Dopamine.
- to matrix from cell group A8 (retrorubral area) and parts of SNpc.
- to striosomes from some SNpc.

from amygdala.
- to striosomes from basolateral nucleus.
- to matrix from other amygdaloid nuclei.

from dorsal raphe nucleus. To matrix. Serotonin.

from subthalamic nucleus. Glutamate.

from pallidum. GABA.

from pedunculopontine nucleus.

outputs. GABA, neuropeptides.

to pallidum. Mainly from matrix.
- to GPe. GABA and enkephalin.
- to GPi. GABA, substance P, dynorphin. Some enkephalin to inner GPe.

to substantia nigra.
- to SNpr. From matrix, mainly from caudate nucleus. GABA, substance P, dynorphin.
- to SNpc. From striosomes. GABA, substance P, dynorphin.

VENTRAL STRIATUM

inputs

from limbic cortex. Hippocampus; piriform, cingulate, and temporal cortex. Glutamate.

from thalamus. Midline nuclei. Glutamate.

from SNpc and ventral tegmental area. Dopamine.

from amygdala.

from dorsal raphe nucleus. Serotonin.

from locus coeruleus. Norepinephrine.

outputs. GABA.

to ventral pallidum.

to ventral tegmental area.

to lateral hypothalamus.

to substantia nigra.

to medial thalamus.

to bed nuclei of stria terminalis.

to pedunculopontine nucleus.

to brainstem.

Table 1-2. Connections of the pallidum.

EXTERNAL SEGMENT OF PALLIDUM (GPe)

inputs

from striatum. From matrix cell clusters. GABA, enkephalin.

from subthalamic nucleus. Glutamate.

from thalamus. Primarily from centre median nucleus.

from pedunculopontine nucleus.

from SNpc. Sparse.

outputs. GABA.

to subthalamic nucleus.

to striatum.

to GPi.

INTERNAL SEGMENT OF PALLIDUM (GPi)

inputs

from striatum. From matrix cell clusters. GABA and substance P.

from subthalamic nucleus. Glutamate.

from thalamus. Primarily from parafascicular nucleus.

from pedunculopontine nucleus

from SNpc. Sparse.

outputs. GABA.

to VA-VL.

to CM-PF.

to pedunculopontine nucleus.

to lateral habenular nucleus.

to striatum.

to GPe

ventral pallidum

inputs

from ventral striatum.

from amygdala.

from dorsal raphe nucleus.

from locus coeruleus.

from SNpc and ventral tegmental area.

outputs

to mediodorsal nucleus of the thalamus.

to hypothalamus.

to amygdala.

to lateral habenular nucleus.

Table 1–3. Connections of the substantia nigra.

SUBSTANTIA NIGRA, PARS RETICULATA (SNpr)

inputs

from striatum. Matrix in caudate nucleus and parts of putamen. GABA, neuropeptides.
from subthalamic nucleus. Glutamate.
from SNpc. Dopamine.
from pedunculopontine nucleus.

outputs. GABA.
to VA–VL thalamus.
to superior colliculus.
to MD thalamus.
to pedunculopontine nucleus.

SUBSTANTIA NIGRA, PARS COMPACTA (SNPC) AND VENTRAL TEGMENTAL AREA (VTA)

inputs

from striatum. GABA, neuropeptides.
from striosomes to SNpc.
from ventral striatum to ventral tegmental area.
from amygdala
from lateral preoptic hypothalamus
from dorsal raphe nucleus
from frontal cortex
from pallidum. Sparse.
from subthalamic nucleus. Sparse.

outputs. Dopamine.
to striatum.
from cell group A8 and part of SNpc to matrix.
from part of SNpc to striosomes.
from SN pars lateralis to both striosomes and matrix.
from cell group A10 to ventral striatum and amygdala.
to pallidum. Sparse.
to subthalamic nucleus. Sparse.

Table 1–4. Connections of the subthalamic nucleus.

SUBTHALAMIC NUCLEUS

inputs

from GPe. GABA.

from cortex, especially motor cortex. Glutamate.

from pedunculopontine nucleus.

outputs.

to GPi. Glutamate.

to GPe. Glutamate.

to SNpr.

to ventral pallidum.

to VA-VL

to striatum.

to pedunculopontine nucleus.

Table 1-5. Connections of the basal ganglia-related thalamus.

VENTRAL ANTERIOR (VA) AND VENTRAL LATERAL (VL) NUCLEI

inputs

from GPi to VA and some VL.
from SNpr to some VA.
from cerebellum to VL.

outputs

to frontal cortex

from VA to areas including supplementary motor area, frontal eye fields.
from VL to areas including motor cortex.

CENTRE MEDIAN (CM) AND PARAFASCICULAR (PF) NUCLEI

inputs

from GPi.
from cortex.
from motor cortex to CM.
from premotor cortex to PF.
from amygdala to subparafascicular nucleus
from SNpr.
from superior colliculus.
from pedunculopontine nucleus.
from locus coeruleus.
from dorsal raphe nuclei.
from brainstem reticular formation.
from spinothalamic tracts.

outputs.

to striatum

from CM to matrix in sensorimotor region of putamen.
from PF to matrix in caudate nucleus and part of putamen.
from subparafascicular nucleus to ventral striatum.

to pallidum

from CM to GPe, some GPi.
from PF to GPi, some GPe.

to cortex.

MEDIODORSAL NUCLEUS

inputs

from basolateral amygdala.
from hypothalamus.
from olfactory bulb.
from ventral pallidum.
from SNpr.
from pontine reticular formation

outputs

to prefrontal cortex, also cingulate cortex and supplementary motor area.
to basolateral amygdala.

FIGURES

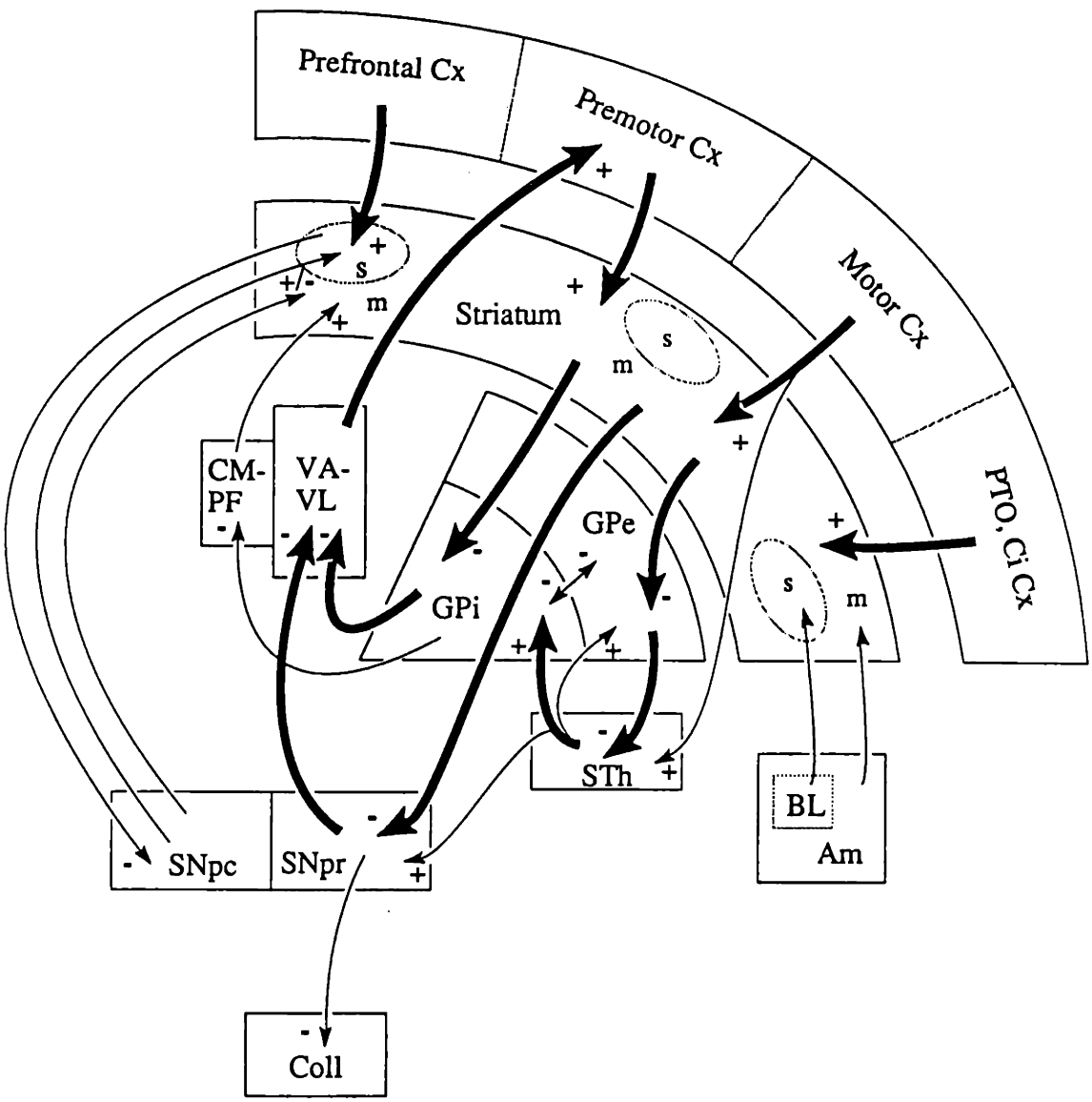

Fig. 1-1. A diagram of basic basal ganglia pathways. What is thought to be the primary flow of cortical information is shown with thick arrows. Excitatory and inhibitory inputs are indicated with plus and minus signs. The connections of the limbic system-associated ventral striatum and ventral pallidum are not shown. Abbreviations: **Am**: amygdala; **BL**: basolateral nucleus of the amygdala; **Ci**: cingulate; **CM-PF**: centre median and parafascicular thalamic complex; **CN**: caudate nucleus; **Cx**: cortex; **GPe**: external pallidal segment; **GPi**: internal pallidal segment; **m**: matrix; **M,S**: motor and somatosensory; **PF**: prefrontal; **PM**: premotor; **PTO**: parieto-temporo-occipital; **Pu**: putamen; **s**: striosome; **S Coll**: superior colliculus. **SNpc**: substantia nigra, pars compacta; **SNpr**: substantia nigra, pars reticulata; **STh**: subthalamic nucleus; **VA-VL**: ventral anterior and ventral lateral thalamic nuclei.

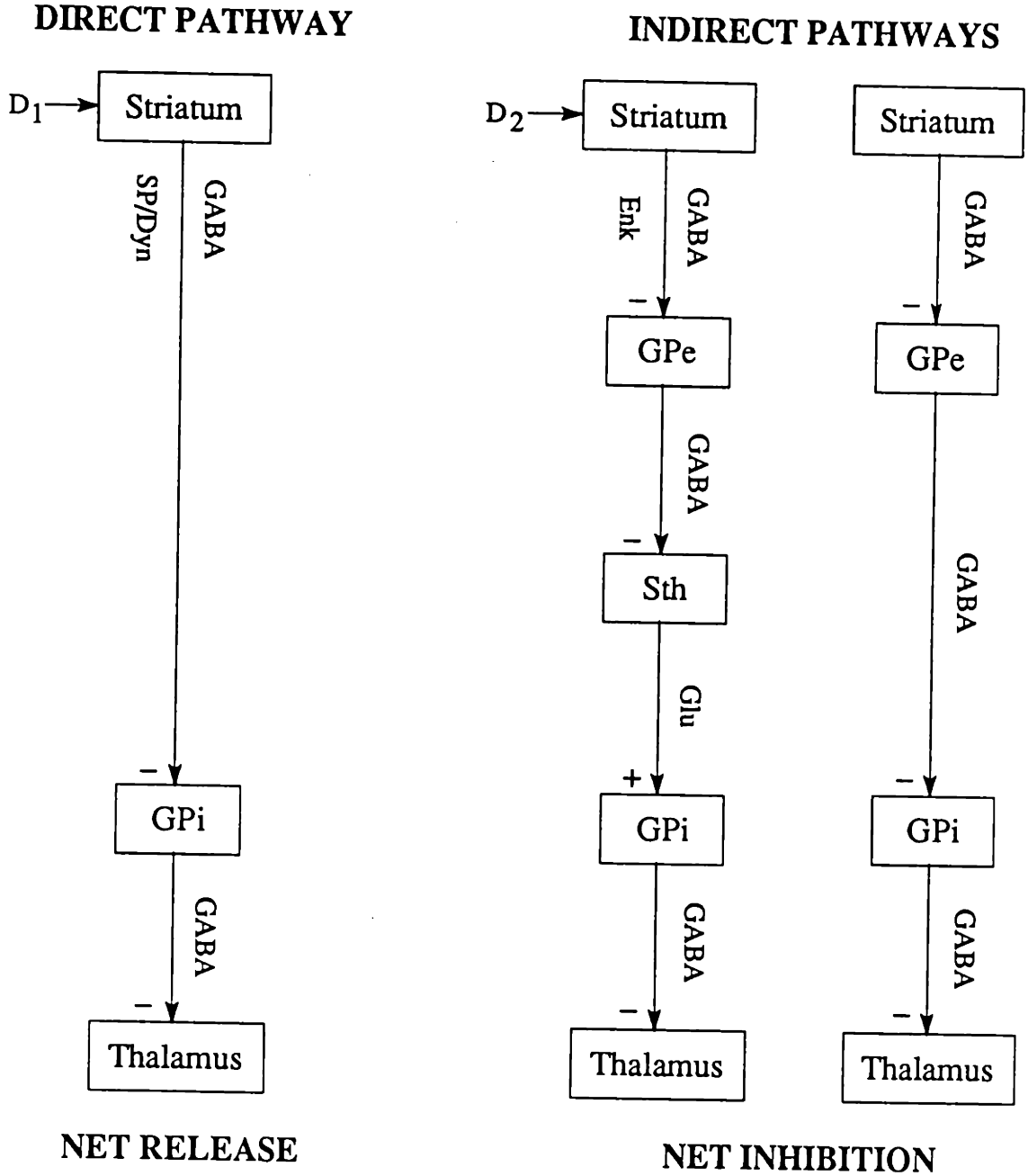

Fig. 1–2. Direct and indirect pathways through the basal ganglia are thought to have opposite effects on the thalamus and cortex. On the left, the doubly inhibitory pathway through GPi has the net effect of releasing the thalamus from pallidal inhibition. At center, the pathway through GPe and the subthalamic nucleus contains three inhibitory steps, resulting in thalamic inhibition. On the right, a projection linking GPe and GPi via the subthalamic nucleus also contains three inhibitory steps, producing thalamic inhibition. The neurotransmitters and neuropeptide co-transmitters used in these projections differ in the three pathways. Abbreviations are as in Fig. 1–1 and **Dyn**: dynorphin; **Enk**: enkephalin; **GABA**: gamma-amino butyric acid; **Glu**: glutamate; **SP**: substance P.

CHAPTER 2. CORTICOSTRIATAL TRANSFORMATIONS IN THE PRIMATE SOMATOSENSORY SYSTEM

> I know I am seated, my hands on my knees, because of the pressure against my rump, against the soles of my feet, against the palms of my hands, against my knees. Against my palms the pressure is of my knees, against my knees of my palms, but what is it that presses against my rump, against the soles of my feet? I don't know. My spine is not supported. I mention these details to make sure I am not lying on my back, my legs raised and bent, my eyes closed. It is well to establish the position of the body from the outset, before passing on to more important matters.
>
> - Samuel Beckett, *The Unnameable*

ABSTRACT

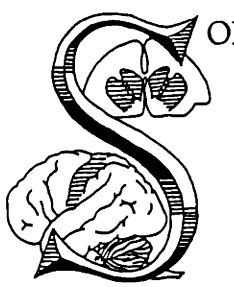

OMATOSENSORY INPUT to the basal ganglia of primates is carried largely by corticostriatal fibers. To determine whether map-transformations occur in this corticostriatal system, we investigated how electrophysiologically-defined regions of the primary somatosensory cortex (SI) project to the striatum in the squirrel monkey (*Saimiri sciureus*). Receptive fields in the hand, mouth, and foot representations of cortical areas 3a, 3b, and 1 were mapped by multiunit recording, and small volumes of distinguishable anterograde tracers were injected into different body-part representations in single SI areas.

Analysis of labeled projections established that at least four types of systematic remapping occur in the primate corticostriatal system. *1)* An area of cortex representing a single body part sends fibers which diverge to innervate multiple regions in the putamen, forming branching, patchy fields that are densest in the lateral putamen. The fields do not form elongated cylindrical forms; rather,

they are nearly as extended mediolaterally as they are rostrocaudally. *2)* Cortical regions representing hand, mouth and foot send globally somatotopic, non-overlapping projections to the putamen, but regions with closely related representations (such as those of the thumb and fifth finger in area 3b) send convergent, overlapping corticostriatal projections. The overlap is fairly precise in the caudal putamen, but in the rostral putamen, the densest zones of the projections do not overlap. *3)* Regions representing homologous body parts in different SI cortical areas send projections that converge in the putamen. This was true of paired projections from area 3a and 3b, and from areas 3b and 1. Thus, corticostriatal inputs representing distinct somatosensory submodalities can project to the same local regions within the striatum. Convergence is not always complete, however: in the rostral putamen of two cases comparing projections from areas 3a and 1, the densest zones of the projections did not overlap. *4)* All projections from SI avoid striosomes and innervate discrete patches within the matrix.

These experiments demonstrate that the somatosensory representations of the body are reorganized as they are projected from SI cortex to the somatosensory sector of the primate putamen. This remapping suggests that the striatal representation of the body may be functionally distinct from that of each area of SI cortex. The patchy projections may provide a basis for redistribution of somatic sensory information to discrete output systems in the basal ganglia. Transformations in the corticostriatal system could thus be designed for modulating different movement-related programs.

INTRODUCTION

In the past ten years, two types of reorganization have been demonstrated in pathways leading from the cortex to the striatum. First, cortical areas projecting to the striatum preferentially innervate or avoid striosomes, which form neurochemically distinct three-dimensional labyrinths embedded in a large

surrounding matrix (Ragsdale and Graybiel, 1981; Gerfen, 1984; Donoghue and Herkenham, 1986). Patterns of striosome–matrix innervation are specific to the layers of origin of corticostriatal neurons (Gerfen, 1989), and set up an ordering of cortical association areas (Ragsdale and Graybiel, 1990). This redistribution of cortical inputs gains importance because striosomes and matrix have different outputs as well. Neurons in striosomes project to the dopaminergic substantia nigra pars compacta and adjacent regions, whereas neurons in the matrix project to both segments of the globus pallidus, and to the non–dopaminergic substantia nigra pars reticulata (Graybiel et al., 1979; Gerfen, 1984; Gerfen, 1985; Jiménez–Castellanos and Graybiel, 1989c). Thus, the striosome–matrix redistribution of cortical inputs to the striatum may direct cortical information to neurochemically distinct parts of the striatum which in turn project to functionally distinct parts of the pallidum and substantia nigra.

The second reorganization of corticostriatal projections occurs within the matrix. Some matrix–directed corticostriatal projections innervate only discrete zones within the matrix, rather than innervating the matrix uniformly (Malach and Graybiel, 1984; Alexander et al., 1988; Fotuhi et al., 1989; Parthasarathy et al., 1990). Evidence that the matrix contains clusters of efferent neurons suggests that there may be distinct sub–channels within the corticostriatopallidal and corticostriatonigral pathways (Desban et al., 1989; Jiménez–Castellanos and Graybiel, 1989b; Giménez–Amaya and Graybiel, 1990; Selemon and Goldman–Rakic, 1990; Giménez–Amaya and Graybiel, 1991; Graybiel et al., 1991).

An interesting aspect of the non–striosomal patchiness of striatal inputs is that, at least in the cat, it characterizes the projection from the somatic sensory and motor cortex to the matrix. This arrangement suggests that sensory–motor representations in the striatum may not be continuous. In the cat, the somatic sensory projection to the striatum is patchy, although generally somatotopic, and that patchiness imposes a partial segregation of inputs to the striatum from areas 3a and SI (thought to be the feline equivalent of primate area 3b) (Malach and

Graybiel, 1986). In the primate, a number of studies starting with those by Künzle (Künzle, 1975; Künzle, 1977) have demonstrated a general somatotopic organization in cortical sensorimotor projections to the striatum. One report in the macaque suggested that projections from areas 3b, 1, and 2 do not overlap in the striatum, but these comparisons were made across, rather than within, individual cases, and without physiological identification of the injection sites (Jones et al., 1977). There is preliminary evidence that the motor cortex projects to the same zones in the striatum as receive inputs from primary somatosensory cortex (SI) (Fotuhi et al., 1989), but avoids parts of the striatum receiving from supplementary cortex (Alexander et al., 1988). The relationship of these inputs to striosomes is not well-understood. There is also electrophysiological evidence for clustering of striatal neurons with similar somatic sensory receptive fields (Schneider and Lidsky, 1981; Crutcher and DeLong, 1984; Liles and Updyke, 1985) and evidence for "microexcitable zones" in which electrical stimulation produces discrete motor responses (Alexander and DeLong, 1985a). These physiologically-identified clusters correspond with projections from the cortical region representing the same body part (Liles and Updyke, 1985; DeLong et al., 1988).

In the study reported here, and briefly earlier (Flaherty et al., 1989), we electrophysiologically mapped somatic sensory cortex (SI) and anatomically marked the corticostriatal projections of defined parts of the SI map. We chose to study the squirrel monkey (*Saimiri sciureus*), because its brain has a shallow central sulcus that leaves cortical areas 3a, 3b, and 1 exposed on the cortical surface (Sur et al., 1982). We set out to answer four questions: 1) How does a discrete, physiologically-defined body part representation in a given cortical map project to the striatum 2) What relationship holds in the striatum between projections from different body part representations in a single cortical map? 3) How are projections from homologous body part representations in different cortical maps related in the striatum? 4) How are projections from these cortical areas distributed with respect to striosome/matrix boundaries?

METHODS

In 16 adult squirrel monkeys, SI was physiologically mapped to guide the placement of 30 anterograde tracer injections into cortical areas 3a, 3b, or 1. In 13 of the 16 monkeys, we injected pairs of differentiable tracers into different regions of SI. Table 2–1 summarizes the protocols for the 30 injections.

Animals were treated with trimethoprim and sulfadiazine (Tribrissen 24%, 0.1 ml/mg SC), atropine (0.04 mg/kg SC) and, in some experiments, dexamethasone (0.8 mg/kg SC) before surgery. They were anaesthetized with an initial dose of ketamine hydrochloride (Ketaset, 30 mg/kg IM) and sodium pentobarbital (Nembutal, 10 mg/kg IP), and were given supplementary doses of ketamine (10 mg/kg IM) as needed during the experiment to maintain anaesthesia. Body temperature was maintained at 35–37°C, and lactated Ringer's solution with 1% dextrose was provided (2–4 cc/hr, IV). The somatic sensory cortex was exposed unilaterally with sterile technique. Throughout the experiment the cortex was covered with high-viscosity silicon fluid held in a recording well.

Electrophysiological recordings. Multi-unit neuronal activity was recorded with tungsten microelectrodes (Microprobe) that had impedances between 1.0 and 1.5 MΩ at 1 Khz. The location of each cortical electrode penetration was marked on an enlarged photograph of the brain surface, and the stereotactic coordinate of the penetration site was also recorded. In a few experiments, recording sites were marked by inserting the electrode 4–6 mm below the cortical surface. Typically, penetrations in areas of interest were 500 μm apart, and recordings were made at depths of 0.8–1.4 mm. Receptive fields were identified as cutaneous or noncutaneous by stimulating the skin with fine hand-held probes. Cutaneous fields were defined as regions from which a vigorous neural response could be elicited with very gentle tactile stimulation of the skin. Noncutaneous fields were defined as those unresponsive to light touch but sensitive to forceful taps or to manipulation of underlying tissues or joints. In each animal we made detailed

maps of the regions of the intended tracer injection, such as the hand, mouth, or foot representations, rather than mapping SI completely. We identified the transition from area 4 to area 3a by a sharp increase in the activation of neurons by stimulation of deep tissues while moving caudally from less responsive cortex. The transition from area 3a to area 3b was marked by an abrupt increase in neuronal activation by gentle cutaneous stimulation of the glabrous or hairy skin. The border between area 3b and area 1 was defined by a reversal of receptive field progression and an increase in receptive field sizes. The area 1–area 2 border was identified by a decrease in sensitivity to cutaneous stimuli.

Tracer injection and histology. Injection pipettes were placed at physiologically-defined sites by reference to the photographic records made during the mapping session. Wheatgerm-conjugated horseradish peroxidase (HRP-WGA, 15%) and ^{35}S-methionine (200 μCi/ul) were pressure-injected with a Picopump (World Precision Instruments). In one case (19) the lectin PHAL (2.5% solution) was injected electrophoretically (Gerfen and Sawchenko, 1984).

Following a survival time of two days (except for the case with a PHAL injection, in which the survival time was 14 days), the animals were deeply anaesthetized with Nembutal and were perfused with heparinized saline followed by 4% paraformaldehyde and 5% sucrose in 0.1 M phosphate-buffered saline (PBS), and then 5% sucrose in PBS. Case 19 was perfused by a two-pH fixation protocol, in which 4% paraformaldehyde at pH 6.5 in 0.1 M acetate buffer was followed by 4% paraformaldehyde at pH 11 in 0.1 M borate buffer (Berod et al., 1981). Brains were blocked *in situ* in a stereotaxic device, and blocks were soaked overnight in 20% sucrose in PBS, frozen in dry ice, and cut coronally or sagittally in 40 μm sections on a sliding microtome. Adjacent sections were processed in series to compare the distributions of injected tracers and histochemical markers.

To demonstrate ^{3}5S-methionine, mounted defatted sections were dipped in Kodak NTB-2 emulsion diluted 1:1 in 0.1% Dreft (Cowan et al., 1972; Hendrickson et al., 1972). Sections were exposed for 1–6 weeks, developed in Kodak D-19, counterstained with cresylecht violet, and coverslipped. HRP

reaction product was demonstrated by the tetramethyl benzidine procedure of Mesulam (Mesulam, 1978) (0.015% H_2O_2), with changes of the incubating solution every 3 minutes for twenty minutes (Illing and Graybiel, 1985)). To demonstrate PHAL, sections were incubated for 36 hours in anti-PHAL (Vector Labs, diluted 1:1000 in saline containing 0.29 M Tris buffer), and bound antibody was labeled with the avidin-biotin peroxidase technique (Vectastain Kit, Vector Labs). Striosomes were identified as zones of low met-enkephalin-like cell body immunoreactivity (Graybiel and Chesselet, 1984). Sections were incubated for three to five days in anti-met-enkephalin (1:2000 dilution of antiserum R176, from Dr. R. P. Elde), and processed with the peroxidase-antiperoxidase method (Sternberger, 1979) by the "protocol B" procedure described elsewhere (Graybiel and Chesselet, 1984).

Data analysis. Sections were studied under bright- and dark-field illumination, and slides stained for HRP were placed between crossed polarizers (Illing and Wassle, 1979). The distribution of tracers in the striatum were charted at 10-40x with a drawing tube, or with a computer graphical data analyzer (Biocom). Although the boundaries between labeled and unlabeled zones were sometimes abrupt, in the cases where they were more gradual, the precise position of the borders as drawn in this paper's figures were somewhat arbitrary, even when the computer was used to determine contours of a given optical density. Consequently, for the purposes of comparison, we have shown both photographs and drawings for the sections illustrated in Figs. 2-5 and 2-7C. Adjacent sections were aligned with reference to local blood vessels. Injection sites, charted on coronal sections with the drawing tube or computer, were reconstructed on the cortical surface with respect to the *in vivo* electrophysiological map by reference to the tracks of the injection pipettes, electrode penetrations, stereotaxic coordinates, and sulcal patterns. The sizes of the injection sites were measured both directly and by computerized labeling-density threshold analysis, taking into account the greater shrinkage of tissue processed by the Mesulam tetramethylbenzidine method. Because injections that

did not penetrate to cortical layer V did not produce analyzable amounts of label in the striatum, injection site widths were measured at the level of layer V, rather than at the surface of the cortex (Flaherty and Graybiel, 1991b). In reconstructing locations of recording and injection sites with respect to the limits of SI cortical areas, we relied primarily on physiological data, but considered cytoarchitectural details as a complementary guide (Jones et al., 1978).

RESULTS

Physiological recordings and injections in SI areas 3a, 3b, and 1

Reconstructed SI maps resembled those described previously in the squirrel monkey (Sur et al., 1982). In some of the monkeys in which the hand region of area 3a was explored, we could, in addition, detect a rostrocaudal progression of receptive fields in which more distal joints in the hand were represented caudally.

Four types of tracer deposits were most useful for analysis: small deposits contained within restricted body part representations in single SI areas (monkeys 23L, 28R, 19), large deposits spanning multiple representations and areas (monkeys 2 and 4), paired deposits of differentiable tracers placed in different SI areas or representations (monkeys 9, 10, and 14–18), and paired deposits of tracers covering the same area (monkey 19). The smallest injection sites had areas that ranged from 0.5% to 5% of the largest injection sites.

Histological reconstruction of injection sites in comparison to the electrophysiological maps showed that all tracer deposits in parts of the hand region were contained entirely within the hand region; the same was true for mouth and foot injection sites. Most injections large enough to produce visible transport were not small enough to be contained entirely within a single sub-region, such as a finger tip within the hand representation; they also infiltrated

adjacent representations (such as adjacent finger tip representations). In areas 3a and 1, single recording sites occasionally had receptive fields extending onto more than one digit. Table 2-1 lists the body part representation predominantly labeled by each injection. In two cases the injection sites did not spread outside even the sub-region injected: the area 1 upper lip representation in monkey 9, and the area 3b foot sole representation in monkey 23L. Fig. 2-1 shows the injection site, relevant receptive fields, and striatal projections in monkey 9.

In a single control case, monkey 19, we injected PHAL and ^{35}S-methionine into the same site in area 3b (the third finger representation). Regions of densest ^{35}S-methionine labeling corresponded to regions with the highest density of PHAL-labeled fibers and varicosities (Fig. 2-2), suggesting that corticostriatal distributions labeled with ^{35}S-methionine correspond to regions enriched in corticostriatal terminals. Because PHAL-labeled fibers are difficult to analyze at low power for macroscopic patterning, the tracer was not used in the main experiments.

Forms of the striatal projection fields traced from single loci in SI

The injection of either HRP-WGA or ^{35}S-methionine into SI produced anterograde labeling in the ipsilateral putamen in all cases except two (monkeys 5 and 6), in which injection sites did not penetrate below layer IV. The caudate nucleus was not labeled except in a few sections of one case (monkey 18), in which we injected cortical representations of the foot. In the one case (monkey 28R) in which the contralateral hemisphere was examined, there was no label in the contralateral striatum, as expected from the findings of Jones, *et al.* (Jones et al., 1977).

Regardless of the cortical area or body part representation injected, the labeled striatal projection zones had extensive mediolateral as well as rostrocaudal dimensions, and all but one (the HRP-WGA injection in monkey 7) were broken

up into patches when viewed in either coronal or sagittal sections. When projection patches were followed through sequential cross-sections, many--but not all--of the patches fused, forming a three-dimensional branching network. Thus the representation of any one body part was not entirely continuous in the striatum. The patches often, but not always, contained one or more zones of denser labeling ("hot spots") within them. Because the patches varied in intensity of labeling, the less densely-labeled border zone of one patch might be more intensely labeled than the hot spots of another patch. Patchiness was more sharply labeled by ^{35}S-methionine than by HRP-WGA.

Fig. 2-3 illustrates the typical features of projections from SI hand areas to the striatum. The deposit in this case (monkey 15) was centered on the index finger representation of area 3a. In rostral sections (Fig. 2-3A), the labeled fibers clustered in one to five (in most sections two or three) separate patches (about 0.1 mm to as much as 1.0 mm wide) that could be followed as separate entities in successive sections. Farther caudally, many of the patches fused, so that in individual transverse sections they tended to form diagonal bands running for about 3-4 mm along a ventrolateral-dorsomedial axis. This fusion, and the resulting branch points of labeled bands, can be seen in Fig. 2-3B. Some projection patches remained isolated throughout their rostrocaudal length. At the caudal end of the putamen, most of the labeled patches coalesced into a large splotch of labeling (Fig. 2-3C).

Labeled projections from mouth and foot areas formed similar, but not identical, patterns in the putamen. They differed most notably in their dorsal-ventral positions (see Fig. 2-7 A'-C'). All projections were most patchy in the rostral putamen and formed diagonal bands at mid-putaminal levels, but differed at the most caudal levels in that the foot projection was the patchiest caudally, the mouth projection least patchy, and the hand intermediate. The greatest diagonal dimension of the labeled patches, observed at mid-putaminal levels, was about 5.5 mm (monkey 14). The rostrocaudal extent of the corticostriatal projection in the same case was about 6.5 mm. The projection field thus was nearly as broad

at its middle levels as it was long.

Fig. 2-5A shows a sagittal view of an SI corticostriatal projection in monkey 17, in which a finger representation in area 3b was injected. The projection field forms an anteroposterior band, with "hot spots" of especially dense label appearing along the band like beads on a string. This sagittal view demonstrates the extended rostrocaudal distribution of striatal label from a single discrete locus in the cortex. The rostrocaudal dimensions--about 6 mm in this case--were greater than the maximum mediolateral dimensions--about 2.5 mm--of the same distribution. However, cases cut in the coronal plane, as in Fig. 2-3, show that this difference in mediolateral and rostrocaudal extents reflects the fact that the distributions cut diagonally across the width of the putamen. When these diagonal widths are taken into account, the entire projection field from a single locus in the hand region has a breadth nearly as extended as its length.

Injection site areas varied about 100-fold from the smallest (monkey 23L) to the largest (S2). Even though small injection sites (monkeys 5, 23L and 28R) had striatal projections that were much more faintly labeled than those from large injection sites (monkeys 2 and 4), the distributions of projections from small injection sites were remarkably similar to those from large sites in having about the same numbers and distributions of hot spots (Fig. 2-4), and about the same anteroposterior extent. The smallest injection site that produced visible striatal labeling also produced multiple patches in the striatum, and, as after larger injections, not all of these patches fused when followed through adjacent sections. The two cases in which injection sites were contained within a single sub-part of a body part representation -- the upper lip region of area 1 in monkey 9, and the foot sole region of area 3b in monkey 23L, had projection patterns similar to those labeled by injection sites that involved more than one digit or lip representation. In particular, there were multiple projection patches even from injection sites containing only these small single body part representations (Figs. 2-1 and 2-4B).

Corticostriatal projections from different representations in a single SI map

SI corticostriatal projections conformed to the somatotopic pattern well-known for the sensorimotor sector of the primate putamen (Künzle, 1975; Künzle, 1977): the foot was represented in the rostral and dorsal putamen, the hand in the central putamen, and the face in the ventral putamen. This global somatotopic organization held regardless of the area in SI injected. Although striatal termination zones differed in location, in coronal sections they were approximately the same size and shape (a branching ventrolateral-to-dorsomedial band) regardless of the body part representation injected. Typical projections from the hand region are shown in Fig. 2-3 and Figs. 2-5 through 2-8, from the foot region in Figs. 2-4 and 7, and from the mouth region in Figs. 2-5B and 2-7.

To determine the grain of the corticostriatal map at a finer level, we directly compared the putaminal fiber labeling elicited by dual injections into different body-part representations in a single cortical map. In monkey 17 we made non-overlapping injections into distant body parts: the lower lip representation and the index finger representation of area 3b. The centers of the injection sites were about 3.0 mm apart, and their nearest edges were about 0.6 mm apart. These non-overlapping cortical loci projected to non-overlapping but adjacent regions at all levels of the putamen (Fig. 2-5). In monkey 16 we made non-overlapping injections into representations of nearby body parts (the thumb and fifth finger representations of area 3b). The centers of the injection sites were about 3.2 mm apart, and their nearest edges were about 0.5 mm apart, so that monkeys 16 and 17 did not differ dramatically in the separation of their injection site pairs. These non-overlapping cortical loci projected to regions of the putamen that overlapped substantially, although not completely (Fig. 2-6). Thus, cortical sites in area 3b representing nearby body part representations (digits of the hand) projected to overlapping regions of the putamen, whereas cortical sites about the same distance from each other, but representing distant body parts (hand and lip)

projected to non-overlapping regions of the putamen.

The thumb and fifth finger projections, although quite convergent caudally, were not fully overlapped rostrally. In particular, although the broad extent of each projection was almost completely overlapping at all coronal levels, the densest parts of the projections -- the hot spots -- were shifted relative to one another in their rostral third (about 2 mm). The lack of overlap of the hot spots rostrally contrasted with their consistent superposition in the caudal two-thirds the two projections (although even caudally these foci were not always exactly the same size or shape). This suggested that the grain of the map might be finer rostrally than caudally, at least for the hand representation, a feature found also in experiments described below.

Corticostriatal projections from the same representations in different cortical maps

In five cases we made non-overlapping injections of HRP-WGA and $^{3}5S$-methionine into homologous body part representations of two different SI areas. We compared corticostriatal projections from areas 3a and 3b, 3b and 1, and 3a and 1. In every case there was considerable overlap in the distributions of fibers labeled with the two tracers, and the number and pattern of projection patches were similar for the pairs of projections in most sections. This overlap of projections to the striatum was confirmed for homologous parts of the foot, mouth, and hand representations (Fig. 2-7). Anteroposterior differences in the degree of overlap were again apparent, however, especially in the two cases in which finger regions of areas 3a and 1 were injected (Fig. 2-7C). For comparison, serial photographs corresponding to the second drawing in Fig. 2-7C' are shown in Fig. 2-8. In the rostral parts of the projection fields -- about the first 3 mm of the projection -- the densest parts of the projections were shifted with respect to each other. In the caudal half of the putamen, the overlap of hot spots in the projections from areas 3a and 1 resembled that of the hot spots labeled from the foot representations of areas 3a and 3b, and from the mouth representations of

areas 3b and 1.

Relation between SI corticostriatal projections and the striosomal system

To determine whether fiber projections from SI to the striatum have a systematic relationship to striosomal boundaries, we compared sections showing transported label with serially adjoining sections showing enkephalin-like immunoreactivity to mark the striosomal system. Striosomes are difficult to demonstrate in much of the middle and mid-caudal putamen--the sector where most of the fibers from SI terminate. Nonetheless, in all of our cases, there were levels at which both striosomes and transported label were clearly visible in adjacent sections.

In no case was there any significant overlap of SI projection patches with the striosomal system. Fig. 2-9 shows some typical examples. Very sparse labeling was sometimes seen outside of the main projection patches, and, as can be seen in Fig. 2-9, some of this label was occasionally in striosomes. It is not clear whether this label represents terminals or fibers. The main projection patches, however, were never in striosomes. This preferential innervation of the extrastriosomal matrix held for all SI cortical areas and body part representations injected, and was independent of the tracer used. Even with the largest injections (monkeys 2 and 4), labeled projections from SI did not uniformly innervate the matrix, but innervated discrete regions within it.

We found no consistent relation between the position of striosomes and terminal projection clusters in the matrix. Striosomes and projection patches occasionally shared part of their boundaries, as at the arrows in Fig. 2-9B, but the arrangement shown in Fig. 2-9A, in which striosomes and projection patches did not abut each other, was more common. The spacing between striosomes and projection patches did not have any obvious periodicity.

DISCUSSION

Corticostriatal remapping

This study demonstrates that re-mapping of body part representations occurs in corticostriatal representations, and documents two striking features of this reorganization: a divergent, one-to-many mapping onto the striatum of projections from a given SI locus, and a concomitant many-to-one convergence of such projections with those from a limited number of other SI loci. These transformations characterized the corticostriatal projections from different SI areas, body part representations, and individual animals. We conclude that a systematic reshuffling of SI inputs occurs within the somatic sensory sector of the striatum, and that, as a consequence, functional categories in striatal mapping of the body may be distinct from those seen in SI cortical maps.

Divergence from a single locus in SI cortex. Despite the fact that large injections of tracer into the cortex produce patchy or fenestrated projections to the striatum, the corticostriatal projection may nonetheless have a parallel, one-to-one arrangement (Jones et al., 1977; Goldman-Rakic and Selemon, 1990). That is, if injections could be made small enough to be confined to a single functional unit in the cortex -- perhaps a single body part representation, or a single cortical column -- then the hypothesis is that only a single patch of anterograde label would be seen in the striatum. If, for instance, single body part representations in SI projected to single representations in the striatum, the multiple projection patches we saw after an injection into an SI index finger representation could be explained by spread of label into the SI thumb and third finger representations.

Five sorts of evidence suggest that this is not the case. First, even when tracer injections were contained entirely within a single body part representation such as the upper lip, the labeled projections formed more than one cluster (band)

in the striatum. Second, tracer injections centered, respectively, on the second and fifth finger representations in area 3b labeled very similar, partly superimposed sites in much of their fields of termination. This indicates that even in cases in which a single tracer injection extended across multiple body part representations, the multiple representations did not contribute to the multiple patches in the striatum. Third, the cases in which we injected paired representations in different SI areas showed that the patchy projections from the two areas also superimposed in much of their distributions and, even when they interdigitated, they were very close together. Thus spread of tracer from a single small injection site across the boundaries of these cortical areas would not in itself produce widely-distributed projection patches. Fourth, the smallest cortical injections that were large enough to produce visible transport to the striatum produced patchy projections. In fact, the largest injections -- which covered up to 100 times more surface area than the smallest injections -- did not give rise to a proportional increase in the number of projection patches, although they did produce somewhat larger patches. Finally, the corticostriatal axon morphology seen in this and other studies (DiFiglia et al., 1978) indicates that corticostriatal axons innervating the matrix do not terminate on single sites in the striatum, but have widely-distributed synapses. Thus, although our experiments do not settle whether a single cortical column can project divergently to the striatum, they indicate that single cortical body part representations do.

Convergence on a single locus in the striatum. The extent to which information from different cortical areas is combined in the striatum and subsequent nuclei of the basal ganglia has been extensively discussed (Alexander and Crutcher, 1990; Goldman-Rakic and Selemon, 1990; Percheron and Filion, 1990). Our results support the view that, at least within the sensorimotor sector of the striatum, inputs representing different somatic sensory submodalities can converge. This convergence is systematic in that projections from homologous body part representations in different areas and from nearby representations within a single area converge substantially, whereas SI projections unrelated in

these ways do not converge. Moreover, the relative precision with which labeled fiber clusters from related areas of SI lined up in serial-section comparisons, and the consistent similarity in number and pattern between the projection clusters, make it likely that the anatomical overlap is regulated. The precision and specificity of the inputs to a given set of patches, such as the "hand" set, suggests that the modules are real entities, and probably functional units.

It is particularly interesting that somatosensory inputs with separate representations in the cortex, for instance the muscle spindle inputs to area 3a and the cutaneous inputs to area 3b, project to the same striatal patchworks. If different patches within the striatal hand representation do have different physiological characteristics, it is unlikely that these simply reflect the differences between the different cortical body maps.

Our results also indicate, however, that the corticostriatal projections from related parts of SI do not overlap completely. In the anterior putamen of some cases (chiefly monkeys 14, 15, and 16) the zones of densest labeling by the two tracers were shifted with respect to each other, even though *in toto* the two distributions overlapped. The offset of hot spots from area 3a and area 1 is similar to, but less extensive than that of SI and area 3a projection patches in the cat's striatum (Malach and Graybiel, 1986). In the cat, as in the primate, a single pair of corticostriatal projections may both overlap and interdigitate, depending on the region of the striatum. More than one remapping pattern may thus hold for homologous body-part representations in the striatum of both species. In the zones of overlap, the degree of functional segregation would depend on the precise synaptic arrangements present. Functional segregation might also be increased by the effects of lateral inhibition (Groves, 1983), as it is in somatosensory cortex (Hicks and Dykes, 1983).

It was striking that the lack of convergence from related cortical loci, like the divergence of projections traced from single cortical loci, was most pronounced in the anterior parts of the projection fields. The SI projections to the anterior putamen formed scattered clusters that did not fully overlap projections from

homologous regions, whereas farther caudally they formed projection bands which fully overlapped. Either the grain of somatotopic mapping is not uniform along the anteroposterior dimension of the somatosensory sector of the putamen, or there are representations at its anterior and posterior ends. As we will describe elsewhere, anterior and posterior regions of the squirrel monkey putamen also differ neurochemically. It should be noted that the cases in which there was lack of convergence in the anterior putamen all happened to be cases in which cortex representing the hand was injected, raising the possibility that antero-posterior differences in convergence could be specific to this body part.

Organization of the striatal matrix

Our observations establish that projections from functionally-related parts of areas 3a, 3b, and 1 not only innervate the extrastriosomal matrix of the putamen, they form discrete zones within it. Of interest here is the evidence for clusters in the primate putamen of other input fiber-clusters (Alexander et al., 1988; DeLong et al., 1988; Fotuhi et al., 1989), output cell-clusters (Desban et al., 1989; Jiménez-Castellanos and Graybiel, 1989c; Giménez-Amaya and Graybiel, 1990; Giménez-Amaya and Graybiel, 1991; Selemon and Goldman-Rakic, 1990), and clusters with similar physiological properties (Crutcher and DeLong, 1984; Alexander and DeLong, 1985a; Liles and Updyke, 1985; Brown et al., 1987). If these clusters of input, output, and physiological characteristics are related in a systematic way, the patchwork of corticostriatal input described here could indeed form a discrete sensorimotor input-output processing system within the matrix. In fact, although corticostriatal projections have often been described as forming rostrocaudal tubes in the striatum (DeLong and Georgopoulos, 1981), our evidence suggests that the somatic sensory projections are nearly as wide as they are long, and that they form patches and branching bands that are precisely the forms noted in the organization of output neurons in the squirrel monkey's putamen (Giménez-Amaya and Graybiel, 1991). The similarity favors the

possibility that the matrix clustering underlies formation of input–output assemblies and thus potential processing units.

The functional role of the striatal body map.

Our results do not establish whether there is a single, fragmented body map in the striatal matrix, or whether there are functionally distinct, multiple maps. The multiple regions in the striatum that receive input from the SI hand area might function as a unit, forming a single -- if interrupted -- striatal hand area. On the other hand, if the regions have different physiological roles or input–output connections, they might function as multiple hand representations in a way analogous to (but clearly not identical to) the multiple hand representations within SI. The hints of anteroposterior differences in patchiness and convergence, discussed above, may indicate more than one type of mapping along the length of the striatum, although there does not appear to be an abrupt border between different striatal domains.

With respect to the patchiness of the SI corticostriatal projection, our findings do provide evidence against certain types of functional subdivisions. First, they indicate that different SI projection clusters/bands in the striatum do not uniquely represent single small body parts. Individual projection patches receive convergent inputs from nearby body part representations, at least judging from our evidence for different finger representations of the same hand. Second, our findings suggest that different SI projection patches do not uniquely represent different submodalities of somatic sensation. The convergence in the putamen, especially posteriorly, of projections from different SI cortical maps with different receptive field properties shows that the striatal body map does not make the same distinctions between submodalities, at least on a macroscopic scale, as different SI cortical areas do.

This evidence for recombination of cutaneous and deep inputs, together with physiological evidence that most striatal cells with somatosensory responsiveness

respond to movement around a joint, and that only a very few have cutaneous receptive fields, suggests a third possible functional organization of the striatal body map: perhaps the cutaneous input could undergo reorganization according to muscle or joint domains. This would also make sense of our evidence that corticostriatal projections from cutaneous representations of the fingers converge with each other but are segregated from face inputs: information about regions that tend to move together could be combined in the striatum, whereas inputs representing regions that do not could be kept separate.

TABLES

Table 2-1. Injection sites.

	HRP-WGA injection			^{35}S-met. injection			Inj. site	
Case	area	RF	diam.	area	RF	diam.	overlap	Figure nos.
2	SI	hand	6.1	SI	fingers	3.6	partial	2-4
4	3b	fingers	2.5	3a	fingers	3.3	partial	
5	3b	finger 3	1.7	3b	finger 2	0	none	
6	1	upper lip	0	1	palm	1.2	none	
7	1	lower lip	2.2	3b	lower lip	2.7	partial	
8	3b	lower lip	2.0	1	lower lip	2.0	partial	
9	1	upper lip	1.4	3b	upper lip	1.3	none	2-1, 2-7B
10	1	upper lip	2.1	3b	upper lip	1.9	none	
14	1	fingers	1.9	3a	fingers	1.6	none	2-9A
15	1	fingers	1.8	3a	fingers	1.2	none	2-3, 2-7C,
16	3b	finger 1	2.4	3b	finger 5	2.0	none	2-8
17	3b	lips	1.6	3b	finger 2	1.2	none	2-6
18	3b	toes 2-3	1.8	3a	toes 2-3	1.2	none	2-5
19	☼			3b	finger 3	0.9	complete	2-7A, 2-9B
23L	--			3b	foot sole	0.6	--	2-2
28R	--			1	toes 2-3	0.7	--	2-4

Table 1 footnotes

☼ S19 had no HRP-WGA injection, but had a PHAL injection (diam. ca. 1.8 mm) at the same site as the ^{35}S-methionine injection (area 3b, finger 3).

Area = Brodmann area of cortex at the injection site. RF = principle receptive fields of the cortex at the injection site. Diam. = diameter of the injection site at layer V of cortex, in mm. Overlap = degree to which the two injection sites impinged on each other.

FIGURES

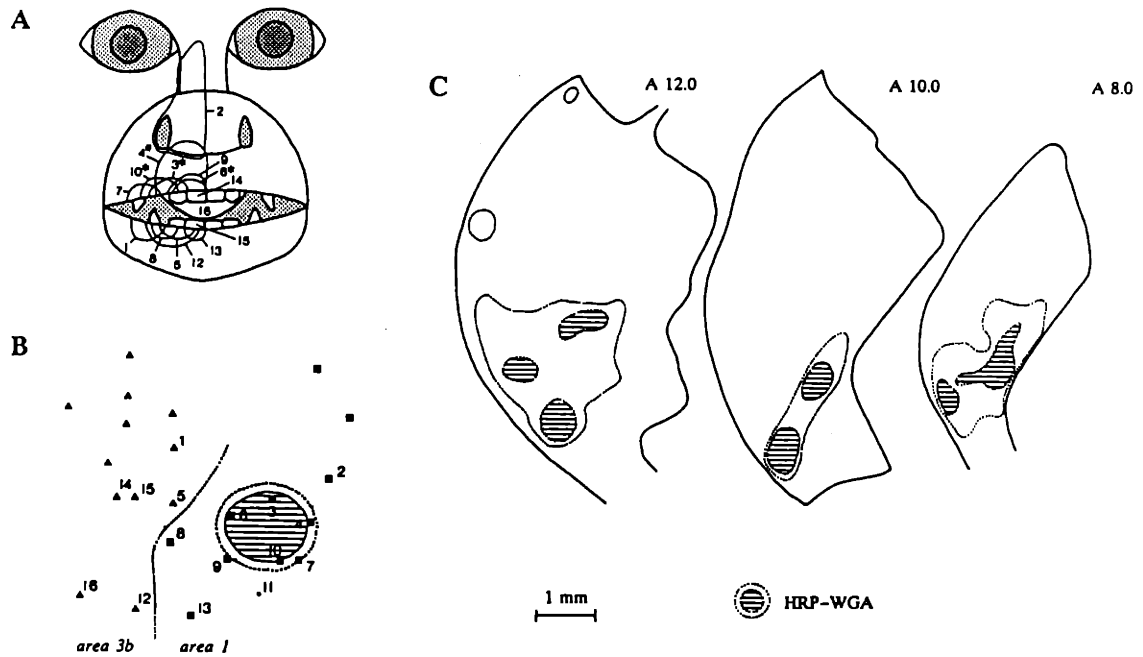

Fig. 2–1. Patches of corticostriatal fibers labeled by an injection of HRP-WGA confined to the upper lip region in area 1. (Case S9) **A.** Receptive fields for the SI cortical recording sites shown in Fig. 2–1B are indicated by corresponding numbers. Asterisks mark the receptive fields of cortex within the injection site. All receptive fields shown were cutaneous. **B.** Cortical recording map illustrating the extent of HRP-WGA labeling in cortical layer V at the injection site. Hatching shows dense labeling; dotted outline encloses more weakly labeled periphery. Recording sites in area 1 are marked by squares (■), sites in area 3b by filled triangles (▲), sites in area 3a by filled circles (●), and dots (.) indicate sites for which the cortical area was not identified. The numbered recording sites had the receptive fields shown in Fig. 2–1A. The receptive fields of unnumbered sites are given in Fig. 2–7B, which also shows the ^{35}S-methionine injection site placed in area 3b in this brain. **C.** Distribution of anterograde labeling in three cross-sections through the putamen. Atlas coordinates are indicated above sections. Multiple projection "hot spots" are present even though the tracer was deposited at a single site contained within a single body part representation. The scale bar applies to both Figs. 2–1B and 1C.

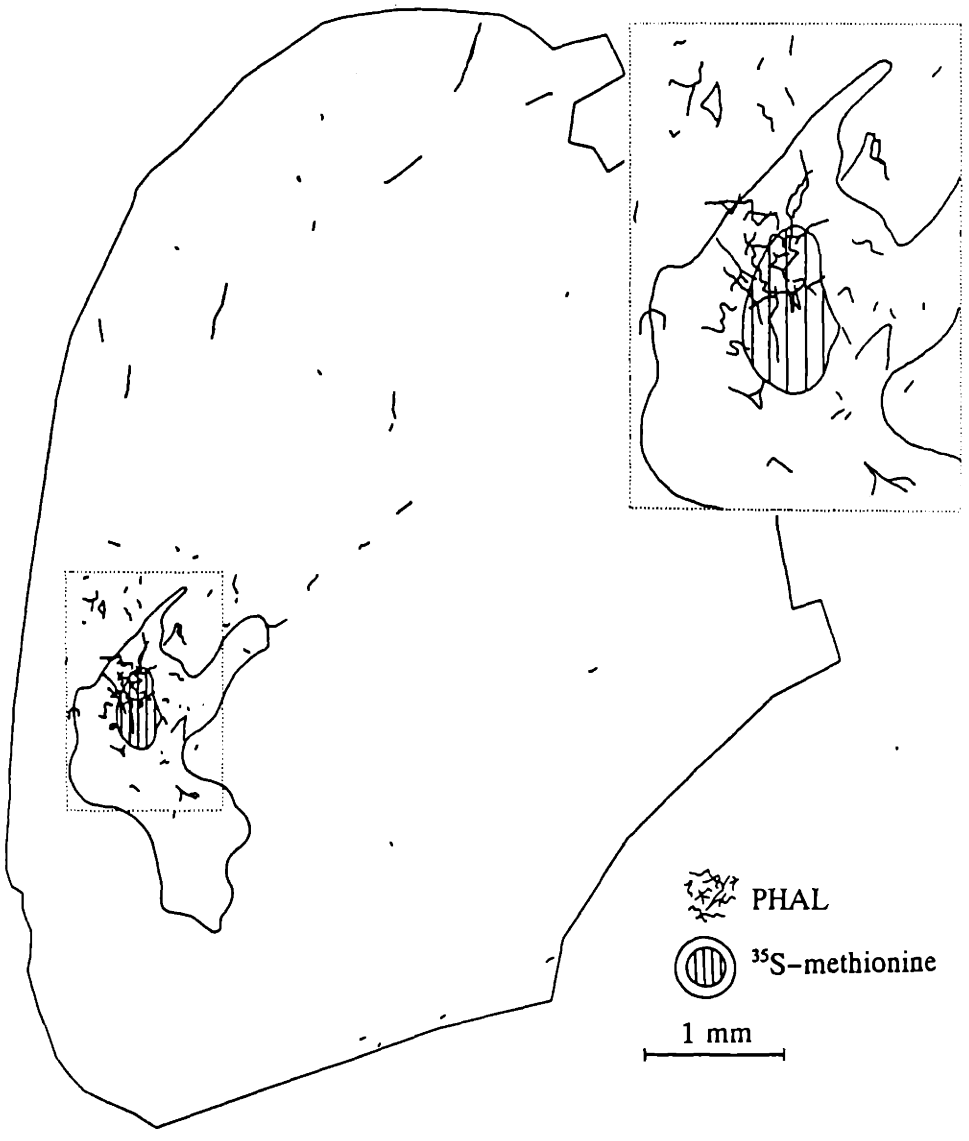

Fig. 2-2. A patch of corticostriatal fibers in the putamen labeled by PHAL and ^{35}S-methionine deposited at the same site in area 3b. (Case S19) Both tracers were deposited at the representation of the third finger. PHAL-labeled fibers were plotted at 20x using Biocom software on a computer coupled to a microscope, and a serial section demonstrating ^{35}S-methionine was projected onto the PHAL plot and charted. Scale bar = 1 mm; inset shows a two-fold enlargement of the main projection site.

Fig. 2–3. Patchwork of corticostriatal fibers labeled by a single tracer injection in area 3a. (Case S15) Reverse–contrast photos of three coronal sections taken at 3.5 mm intervals through the putamen, showing ^{35}S–methionine transported from an injection at the finger representation of area 3a. **A.** illustrates the multiple patches characteristic of the projection from SI to the rostral putamen. **B.** shows the branching diagonal bands characteristic of the projections to the middle of the putamen. **C.** illustrates the large region of labeling characteristic of the caudal putamen. The borders of the putamen are indicated by white outlines. P – putamen, CN – caudate nucleus. Scale bar = 1 mm.

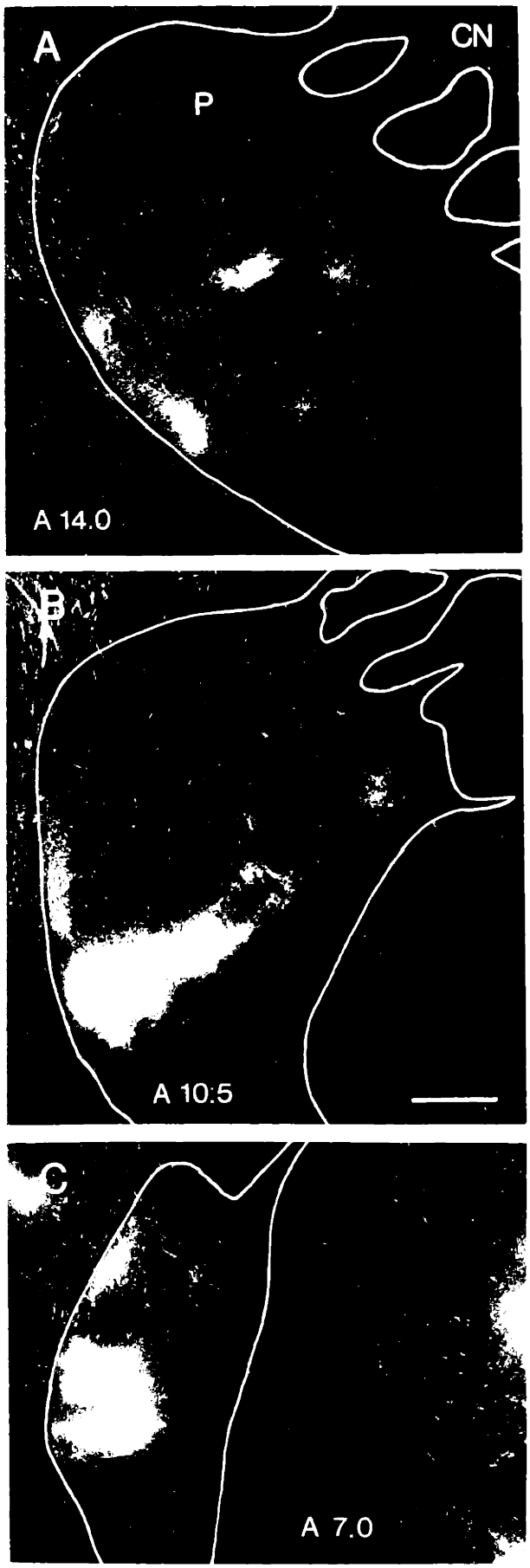
A
CN
P
A 14.0
B
A 10.5
C
A 7.0

Fig. 2–4. Corticostriatal projections labeled by small and large injection sites in SI to the striatum. **A.** and **B.** show reverse-contrast photographs of projection fields in the putamen at the level at which they were most patchy. **A.** Case S2, with an HRP-WGA-labeled injection site in SI of approximately 36 mm^2. **B.** Case S23L, with a methionine-labeled injection site of approximately 0.25 mm^2. Although a much greater amount of striatum was labeled in the cases with large injections, the number and distribution of labeled hot spots was similar to those in cases with small injections. Scale bar = 1 mm.

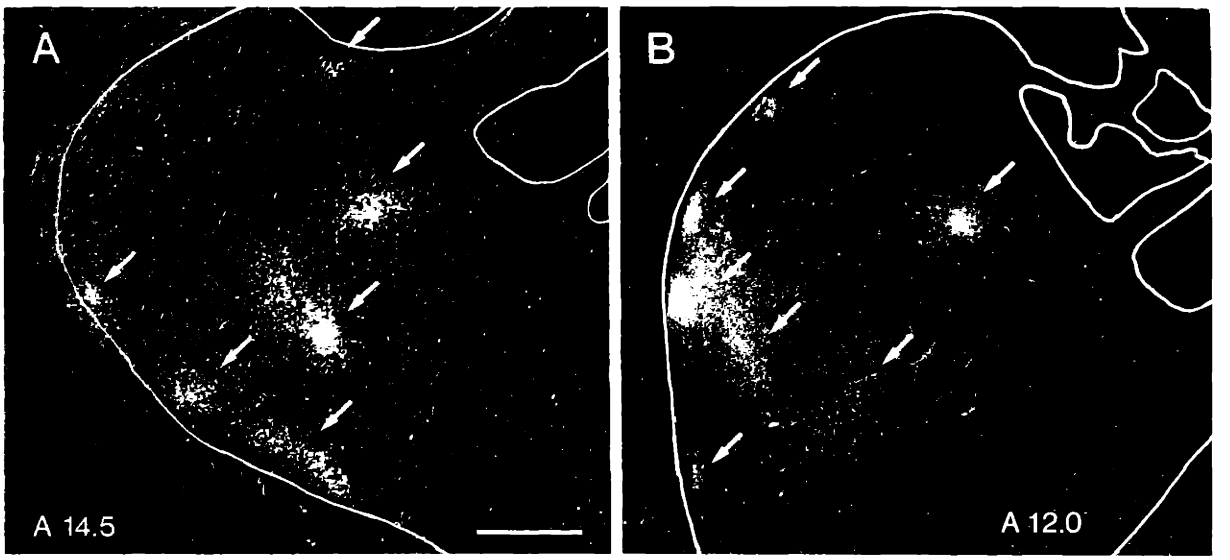
A
A 14.5
B
A 12.0

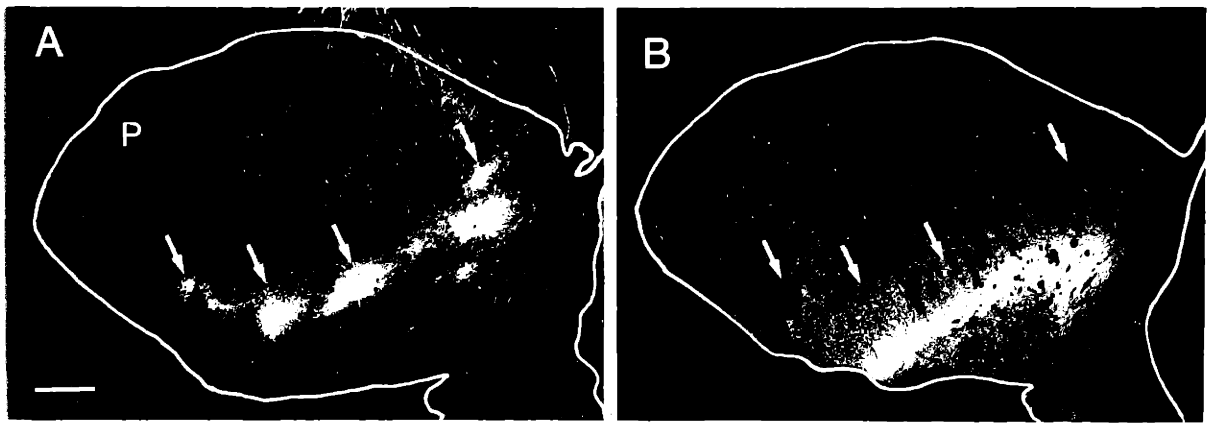
A
P
B

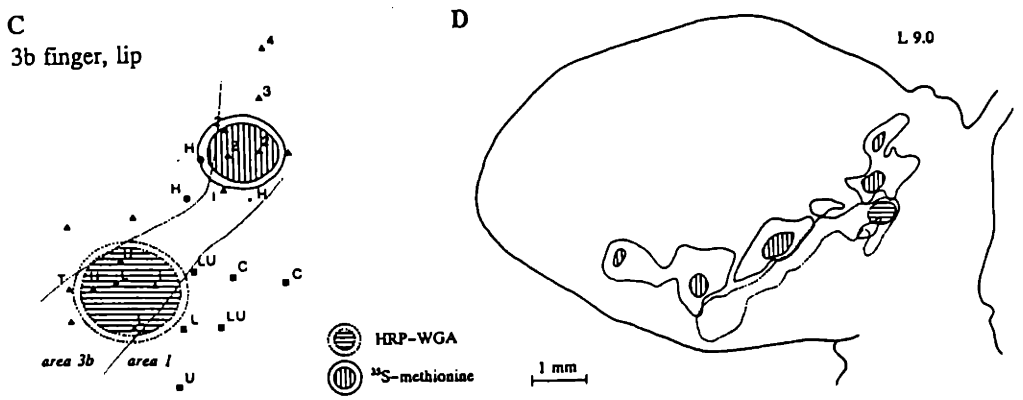

Fig. 2-5. Non-overlap of corticostriatal projections from two unrelated body part representations in the same SI cortical area. Case S17, in which cortex at the finger and lip representations in area 3b was injected. **A.** and **B.** are reverse-contrast photographs of adjacent sagittal sections through the putamen. **A.** shows ^{35}S-methionine-labeled projections putamen from the second finger representation. P - putamen. Scale bar = 1 mm. **B.** shows HRP-WGA-labeled projections from the lip representation. Arrows mark corresponding points in the two sections. **C.** A cortical recording map illustrating the extents of the HRP-WGA and ^{35}S-methionine injection sites. Recording sites in area 1 are marked by squares (■), sites in area 3b by filled triangles (▲), and sites in area 3a by filled circles (●). Dots (·) indicate sites at which the cortical area was not identified, and open triangles (△) indicate sites at which no somatosensory response was identified. Receptive fields for each recording site are indicated by labels. 1 - 5 = first through fifth fingers, H = whole hand, U = upper lip, L = lower lip, LU = upper and lower lips (mouth corner), C = chin, T = teeth. **D.** Overlay chartings of the serial sections shown in Figs. 2-5A and 2-5B. Projections from the second finger and lip areas are directly adjacent, but do not overlap substantially. The scale bar and hatching conventions apply to both Fig. 2-5B and 2-5C. Hatched areas mark the hot spots of densest label; fainter label is outlined by dotted or thin solid line.

Fig. 2–6. Partial overlap of projections to the striatum from two related body part representations in the same SI cortical area. Case S16, in which two separate finger representations in area 3b were injected. **A**. A cortical recording map showing the extents of the HRP–WGA and ^{35}S–methionine injection sites. Recording sites in area 1 are marked by squares (■); sites in area 3b by filled triangles (▲); sites in area 3a by filled circles (●); sites for which the cortical area was not identified, by dots (•); and sites for which no somatosensory response was identified, by open triangles (△). Receptive fields for each recording site are indicated by labels. 1 – 5 = first through fifth fingers, D = multiple digits, P = palm. **A'**. Three overlay chartings of cross–sections at different anteroposterior levels, indicated by atlas coordinates. Although the distribution of each label (indicated by outlines) was substantial at all levels of the putamen, the overlap of the labeled hot spots (indicated by hatches) was substantial only in the caudal putamen. The scale bar and hatching conventions apply to both Fig. 2–6A and 2–6A'.

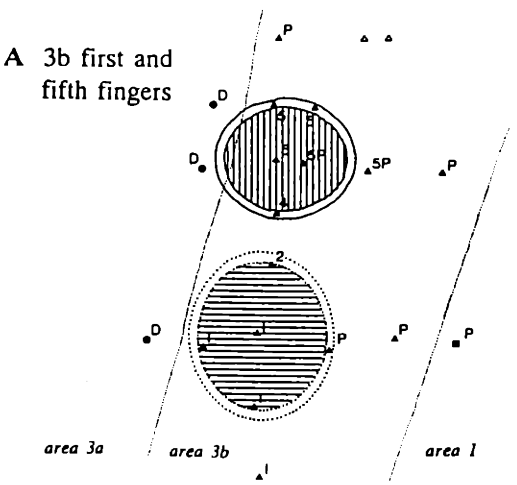
A 3b first and fifth fingers
P
D
5P
area 3a
area 3b
area 1

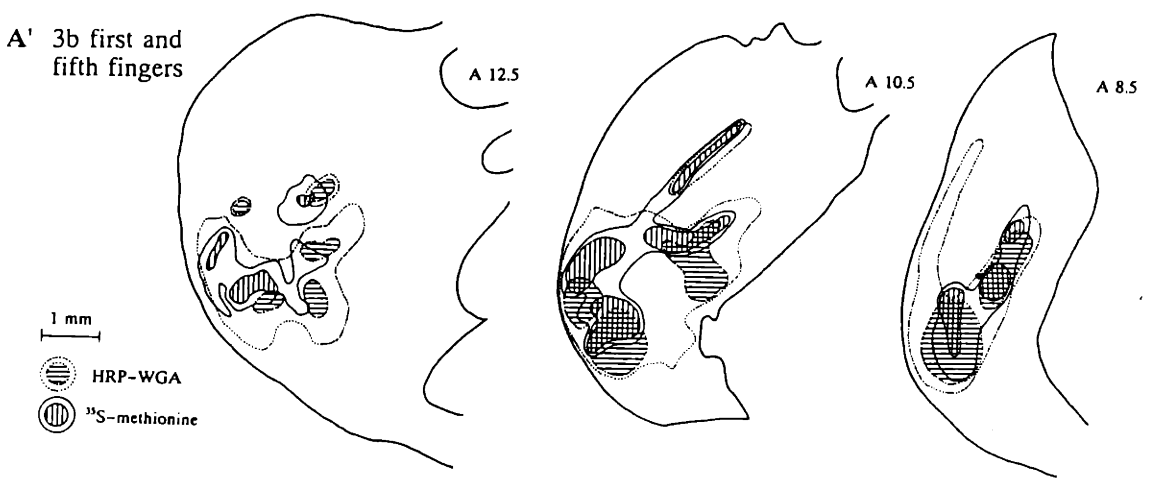
A' 3b first and fifth fingers
A 12.5
A 10.5
A 8.5
1 mm
HRP-WGA
35S-methionine

Fig. 2–7. Overlap of projections to the striatum from the same representations in different cortical maps. Projections from areas 3a, 3b, and 1, and from the foot, mouth, and hand representations, are shown. **A–C.** Cortical recording maps for three cases, showing the extents of the HRP–WGA and ^{35}S–methionine injection sites. ■ = recording sites in area 1; ▲ = sites in area 3b; ● = sites in area 3a; • = unidentified response; Δ = no somatosensory response was identified. Receptive fields for each recording are indicated by labels. 1 – 5 = first through fifth digits (in Fig. 2–7A, the digits are toes, but in Fig. 2–7C, the digits are fingers), D = multiple digits, P = palm, H = whole hand S = foot sole, L = lower lip, U = upper lip, N = nose, C = chin, T = teeth, To = tongue. **A'–C'.** Overlay chartings of cross–sections at different anteroposterior levels for three cases. **A.** (Case S18) Injections in the toe representations in areas 3a and 3b. Both the hot spots (hatched) and overall extent of labeled projections (outlined) overlapped almost completely. **B.** (Case S9) Injections in the upper lip representations of areas 3b and 1. Both the hot spots and overall extent of labeled projections overlapped almost completely. **C.** (Case S15) Injections were made at the finger representations of areas 3a and 1. The overall extent of each label (outlined) was substantial at all levels of the putamen, but the overlap of the labeled hot spots (hatched) was substantial only in the caudal putamen. Photographs from which the second overlay charting of the series was made are shown in Fig. 2–8.

A 3a–3b foot

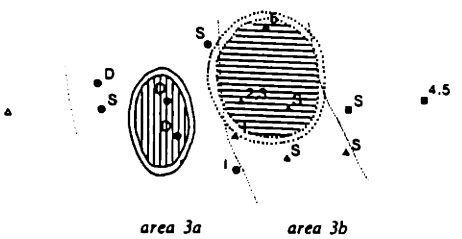

B 3b–1 mouth

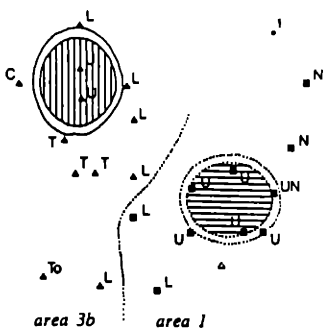

C 3a–1 hand

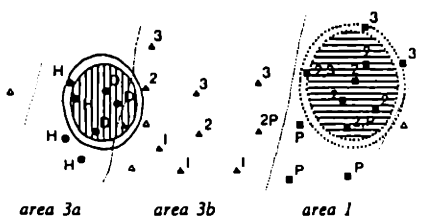

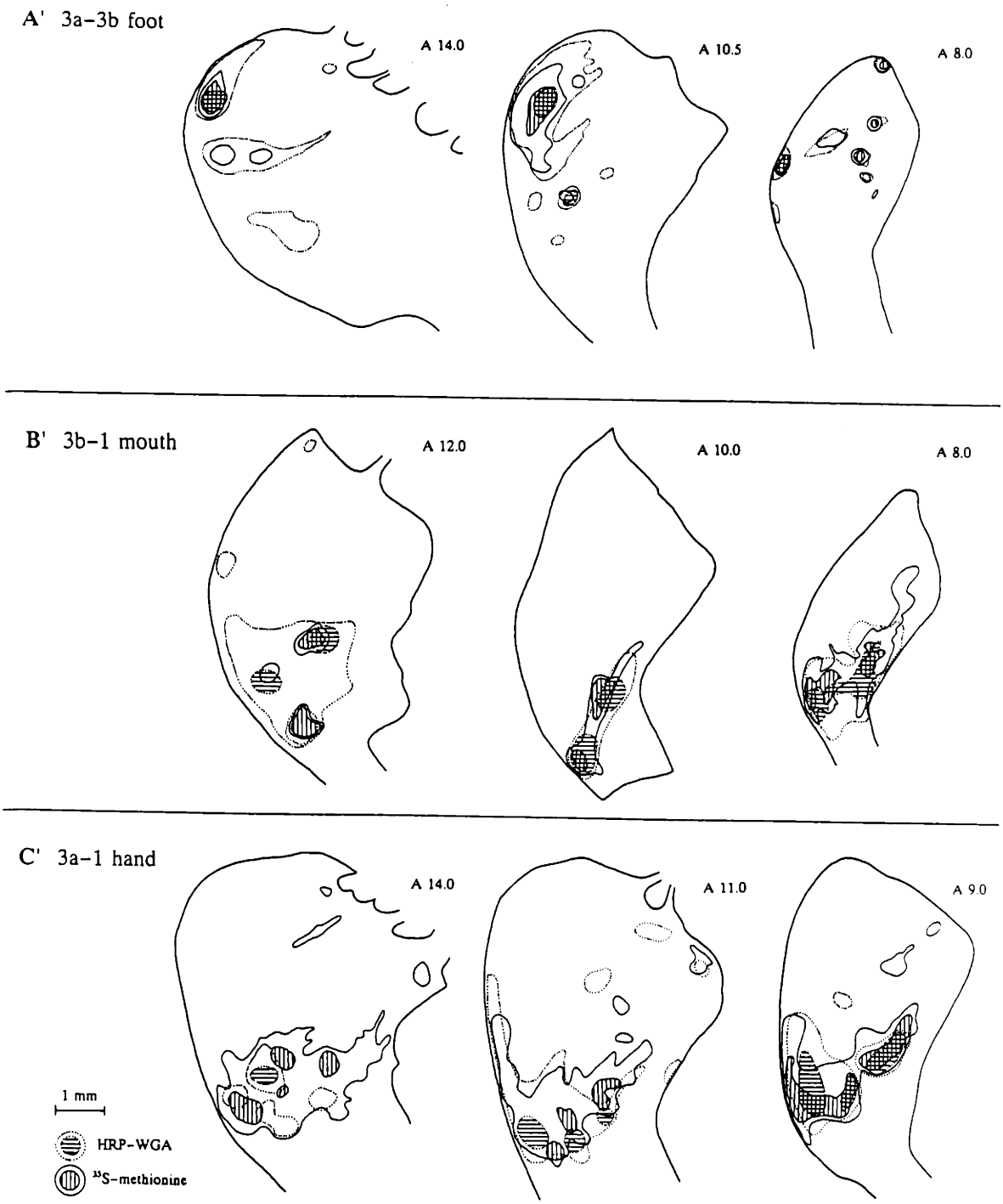
A' 3a–3b foot
A 14.0
A 10.5
A 8.0
B' 3b–1 mouth
A 12.0
A 10.0
A 8.0
C' 3a–1 hand
A 14.0
A 11.0
A 9.0
1 mm
HRP-WGA
35S-methionine

Fig. 2–8. Corticostriatal projections from the same body part representations in cortical areas 3a and 1. Reverse-contrast photographs of serial cross-sections from case S15. The two labeled fiber projections were distributed within overlapping regions in the putamen, but at the anteroposterior level illustrated, the spots of densest labeling did not overlap. The labeling shown in the two photographs is depicted as the second overlay charting in Fig. 2–7C'. **A.** ^{35}S-methionine-labeled projection from the finger representation in area 3a. **B.** HRP-WGA-labeled projection to the putamen from the finger representation in area 1. Asterisks mark corresponding points in the two sections. P – putamen, CN – caudate nucleus. Scale bar = 1 mm.

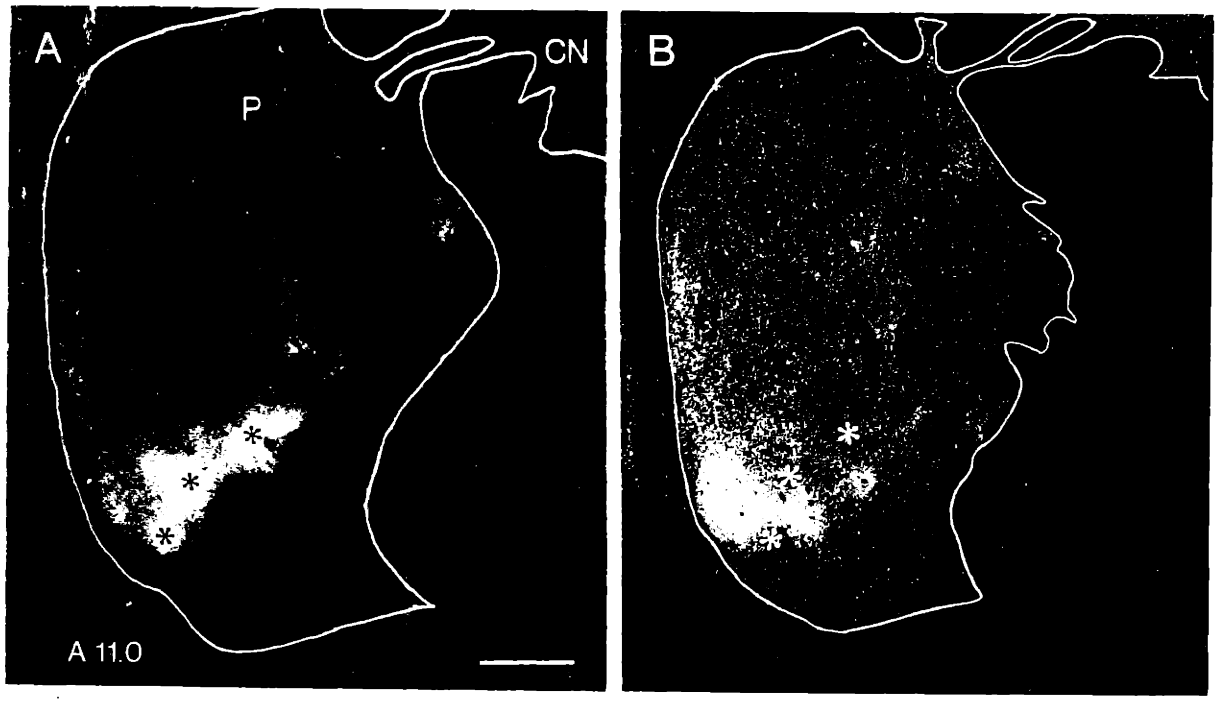
A
CN
P
A 11.0
B

Fig. 2–9. Relation of the SI cortical projections to striosomes. The labeled projection patches predominantly avoided striosomes, and innervated discrete regions within the matrix. **A–B.** Met–enkephalin immunostaining in the putamen of case S14 (A) and case S18 (B). The striosomes appear as zones of very weak staining. **A'**. A section serial to that in Fig. 2–9A, showing methionine–labeled projections from the finger representation of area 1. **B'**. A section serial to that in Fig. 2–9B, showing HRP–WGA–labeled projection from the toe representation of area 3b. Asterisks mark examples of corresponding striosomes in A and A', and in B and B'. The projection patches are at variable distances from the nearest striosome. Arrows mark a place, rare in the case material, where striosomes and SI projection patches share a common border. Scale bar = 1 mm.

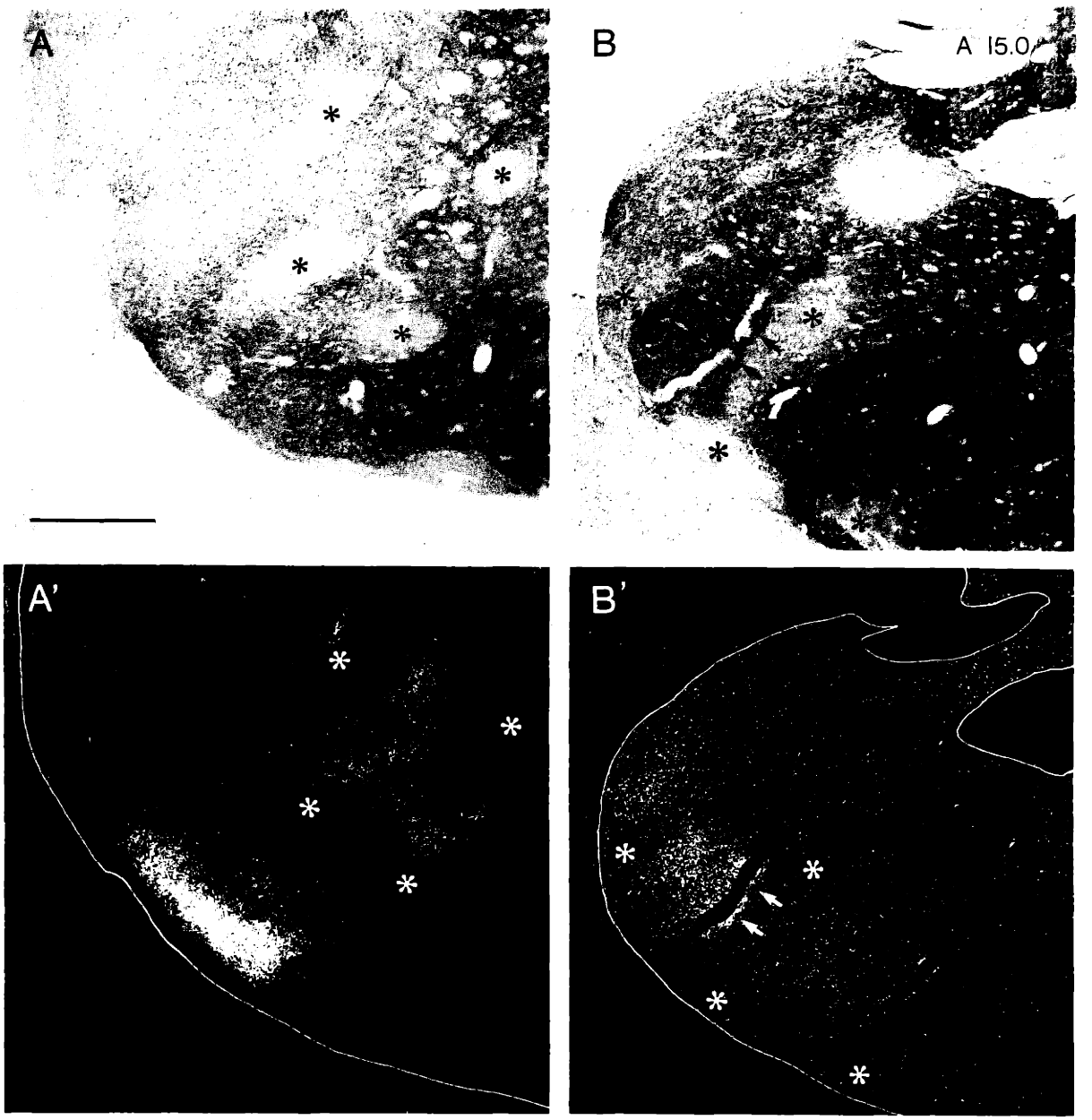
A
A
B
A 15.0
A'
B'

CHAPTER 3. TWO INPUT SYSTEMS FOR BODY REPRESENTATIONS IN THE PRIMATE STRIATAL MATRIX

Étrange paradoxe qui veut que l'homme de son côté soit appelé non un bimane, mais un bipède.... Ainsi donc si l'homme doit une bonne part de son humanité à ses deux mains, ce serait pour lui tomber au niveau du singe, si un caprice de la nature le dotait de deux autres mains à la place de ses pieds. Des mains donc... mais point trop n'en faut!

(It is a strange paradox that man is not called a *biman* but a *biped*. Thus although man owes a good part of his humanity to his two hands, it would bring him down to the level of monkeys if a caprice of nature had given him two more hands in the place of feet. Hands then... but not too many.)

- Michel Tournier, *Petites Proses* (1986)

ABSTRACT

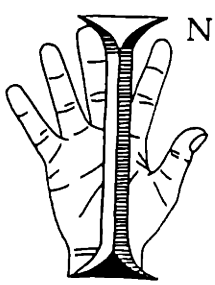

IN THIS STUDY we demonstrate the existence of two distinct sensorimotor cortical input systems to the primate striatum. The first is a series of discrete zones in the extrastriosomal matrix of the putamen ("matrisomes") that receive somatotopically organized projections that from both the body map in ipsilateral primary motor cortex (MI) and maps in ipsilateral primary somatosensory cortex (SI). The second system comprises matrisomes, in largely different locations, that receive somatotopically-organized inputs from contralateral MI but not SI.

Intracortical microstimulation and multiunit recording were used to guide deposits of multiple anterograde tracers in MI and SI, and striosome/matrix architecture was demonstrated by enkephalin immunohistochemistry. We found that inputs from regions of ipsilateral MI and SI that represented the same body parts sent projections to the same matrisomes of the ipsilateral putamen. Contralateral MI sent its strongest inputs to matrisomes that tended to interdigitate with

those receiving inputs from ipsilateral SI and MI, except the contralateral MI face region, which sent projections that instead overlapped those from the ipsilateral MI face region. MI regions representing axial body parts (trunk and face) sent stronger representations to the contralateral putamen than did those representing distal parts (hand and foot). SI sent no contralateral projection. Thus, with the exception of the face representation, inputs representing the contralateral and ipsilateral body may alternate in the primate striatal matrix, an arrangement reminiscent of the alternating ocular dominance columns in visual cortex. Ipsilateral SI and MI, and contralateral MI all innervated matrisomes intermingled with striosomes and also intermingled with matrisomes not receiving sensorimotor cortical input. The patchiness of these maps is thus unlike the smoother somatotopic maps of sensorimotor cortex, and is also unlike the fractured somatotopy reported for the cerebellum.

INTRODUCTION

To understand the differences between the way the cerebral cortex and basal ganglia control movement, it has been useful to compare their motor and somatosensory representations of the body (Crutcher and Alexander, 1990; Mink and Thach, 1991c). In this study we focused on the map transformations that occur when information about the body is sent from the cortex to the striatum. Electrophysiological and anatomical experiments have shown that the representation of the contralateral body in the primate putamen is unlike its representations in primary somatosensory and motor cortex in being distinctly patchy. Microexcitable zones and input zones for corticostriatal projections are surrounded by tissue thought to be without strong sensorimotor input (Künzle, 1975; Künzle, 1978; Crutcher and DeLong, 1984; Alexander and DeLong, 1985a; Liles and Updyke, 1985). Although there has been continuing debate about the extent to which inputs from different areas of cerebral cortex are integrated at successive stages within the basal ganglia (Percheron and Filion, 1990), there is

now evidence for anatomical convergence in the putamen of somatotopically related inputs from SI cortical areas with different somatosensory submodalities (Flaherty and Graybiel, 1991a).

It is not obvious *a priori* whether MI projections also converge with the SI projections, because, aside from their grossly equivalent somatotopy, body representations in MI and SI could be fundamentally different in organization and in their influence on motor control by the basal ganglia. There has been one preliminary report of the relation between ipsilateral MI and SI projections to the primate striatum (Fotuhi et al., 1989), but the body part representations of the cortical areas studied were not electrophysiologically identified. The degree to which MI and SI inputs to the putamen are somatotopically related, the relative contributions of different body part representations, and the role of the contralateral projection have not been previously studied.

Many neurochemical and anatomical distinctions between the striosomes and matrix of the striatum have been documented (Graybiel, 1990), but much less is known about the internal organization of the matrix. Yet the matrix is of particular importance to motor control by the basal ganglia: it is a target of MI and SI input, and it projects to other nuclei with movement-related activity -- the globus pallidus and substantia nigra pars reticulata. Recent work in primates has demonstrated that the somatosensory cortex projects to the striatal matrix (Flaherty and Graybiel, 1991a), but it is not known whether in primates the MI inputs are contained entirely in the extrastriosomal matrix (Koliatsos et al., 1988), and, if so, whether they fill the matrix homogeneously or interact with other, interdigitating matrix systems. In light of evidence that corticostriatal projections may be organized by cortical layer rather than cortical area, at least in the rat (Gerfen, 1989), it was important to confirm that the primate MI projects to the matrix.

Consequently, we combined electrophysiological stimulation and recording, multiple tract tracers, and immunohistochemistry to determine the relationship between striatal architecture and projections from ipsilateral and contralateral

body part representations. The following work has been reported in abstract form (Flaherty and Graybiel, 1991c).

METHODS

In 11 adult squirrel monkeys (*Saimiri sciureus*), bilateral electrophysiological maps of motor and somatosensory cortex were made to guide the placement of the anterograde tracers ^{35}S-methionine and wheatgerm agglutinin-conjugated horseradish peroxidase (WGA-HRP) into selected sites within motor and somatosensory cortex. The distributions of the tracers transported to the striatum were compared to each other, and to striosomes demonstrated by enkephalin-like immunoreactivity, in serial sections. Table 3-1 summarizes the protocols for the 11 monkeys. In the course of the experiments, distinguishable retrograde tracers were also deposited elsewhere in the brains for experiments to be reported separately.

Surgeries and histology were performed as described previously (Flaherty and Graybiel, 1991a). Briefly, each monkey was anesthetized with ketamine (10 mg/kg/hr IM) and a single initial dose of sodium pentobarbital (5 mg/kg IP), large bone and dural flaps were turned with sterile technique, the cortical surface was covered with high-viscosity silicon oil, and microelectrode penetrations were made at 500-1000 μm intervals to determine the boundaries of body part representations in cortical areas 4, 3a, 3b, and 1. The location of each cortical electrode penetration was marked on an enlarged photograph of the exposed cortex, and the stereotactic coordinate of each penetration was noted.

Multiunit neuronal activity was recorded with parylene-coated tungsten electrodes (Microprobe) with impedances of 0.8 MΩ ±15% at 1 Khz. The borders of areas 3a, 3b, and 1 were determined as described previously (Flaherty and Graybiel, 1991a). Area 4 was defined according to the criteria of Sessle and Wiesendanger (Sessle and Wiesendanger, 1982), and was mapped with standard intracortical electrical stimulation. Trains of symmetric biphasic paired pulses, 0.3

msec each, were delivered at 300 pulse-pairs/sec. Stimuli were delivered from an optically-coupled stimulus isolator (Bak BSI-2) driven by a biphasic pulse generator (Bak RP-1), through platinum-iridium microelectrodes (Microprobe) with impedances of 0.8 MΩ ±15% at 1 Khz. Current amplitude and pulse waveform were monitored intermittently on an oscilloscope by recording differentially across a 1 kΩ resistor in series with the microelectrode. Motor responses to microstimulation were considered to be present when either visible movement about a joint or visible muscle contraction occurred in a reproducible manner at a constant stimulus. If movement was detected at 100 μA, the current was gradually lowered until the threshold value was reached. If no movement was detected, currents up to 400 μA were tried briefly. As little as 3 μA was sufficient to stimulate movement in many monkeys.

At the end of the mapping session, ^{35}S-methionine (200 μCi/μl in sterile saline) and WGA-HRP (15% in sterile saline) were placed at physiologically-characterized sites in SI and MI by reference to the photographic records made during the mapping session. Tracer deposits in SI were centered in area 3b. Two types of injections were made: small deposits designed to be within a given body part representation of a single cortical area (monkeys 32, 37, and 40-42), and large injections intended to completely fill, but not exceed, most or all of the body part representations in a given area (monkeys 33-35). Post-operatively, animals were maintained on the analgesics butorphanol tartrate (0.025 mg/kg s.c., t.i.d.) or buprenorphine HCl (0.01 mg/kg s.c., b.i.d.). Two to three days after surgery, animals were perfused through the heart with 0.9% saline, then 4% paraformaldehyde in a 0.1 M phosphate-buffered 5% sucrose solution, and finally a post-wash with phosphate-buffered sucrose. Brains were blocked in a stereotaxic device, and blocks were soaked 1-3 days in 20% glycerol, frozen, and cut coronally in 40 μm sections on a sliding microtome. Adjacent sections were processed in series to compare the distributions of injected tracers and enkephalin immunoreactivity.

To demonstrate ^{35}S-methionine, slide-mounted sections were dipped in

diluted Kodak NTB-2 emulsion, stored in the dark at -20°C for 7 days to 7 months, developed in Kodak D-19, counterstained with cresylecht violet, and coverslipped. WGA-HRP reaction product was demonstrated by the tetramethyl benzidine (TMB) procedure of Mesulam (Mesulam, 1978), except that the incubation solution was changed every 3 minutes to prevent precipitation (Illing and Graybiel, 1986). For enkephalin immunohistochemistry, sections were incubated for 2 days in anti-met-enkephalin (Incstar, 1:2000 dilution), and bound antibody was labeled with the avidin-biotin peroxidase technique. Striosomes were identified as zones of low met-enkephalin-like immunoreactivity (Graybiel and Chesselet, 1984).

Sections were studied under bright- and dark-field illumination, and those stained with TMB were placed between crossed polarizers (Illing and Wassle, 1979)](Illing and Wassle, 1979). The distributions of tracers in the striatum were charted at magnifications between 10-40x with a drawing tube or with a Biocom image analyzer. Corticostriatal labeling was classified in two categories, "hot spots" of dense labeling and surrounding zones of weaker labeling. These categories were generally assigned by eye, but were occasionally checked by computerized optical density threshold analysis. Adjacent sections were aligned with reference to local blood vessels. Injection sites charted in the coronal sections were reconstructed on the cortical surface with respect to the *in vivo* electrophysiological map by reference to the tracks of the injection pipettes, electrode penetrations, stereotaxic coordinates, and sulcal patterns, as previously described (Flaherty and Graybiel, 1991a), taking into account the greater shrinkage of the TMB-stained sections. Because injections that did not penetrate to cortical layer V did not produce analyzable amounts of label in the striatum, injection site widths were measured at the level of layer V, rather than at the surface of the cortex (Flaherty and Graybiel, 1990). The locations of the tracer deposits were also mapped with respect to the distribution of the giant pyramidal cells of area 4. Anteroposterior (A-P) levels of sections were assigned according to the atlas of Gergen and McLean (Gergen and MacLean, 1962).

RESULTS

Motor and somatosensory cortex each send modular inputs to the putamen

Bilateral inputs from MI to the striatum. When large tracer deposits were made along much of the length of MI (4 hemispheres), anterograde labeling in the ipsilateral putamen filled multiple clusters and bands that appeared as discrete patches in cross-section. At the densest part of its anteroposterior extent (about A 10.0 to A 12.0), the corticostriatal projection formed a nearly-confluent "main field" of label with faint satellite zones around it (Fig. 3-1C). But even the largest of the tracer deposits in MI produced multiple discrete zones of labeling at more anterior and posterior levels of the putamen (see, for instance, Figs. 3-5B and 3-8A). Occasionally the lateral edge of the rostral caudate nucleus contained weak labeling as well.

When small tracer deposits were placed in restricted regions of MI (11 hemispheres), the clusters and bands were smaller and more discrete than those labeled by large cortical injections (Fig. 3-2B). The bands were similar in shape and location to the previously-described pattern of ipsilateral labeling following small tracer deposits in somatosensory cortex (Flaherty and Graybiel, 1991a), but when MI and SI injection sites were the same size, the MI projections tended to be larger and more densely labeled. The distributions of labeled projections in the ipsilateral putamen showed the expected rough somatotopy -- projections from the foot region tending to be most dorsal, and head most ventral.

Labeled projections from MI to the contralateral putamen appeared at approximately the same A-P levels as they did in the ipsilateral putamen, and they had a similar somatotopic organization. Contralateral inputs also resembled ipsilateral inputs in being broken into distinct zones. These were, however, smaller and fainter than those on the ipsilateral side, and their distribution was roughly the inverse of those on the ipsilateral side. For instance, the lateral edge of the putamen was often studded with discrete patches of label on the

contralateral but not on the ipsilateral side, and the zone in the central putamen that received the confluent main field of the ipsilateral projection was often free of label contralaterally (Fig. 3-1B).

Ipsilateral inputs from SI to the striatum. To compare the projections from SI to the striatum with those from ipsilateral and contralateral MI, it was necessary to confirm, for all of area 3b and adjacent SI areas, previous reports that there is no cross-projection to the primate striatum from SI cortex (Jones et al., 1977; Flaherty and Graybiel, 1991a). We therefore made an extensive tracer deposit in SI, depositing a total of 120 nl of ^{35}S-methionine in 11 spaced injections along area 3b, and labeling somatosensory cortex from the foot through the hand representations (Fig. 3-1D). The labeling produced in the ipsilateral putamen by this injection was intense (Fig. 3-1F). The contralateral putamen is shown in Fig. 3-1E. Even after a seven-month exposure of the autoradiographic slides, no transport to the contralateral putamen was visible in the foot, leg, trunk, arm, or hand regions of the putamen. By contrast, small (10 nl) injections of ^{35}S-methionine into MI produced faint labeling in the contralateral striatum after an exposure time of about 10 days.

Somatotopically-related inputs from SI and ipsilateral MI predominantly converge in the putamen.

To determine whether ipsilateral SI and MI corticostriatal projections project to the same zones in the putamen, we made both small and very large paired injections in the two cortical areas, at pairs of sites representing either the same or different body parts.

In both hemispheres of monkey 32 (32L and 32R), we made small deposits of ^{35}S-methionine and WGA-HRP at, respectively, the foot representations of area 4 and area 3b. The injection sites for 32L are shown in Fig. 3-2A. The deposits in area 3b extended into adjacent parts of area 3a, but there was little or no overlap with the injection site centered in area 4. In both hemispheres, the zones

in the putamen that were densely labeled by the two tracers overlapped extensively, and the shapes, orientation, and numbers of the projection zones were similar (Fig. 3-2B through 3-2D). The correspondence held for both the zones of dense labeling and for the surrounding haloes of diffuse labeling.

There was some danger that the ipsilateral projections from MI to the striatum in monkey 32 were augmented by faint contralateral MI projections. To minimize this possibility, we first analyzed slides in which the autoradiographic emulsion had been exposed for only 10 days, an exposure time which produced only faint contralateral labeling in other monkeys with foot region injection sites. Second, as we will describe below, the contralateral projection is largely non-congruent with the ipsilateral projection, and, if present, would only have obscured the correspondence seen here, rather than artifactually creating it. Third, in other monkeys (33 and 34, discussed below) there was no possibility of cross-projection contamination, and yet the overlap between SI and ipsilateral MI seen in these monkeys was similar to monkey 32.

To determine the degree to which this overlap between MI and SI inputs was somatotopically specific, in two monkeys (hemispheres 36L and 37L) we made small injections in the foot region of are 4 and the trunk region of area 3b (Fig. 3-3A). These non-homologous injection sites labeled projection fields in largely different regions of the putamen. However, the two sets of projection patches sometimes lay adjacent to each other or even partially overlapped (Fig. 3-3A'). Projections from cortex representing body parts even further apart in the cortical map -- the foot and the hand -- showed this same pattern of predominant but not total segregation (Fig. 3-3B').

To study the degree of overlap when larger amounts of SI and MI were labeled, in two monkeys (hemispheres 33R and 34R) we made large confluent deposits of one tracer throughout the foot, leg, trunk, arm, and hand representations of SI, and the other tracer throughout the foot and leg representation of MI of the same hemisphere (Fig. 3-4A). The larger SI injection site labeled regions in the putamen that overlapped with, but were more

extensive than, those labeled by the smaller MI injection. The overlap was somatotopically restricted: in the leg region of the ipsilateral putamen, the SI and MI projection patches overlapped, whereas in the trunk and arm regions of the putamen only SI projection patches were labeled. Fig. 3-4B shows an overlay charting of typical pairs of cross-sections.

In monkeys in which tracers were deposited in matched body part representations in MI and SI, marked exceptions to the correspondence between MI and SI input zones were rare. However, the precision of alignment of the two sets of projection patches varied. Hemispheres 32L and 33R had very close zone-for-zone correspondence whereas hemispheres 32R and 34R had labeled projection zones that were not always in exact register; they were sometimes either offset slightly from each other or interdigitated with each other. There was a rough correlation between degree of projection-field overlap in the putamen and injection site sizes: in the hemispheres with less precise overlap, the injection sites were somewhat smaller. There was also a rough correlation between degree of overlap of the projections in the putamen and in the second somatosensory area (SII). In hemispheres 32L, 33R, and 34R, the projections from MI and SI overlapped in SII, but in 32R, they were adjacent to each other, suggesting that in 32R the MI and SI injection sites were not in perfectly matched body part representations (data not shown).

Inputs from ipsilateral and contralateral sensorimotor cortex rarely converge in the putamen.

SI and contralateral MI send inputs to predominantly different regions of the putamen.

In sharp contrast to the convergence of the ipsilateral projections from MI with those from SI, the most densely-labeled projections from contralateral MI tended to innervate zones between or next to ipsilateral SI projection zones. Typical interdigitation of SI and contralateral MI projections is shown in Fig. 3-

4C, for monkey 33. In that monkey, we injected ^{35}S-methionine throughout the foot, leg, trunk, arm, and hand representations of the left SI cortex, contralateral to a deposit of WGA-HRP filling the foot and leg MI cortex in the right hemisphere (Fig. 3-4A). The amount of overlap between the cross-projections (Fig. 3-4C) was much less than that seen between the ipsilateral projections labeled in the other hemisphere of the same monkey (Fig. 3-4B, described above). Similar results were obtained in a second monkey (34), in which the same experimental design was followed with the tracers reversed.

In both of these monkeys, the zones of the putamen densely labeled by ipsilateral SI and contralateral MI tended to be adjacent to each other, and sometimes the ipsilateral and contralateral projection zones curved around each other as if both were governed by the same boundary conditions. This proximity suggested that the lack of overlap of the hot spots was not simply the result of a wide dispersal of inputs from SI and contralateral MI. The interdigitation of the two corticostriatal projections was not, however, invariant in either monkey: in a few sections in each case, the projection zones labeled from one hemisphere overlapped the projection zones from the other hemisphere. Furthermore, in contrast to the interdigitation of the zones of dense labeling, there was weak labeling surrounding these hot spots that was not well-separated. Nonetheless, the tendency for SI and contralateral MI projection patches to avoid each other was dramatically different from the characteristic overlap of SI and ipsilateral MI projections, as can be seen in Fig. 3-4.

Ipsilateral and contralateral MI send inputs to predominantly different regions of the putamen. The results just described suggested that the corticostriatal projections from ipsilateral and contralateral MI form distinguishable input systems in the putamen. To test this conclusion directly, we injected distinguishable tracers in MI of the two hemispheres in monkey 35, filling all of MI except the face region (Fig. 3-5A). In the putamen of both hemispheres, the dense zones of labeled ipsilateral and contralateral projections from MI predominantly avoided each other. Charts of three sections through the right

putamen are shown in Fig. 3–5B. The degree of overlap for these ipsilateral and contralateral MI projections was similar to that found in the monkeys with injections of ipsilateral SI and contralateral MI. In contrast to the densely–labeled projection zones, the haloes of weak label overlapped, as in the monkeys with SI and MI injections.

Judging from the foot–dorsal, head–ventral somatotopic organization of the putamen's motor sector, the degree of overlap of the ipsilateral and contralateral MI projections did not appear to vary with the body part labeled: the leg, trunk, and arm regions showed equivalent small amounts of overlap. However, the face region of MI was not labeled in these hemispheres, and the possibility for variations by body part in this monkey could only be estimated roughly. Consequently, to make comparisons of the projections from ipsilateral and contralateral MI representing individual body parts we made small injections in single body part representations of MI in three monkeys, again using distinguishable tracers in each pair of hemispheres.

Because the foot and face regions of MI project to parts of the putamen far enough apart that their projections are easy to distinguish from each other, we could inject both regions in a single monkey by reversing the tracers used for each hemisphere. We did this in monkey 40 (Fig. 3–6), depositing WGA–HRP in the foot region and ^{35}S–methionine in the face region in the left hemisphere, and reversing the tracers in the right hemisphere. The relationship between the ipsilateral and contralateral MI projections could thus be compared independently in two different hemispheres for each of the two body parts. The foot region of MI in both hemispheres sent a cross–projection that was fainter and had a more lateral distribution in the dorsal putamen than the ipsilateral foot projection. In both hemispheres, the dense contralateral input zones predominantly avoided the zones receiving heavy inputs from the ipsilateral foot region. Fig. 3–6A' shows the results for the right hemisphere. The projections from the two MI face cortex injections, in sharp contrast, were squarely overlapping in the putamen on both sides. Fig. 3–6B' shows the results for the right hemisphere. The face region of MI

also differed from the foot region in sending relatively stronger cross-projections to the putamen.

In monkey 41 we placed different tracers in the MI trunk region of the two hemispheres (Fig. 3-7A). The regions of the putamen labeled by these injections tended to be slightly ventral to those labeled by the foot MI injections, and dorsal to the regions labeled by face MI injections (cf. Figs. 3-6A', 3-7A', and 3-6B'). The trunk region of MI sent stronger cross-projections to the putamen than did the foot region of MI. In both hemispheres the ipsilateral and contralateral MI trunk projections predominantly interdigitated, although there was some overlap along the borders of the two projections' most densely labeled zones. Thus, the MI trunk projections avoided each other as had the MI foot projections, rather than overlapping, as had the MI face projections.

Finally, we compared the inputs from the MI hand cortex of the two hemispheres (monkey 42). The regions of the putamen labeled by these injections tended to be slightly ventral to those labeled by the trunk MI injections, and dorsal to the regions labeled by face MI injections (cf. Figs. 3-7A', 3-7B', and 3-6B'). A few projection zones were far dorsal to the main hand projection zone (Fig. 3-7B). The ipsilateral and contralateral hand MI projections had a relation to each other that was similar to the projections from foot MI: they innervated different zones in the putamen, and the cross-projection was significantly weaker than the ipsilateral one.

MI innervates discrete zones in the matrix.

In the mid-caudal putamen of the primate -- the sector where most of the corticostriatal fibers from SI and MI terminate -- striosomes are relatively scarce or difficult to demonstrate. Farther rostrally, however, both striosomes and labeled corticostriatal inputs were clearly visible. For all levels at which both striosomes and projection zones were present, both ipsilateral and contralateral MI projected predominantly to the extrastriosomal matrix (Fig. 3-8). This

preferential targeting of the matrix held not only for hemispheres with relatively small tracer injections in foot, trunk, hand, and face MI, but also for hemispheres in which large tracer deposits filled most of MI. There were occasional exceptions in which small projection zones from motor cortex overlapped striosomes. Such exceptions were more frequent for the contralateral than for the ipsilateral MI projection (see Fig. 3-8). The SI projection to the putamen, as reported previously (Flaherty and Graybiel, 1991a), was also directed predominantly towards the matrix.

Even when MI was labeled heavily along most of its length, the labeled systems of zones within the matrix did not fill the matrix completely. Patchiness was most apparent at the borders of the projection, but was apparent at all rostrocaudal levels. Even in the main field of the MI projection (about A 10.0 to A 12.0), the matrix was not uniformly labeled. Similarly, when SI was similarly injected with tracer, the labeled corticostriatal projection also did not completely fill the matrix within its target zone. We therefore tested the possibility that the remainder of the matrix in the sensorimotor sector of the putamen might be filled in by the projection of contralateral MI project to non-overlapping parts of the matrix. We compared closely spaced triplets of sections for the relative distributions of ipsilateral MI projections, contralateral MI projections, and striosomes in the putamen. Even when ipsilateral and contralateral motor cortical projections were combined, there were still regions within the sensorimotor termination zones of the matrix which were not heavily labeled. Fig. 3-9 illustrates this point with an overlay drawing of the triplet of cross-sections photographed in Fig. 3-8A through 3-8C, in which the most intense fields of labeling are charted along with striosomes.

DISCUSSION

These experiments demonstrate the existence of two sets of motor cortical input zones within the matrix of the primate striatum (Fig. 3-10). The first

receives somatotopically-matched, largely convergent inputs from ipsilateral MI and SI. The second receives inputs from contralateral MI. Both sets of zones are distinctly modular, and -- with the apparent exception of those in the face region of the putamen -- the two sets are most often non-overlapping. Our results suggest 1) the putamen does not segregate motor and somatosensory information about the same side of the body as much as it segregates information about the ipsilateral and contralateral body. 2) The putamen receives more contralateral information about axial body parts than distal ones. 3) Matrisomes receiving motor and somatosensory information about a given body part are positioned so that they can interact along their borders with striosomes, with matrisomes receiving information from nearby ipsilateral body parts, with matrisomes receiving information from the contralateral body part, and with other matrisomal systems with unknown inputs. The sensorimotor input map in the putamen is thus considerably patchier than that seen in other central nervous system representations of the body.

Organization of the matrix in the sensorimotor region of the putamen

In a previous study we demonstrated that small tracer injections in electrophysiologically-identified SI cortex innervate discrete zones within the matrix of the putamen, rather than innervating the matrix uniformly (Flaherty and Graybiel, 1991a). What innervated the adjacent regions of matrix was not identified. We show here that the matrix inputs are patchy even when labeled by extensive injections in SI cortex, as is true also in the cat (Malach and Graybiel, 1986). Ipsilateral MI does not innervate the adjacent matrix; it innervates approximately the same zones as SI does. The projections labeled by injection sites filling all of SI or MI were less patchy in the center or main field of the projection than in more peripheral parts of the projection field, and contralateral MI innervates some matrix regions adjacent to the ipsilateral MI input zones. But even in monkeys in which very large deposits of tracer were placed in MI of both

hemispheres, there were still zones of matrix in the sensorimotor part of the putamen in which little labeling appeared. Our findings thus not only establish the presences of at least two sets of inputs to matrix modules or "matrisomes" (Graybiel et al., 1991) in the sensorimotor sector of the primate putamen, but also suggest there may be other sets of matrisomes there as well.

It is often assumed that MI projects to the matrix in the primate putamen, as it does in the rat (Donoghue and Herkenham, 1986). The present study provides direct evidence for this assumption. At all levels of the striatum at which both striosomes and MI projections were visible, both ipsilateral and contralateral motor cortex projections predominantly avoided striosomes. There were occasional exceptions to this rule, more often in the contralateral than in the ipsilateral projection. However, most of the inputs to the putamen from MI on both sides terminated in discrete zones outside striosomes.

The existence of multiple distinguishable matrisomal systems raises again the question first raised when striosomes were discovered: what is the purpose of all this patchiness in the striatum? Recent evidence suggests that the outputs of the striatal matrix are as patchy as its inputs (Desban et al., 1989; Jiménez-Castellanos and Graybiel, 1989a; Giménez-Amaya and Graybiel, 1990; Selemon and Goldman-Rakic, 1990). The next step in studying this mosaic, therefore, will be to determine the relations between these input and output zones.

Convergence of ipsilateral SI and MI inputs to the putamen.

We show here that SI and MI project to overlapping matrisomes in the ipsilateral putamen. Convergence of labeled SI and MI inputs was seen both in monkeys in which relatively small injections centered in one body part, and in monkeys in which much larger injection sites were made. Because the overlap occurred for the projections of all pairs of matched body representations we tested, convergence may be a general rule for all of the MI and SI projection fields. This hypothesis is consistent with the findings of Fotuhi et al. (Fotuhi et al.,

1989), who noted overlap of corticostriatal inputs from regions of MI and SI cortex injected without electrophysiological guidance. In previous work we showed that there is convergence onto the primate putamen of different SI maps: areas 3a, 3b and 1 send somatotopically-organized, largely overlapping inputs to the putamen (Flaherty and Graybiel, 1991a). Thus the evidence we present suggests that there is a set of matrisomes in the striatum that receives input from somatotopically-related parts of the four adjacent body maps in areas 4, 3a, 3b, and 1.

Three-dimensional reconstructions indicate that these matrisomes have branching, often discontinuous structures (Malach and Graybiel, 1986; Flaherty and Graybiel, 1991a). Single body part representations in the cortex thus send projections to multiple matrisomes. Electrophysiological recording experiments support the claim that the inputs carry information about the contralateral body (Crutcher and DeLong, 1984; Liles and Updyke, 1985), although in the monkey, to a greater extent than in the rat, it may be somewhat different from that sent to the spinal cord (Donoghue and Kitai, 1981; Bauswein et al., 1989). It is still unclear whether this multiplicity indicates a single, discontinuous body map in the putamen or whether each matrisome is part of a separate, functionally-differentiated body map. Like the "fractured somatotopy" described for the cerebellum (Kassel et al., 1984), the map or maps in the putamen are discontinuous in that multiple patches representing unrelated body parts are intermingled. Unlike the cerebellum, however, the putamen contains regions with sensorimotor input that are interrupted by tissue with no strong sensorimotor input (Figs. 3-4, 3-9) or responsiveness (Crutcher and DeLong, 1984; Alexander and DeLong, 1985a). In addition, there is no evidence for somatotopy within individual putamen sensorimotor zones, as there is within the fractured representations in the cerebellum.

Thus the corticostriatal projection transforms cortical body maps in at least two respects (Fig. 3-10). First, inputs from cortical areas with different sensorimotor modalities, such as the motor map of area 4, the deep receptor map of area 3a, and the cutaneous map of area 3b -- maps that are anatomically

distinct in the cortex -- project to the same regions of the putamen. Second, the relatively continuous cortical maps are reorganized into a patchy map or maps in the putamen. Patchy somatotopic representations may be more efficient than continuous ones in performing sensorimotor computations that involve non-local as well as local interactions (Nelson and Bower, 1990). These two differences, then, may reflect fundamental differences in the constraints or goals of movement control by the sensorimotor cortex and the putamen.

Although somatotopically-organized convergence was the rule for ipsilateral MI and SI inputs to the putamen, the rule was not always followed perfectly. We were interested in the nature of the exceptions, which fell into roughly three categories: lack of overlap between some projection fields from the same body part representations in different cortical maps, overlap between projections from different body part representations, and changes in degree of overlap at different A-P levels.

We considered four possible explanations of the instances of non-overlap between projections from homologous body part representations in MI and SI cortical maps. First, they could reflect our experimental techniques. Larger injection sites labeled projections that overlapped each other somewhat more than smaller ones. Second, the precision with which exactly matched body part representations were injected was also a factor. We therefore used projections from MI and SI to the second somatosensory region (SII) as an independent check of our injection site reconstructions. Because SII has somatotopically-organized connections with SI and MI (Friedman et al., 1980; Yumiya and Ghez, 1984; Mori et al., 1989), lack of overlap of labeled regions in SII indicates an imperfect match between body part representations injected in MI and SI. This was seen in only one hemisphere, 32R. Third, the occasional failure in overlap might instead have reflected differences in the rostrocaudal location of the MI injection sites, as rostral and caudal MI differ in their connections, cytoarchitecture, and electrophysiology (Strick and Preston, 1978b; Tanji and Wise, 1981; Strick and Preston, 1978a; Gould et al., 1986; Donoghue, 1985; Holsapple et al., 1991). However, our injection sites

included most of the anteroposterior extent of MI in most monkeys, and there was no obvious correlation between the A–P locations of the injection sites and the degree of MI and SI projection overlap in the putamen. Fourth, the imperfect overlap between SI and MI projections from homologous representations may reflect the fact that SI and MI representations are never perfectly homologous: the relatively strict cutaneous somatotopy of SI area 3b, for instance, could only roughly parallel the mosaic agonist and antagonist muscle representations in area 4.

Overlap between corticostriatal projections from different body part representations was uncommon for between the dense zones of the projection, but was the rule for the faint haloes of label surrounding these dense zones. This overlap of weakly labeled zones occasionally was present even when the body parts were as distant as foot and hand. It is not known whether any individual neurons within these zones receive inputs related to more than one such body part, or whether such convergence is functional -- for instance, it might normally be suppressed by lateral inhibition. On the other hand, the overlap might allow interactions between information about different body parts, or permit plasticity of body part representation, as it does in SI and MI (Jenkins et al., 1990; Jacobs and Donoghue, 1991).

The overlap of body-part input fields varied at different anteroposterior levels of the putamen, as they do in the cat and rat (Malach and Graybiel, 1986; Brown, 1991). Even the foot-dorsal, head-ventral somatotopy was not entirely constant along the anteroposterior axis. For instance, some "foot matrisomes" were ventral to some trunk matrisomes, and even to some hand matrisomes. This could allow different interactions between inputs at different anteroposterior levels, and might underlie differences in sensorimotor processing in anterior and posterior parts of the putamen. Our experimental protocol limited us to categorizing cortical sites by somatotopy. Another criterion, for instance by directional population coding in MI (Georgopoulos et al., 1989), might have yielded a different set of neighbor relations between input patches.

Non-convergence of contralateral MI inputs to the putamen with ipsilateral MI and SI inputs

The second set of input matrisomes that we identified was innervated by afferents from contralateral MI. Like the ipsilateral MI projection, the projection from contralateral MI to the putamen was divergent, innervating multiple matrisomes. These zones tended to be spatially separate from the hot spots of ipsilateral MI and SI projections, although often the haloes of weaker labeling were not well-separated. The contralaterally-labeled input matrisomes resembled the ipsilateral ones in being broadly distributed throughout the putamen, but the contralaterally-labeled matrisomes tended more frequently to be along the lateral border of the putamen than did the ipsilateral ones. This relative shift is reminiscent of that reported for the rat, in which contralaterally-activated sensorimotor zones appear to be displaced in the putamen with respect to ipsilateral ones (Brown, 1991).

Variation with body part representation of MI corticostriatal projections. The relative strength of the MI corticostriatal cross-projection varied with body part representation. Regions of cortex representing axial muscles -- the face and trunk regions -- had stronger cross-projections than did those representing appendicular muscles -- the foot and hand regions. In this regard MI's corticostriatal projection resembles its corticocortical projections to contralateral MI, as MI cortex representing trunk and face has stronger callosal connections than does that representing foot and hand representations.

The most dramatic variation with body part representation was the difference in the degree of ipsilateral and contralateral MI projection overlap in the putamen for the face and other parts of the MI map. The consistent overlap of left and right MI face projections contrasted strongly with the predominant non-overlap of paired inputs traced from other MI sites. This difference was documented in the projection patterns in single hemispheres, and not simply in

cross-animal comparisons, but our findings are so far limited to two hemispheres of one monkey (monkey 40). However, such a pronounced variation in innervation by inputs carrying information about different body parts points to the danger of generalizing about an entire body representation from information about a single part of it.

Overlap in the putamen between inputs from left and right face MI, but not between inputs from hand or foot MI, might reflect a difference between central control of axial versus appendicular movements. Left and right MI trunk projections did overlap to some extent, but the overlap was much less than that between left and right mouth projections. In addition, the trunk projections tended to overlap only along their borders, whereas the mouth projections overlapped squarely: the left and right mouth projections seemed to be centered on the same matrisomes. The face has special status in expressive or emotional gesturing, which might cause the basal ganglia to treat face inputs differently from trunk inputs.

Body representations in the putamen. The main representation in MI cortex is of the contralateral body. If the corticostriatal projections from MI carry that information to the putamen, then our results suggest the presence of two body maps in the putamen -- one receiving inputs from ipsilateral MI and SI and representing the contralateral body, and the other receiving inputs from contralateral MI and representing the ipsilateral body.

Electrophysiological recording shows that inputs from ipsilateral sensorimotor cortex create a representation of the contralateral body in the putamen, but the effects of contralateral MI inputs have not been well-studied. Stimulation of the putamen of alert monkeys sometime produces bilateral movements (Alexander and DeLong, 1985b), and in the striatum of alert cats and rats, neurons with bilateral receptive fields have been recorded (Schneider and Lidsky, 1981; West et al., 1990). Monkeys given MPTP show an increased number of pallidal neurons with bilateral somatosensory receptive fields -- possibly because there is decreased dopaminergic inhibition of crossed sensorimotor

inputs. These crossed inputs need not be originating in MI, however. The supplementary motor area (SMA), for instance, has a role in bilateral movements (Brinkman, 1984), and sends overlapping bilateral projections to the striatum (McGuire et al., 1991). Initial reports suggests that SMA and ipsilateral MI project to separate regions of the striatum (Alexander et al., 1988) and receive inputs via the thalamus from different regions of the globus pallidus (Hoover and Strick, 1991). Our findings raise the possibility that SMA projects to the same matrisomes in the putamen as contralateral MI inputs do.

The tendency for right and left MI input matrisomes to alternate in the putamen could bring representations of the homologous parts of the right and left sides of the body into proximity. In some respects the roughly alternating matrisomes are reminiscent of ocular dominance columns (slabs) in the visual cortex. In that system, right and left eye inputs carrying information about approximately the same part of visual space innervate adjoining cortical columns, and processing operations are carried out across pairs of columns (Hubel and Wiesel, 1962). The placement of the left and right input matrisomes does not appear to be a strict alternation, however; nor are the two inputs equally strong. Even so, such a system of nearby left and right input matrisomes might facilitate the control of bilateral movements.

Some neurons in MI fire in relation to movements of the ipsilateral body -- especially units in the face region (Huang et al., 1988; Tanji et al., 1988). Thus another possible interpretation of our findings is that the contralateral MI inputs to the putamen are selectively from the neurons in MI representing the ipsilateral body. If the ipsilateral and contralateral inputs do carry information about the same side of the body, then their segregation in the putamen suggest that they either form two maps, perhaps dealing with different features of the representation, or that they combine to form a single map having inhomogeneous input regions. It would clearly be of interest to identify the cells of origin of the two projections.

Relation between corticocortical and corticostriatal projections.

Our findings indicate that MI's crossed corticostriatal projection is similar to its callosal corticocortical projections in being stronger for regions of MI representing axial body parts than appendicular ones. Some years ago, Yeterian and van Hoesen proposed that cortically interconnected areas project to overlapping zones in the striatum, whereas cortical areas that are not interconnected do not (Yeterian and Van Hoesen, 1978). Selemon and Goldman-Rakic later reported exceptions to this proposed rule in monkeys in which large cortical injections had been made (Selemon and Goldman-Rakic, 1985), but there is renewed interest in Yeterian and van Hoesen's hypothesis, as it seems to apply to certain cortical regions (Yeterian and Pandya, 1991; Parthasarathy et al., 1992). McGuire *et al.* have proposed the alternate hypothesis that projections from homotopic cortical regions -- the same areas in different hemispheres -- overlap in the striatum, whereas heterotopic ones do not (McGuire et al., 1991).

The present experiments, however, show counterexamples to both proposed schemes. First, although MI and SI, and areas 3a, 3b, and 1 within SI, are not homotopic, they send convergent inputs to the striatum (Flaherty and Graybiel, 1991a). Second, of these cortical regions with convergent striatal inputs, areas 4 and 3b are thought not to be cortically connected (Jones et al., 1978). Whether there are corticocortical connections between areas 4 and 3a is controversial (Huerta and Pons, 1990). But even if these areas are interconnected, the spread of the 3b tracer deposit into parts of area 3a in the present experiments would not change the position of the labeling in the putamen, because the projection from areas 3a and 3b themselves converge. Third, ipsilateral and contralateral area 4 are not only cortically connected but homotopic, yet their inputs to the striatum are predominantly non-overlapping, unlike those of ipsilateral and contralateral SMA.

It appears, then, that neither cortical connectivity nor homotopical relationships are infallible predictors of corticostriatal overlap. We suggest that

whether inputs from particular cortical regions converge in the striatum depends on aspects of their function that are only sometimes mirrored by their cortical connectivity. This view allows for different demands of cortical and striatal processing, and for those demands to influence the patterns of connectivity.

TABLES

Table 3-1. Summary of experiments.

Exp.	Hemi-sphere	Tracer	Inj. area	Injected Representation	Figs.
29	L	Met	SI	all but head	3-1D,E,F
		HRP	MI	foot	
	R	HRP	SI	foot	
30	L	Met	SI	hand	3-3B,B'
		HRP	SI	foot	
	R	Met	SI	foot	
		HRP	SI	hand	
32	L	Met	MI	foot	3-2A,B,C,D
		HRP	SI	foot	
	R	Met	MI	foot	
		HRP	SI	foot	
33	L	Met	SI	all but head	3-4A,B,C
	R	Met	SI	all but head	
		HRP	MI	foot and leg	
34	L	HRP	SI	all but head	
	R	HRP	SI	all but head	
		Met	MI	foot and leg	
35	L	HRP	MI	all but head	3-1A,B; 3-5A,B
	R	Met	MI	all but head	3-1A,C; 3-5A; 3-8; 3-9
36	L	HRP	MI	foot	
		Met	SI	trunk	
	R	Met	SI	trunk	
37	L	HRP	MI	foot	3-3A,A'
		Met	SI	trunk	
	R	Met	SI	trunk	
40	L	HRP	MI	foot	
		Met	MI	mouth	
	R	Met	MI	foot	3-6A,A'
		HRP	MI	mouth	3-6B,B'
41	L	HRP	MI	trunk	
	R	Met	MI	trunk	3-7A,A'
42	L	HRP	MI	hand	3-7B,B'
	R	Met	MI	hand	

FIGURES

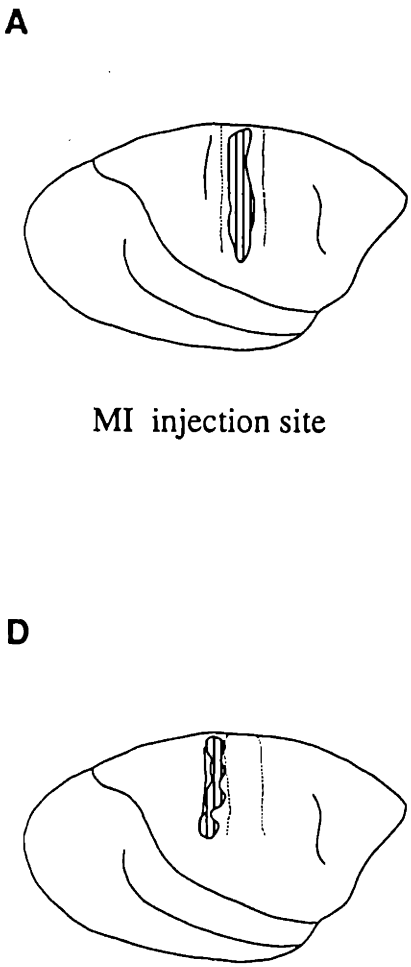

Fig. 3-1. Motor cortex (MI) projects bilaterally to the putamen (A, B, C; monkey 35), but somatosensory cortex (SI) projects ipsilaterally (D, E, F; monkey 29). A, D: Reconstructions of the 35S-methionine tracer injection sites. Dotted lines indicate the boundaries of Betz cell distribution. Fig. 3-5A shows a more detailed view of A. **B-C**: Dark-field photomicrographs of a coronal section through the putamen of monkey 35 at A 11.5, showing labeled ipsilateral (C) and contralateral (B) corticostriatal projections **E-F**: Dark-field photomicrographs of a coronal section through the putamen of monkey 29 at A 10.5, showing the ipsilateral SI corticostriatal projection (F) and absence of contralateral SI projection (E). Borders of the putamen are outlined in white. D-F are printed backwards for ease of comparison with A-C. Scale bar, 1 mm.

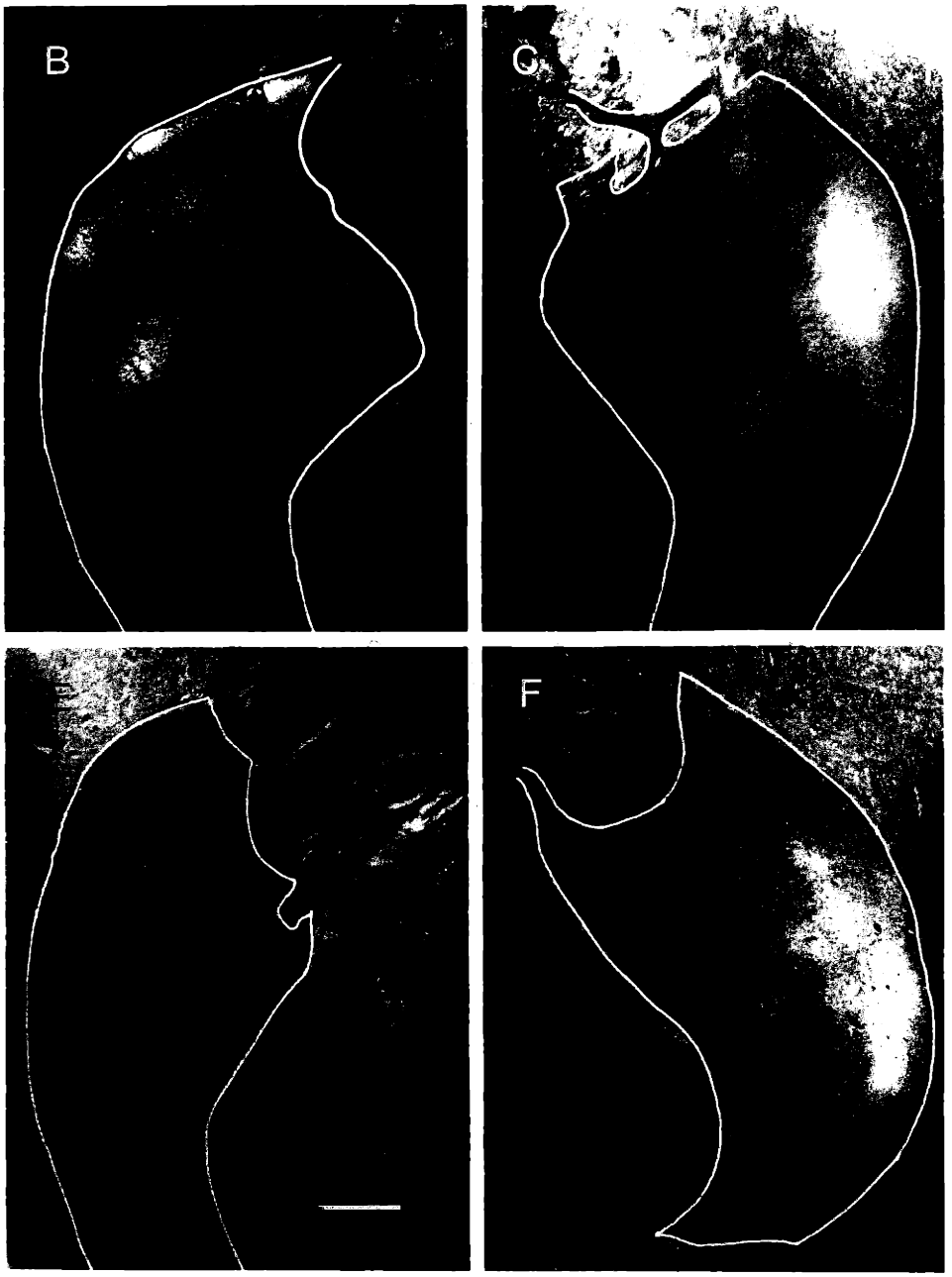
B
C
F

Fig. 3-2 (*overleaf*). Regions representing matched body parts in MI and SI project mainly to overlapping regions of the putamen (monkey 32L). **A**: Reconstructions of tracer injection sites in the MI and SI foot areas, superimposed on the stimulation and recording maps. Hatched regions = regions in which the tracer penetrated to cortical layer V. Dotted lines = boundaries of Betz cell distribution. CS = central sulcus. Stimulating and recording electrode penetration sites are marked by symbols: ▽ = area 3a, ▲ = area 3b, Δ = area 1, ○ = area 2, × = no recorded response, ■ = movement stimulated less than 100 μA, □ = movement stimulated ≥ 100 μA, + = no stimulated response at 400 μA. **B, C**: Dark-field photomicrographs of serial coronal sections through the putamen at A 12.5, showing ^{35}S-methionine-labeled inputs from MI (B) and SI (C) foot regions. The two micrographs are also shown as an overlay charting in the middle of D. **D**: Overlay chartings of serial coronal sections through the putamen at three anteroposterior levels, showing the overlap (black regions) of the densest zones of the MI input zones (horizontal hatches) and SI input zones (vertical hatches). Because in this monkey the MI injection site is smaller than the SI injection site, the MI input zones are smaller than the SI input zones, and are almost entirely within the SI zones in this monkey. Thus most of the horizontal hatches indicating MI hot spots are covered with black overlay. Atlas coordinates are given below sections.

A. Injection sites

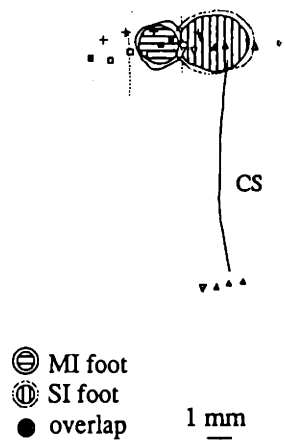

D. Ipsi. putamen

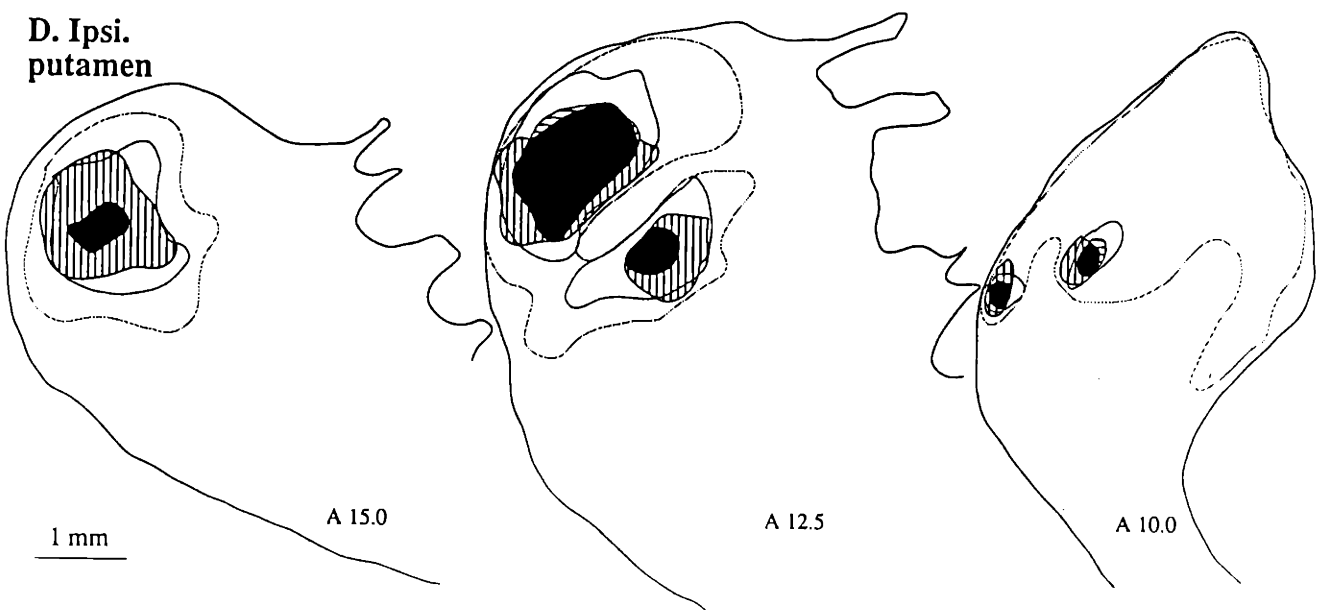


B
C

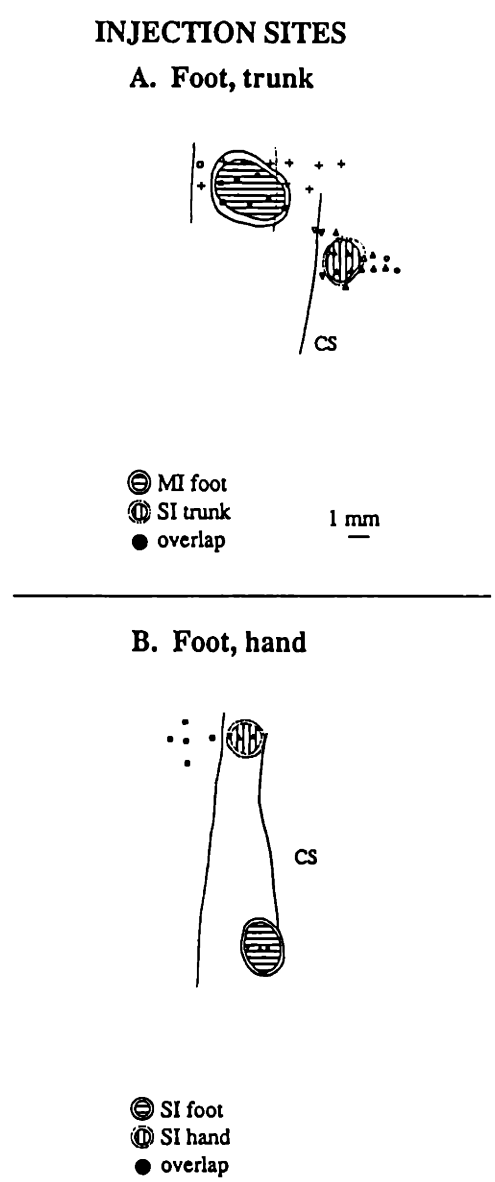

Fig. 3–3. MI and SI regions representing different body parts project to largely but not completely separate regions in the putamen (monkeys 37L and 30R). **A, B**: Reconstructions of MI and SI tracer injection sites in both hemispheres, superimposed on the stimulation and recording maps. Abbreviations and symbols are explained in the legend to Fig. 3–2. **A', B'**: Overlay chartings of serial coronal sections through the putamen at three anteroposterior levels, showing the predominant separation of patches from two different body parts, but also the occasional interdigitation or overlap. Atlas coordinates are given below sections. Scale bars in A and A' apply to B and B' respectively. B and B' (monkey 30R) are printed in reverse for ease of comparison with A and A'.

IPSI. PUTAMEN

A'. Foot, trunk

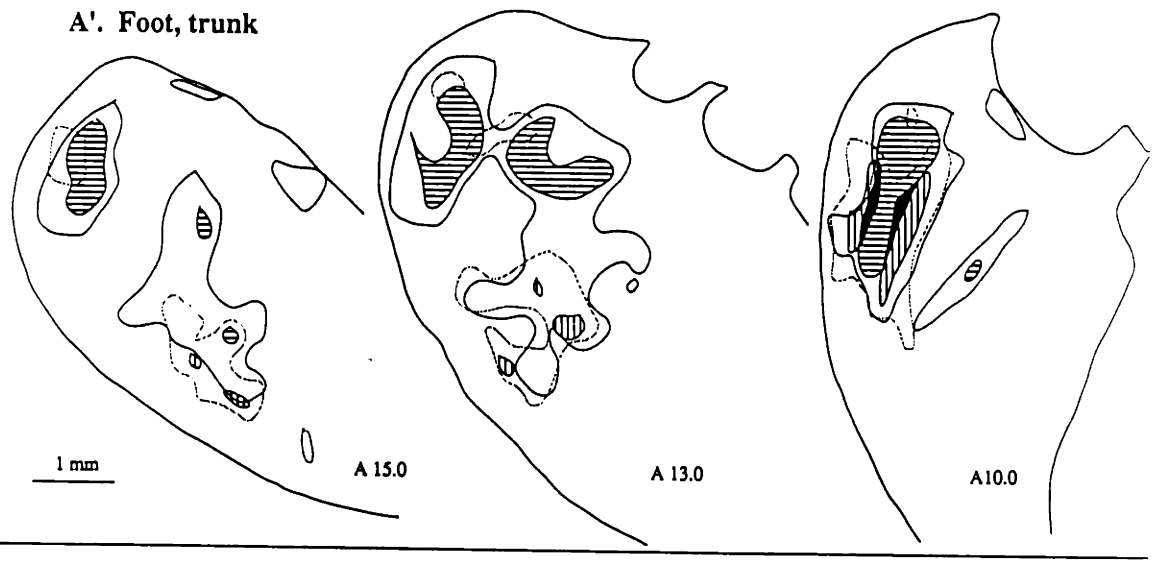

B'. Foot, hand

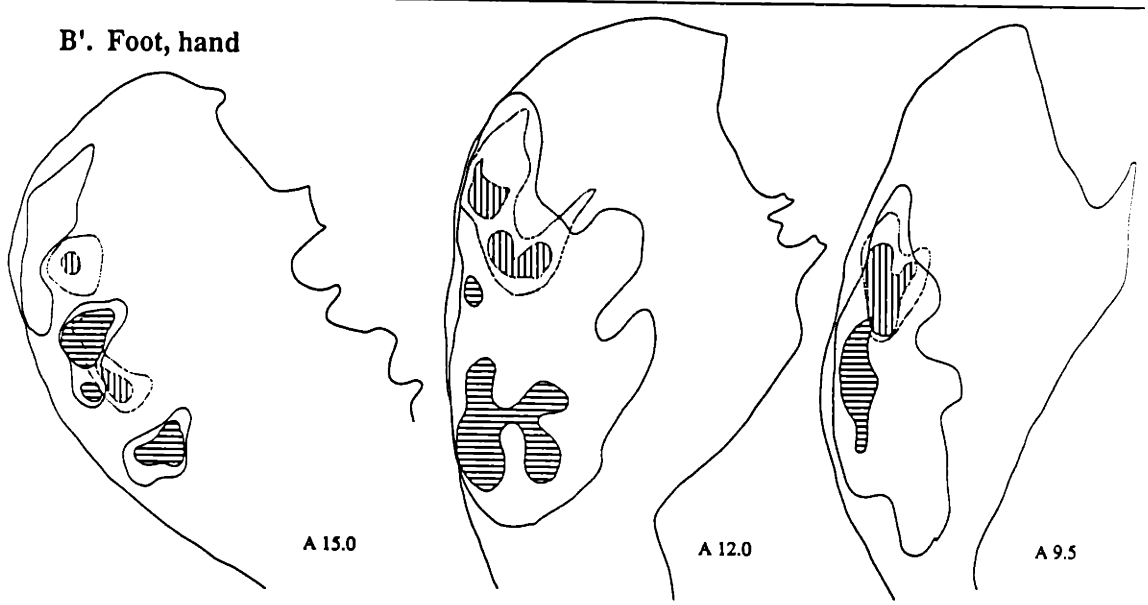

Fig. 3–4. Although SI and ipsilateral MI project to overlapping regions in the putamen, SI and most of contralateral MI do not (monkey 33). **A.** Reconstructions of MI and SI tracer injection sites in both hemispheres, superimposed on the stimulation and recording maps. The right MI injection site filled foot and leg regions; the left and right SI injection sites filled foot, leg, trunk, arm, and hand regions. Abbreviations and symbols are explained in the legend to Fig. 3–2. **B**. Overlay chartings of serial coronal sections through the putamen at three anteroposterior levels, showing the overlap (black regions) of the dense zones of the two labels transported from the ipsilateral MI and SI injection sites shown on the right side of 3A. **C**. Overlay chartings showing the lack of overlap of label transported from the ipsilateral SI injection site shown on the left side of 3A and the contralateral MI injection site shown on the right side. The scale bar in B applies to C.

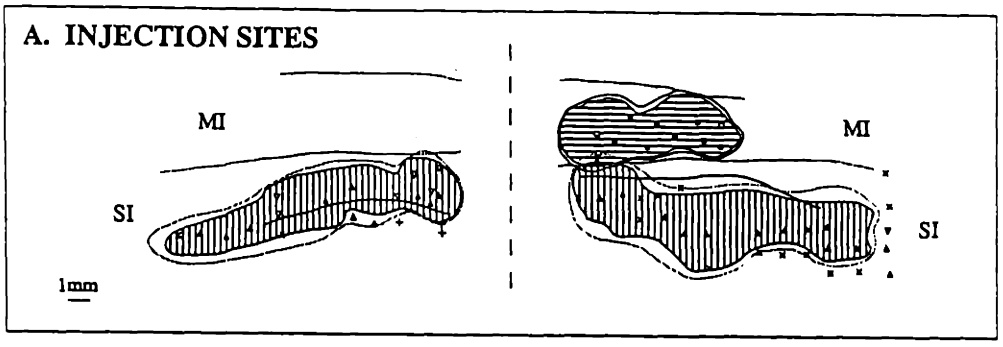

B. IPSI. PROJECTIONS

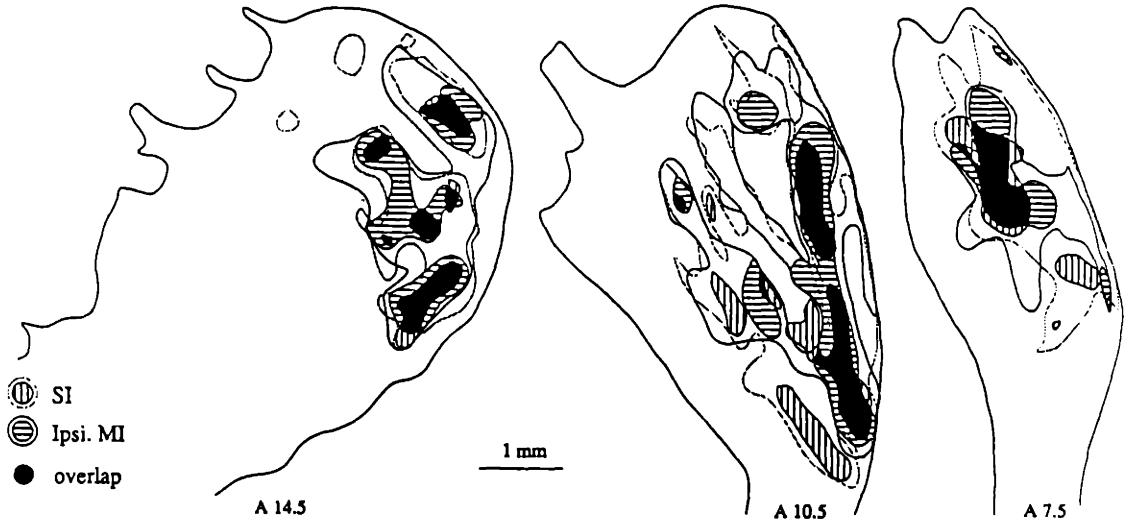

C. CONTRA. PROJECTIONS

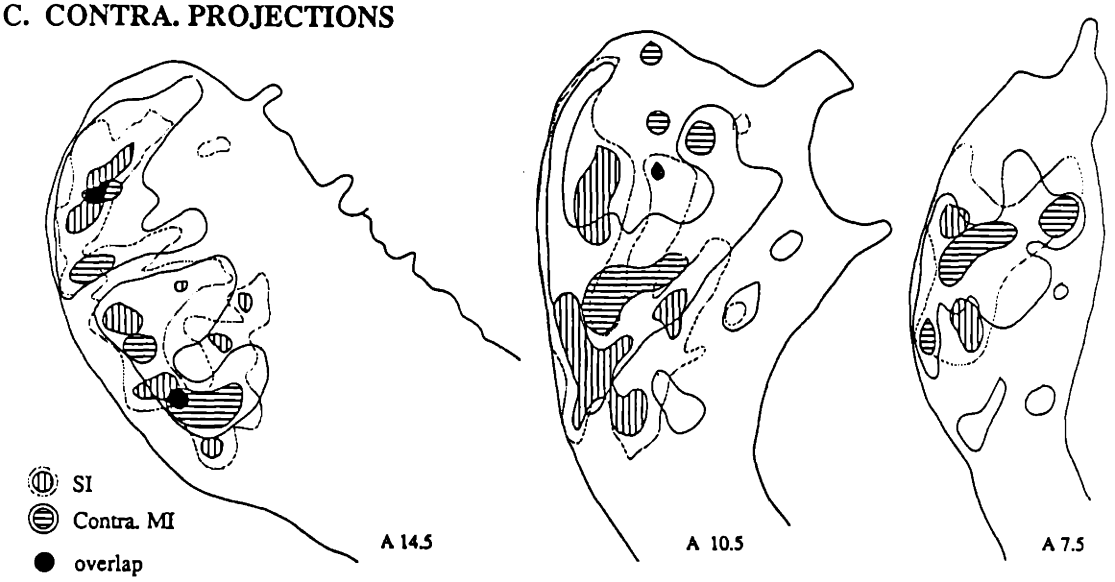

Fig. 3–5. Ipsilateral and contralateral MI project to predominantly segregated regions in the putamen (monkey 35). **A.** Reconstructions of MI tracer injection sites in both hemispheres, superimposed on the stimulation and recording maps. MI was filled bilaterally in the foot, leg, trunk, arm, and hand regions. Abbreviations and symbols are explained in the legend to Fig. 3–2. **B.** Overlay chartings of serial coronal sections through the putamen at three anteroposterior levels, showing the lack of overlap (black regions) of the two labels transported from ipsilateral and contralateral MI.

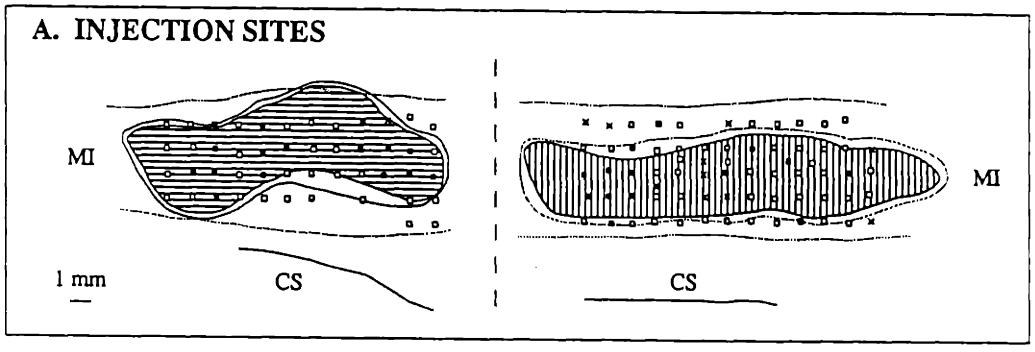
A. INJECTION SITES
MI
1 mm
CS
CS
MI

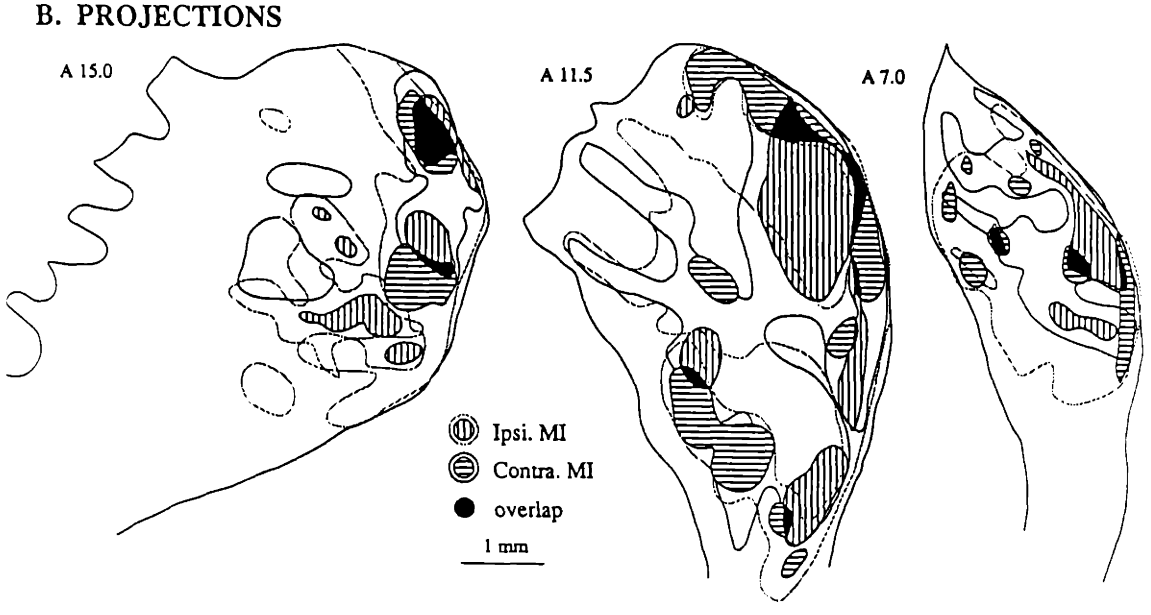
B. PROJECTIONS
A 15.0
A 11.5
A 7.0
Ipsi. MI
Contra. MI
overlap
1 mm

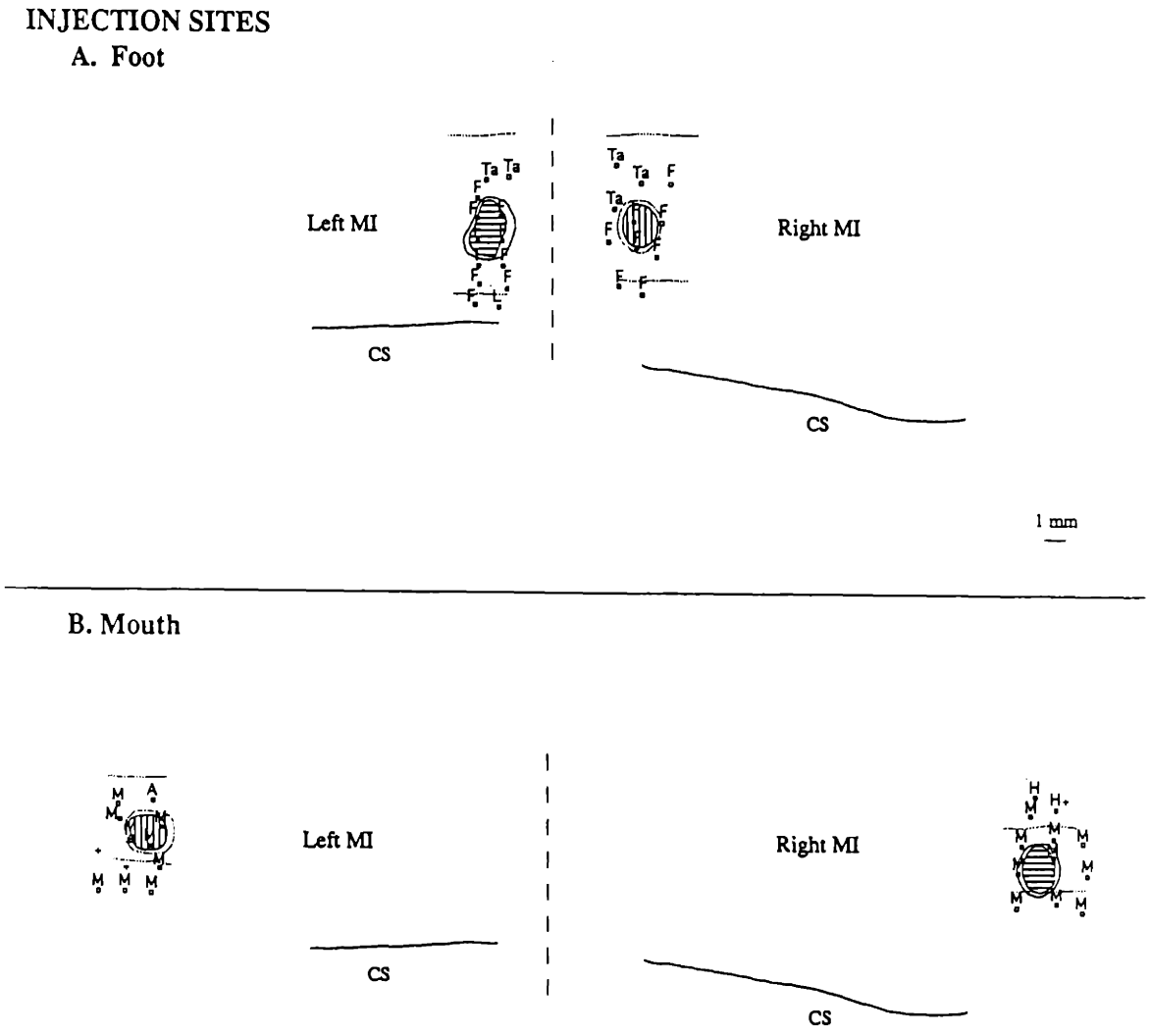

Fig. 3–6. Projections from the foot MI representations interdigitate in the putamen, but those from the mouth representations overlap (monkey 40). **A–B.** Reconstructions of MI tracer injection sites in both hemispheres, showing paired injections of the foot region (A), and mouth region (B). Letters indicate sites of stimulated movement: Ta = tail, F = foot, T = trunk, A = arm, H = hand, M = mouth. Other abbreviations and symbols are explained in the legend to Fig. 3–2. **A'–B'.** Overlay chartings of serial coronal sections through the right putamen at three anteroposterior levels, showing the interdigitation of labeled inputs from the ipsilateral and contralateral MI foot region (A'), in contrast to the overlap (black regions) of the densest regions of labeled inputs from ipsilateral and contralateral MI mouth regions (B').

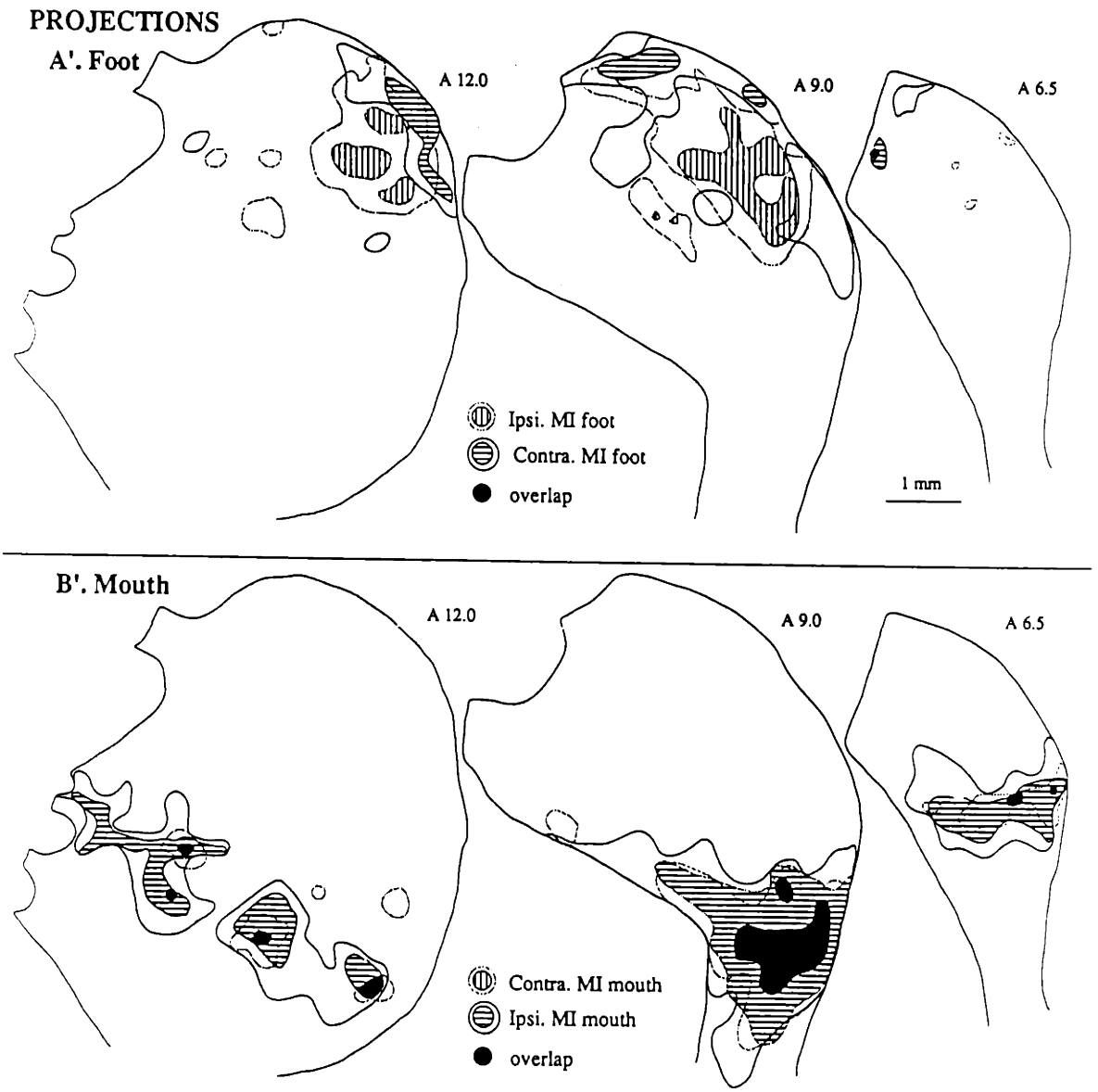
PROJECTIONS
A'. Foot
A 12.0
A 9.0
A 6.5
Ipsi. MI foot
Contra. MI foot
overlap
1 mm
B'. Mouth
A 12.0
A 9.0
A 6.5
Contra. MI mouth
Ipsi. MI mouth
overlap

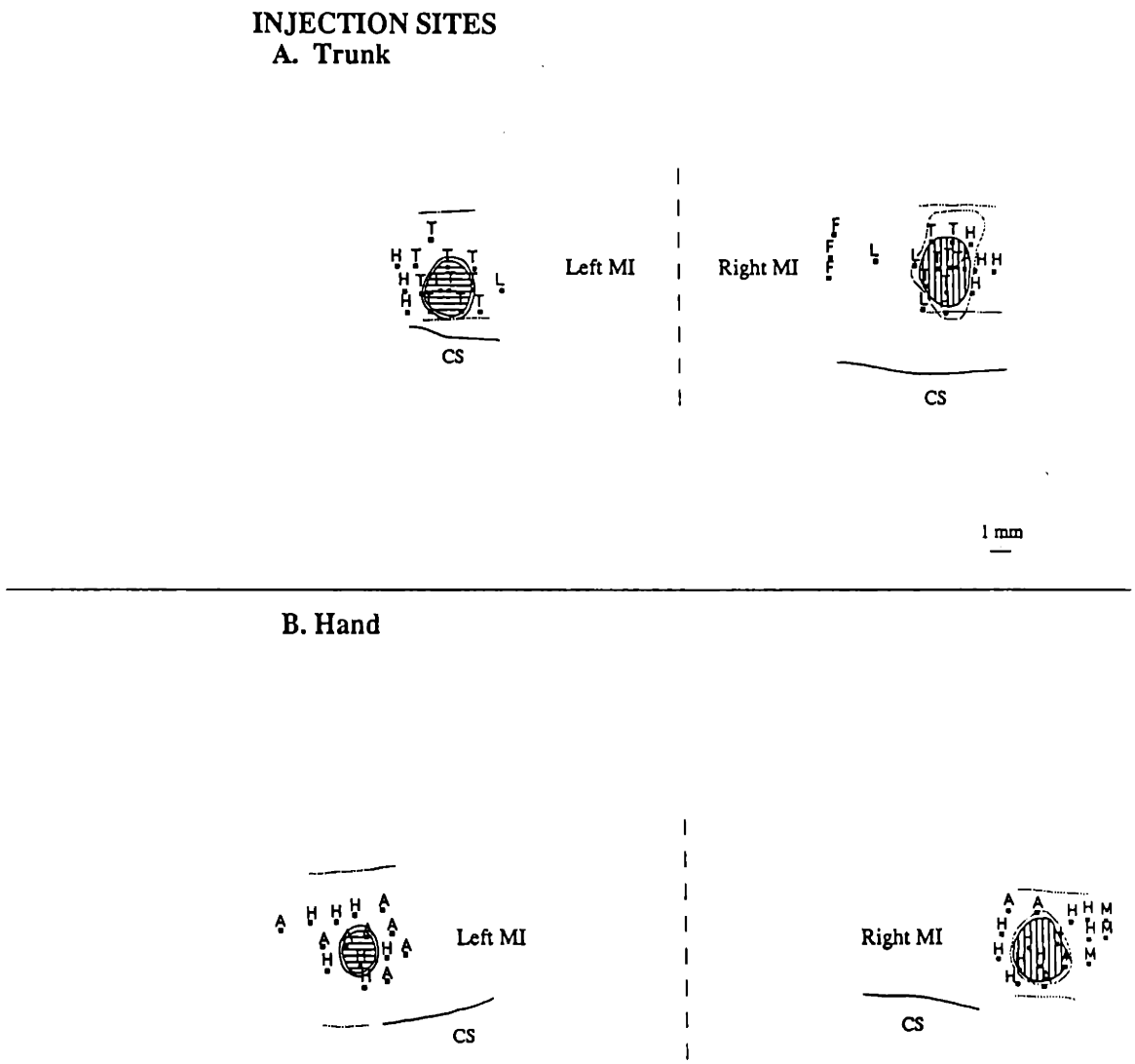

Fig. 3–7. Projections from the ipsilateral trunk and hand MI representations to the putamen interdigitate with their homologues from contralateral MI (monkeys 41, 42). **A–B**. Reconstructions of the MI tracer injection sites in both hemispheres, showing paired injections of the trunk region (A), and hand region (B). Abbreviations and symbols are explained in the legends to Figs. 3–2 and 3–6. **A'–B'**. Overlay chartings of serial coronal sections through the right putamen at three anteroposterior levels, showing the interdigitation of the densest regions of labeled inputs from ipsilateral and contralateral MI trunk regions (A'), similar to the interdigitation of labeled inputs from the ipsilateral and contralateral MI hand region (B'). B and B' are printed in reverse, for ease of comparison with A and A'.

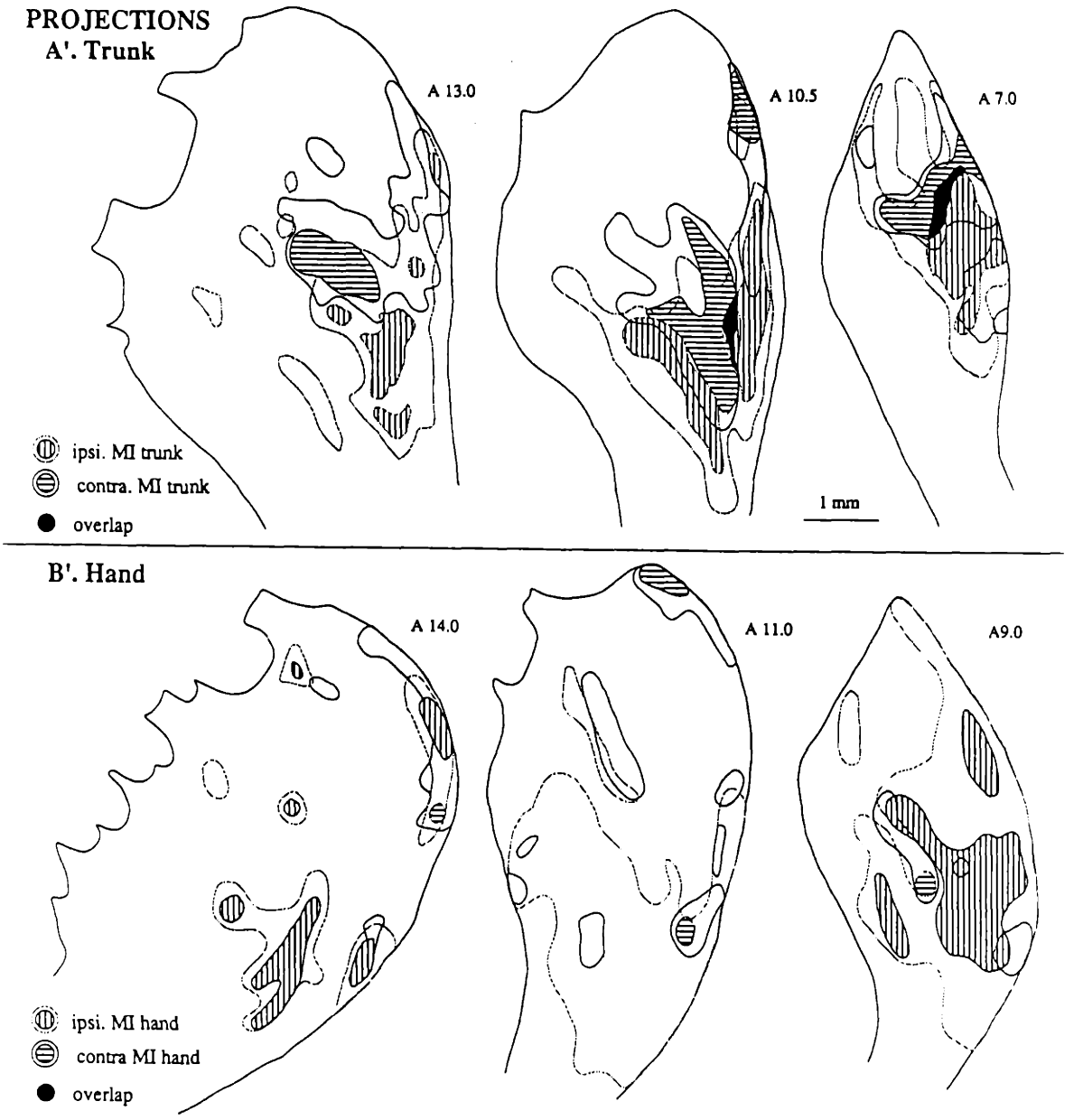
PROJECTIONS
A'. Trunk
A 13.0
A 10.5
A 7.0
ipsi. MI trunk
contra. MI trunk
overlap
1 mm
B'. Hand
A 14.0
A 11.0
A9.0
ipsi. MI hand
contra MI hand
overlap

Fig. 3–8. Ipsilateral and contralateral MI send projections to multiple zones ("matrisomes") in the extrastriosomal matrix of the putamen (monkey 35). Asterisks mark locations of striosomes in A, B, and C. **A.** A coronal section through the putamen at A 14.0, showing inputs to the putamen from ipsilateral MI, labeled with HRP–WGA. **B.** Striosomes in a putamen section serial to that shown in A. Striosomes appear as regions of weak met-enkephalin immunostaining. **C.** Inputs from contralateral MI, labeled with ^{35}S–methionine. Arrows mark the location of an exception, in which contralateral MI innervates a small striosome. In A and C, borders of the putamen are outlined in white. Scale bar, 1 mm.

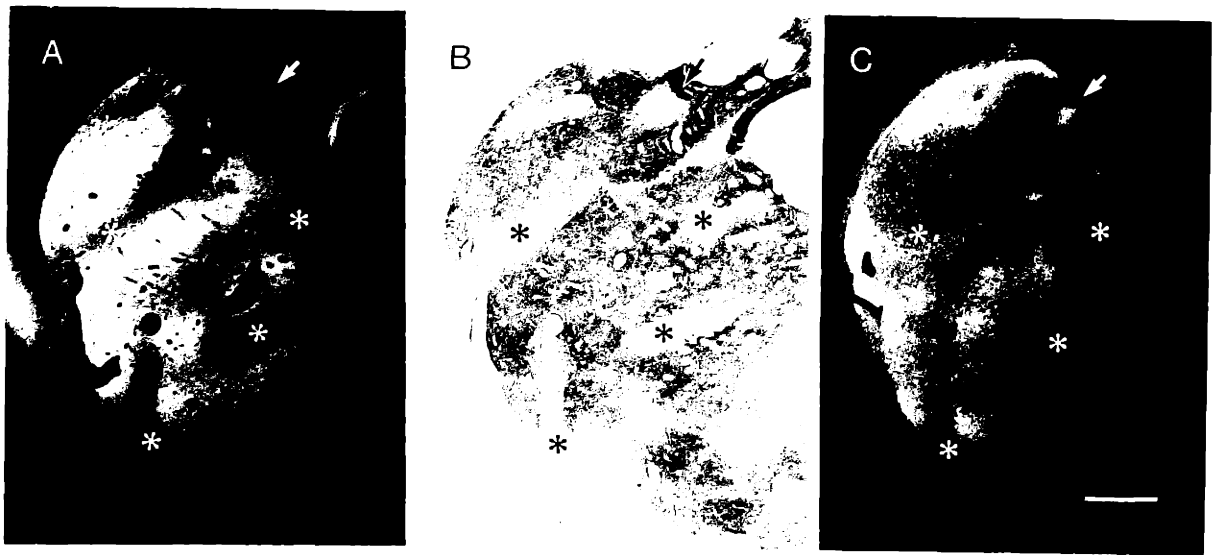
A
B
C

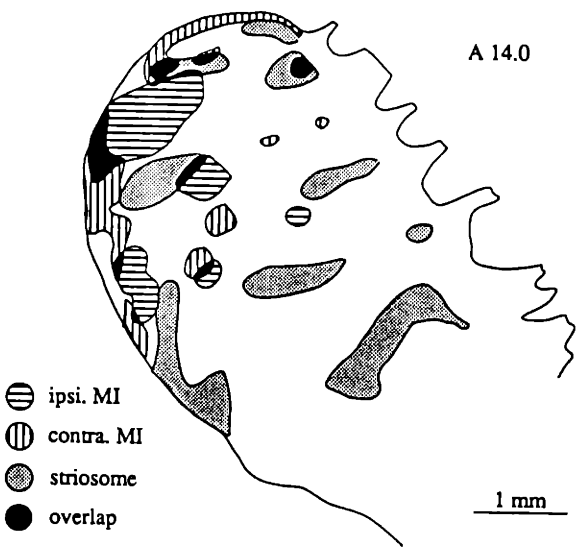

Fig. 3–9. Ipsilateral and contralateral MI projections do not uniformly fill the matrix, and form separate subsystems within it. An overlay charting of the three putamen sections photographed in Fig. 3–8, showing the location of the densest zones of the ipsilateral and contralateral inputs from MI with respect to striosomes.

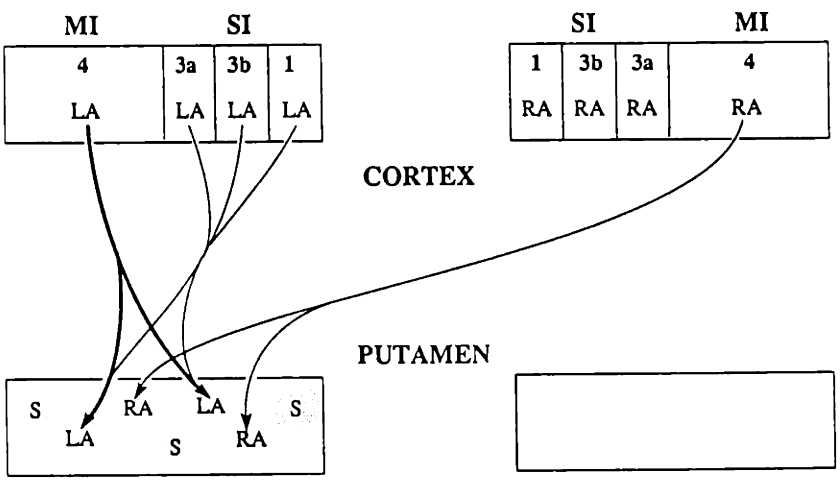

Fig. 3–10. A summary of the sensorimotor cortical arm region inputs to the left putamen; inputs to the right putamen are not shown. Five aspects of the corticostriatal map transformations are shown. 1) Different ipsilateral cortical representations of sensory and motor modalities (areas 4, 3a, 3b, and 1) are combined in the putamen. 2) MI inputs are stronger than SI inputs, and only the former are bilateral. 3) Single cortical representations innervate multiple, patchy zones in the putamen. 4) The input patches are within, but do not fill, the matrix. 5) The inputs interdigitate with patchy inputs from other, unrelated body parts in ipsilateral MI, with inputs from contralateral MI, with matrix regions that do not receive sensorimotor cortex inputs, and with striosomes. LA = left arm representation; RA = right arm representation, s = striosome.

CHAPTER 4. MODULAR OUTPUT ORGANIZATION OF THE STRIATUM

"Matrisomes"

"*Must* a name mean something?" Alice asked doubtfully.
"Of course it must," Humpty Dumpty said: "*my* name means the shape I am. With a name like yours, you might be any shape, almost."

– Lewis Carroll, *Through the Looking Glass and What Alice Found There*

ABSTRACT

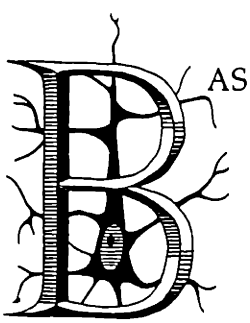

ASAL GANGLIA PATHWAYS from the striatum to the external segment of the globus pallidus (GPe), the internal segment of the globus pallidus (GPi), and the substantial nigra pars reticulata (SNr) are important for motor control in primates. In squirrel monkeys, we combined multiple retrograde tracers and immunocytochemistry in single and serial sections to determine the relationship between striatal neurons sending inputs to these three targets. Striatal neurons labeled by small injections confined to either GPe or GPi formed small cluster in the matrix, or matrisomes. Labeled projections from the matrix to SNr were more diffuse, but also showed some sign of matrisomal organization. Serial section comparisons showed that contrary to previous hypotheses, GPe- and GPi-projecting matrisomes were not segregated by target, but could overlap. The degree of overlap depended on the injection site location within each segment, suggesting that a given matrisome sends inputs to two sites, one in GPe, and one in GPi. Cell density measurements and single section double-retrograde labeling analysis confirmed that GPe- and GPi-projecting neurons are extensively

intermingled in the striatum. However, in contrast to previous reports in the rat, individual primate striatopallidal neurons form two discrete classes. Only 1.25 ± 1.73% of labeled striatal neurons were doubly labeled from both GPe and GPi -- a number not significantly different from zero. Enkephalin content differed very significantly between GPe- and GPi-projecting neurons: 71.3 ± 7.6 % of the labeled GPe-projecting neurons showed enkephalin-like immunoreactivity, in contrast to 10.0 ± 3.6% of the labeled GPi-projecting neurons.

These results suggest that in the primate a given input to the striatal matrix has a terminal field containing both GPe- and GPi-projecting neurons, rather than having its terminals channeled to a region projecting to a single target. However, the striatopallidal neurons themselves form two anatomically and neurochemically discrete classes.

INTRODUCTION

Two pathways for cortical information through the basal ganglia, the "direct" pathway through GPi and SNr, and the "indirect" pathway through GPe and the subthalamic nucleus, appear to have opposite effects on many aspects of basal ganglia and cortical activity, and to be differentially affected by basal ganglia disorders such as Parkinson's disease and Huntington's disease. The striatum, the principle stage in basal ganglia processing of cortical information, is anatomically and physiologically structured in such a way that it may be the switching station that directs certain inputs to GPe and others to GPi. There is controversy, however, over the degree to which striatal neurons projecting to GPe and GPi are segregated, and at what level.

Injections of retrograde tracer into GPe, GPi, and SNr label clusters of output neurons in the extrastriosomal matrix of the striatum. Input fibers to the matrix also form patchy terminations in the matrix. These discrete input and output zones are similar in size and shape to striosomes or patches, although they are entirely within the matrix (Malach and Graybiel, 1986; Flaherty and Graybiel,

1991a; Giménez-Amaya and Graybiel, 1990; Desban et al., 1989). Consequently, to avoid the confusion of the term "patches in the matrix," they have been called matrisomes (Graybiel et al., 1991). Input matrisomes receiving projections from somatosensory, motor, and oculomotor regions of cortex have been studied; they can be distinguished by the cortical areas and by the body or movement representation within a given cortical area (Malach and Graybiel, 1986; Flaherty and Graybiel, 1991a; Parthasarathy et al., 1992). Less is known about the principles of organization of the output matrisomes. The possibility has been repeatedly raised that different matrisomes project to different target nuclei (Divac, 1984; Feger and Crossman, 1984; Jiménez-Castellanos and Graybiel, 1989a; Giménez-Amaya and Graybiel, 1990; Selemon and Goldman-Rakic, 1990), but experiments so far have tested this proposal only indirectly.

Striatal neurons projecting to GPe have been differentiated from those projecting to GPi and SNr by their neurochemistry. Although both sets of neurons are GABAergic, striatal axon terminals in GPe tend to contain enkephalin as a co-transmitter, whereas those in GPi and SNr tend to contain substance P and dynorphin. They also differ in their dopamine receptor subtypes (Gerfen et al., 1990) and perhaps their physiological response to dopamine. If striatal output matrisomes are indeed separated by their target nucleus, there should be a patchy and complementary distribution of enkephalin- and substance P-containing cell bodies (and of dopamine receptor subtypes) in the matrix, similar to the distinct differences between enkephalin and substance P staining in the striosomes compared to the matrix. However, systematic matrisome-sized inhomogeneities of the compounds within the matrix have been hard to demonstrate.

Moreover, when striatal cell bodies rather than pallidal and nigral axon terminals are examined, the segregation of transmitter-related substances is not as dramatic: in the rat and cat some neurons express enkephalin as well as substance P, D1-like receptors as well as D2-like receptors (Penny et al., 1986; Besson et al., 1990; Surmeier et al., 1991; Meador-Woodruff et al., 1991). It is not known whether neurons that coexpress these molecules also project to both GPe

and GPi/SNr, nor whether such coexpression is seen in the primate striatum, which differs from that of non-primates.

Previous studies of striatal output neurons have given widely different estimates of the number of striatal output neurons sending collaterals to more than one target nucleus has varied from very few (Feger and Crossman, 1984) to the proposal that all neurons projecting to SN also project to GP (Kawaguchi et al., 1990). Moreover, because of the difficulty of making tracer injections in a single segment of the GP that do not contaminate the other segment, the relative frequency of striatal neurons projecting respectively to GPe and to GPi has not previously been studied.

In the experiments described here, and briefly elsewhere (Flaherty and Graybiel, 1992), we addressed four questions about the output organization of the primate striatum. 1) Do output matrisomes in the putamen project to a single target nucleus? 2) If not, what are their organizing principles? 3) Do individual neurons project to both GPe and GPi? 4) To what extent are enkephalinergic neurons found only in the indirect pathway? In a second paper we describe how input and output matrisomes are related.

METHODS

In 17 adult squirrel monkeys (*Saimiri sciureus*) weighing 0.53–1.14 kg, we injected the retrograde tracers wheatgerm agglutinin conjugated to enzymatically-inactivated apo-horseradish peroxidase and labeled with colloidal gold (HG), wheatgerm agglutinin conjugated to horseradish peroxidase (WGA-HRP), the beta subunit of cholera toxin (CTB), and Fluorogold bilaterally into GPe, GPi, and SN under stereotaxic guidance. Table 4-1 lists the injection sites for each animal. The distributions of the tracers transported to the striatum were compared to each other, and to distributions of enkephalin and tyrosine hydroxylase immunoreactivity. Serial section analysis, and also single, doubly labeled section analysis was performed. In the course of the surgeries, distinguishable

anterograde tracers were deposited in the cerebral cortex under electrophysiological guidance, for experiments reported elsewhere (chapters 2 and 3).

Surgeries were performed as described previously (Flaherty and Graybiel, 1991a). A saturated solution of CTB (Sigma, Inc.) was prepared by adding 0.5 mg CTB to 20 µl sterile water, stirring vigorously, and letting the precipitate settle for 5 min before filling the injection pipette. Fluorogold (1% solution, Fluorochrome, Inc.) and WGA-HRP (15% solution Sigma) were administered in sterile saline. HG was prepared in advance according to the method of Basbaum and Menetrey (Basbaum and Menetrey, 1987) and stored at -20 °C. HG could be repeatedly thawed and used for more than one year without detectable loss of sensitivity.

Neuroanatomical tracers were placed, under a layer of mineral oil, in glass micropipettes with internal tip diameters of 25-35 µm, and were pressure-injected with a Picopump (World Precision Instruments). Typical volumes injected were 20 nl of CTB, 10 nl of Fluorogold, and 90 nl of HG. The size of the HG injection site, however, did not increase much as the volume injected increased -- presumably because its high density inhibited diffusion away from the injection site. Injection sites were chosen by combining stereotaxic coordinates from the atlas of Gergen and MacLean (Gergen and MacLean, 1962), an anteroposterior (AP) correction factor determined from previous cases (subtract 0.5 from all AP values), and brain landmarks. The most useful brain landmark was the position of the central sulcus, which was normally located at A 6.0. When it was more than 1 mm different from this, we averaged its actual AP location with the normal atlas location and added this second correction factor to the stereotaxic coordinates.

After a two-day survival time, during which buprenorphine (0.01 mg/kg SC) was given twice daily, the animal was perfused under deep anesthesia, and the brain was blocked, cryoprotected, and sectioned coronally at 40 µm as described previously (Flaherty and Graybiel, 1991a). Adjacent sections were processed in series, or single sections were doubly stained, to compare the distributions of

injected tracers, neurotransmitter-related compounds (enkephalin, tyrosine hydroxylase), and cell bodies (Nissl substance).

The location of WGA-HRP was demonstrated with the tetramethylbenzidine (TMB) method of Mesulam (Mesulam, 1978) with minor modifications (chapter 3). Fluorogold was observed in sections processed for WGA-HRP, HG, or fluorescent antibodies; it tended to be obscured in diaminobenzidine (DAB) immunostained sections. Nissl substance was stained with cresyl violet on mounted defatted slides.

HG was demonstrated by 3 to 6 20-min incubations of loose sections in a 1:1 mixture of the initiator and enhancer solutions of the IntenSe BL silver enhancement kit (Amersham), alternated with brief washes in 0.1 M phosphate buffer (PB). The silver-enhanced tissue was fixed with a 5-min incubation in 2.5% sodium thiosulfate in PB, mounted, dehydrated, and coverslipped. The mounting medium Eukitt was found to cause rapid fading of HG staining, but sections coverslipped in Permount (Fisher) have not faded detectably in two years. Analysis of many sections containing HG injection sites or regions of retrograde transport, processed with diaminobenzidine (DAB) for immunoperoxidase staining, or with tetramethylbenzidine (TMB) for wheatgerm agglutinin-horseradish peroxidase staining showed that HG did not cross-react with these methods.

Enkephalin, CTB, and tyrosine hydroxylase were demonstrated immunohistochemically. Enkephalin staining was relatively sensitive to endogenous peroxidase activity and detergent levels; consequently we stored tissue in 0.1% sodium azide in PB, pretreated it for 5 min in 10% methanol and 3% hydrogen peroxide in PB, and exposed it to 0.3% Triton x-100 in PB in only one 5-min incubation before beginning the immunostaining. Sections were incubated with antibodies against CTB (List Biolabs, 1:2000 dilution), enkephalin (Incstar anti-met-enkephalin, 1:1000 dilution), or tyrosine hydroxylase (Eugenetech, 1:1000) for two days. Sections to be singly stained were then incubated with a biotinylated secondary antibody, stained with the DAB-avidin-

biotin peroxidase technique (Vector), mounted, dehydrated, and coverslipped. Striosomes were identified as striatal regions in which neurons expressed low enkephalin immunoreactivity (Graybiel and Chesselet, 1984). The borders of GPe were determined by enkephalin staining (Haber and Elde, 1982). SNc was delimited from SNr by its greater tyrosine hydroxylase staining.

For sections immunostained and then doubly stained for HG, bound antibody was labeled with a secondary antibody conjugated to the fluorochrome CY3 (Jackson Immunoresearch), mounted, and coverslipped in 90% glycerol/10% PB with 5 mg/ml DABCO (1,4--diazabicyclo-[2,2,2]-octane, Aldrich) added to retard fading. (HG was also compatible with DAB peroxidase immunohistochemistry, except that in cells darkly stained with DAB it was sometimes hard to detect whether HG granules were present.)

Putamen neurons in singly-stained non-fluorescent sections were counted at 250x with a Leitz Ortholux microscope coupled to a Cohu CCD video camera and a Biocom computerized image analyzer. Counts were made within multiple sample squares $3.8x10^4$ μm^2 in area and 40 μm in thickness. Samples of retrogradely labeled neurons were not taken randomly; rather, they were placed in the regions with the highest density of labeled neurons. Nissl-stained neurons were counted in the same hemispheres in equivalent regions of the putamen. Small Nissl-stained cells with dark nuclei (diameters of 7 μm or less) were considered to be glia and were not counted. In determining cell counts per mm^3, the relative shrinkage of tissue processed with different techniques was taken into account by comparing the total area of the putamen for each slide with the total area of a serial, Nissl-stained slide.

Doubly stained fluorescent sections were examined on a laser scanning confocal imaging system (Bio-Rad MRC 600) coupled to a Zeiss Axioplan microscope. The laser confocal system had two photodetector channels, permitting simultaneous analysis of the fluorescent label in the same or in depth-summed optical planes. CY3 fluorescence was examined with a YHS filter block; HG granules were examined with either transmitted or reflected light. Digitized images of the

separate channels were stored and merged to produce pseudocolor composites.

Doubly labeled cells were counted by systematically scanning of sections through the putamen at a magnification of 400x, at which the Bio-Rad screen field was approximately 300 μm in diameter. Sections analyzed were approximately 1 mm apart, and spanned the rostrocaudal extent of the retrograde transport. Within a given section through the putamen, all and only the 300 μm fields that contained more than one cell of each type were counted. This was done in order to avoid diluting the percentage of doubly labeled cells by singly labeled cells in regions where there was no overlap between GPe- and GPi-labeled neurons. Thus, only cases with injection sites in topographically-related areas of GPe and GPi were counted. Cells were counted only in the putamen because most of the injection sites -- and all of them in the cases with overlap between the retrogradely labeled matrisomes -- were in regions of GP that receive inputs from the putamen rather than the caudate nucleus.

Injection site reconstructions and overlay drawings of serial sections were made with a Wild stereomicroscope equipped with a drawing tube, as previously described (chapter 3). The center of the injection site was considered to be the region in which the tracer completely obliterated cytoarchitecture; the injection site halo contained distinct labeled cells and heightened background staining. To determine injection site volume, the coronal area through the center of each injection site was measured with a Biocom computerized image analyzer, the effective radius was determined, and the volume of the equivalent sphere was calculated. The relative shrinkage of tissue processed with different techniques was taken into account.

RESULTS

Striatal projections to GPe and GPi are organized in matrisomal clusters

In 17 monkeys, we made 65 successful differentiable injections of the retrograde

tracers CTB, HG, HRP-WGA, and Fluorogold: 23 centered in GPe, 34 in GPi, and 8 in SN (see Table 4-1). Transport of CTB and HG were analyzed most extensively because CTB and HG had several advantages over WGA-HRP and Fluorogold. First, unlike WGA-HRP, CTB and HG form small, well-defined injection sites with little or no labeled pipette track. Thus they could be used to more easily label a single segment of the pallidum without contaminating the other segment. Further, because WGA-HRP could also be an anterograde tracer, we preferred to save it for cortical injections, the results of which are reported elsewhere (chapters 3 and 5). HG contains enzymatically-inactivated WGA-HRP, but it does not label anterograde projections.) Finally, Fluorogold -- unlike CTB, HG, and WGA-HRP -- did not produce strong, clearly compartmentalized retrograde labeling in the striatum.

Of the 41 CTB or HG injection sites, 32 (78%) were confined entirely to their target nucleus, as opposed to 2 (16%) of the 12 WGA-HRP injection sites. Although less so than WGA-HRP, HG had a tendency to label the bottom part of the pipette track, forming elongated injection sites. Consequently it was a more successful tracer when used for GPe injections because the track was contained in GPe; in GPi injections the track tended to contaminate GPe.

All of the three non-fluorescent tracers, WGA-HRP, HG, and CTB, labeled striatal cell clusters between 0.1-3.0 mm in cross-sectional diameter (Fig. 4-1). Cell clusters labeled with WGA-HRP or CTB were even more apparent because of the tendency of these tracers to label neuropil as well as cell bodies. But even HG, which did not label neuropil, labeled distinct cell clusters.

The cell clusters labeled from GPe and GPi resembled each other in shape, size, number and distribution. They were somewhat smaller and more discrete than those seen in previous studies with large injection sites not completely contained to a single pallidal segment (Giménez-Amaya and Graybiel, 1990; Giménez-Amaya and Graybiel, 1991). Retrograde labeling in the putamen following an approximately 1 mm diameter injection in GPe or GPi was approximately 5 mm in anteroposterior extent and 3 mm in the mediolateral

dimension. In cross-section, the clusters often had a long axis which ran dorsomedially to ventrocaudally, an orientation commonly seen in input matrisomes as well.

Fluorogold produced a sparse, uniform distribution of labeled neurons, with no apparent clusters (Fig. 4-1D). To determine whether this difference in labeling was due to different qualities in the transport of Fluorogold, or whether it was due to the faint fluorescent appearance of the labeled neurons, we also analyzed sections in which CTB had been demonstrated not by standard DAB ABC immunohistochemistry, but by either a secondary antibody conjugated to the fluorochrome CY3, or a fluorochrome ABC method using a Texas Red-conjugated avidin-biotin complex. Such slides showed the same patchy cell distribution seen in DAB-stained sections, indicating that it is not the faintness of fluorescently labeled neurons that makes it difficult to see cell clusters retrogradely labeled with Fluorogold.

Comparison with serial sections DAB-immunostained for met-enkephalin to demonstrate striosomes confirmed previous descriptions of larger tracer injections (Giménez-Amaya and Graybiel, 1990) that the labeled cell clusters projecting to both GPe and GPi were predominantly in the striatal matrix, although striosomes were not entirely free of labeled cells. Doubly labeled single-section comparisons of retrograde label and enkephalin distribution is described below.

Of the 8 hemispheres in which SN was injected with tracer, 4 received multiple injections of the same tracer. Comparison with serial sections immunostained for tyrosine hydroxylase demonstrated that in all cases the injection site included both SNr and SNc. These large SN injection sites produced cell labeling in the matrix of the putamen that was less patchy, and covered more of the striatum, than that labeled by the small GP injections (Fig. 4-2). Some regions of the striatum in each hemisphere showed discrete patches of labeled cells, however. Comparison with serial sections immunostained to demonstrate striosomes showed that some of the SN-labeled cell clusters were contained within striosomes, rather than being matrisomes. Retrograde transport from SN to the

brainstem was not analyzed.

For reasons discussed elsewhere (chapter 5) we tried to inject parts of GP and SN which received inputs from the sensorimotor cortex-recipient striatum. Consequently, injection sites were not randomly distributed in the GP or SN, but tended to be in regions which produced retrograde labeling in the mid-lateral and lateral putamen. There was also retrograde labeling in the subthalamic nucleus, which will be described separately.

Matrisomes projecting to GPe and GPi can overlap

Our results show that clusters of striatal neurons projecting to GPe and GPi, although organized topographically, are not strictly segregated by their target nucleus.

Labeled and unlabeled neurons intermingle in output matrisomes. Within the bounds of these clusters, labeled neurons were not densely packed together, but instead interspersed with unlabeled neurons, suggesting that not every neuron in a cluster projected to the target labeled by the injection site. To determine the percentage of neurons in an output matrisome that were labeled by a retrograde injection in either GPe or GPi, in 6 hemispheres we compared the cell count of all Nissl-stained neurons in the striatum with the maximum count of retrogradely labeled neurons in the most densely labeled regions of output matrisomes (Fig. 4-3A). The maximum cell counts of GPe- and GPi-labeled output neurons, 24,000 ± 6,500 cells/mm^3 and 24,700 ± 3,800 cells/mm^3, respectively, were less than 38% of the total neuronal count, 65,500 ± 8,000 cells/mm^3 ($p < 1 \times 10^4$ for both comparisons). The GPe- and GPi-labeled counts did not significantly differ from each other. We also measured the count of striatal neurons labeled after SN injections. Even in the densest zones of retrograde labeling, this count was only 17,900 ± 3,400 cells/mm^3, or 27% of the total neuronal count.

Because the CTB and HG injection sites in GP were small and did not fill all of one pallidal segment, the possibility remained that the unlabeled neurons

intermingling with neurons projecting to one pallidal segment projected to regions of that segment outside of the injection site. Therefore we also counted neurons labeled by much larger WGA-HRP injections in the pallidum. In 4 hemispheres with WGA-HRP injection sites that filled much of one pallidal segment, and on average had volumes 10-20 times greater than the volumes of the HG or CTB injections, the maximum labeled cell density in the putamen was 20,400 ± 4,500 cells/mm^3, still less than 40% of the Nissl-stained neurons. This value was not significantly dependent on the tracer used (Fig. 4-3A) or on the injection site size over a 75-fold range (Fig. 4-3B). The fact that large injections in one pallidal segment labeled no more neurons in the striatum than small injections did suggests that the other, unlabeled, neurons in that matrisome are not projecting to the same pallidal segment.

Neurons retrogradely labeled from GPe and GPi are intermingled in the putamen. GPe and GPi were injected with different retrograde tracers in 16 hemispheres. In 11 of them, each injection site of the pair was contained in a single GP segment; in the other 5, the injection site in one segment contaminated the other segment to a small extent. Because of the topography of the striatopallidal projection, unless the two injections were in regions of each GP segment that happened to receive projections from the same region of the striatum, the two sets of retrogradely labeled matrisomes in the striatum would not be in comparable regions. Thus, whether or not individual matrisomes project only to a single target nucleus, the labeled cell clusters in such cases would fail to overlap by virtue of striatopallidal topography. Clear topographic mismatch of striatal labeling occurred in 9 of the 16 hemispheres. In the other 7 hemispheres, the retrogradely labeled matrisomes were in the same general region of the striatum for at least some AP levels.

Of these 7, both serial section and doubly labeled single section analysis showed that 6 hemispheres had labeled clusters in the putamen containing both neurons projecting to GPe and neurons projecting to GPi (Fig. 4-4). The hemispheres in the left column of Table 4-1 are listed in order of decreasing

overlap: the last two cases had label in two largely different striatal territories, but when the two labels were in the same general region, the labeled patches overlapped. As a rough measure of the anatomical relationship between the sites in GPe and GPi that received overlapping projections from the putamen, we averaged the stereotaxic coordinates of the injection sites in the 4 hemispheres with the most overlap between GPe- and GPi-projecting matrisomes (Table 4-1, the first 4 entries). The result suggests that a GPi injection which is 1.5 mm posterior, 0.8 mm ventral and 0.2 mm medial to its companion GPe injection will retrogradely label matrisomes that at least partially overlap those labeled by the GPe injection.

The spatial relationship between the labeled matrisomes themselves did not seem to be governed by a single rule: the two sets of matrisomes neither perfectly overlapped nor systematically avoided each other. Rather, GPe- and GPi-projecting matrisomes partially overlapped in a largely random manner. Significantly, in the region of intersection of the two projection topographies, the retrograde patches do not seem constrained to avoid each other.

In 3 of the 6 cases with overlap of GPe- and GPi-projecting matrisomes, there was a small amount of contamination of GPe by the GPi injection site, raising the possibility that the overlapping matrisomes labeled by the two injections both projected to GPe. However, the radial topography of the striatal projections to GPe and GPi is such that the transport from the accidentally injected regions of GPe adjacent to GPi labeled regions of the striatum medial and caudal to the regions labeled by the GPe injection. Moreover, the overlapping matrisomes labeled by the two tracers were also seen in 3 hemispheres in which each injection site was completely confined to a single pallidal segment.

A single one of the 7 hemispheres with retrograde label in the same general region of the striatum had labeled matrisomes projecting to GPe and GPi that were segregated from each other and never overlapped (Fig. 4-5). The pair of pallidal injection sites did not have the same stereotaxic relationship as those pairs which labeled overlapping matrisomes, the most apparent difference being a

greater mediolateral separation. There were no examples in which the boundaries of the two sets of matrisomes seemed to be governed by a single rule; rather, the patches of label were apparently randomly distributed with respect to each other.

Enkephalinergic and GPi-projecting neurons are intermingled in the putamen. Single sections doubly stained to show neurons retrogradely labeled from GPi injections together with enkephalin-positive neurons (presumably projecting to GPe) demonstrated that such neurons are not segregated into different matrisomes in the putamen. These double-staining experiments will be described further below. The intermingling of neurons retrogradely labeled from GPi and neurons containing enkephalin-like immunoreactivity supports our double-retrograde labeling finding that GPe-labeled and GPi-labeled projection neurons are not segregated into different matrisomes in the striatum.

Individual neurons in the putamen project selectively either to GPe or to GPi

Few neurons are retrogradely double-labeled from both GPe and GPi. In 5 of the hemispheres where labeled striatal neurons projecting to GPe and GPi were intermingled, we combined in the same sections the silver enhancement reaction to demonstrate HG with demonstration of CTB by fluorescence immunohistochemistry. When neurons retrogradely labeled with the two tracers were found in the same general region of the striatum, they were not always separated into different clusters, but intermingled, sometimes extensively (Fig. 4-6A). This single-section analysis confirmed the serial-section analysis indicating that GPe- and GPi-projecting neurons are not segregated into different matrisomes in the striatum.

To determine whether individual striatal neurons project to both GPe and GPi, we counted doubly labeled neurons in the 5 hemispheres in which there were regions of intermingling between neurons retrogradely labeled from GPe with those labeled from GPi. Very few cells were doubly labeled (Fig. 4-6B). Labeled striatal neurons were counted only in regions where neurons labeled with the two

tracers were closely intermingled; specifically, when both types of neurons appeared in a microscope field of approximately 300 μm in diameter. A typical field counted is illustrated in Fig. 4-6A. Because of the locations of the GP injection sites, all the regions of intermingling were in the putamen. Within these 5 hemispheres we counted a total of 1907 neurons retrogradely labeled by GPi injections, and 2855 neurons labeled by GPe injections. Expressed as a percent of the total number of counted labeled neurons, the hemispheres had 1.25% ± 1.73% (mean ± S.D.) doubly labeled neurons, a mean that did not significantly differ from zero. Re-expressing doubly labeled neurons as a percent of the less frequent cell type, or as a percent of the GPe- or GPi-labeled neurons, did not yield means significantly different from zero.

Double-labeling of enkephalin-containing neurons and neurons projecting to GPe or to GPi. As a second index of the degree to which GPe and GPi receive separate projections from the striatum, we combined, in single sections, fluorescence immunohistochemistry for met-enkephalin (which preferentially labels neurons projecting to GPe) with silver enhancement to demonstrate HG (Fig. 4-7). This technique was applied to tissue from three hemispheres with HG injections in GPe, and four with HG injections in GPi. We counted 2,126 neurons in the GPi injection cases and 1,695 neurons in the GPe injection cases. Only 10.0±3.6% of the labeled GPi-projecting neurons were enkephalin-positive (2.8±1.6% strongly positive, and 7.2±4.4% weakly positive). In contrast to the GPi cases, 71.3±7.6% of the labeled GPe-projecting neurons were enkephalin-positive (41.1±0.08% strongly positive, and 30.1±7.3% weakly positive). The frequency of enkephalinergic neurons projecting to GPe is significantly different from that of GPi-projecting neurons ($p < 1x10^{-6}$).

DISCUSSION

These experiments demonstrate that even very small retrograde injection sites completely contained in single pallidal segments label multiple matrisomes in the

striatum, and that these matrisomes contain neurons projecting to both GPe and GPi, even though individual neurons within them project only to one or the other target nucleus and can be differentiated into two classes on the basis of enkephalin staining. Thus, channeling of matrix outputs to different target nuclei may happen at the neuronal level, but does not have any larger-scale anatomical organization.

Retrograde tracers: technical considerations

The novel combination of the tracers CTB and HG has allowed the first retrograde double-labeling study in the basal ganglia that can clearly demonstrate compartmental organization as well as doubly-labeled cells. The combination of CTB and HG also allowed injection sites small enough that closely adjacent regions, such as GPe and GPi, could be injected without cross-contamination. Previous studies in which fluorescent retrograde tracers were injected into striatal targets did not demonstrate retrogradely labeled patches in the striatum as clearly as those using WGA-HRP (Feger and Crossman, 1984; Beckstead and Cruz, 1986; Selemon and Goldman-Rakic, 1990). The question then arose whether the patchiness was an artifact of the particular tracer. In this study we demonstrate the retrogradely labeled output patches with two new tracers, CTB and HG. These tracers, in fact, demonstrate the modular output organization even more cleanly than WGA-HRP does, probably because of their smaller injection sites. It is interesting, however, that HG and CTB injection sites an order of magnitude smaller in volume than our typical WGA-HRP injection sites do not produce labeling that is an order of magnitude more patchy. Fluorogold, in contrast to the three other tracers, did not effectively show the patchy retrograde distribution. This was not due to its fluorescence or the fact that it must be observed at high power, when CTB was detected with a fluorescent rather than peroxidase-labeled antibody and observed at high power, its distribution was still patchy.

Striosome–matrix segregation

Previous comparisons of striosomes with retrograde patches labeled by tracer injections in GP showed that the labeled neurons were in clusters located predominantly in the matrix. These output matrisomes are thus added to a growing list of modular matrix systems. However, the previous studies, which had large injection sites, also showed that labeled neurons were not completely absent from striosomes. We were curious whether smaller injections would produce cell labeling that was perfectly confined to the matrix. They did not; even very small injections labeled scattered neurons in striosomes. These apparent exceptions are similar to other examples of striosome/matrix compartmentalization in the striatum; for instance, motor cortex input patches that are predominantly segregated to the matrix nonetheless send a few fibers to striosomes. It would be useful to know whether these minor innervations allow interaction between striosome and matrix processing, or are merely developmental abberations.

Principles of matrix output organization

The patchiness of these output cell clusters, makes it natural to propose that different clusters project to different target nuclei (Divac, 1984; Feger and Crossman, 1984; Jiménez–Castellanos and Graybiel, 1989a; Selemon and Goldman–Rakic, 1990; Giménez–Amaya and Graybiel, 1991) (Fig. 4–8A). Our experiments, however, present several independent lines of evidence against this hypothesis. First, comparisons of cell counts of Nissl–stained neurons with that of neurons retrogradely labeled from GPe or GPi indicate that even at the densest part of an output matrisome, an average of 38% of the neurons were labeled. Even increasing the injection site size within the pallidum over a 75–fold range did not increase this significantly (although the total number of labeled neurons and their distribution across the striatum increased). This suggests that the

remaining, unlabeled neurons project to another target nucleus. The percentage of labeled neurons we found in matrisomes after pallidal injections was similar to percentages reported for the rat, but our SN injections, which labeled a maximum of 27% of the cells in an output patch, were lower than the 50–70% reported for the rat (Bolam et al., 1981; Loopuijt and van der Kooy, 1985). Such differences may reflect the evidence that a much higher percentage of striatal neurons in the rat send branching projections to multiple target nuclei (Kawaguchi et al., 1990).

Second, serial-section analysis of the retrograde tracers at low magnification -- the conditions best for demonstrating matrisomes -- established that GPe- and GPi-projecting matrisomes do not strictly avoid each other, but can overlap. To demonstrate this, we needed to make a large number of paired injections. This constraint was made necessary by two factors: the topography of the striatopallidal projection, and our inability to reliably inject topographically homologous regions of GPe and GPi. The intermingling of GPe- and GPi-projecting neurons was confirmed with high-magnification analysis of the two tracers in doubly-stained single sections.

The precision of the striatopallidal topography has occasionally been questioned (Parent et al., 1984; Feger and Crossman, 1984), but analysis of our single tracer injections confirm previous reports (JM/G, Selemon) of a precise, if complicated, topography in which multiple discrete striatal zones converge on a single GP region. Our dual tracer experiments suggest in addition that any given matrisome in the putamen projects to a pair of regions, one in GPe, the other in GPi. In the pallidal regions that we studied, predominantly those that receive from the sensorimotor region of the putamen, the relations of the regions of GPe and GPi receiving inputs from approximately the same putamen regions can be expressed stereotaxically: the GPi injection site is on average 1.5 mm posterior, 0.8 mm ventral, and 0.2 mm medial to the GPe injection site. These coordinates fit remarkably well with the radial organization of striatopallidal projections. Because the coordinates were determined from injections labeling only the the

sensorimotor region of the putamen, we do not know whether other striatal regions would project to GPe and GPi regions bearing the same anatomical relationship.

In a limited number of cases we also compared the striatal projections to GP with those to SN. In 2 of the 4 hemispheres with HG and CTB injections in GP and SN, there was some intermingling of neurons projecting to the two regions; in the other two, different striatal territories were labeled. The matrix neurons labeled by our SN injections were more sparsely and widely distributed in the matrix than were those labeled by our pallidal injections. Some of this difference may stem from the larger size of our SN injection sites. In one previous report, a single injection in SNr retrogradely labeled discrete zones in the putamen which were similar in appearance to those following our pallidal injections (Selemon and Goldman-Rakic, 1990).

In hemispheres in which GPe- and GPi-projecting matrisomes overlapped, the overlap did not appear systematic. This lack of a consistent relationship contrasted with previous studies of matrisomes in the putamen that receive cortical inputs from regions in motor and somatosensory cortex (chapters 2 and 3). Projections from the foot regions of ipsilateral motor and somatosensory cortex, for instance, send projections to the putamen that overlap each other in a nearly patch-for-patch way, and they predominantly avoid projections from the foot region of contralateral motor cortex. Neither of those two patterns, systematic overlap or systematic avoidance, held for the GPe-projecting and GPi-projecting matrisomes we labeled.

One possibility raised by these findings is that there is no systematic relationship between the location if matrisomes projecting to GPe and to GPi (Fig. 4-8B). A second possibility is that a systematic relationship between the two would be seen if topographically equivalent regions of GPe and GPi could be identified and injected as they could be in studies of cortical projections, so that exactly the same matrisomes would be labeled (Fig. 4-8C).Indirect support for this appears in other experiments, in which the labeled projections from foot

motor cortex overlap in a patch-for-patch way with labeled projections to GPe in one hemisphere and GPi in another (chapter 5). Such evidence suggests -- although because of the dangers of making cross-animal comparisons it does not prove -- that if all three injections had been made in the same brain, the same patches would have been labeled by all three tracers. It also demonstrates that identifying sets of matrisomes by their inputs can be equivalent to identifying them by their outputs. Analogy with the cortical projection suggests that one way to identify homologous regions of GPe and GPi would be by motor and somatosensory mapping. Because anesthesia supresses pallidal stimulation of and response to movement, we could not use that approach in the present work.

A third independent line of evidence that matrisomes projecting to one segment of GP also contain neurons projecting to the other comes from tissue sections with neurons in the putamen retrogradely labeled from GPi and doubly labeled for enkephalin. Such double-labeling confirm the intermingling of neurons projecting to GPe and GPi. The specificity of enkephalin as a marker for GPe-projecting neurons is discussed below. The advantage to this approach over retrograde double-labeling is that there no need to match the topographies of the GPe and GPi projections: the HG-labeled GPi-projecting neurons intermingled with enkephalin-containing, GPe-projecting neurons throughout their distribution. This lends support to the hypothesis that our results apply not only to GP regions receiving from the sensorimotor region of the putamen (the location of most of our overlapping GPe- and GPi-projections) but also to the putamen in general, and presumably to the caudate nucleus as well.

Separation of GPe and GPi pathways through the basal ganglia at the level of single neurons

Retrograde double-labeling experiments. The fact that single matrisomes project to both GPe and GPi does not, of course, imply that GPe and GPi get exactly the same information from the striatum or, ultimately, from the cortex and

other striatal inputs. Our results demonstrate that as detected by retrograde double labeling, the percentage of neurons projecting to both segments of the pallidum did not significantly differ from zero. If these distinct populations either receive different inputs or have different intrinsic properties, GPe and GPi could get very different messages from the striatum. The two populations of projection neurons could thus be receiving different inputs. The low percentage of doubly labeled neurons was also evidence that the overlap of matrisomes projecting to GPe and GPi was not an artifact of transport of the GPe tracer by axons passing through GPe on their way to GPi.

Previous retrograde double-labeling studies have given widely varying percentages of striatal neurons that project to more than one target nucleus. Part of the inconsistency can be attributed to species differences: studies in rats with a variety of techniques have generally indicated a much higher degree of collateralization between the GPe and GPi/SNr pathways. In fact, studies of intracellularly filled striatal neurons suggest that in the rat *all* neurons projecting to SN or the entopeduncular nucleus (the rat homologue of GPi) also project to GP (the rat homologue of GPe) (Kawaguchi et al., 1990). Our data indicate that this is not true in the monkey: GPe injections never labeled more than 43% of striatal neurons even in their densest distributions. Retrograde double-labeling studies in the rat differ from intracellular filling studies in yielding lower percentages of striatal neurons projecting to more than one target nucleus. However, even double-labeling studies show 40–70% of rat striatal neurons projecting to more than one target (Bolam et al., 1981; Loopuijt and van der Kooy, 1985), still a much higher number than that reported for cats and monkeys.

In monkeys the number of striatal neurons that project to more than one striatal target has not previously been rigorously quantified, but appears to be low (Feger and Crossman, 1984; Parent et al., 1989; Beckstead and Cruz, 1986; Selemon and Goldman-Rakic, 1990; Giménez-Amaya and Graybiel, 1990). The experiment is more difficult to do in monkeys, however, because in large animals it is difficult to fill both target nuclei with retrograde tracer in order to label much

of the striatum. Furthermore, most previous papers have described the number of doubly labeled neurons in terms of the total number of labeled neurons. Unless the SN and GP injection sites involve topographically-related portions of the target nuclei, this artificially lowers the percent of doubly labeled neurons, because it includes neurons in large regions of the striatum that have been labeled by only one of the injection sites. One experiment in the cat, however, in which large, well-placed injections of retrograde tracers produced intermingling of labeled neurons almost all the way through the striatum, reported the number of doubly labeled neurons as well under 5% of the total number of neurons.

We counted neurons only in areas where the two labels were intermingled, and, although the proportions of the neurons were not always equal, the percent of doubly labeled neurons did not change significantly when it was expressed as a percent of the smaller or larger number of singly labeled neurons. It is conceivable that one tracer saturated neuronal axon transport mechanisms and blocked transport of the second tracer, or that the GPe injection site disrupted axons from the more distal GPi site, although previous double-labeling studies in the basal ganglia have not reported this problem. Therefore, and to rule out the possibility that we did not inject exactly topographically equivalent regions of GPe and GPi, we also compared neurons retrogradely labeled from either GPe or GPi with neurons immunostained for enkephalin.

Retrograde labeling and enkephalin immunostaining. Enkephalin was a relatively accurate marker for GPe and GPi-projecting neurons in the putamen: 71% of GPe-labeled neurons expressed enkephalin, whereas only 10% of GPi-labeled neurons did. Of course, enkephalin is more than a marker -- it is released from striatal neurons and has physiological effects in the basal ganglia that in many ways are opposite to those of the substance P and dynorphin thought to be released by neurons projecting to GPi and SNr. Our evidence that enkephalin is predominantly restricted to the indirect, GPe pathway through the primate basal ganglia, not only has physiological implications but also suggests the possibility of selective pharmacological manipulation of the indirect pathway.

If enkephalinergic and GPi-projecting striatal neurons form two functionally distinct classes, do the 10% of neurons which are both enkephalinergic and project to GPi form a third functionally distinct class? One possibility is that this group of neurons also projects to GPe. Our double-retrograde labeling result, that only 1% of neurons project to both GPe and GPi, suggests that most do not. Of the 10%, however, only 3% of the GPi-labeled neurons expressed enkephalin strongly, a percentage closer to that of the retrogradely double-labeled neurons. Perhaps, then, only the neurons that strongly express enkephalin also project to GPe. A second possibility is that they project to the medial division of GPi, which has relatively high levels of enkephalin compared to the lateral division of GPi.

Our results are consistent with previous double-labeling studies of striatal output neurons in other species. In the rat, striatal neurons retrogradely labeled from GP (GPe) more often express mRNA encoding enkephalin than do those retrogradely labeled from SN (Gerfen and Young, 1988; Gerfen et al., 1990). These results were not quantified, however. Moreover, since the SN injection sites presumably included both SNc and SNr, the difference might reflect properties of striosomal neurons projecting to SNc, as well as a difference between matrix neurons projecting to GP vs SNr. Double immunostaining shows enkephalin and substance P peptides coexisting in 17% of rat striatal neurons (Penny et al., 1986). In the cat, one study showed 63-76% coexistence of enkephalin and substance P, but these cats were pretreated with colchicine to enhance neuropeptide staining (Besson et al., 1990). Our retrograde double-labeling evidence that there is more segregation between the GPe and GPi/SNr pathways in the primate than in the rat would suggest that coexpression of such markers would be concomitantly less, and that does seem to be the case.

Neurons coexpressing markers for both the GPe and GPi pathways night have different functions than those that do not. On the other hand, they need not necessarily decrease the segregation or specificity of the two pathways. It might be, for example, that in the neurons which coexpress enkephalin and substance P, one compound is always expressed or turned over at a much greater rate than

the other. Different peptides in the same neurons can be differentially regulated (Salin et al., 1990) and perhaps even targeted to different collaterals of the same neuron (Hattori et al., 1991). Consequently, moderate levels of coexistence of the neurotransmitter-related compounds thought to differentiate the GPe and GPe/SNr pathways need not preclude the possibility of independent control of the two pathways.

Why have matrisomes?

If the clustering of output neurons into matrisomes is not a mechanism to channel particular types of cortical information into separate striatal target nuclei, what are matrisomes for? Our small pallidal injections demonstrated that one function of the matrisomal output arrangement is a topographically specific and fractured convergence in which inputs from multiple discrete sites in the striatum all project to the same small region of a segment in GP. And the orientation of GP-projecting matrisomes, which is parallel to the input matrisomes labeled anterogradely from the cortex, suggests an input-output arrangement in which particular cortical inputs are channeled through the striatum to particular GPe and GPi sites -- as opposed to an orthogonal arrangement in which different cortical inputs would be combined into single output matrisomes.

Evidence presented elsewhere (chapter 5) suggests that what unifies the different matrisomes projecting to a single GP region may be the nature of their cortical inputs: anterograde tracer injected in a region of sensorimotor cortex representing a single body part labels multiple matrisomes whose projections in turn reconverge on a single region in either GPe or GPi. That, combined with the overlap of matrisomes projecting to GPe and GPi shown in the present study, make it likely that rather than being randomly distributed with respect to each other, any set of matrisomes projecting to a single region of GPe also projects to a single region of GPi, and perhaps SNr. Thus the striatum may indeed be sorting cortical inputs into different output channels, but in such a way that it guarantees

that GPe and GPi get paired and similar, if not identical, versions of each cortical message.

TABLES

Table 4-1. Retrograde tracer injection site pairs. AHL = the stereotaxic coordinate of the injection site.

OVERLAP when label same territories

Case	GPe	AHL	GPi	AHL
34R	CTB	11.0	HG	9.5
		14.0		13.0
		6.5		7.0
35L	CTB	10.5	HG	9.0
		13.0		12.5
		7.0		6.5
34L	CTB	11.0	HG	9.5
		14.0		13.0
		7.0		7.0
39R	HG	11.5	CTB	10.0
		13.0		12.5
		6.5		6.0
40R	HG	10.0	CTB	9.5
		13.5		11.5
		7.0		6.0
40L	HG	9.5	CTB	9.5
		13.5		11.5
		7.0		6.0

INTERDIGITATE when label same territories

39L	HG	11.0	CTB	10.0
		13.0		12.5
		7.0		4.5

MISS -- always different territories

Case	GPe	AHL	GPi	AHL
27L	CTB	11.0	HRP	9.5
		12.0		12.5
		5.0		5.5
27R	CTB	12.0	HRP	9.5
		13.0		11.5
		6.0		5.0
30L	HG	10.0	CTB	8.5
		13.5		14.0
		6.5		7.5
30R	HG	10.0	CTB	8.5
		14.5		13.5
		7.0		7.0
36L	HG	10.0	CTB	8.0
		13.5		12.0
		7.0		6.5
36R	HG	9.0	CTB	8.5
		13.5		12.0
		6.0		6.5
37L	HG	10.5	CTB	9.0
		12.0		11.0
		7.0		6.0
37R	HG	10.5	CTB	9.0
		12.0		11.5
		8.0		6.5

FIGURES

Fig. 4–1 (*overleaf*). Similar matrisomes project to GPe and GPi. A–C. Retrograde tracer injection sites in the pallidum. There was no labeling in the caudate nucleus of these cases. A'–C'. Dark–field and reverse contrast photographs of labeled cells in the putamen. A. HG in GPe (hemisphere 39L). B. CTB in GPi (hemisphere 39L). C. A typical large WGA–HRP injection site extending through stereotaxic levels and filling much of GPi (hemisphere 25R). A'–C'. Coronal sections through the putamen of these hemispheres, with typical retrogradely labeled matrisomes. A'. HG in hemisphere 39L, stereotaxic level A 12.5. B'. CTB in a section serial to that in A'. C'. WGA–HRP transported from the injection site in C (hemisphere 25R, level A 12.0). Scale bar = 1 mm. Borders of the putamen are outlined in white. B and B' have been printed backwards for ease of comparison.

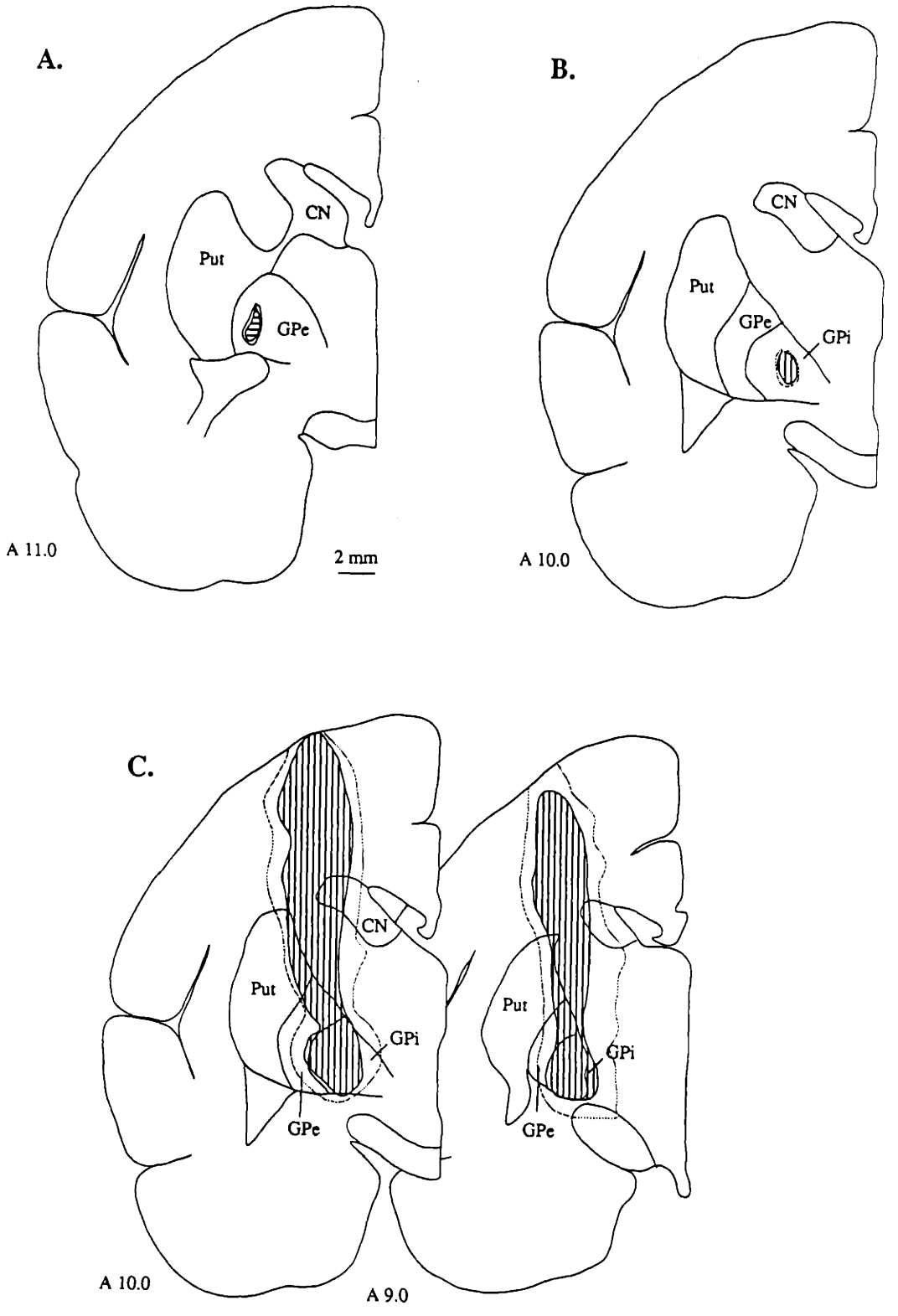
A.
CN
Put
GPe
A 11.0
2 mm
B.
CN
Put
GPe
GPi
A 10.0
C.
CN
Put
GPi
GPe
A 10.0
Put
GPi
GPe
A 9.0

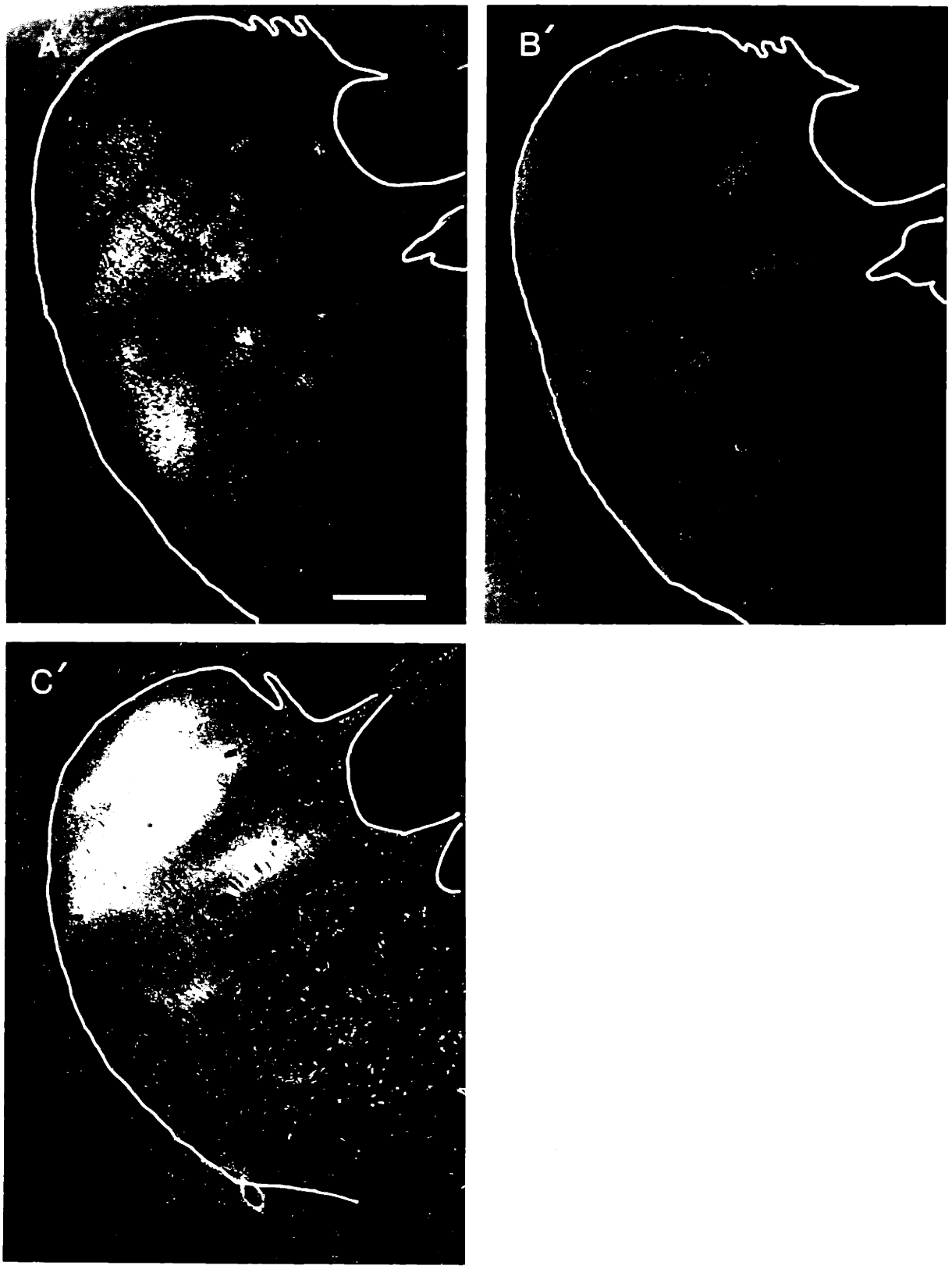
A´
B´
C´

Fig. 4–2 (*overleaf*). Large nigral injections retrogradely label matrisomes more diffusely than do pallidal injections. A. A CTB injection site in both SNc and SNr, spanning several stereotaxic levels, following 3 injections of CTB (hemisphere 42L). B. A CTB injection site in GPi (hemisphere 40L). C. Cells containing CTB in the putamen and caudate nucleus (stereotaxic level A 12.5), transported from the SN injection site in A. D. A serial section immunostained for enkephalin, showing that the clusters of labeled neurons in C are in the matrix in this section. E. Cells containing CTB in the putamen (level A 12.0) transported from the GPi injection site in B. F. A serial section immunostained for enkephalin, showing that the clusters of labeled neurons in C are in the matrix. Striosomes are marked with arrows in both pairs of photographs. Scale bar = 1 mm.

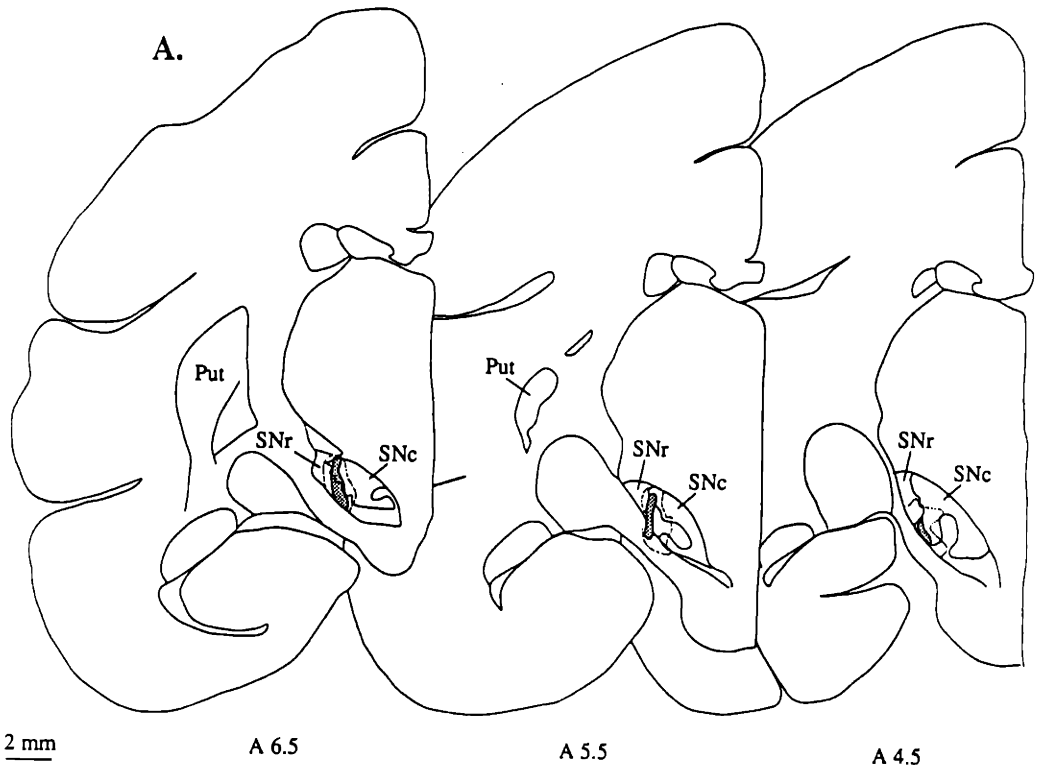
A.
Put
SNr
SNc
Put
SNr
SNc
SNr
SNc
2 mm
A 6.5
A 5.5
A 4.5

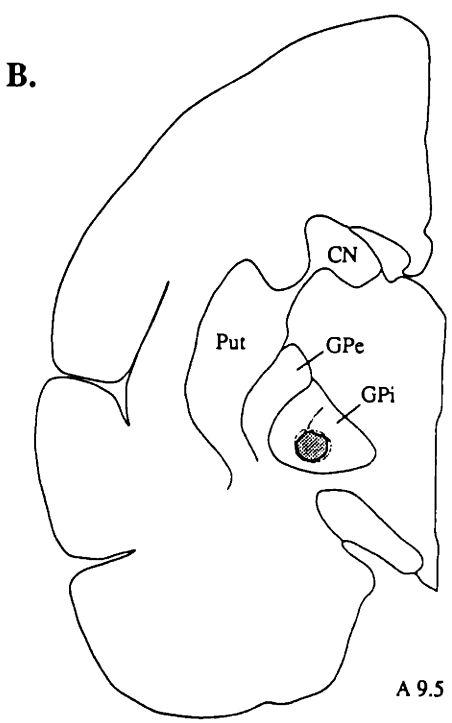
B.
CN
Put
GPe
GPi
A 9.5

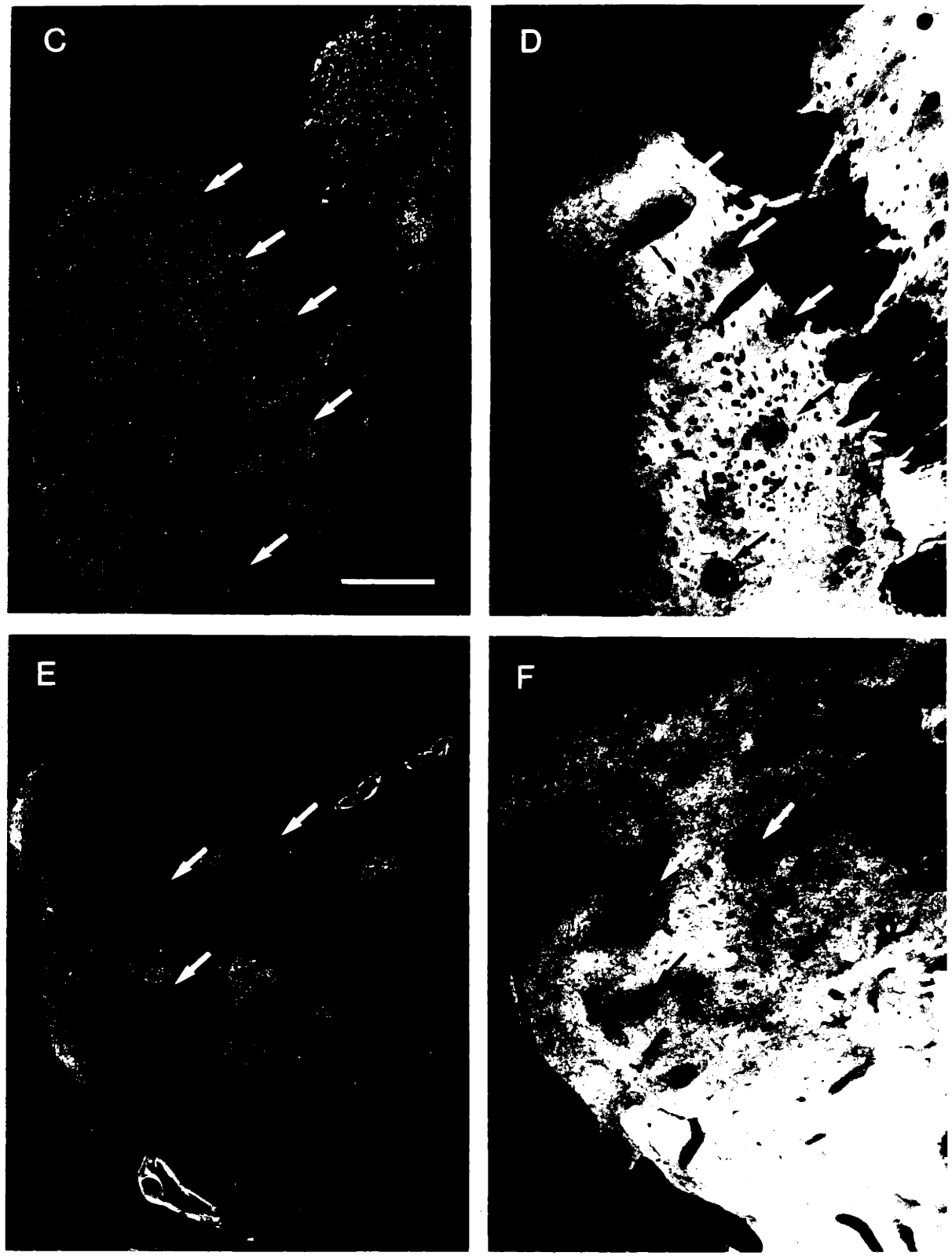
C
D
E
F

Fig. 4–3. Striatal cells projecting to a particular target nucleus make up only a fraction of the cells in an output patch. A. The maximum number of retrogradely labeled striatal neurons in the densest part of the patch, is independent of injection site and tracer, and is less than half of all neurons within the patch. Measurements of the total neuronal count were made on Nissl–stained sections. Error bars are 1 standard deviation. B. The maximum percent of retrogradely labeled striatal neurons is independent of injection site size within the pallidum. Note that the x axis has a logarhythmic scale.

A.

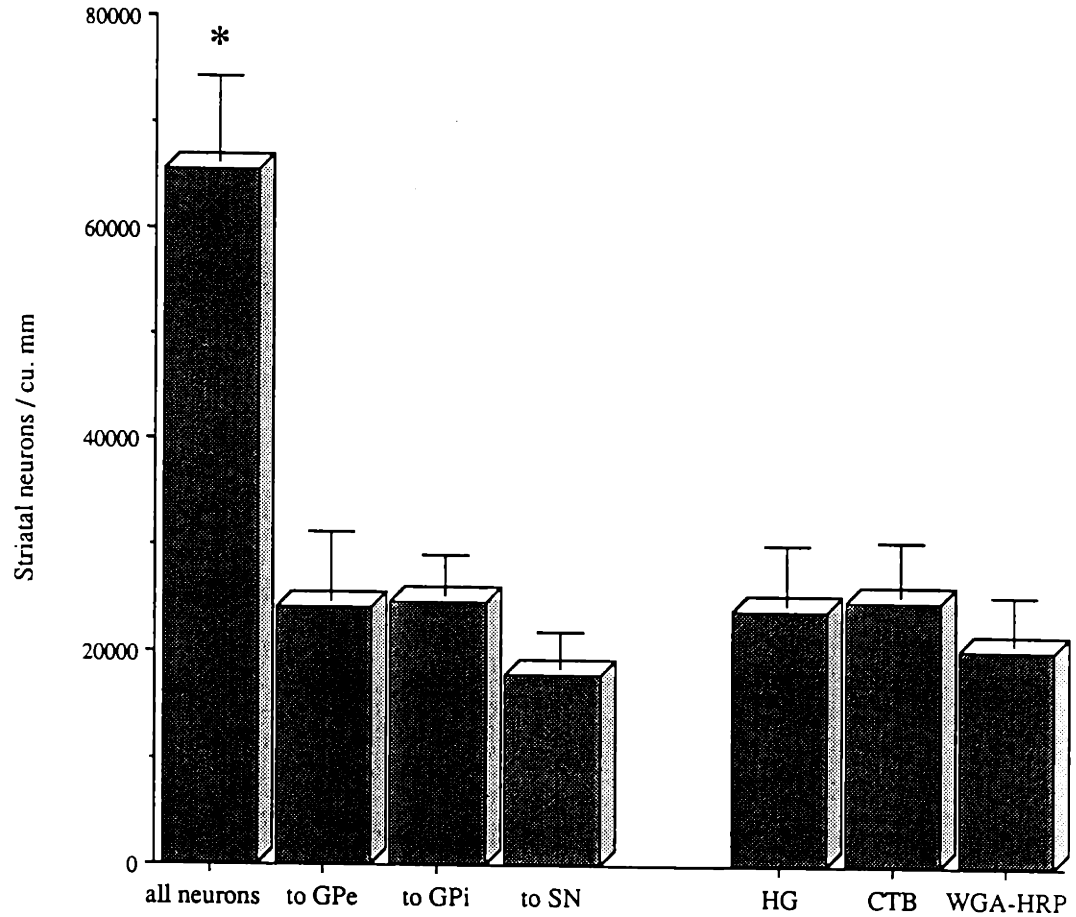
80000
60000
40000
20000
0
*
Striatal neurons / cu. mm
all neurons
to GPe
to GPi
to SN
HG
CTB
WGA-HRP

B.

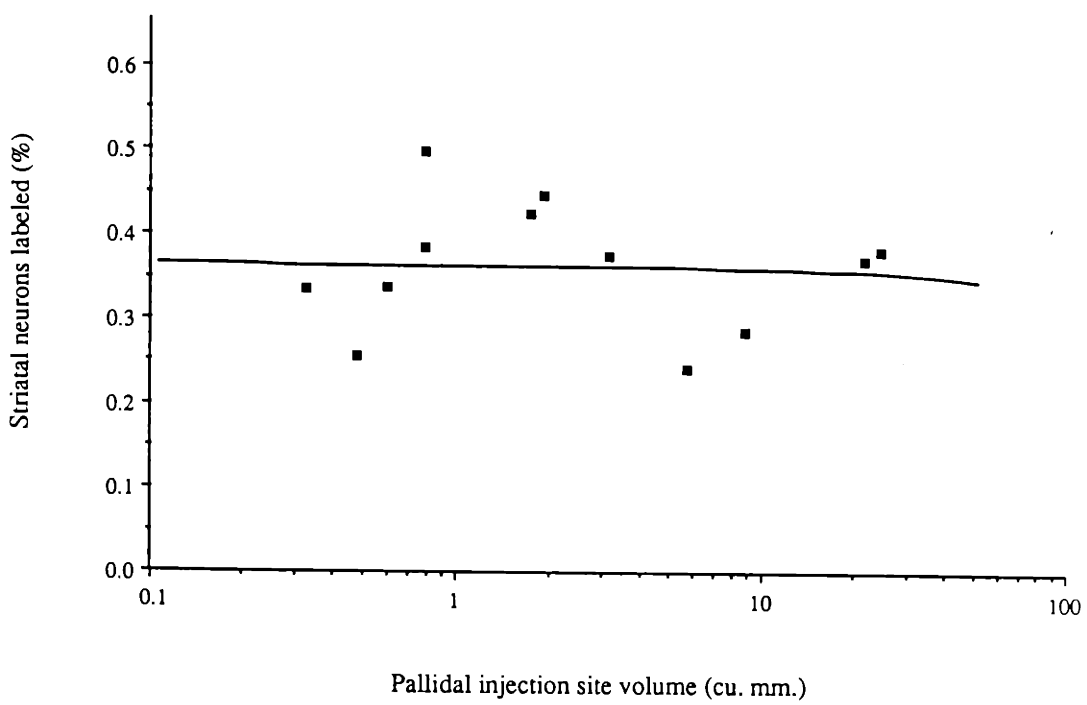
0.6
0.5
0.4
0.3
0.2
0.1
0.0
Striatal neurons labeled (%)
0.1
1
10
100
Pallidal injection site volume (cu. mm.)

Fig. 4–4. Matrisomes projecting to GPe and GPi can overlap. A–B. The positions of retrograde tracer injection sites which labeled overlapping projection fields in two hemispheres (34R and 35L). A'–B'. Overlay drawings of regions of retrogradely labeled cells in coronal sections through the putamen of the two cases (A 13.5 and A 12.5 respectively). Hatched areas represent the dense zones of the two tracers; surrounding outlines represent the lightly–labeled haloes; black represents areas of dense–zone overlap.

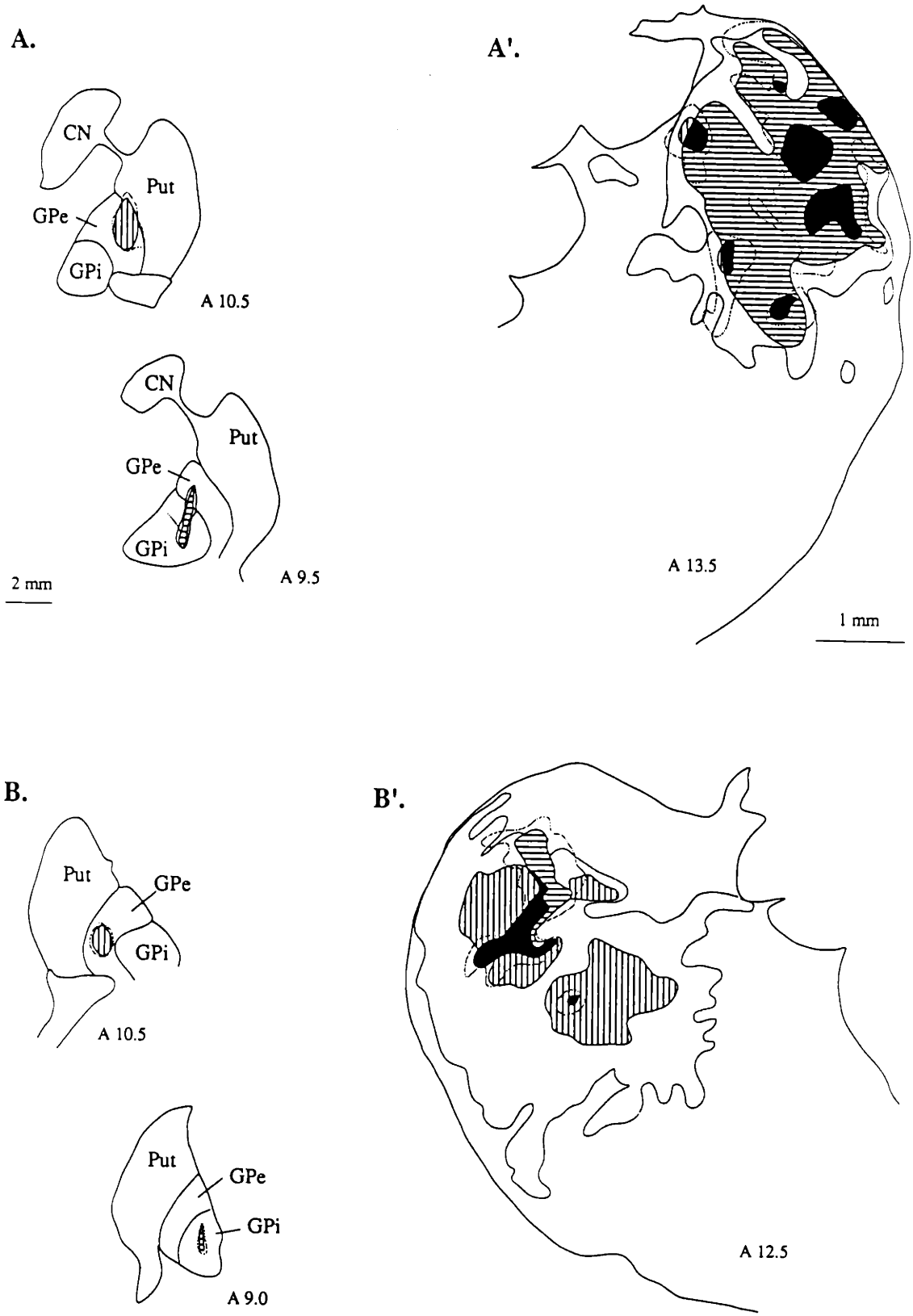
A.
CN
Put
GPe
GPi
A 10.5
CN
Put
GPe
GPi
A 9.5
2 mm
A'.
A 13.5
1 mm
B.
Put
GPe
GPi
A 10.5
Put
GPe
GPi
A 9.0
B'.
A 12.5

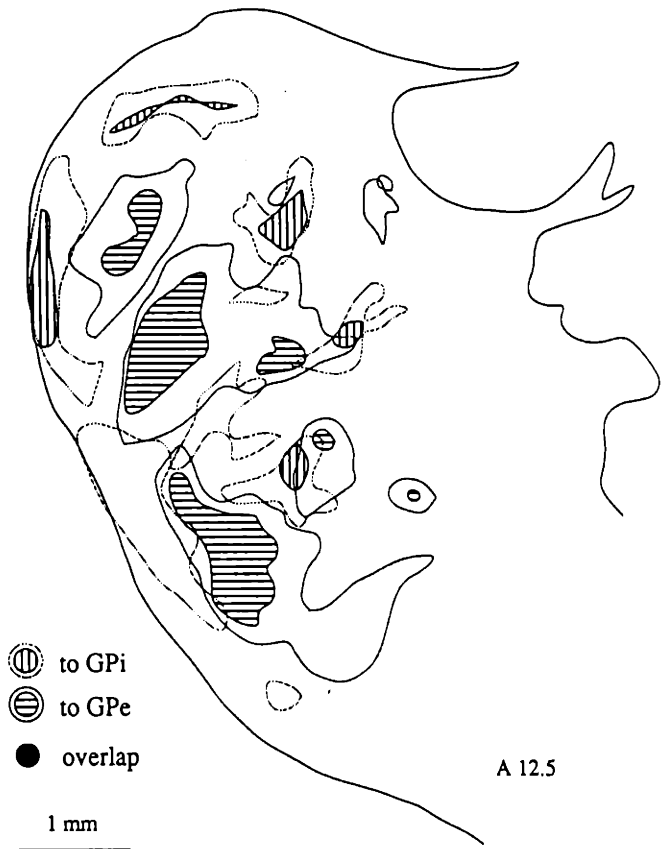

Fig. 4-5 (*above*). Matrisomes projecting to GPe and GPi can interdigitate. Injection sites are shown in Fig. 4-1A and 4-1B hemisphere 39L). Overlay drawings of regions of retrogradely labeled cells in a coronal section through the putamen (A 12.5). The sections drawn are also photographed in Fig. 4-1A' and 4-1B'.

Fig. 4-6 (*right*). GPe- and GPi-projecting striatal neurons are intermingled but few project to both segments. Laser confocal microscope views of coronal sections through the putamen. Neurons projecting to GPe (red) are labeled with a fluorescent antibody to CTB; those projecting to GPi (green) are labeled with HG. A. Low-power view showing the extensive intermingling of GPe- and GPi-projecting neurons. B. Higher-power view showing that cells contain one or the other label but rarely both. Scale bars = 50 μm.

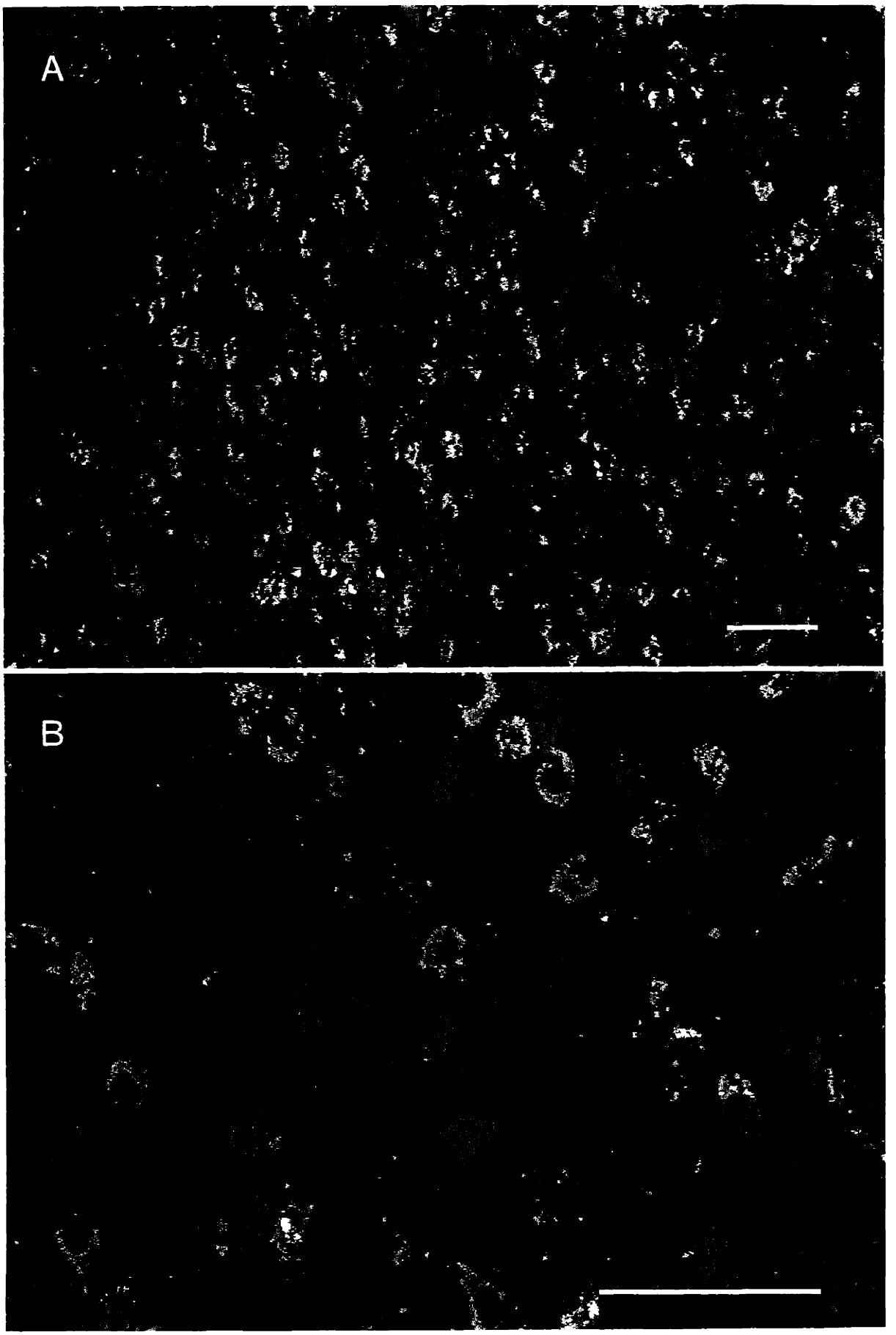
A
B

Fig. 4–7. Striatal neurons projecting to GPi rarely express enkephalin; those projecting to GPe commonly do. Laser confocal microscope views of coronal sections through the putamen. Cells labeled with a fluorescent antibody to enkephalin are red, and those containing HG transported from either GPi or GPe are green. A–B. GPi neurons and enkephalin–containing neurons (hemispheres 41L and 34R), showing that neurons contain only one or the other label. C–D. GPe neurons and enkephalin–containing neurons (hemisphere 39L) – – two photographs of the same field. Doubly labeled neurons are indicated with arrows. Scale bars = 50 μm.

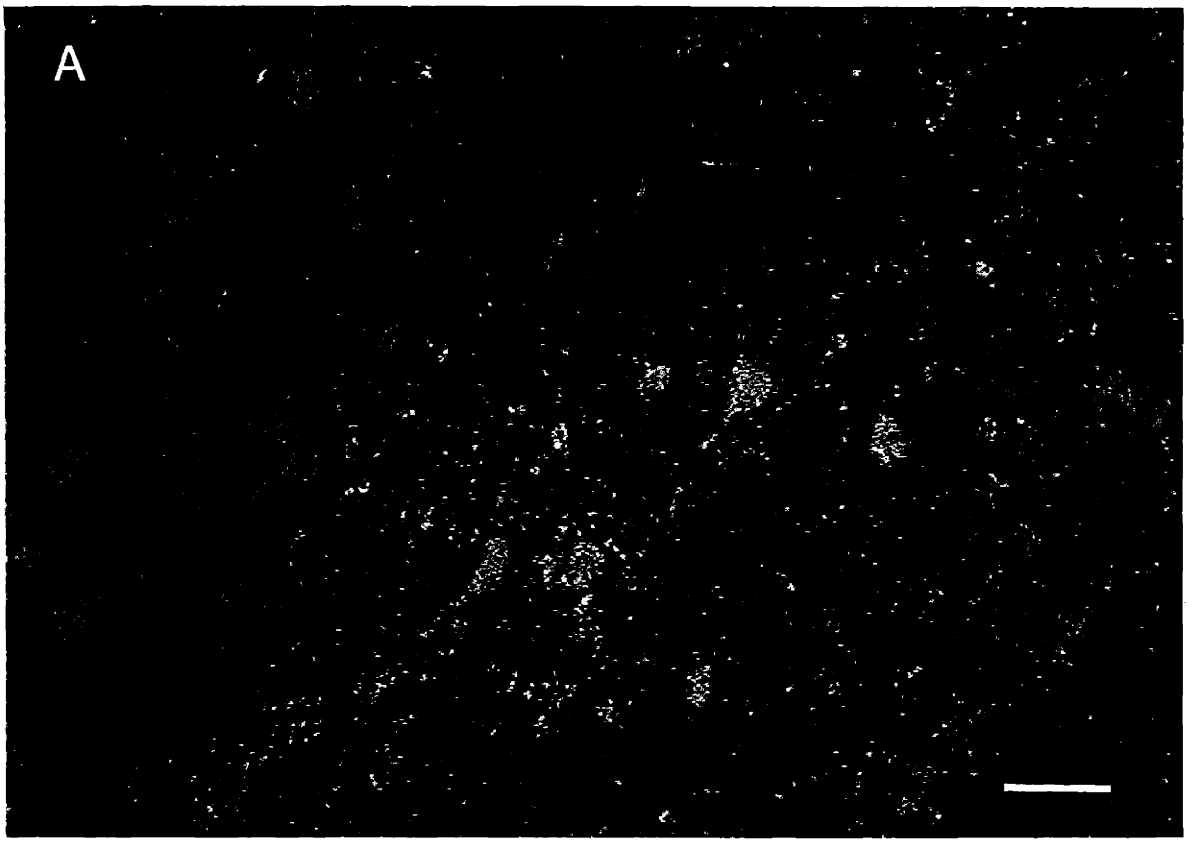
A

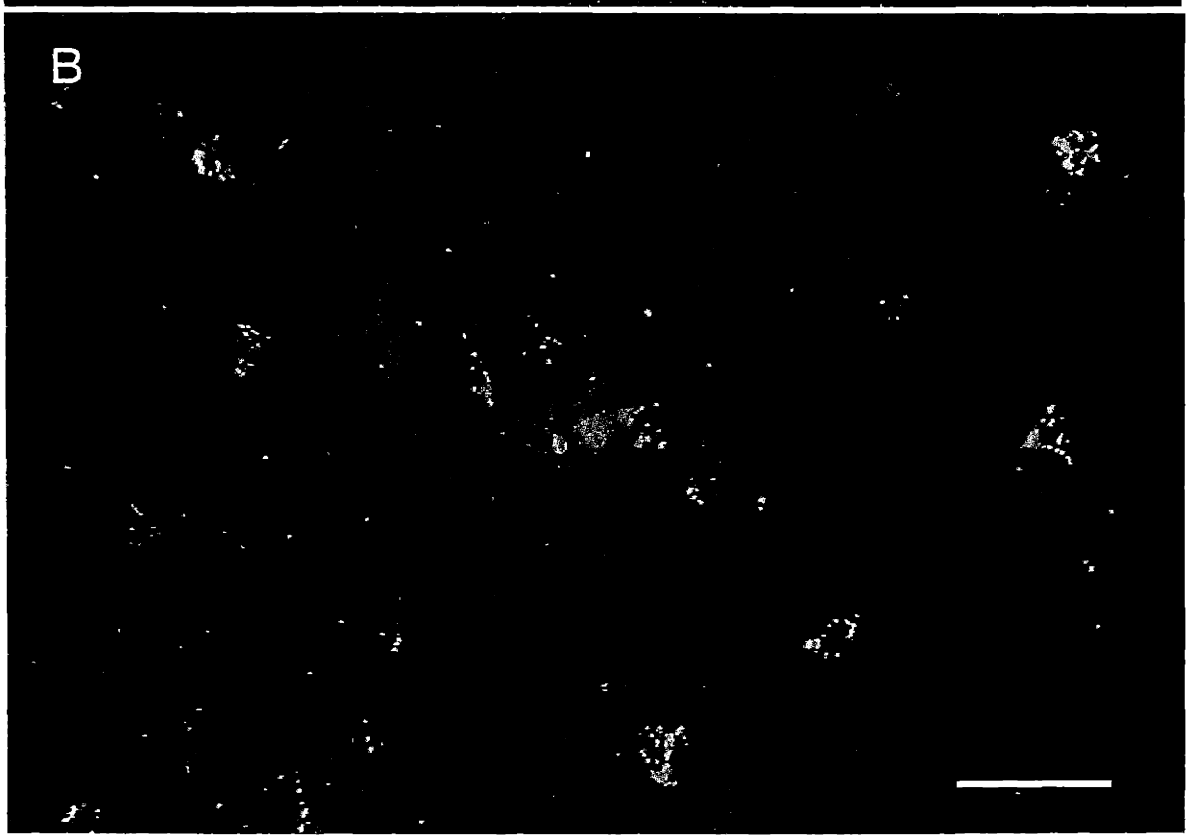
B

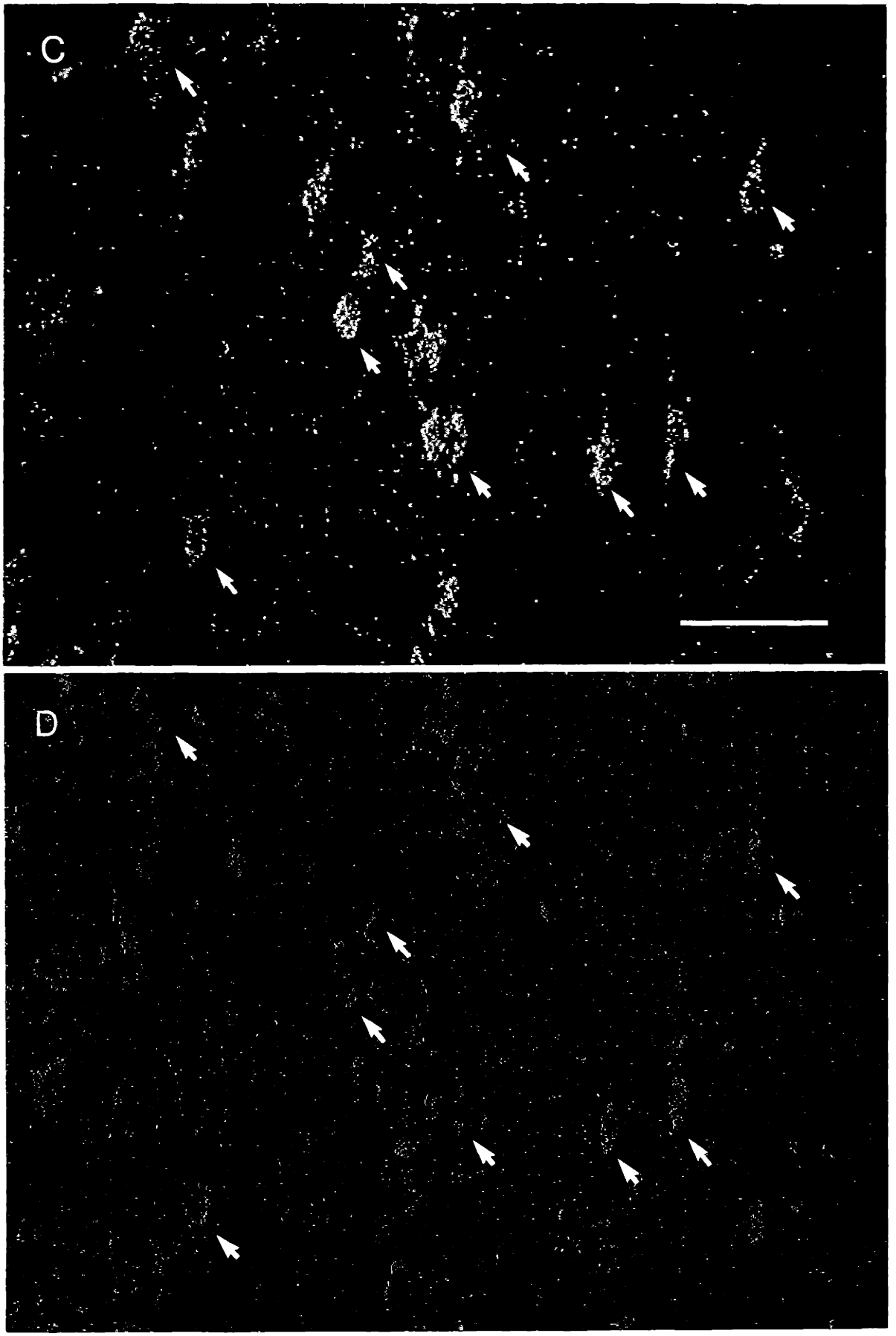
C
D

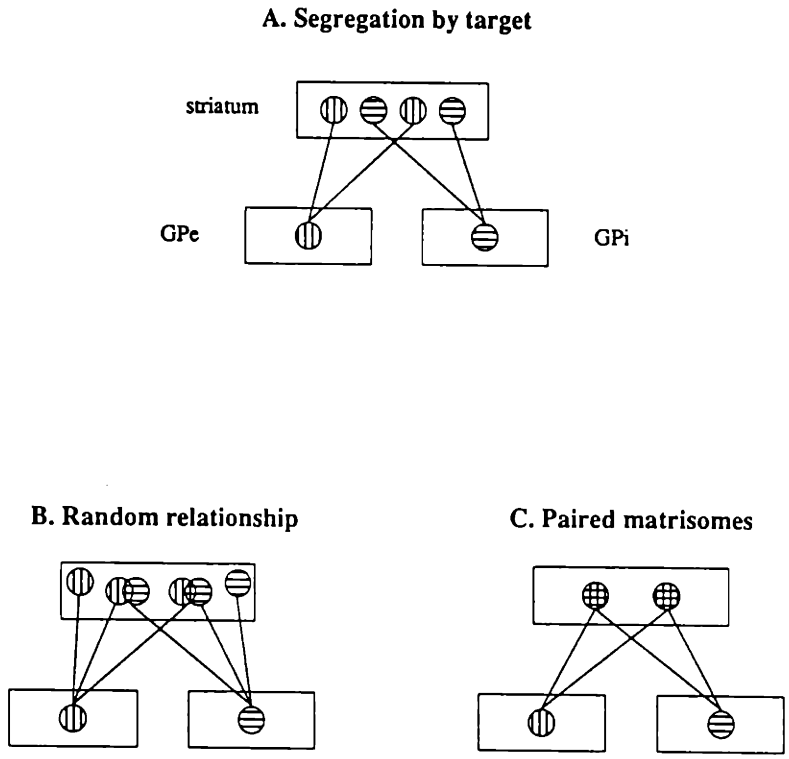

Fig. 4–8. Three models of striatal output organization. A. Matrisomes might project to only a single target nucleus. Our results make this unlikely. B. Matrisomes projecting to GPe and GPi might be randomly organized with respect to each other. C. All matrisomes that converge on a single site in GPe might also converge on a single site in GPi.

CHAPTER 5. INPUT-OUTPUT ORGANIZATION OF THE PRIMATE SENSORIMOTOR STRIATUM

> One often hears of writers that rise and swell with their subject, though it may seem but an ordinary one. How, then, with me, writing of this Leviathan? Unconsciously my chirography expands into placard capitals. Give me a condor's quill! Give me Vesuvius' crater for an inkstand! Friends, hold my arms!
>
> - Herman Melville, *Moby Dick*

> The only difference, after all their rout,
> Is, that the one is in, the other out.
>
> - Charles Churchill, *The Conference (1764)*

ABSTRACT

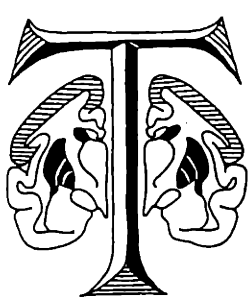

O DETERMINE the relationship between sensorimotor cortical inputs to and pallidal outputs from the striatum, we have combined electrophysiological recording, stimulation, anterograde tracers, retrograde tracers, and immunohistochemistry in single primate brains. 1) Divergent inputs to the striatum from body part representations in cortex can reconverge on specific locations in GPe and GPi. Anterograde and retrograde injections in corresponding parts of cortex and GP labeled the same sets of matrisomes. Dispersed sets of input matrisomes can thus act together as output matrisomes, and specific loci in GPe and GPi may reintegrate information from distributed sets of matrisomes concerned with the same body part. This reconvergence suggests that the divergence of the sensorimotor projection to the striatum, rather than existing to innervating multiple output systems, may increase the lateral interactions between sensorimotor matrisomes and other striatal compartments. 2) GPe and GPi contain

small input modules that may convey cortical information in parallel. Matrisomes projecting to some regions of GPe and GPi are selectively avoided by sensorimotor cortical inputs, yet these GP regions are very near those receiving sensorimotor matrisome inputs. Overall, the systematic convergence and divergence of matrisome connections may allow the putamen to sort cortical information to discrete, paired regions of GPe and GPi.

INTRODUCTION

Current models of basal ganglia processing emphasize a series of stages in which cerebral cortical information is sent first to the striatum, then to the pallidum and substantia nigra, and then to the thalamus before being sent back, presumably transformed, to the cortex. Such models no doubt oversimplify -- for instance they imply a hierarchical, non-parallel model of motor control that does not entirely fit the electrophysiological evidence (Crutcher and Alexander, 1990), and they ignore the complicated back-projections between the two segments of the pallidum and the subthalamic nucleus (Smith and Bolam, 1990; Kincaid et al., 1990; Carpenter and Jayaraman, 1991). Nonetheless, the models have been productive in explaining and predicting both research and clinical results. But progress has been hindered by technical limitations that force most studies of the basal ganglia to focus on a single nucleus or stage of processing. Thus, although there have been many studies of the corticostriatal projection, and many of the striatopallidal projection, little is known about the relationship between the two.

Most corticostriatal neurons synapse directly on striatal output neurons. The relationship between corticostriatal and striatopallidal neurons is therefore fundamental to the way the basal ganglia process information and control movement. Corticostriatal inputs and striatopallidal outputs are organized into compartments or modules within the striatum, rather than being smoothly topographically organized. Tract tracing experiments suggest that a single small region of a given cortical area projects divergently to several such modules (which

may also receive convergent inputs from other parts of the cortex), and a given region of any one of the four striatal target nuclei (GPe, GPi, SNr, and SNc) receives convergent projections from striatal modules similar in shape and size to the input modules.

Why might this modularity exist? Perhaps it is a convenient way for the striatum be to sort different inputs into different output channels. Our recent work provides evidence that these channels are not distinguished by their target nuclei (chapter 4), but it might be that they are aimed at different regions within each target nucleus. A modular, matrisomal organization might also allow lateral interaction between many different inputs.

In this study we have combined electrophysiological recording, stimulation, anterograde tracers, retrograde tracers, and immunohistochemistry to determine in single primate brains the relationship between striatal inputs and outputs. We have focused on sensorimotor regions of the cortex, striatum, and pallidum, to address the following questions. 1) Are input and output zones in the striatum randomly organized with respect to each other, or do sets of matrisomes picked out by one characteristic share any others? For instance, do the multiple matrisomes innervated by a single cortical site have the same output, and, conversely, do the multiple matrisomes innervating a single pallidal site have the same input? 2) Does the relationship between input and output matrisomes vary with cortical input or with the particular region of the pallidum targeted? 3) Is there a modular organization of the pallidum that reflects the modular organization of the striatal matrix?

METHODS

Surgeries, electrophysiology, tracer injections, histology, and injection site reconstructions were performed as described previously (chapters 2, 3, and 4). Briefly, motor and somatosensory cortex were mapped bilaterally in 15 adult squirrel monkeys (*Saimiri sciureus*) maintained under ketamine anesthesia after an

initial small dose of sodium pentobarbital. Anterograde neuronal tract tracers were then injected in defined parts of the cortical body maps, and retrograde tracers were stereotaxically injected in GPe and GPi.

To maximize the number of differentiable tracers per hemisphere, we tried many anterograde and retrograde tracers in different combinations. Anterograde tracers included ^{35}S–methionine (Met) (Cowan et al., 1972), wheatgerm agglutinin conjugated to horseradish peroxidase (WGA–HRP) (Mesulam, 1978), *Phaseolus vulgaris* leukoagglutinin (PHAL) (Gerfen and Sawchenko, 1984), concanavalin A (Matsubara et al., 1987), Fluoro–Ruby (Schmued et al., 1991), biocytin (King et al., 1989), rhodamine–conjugated latex microspheres (Katz et al., 1984), and unconjugated WGA. Retrograde tracers included WGA–HRP, enzymatically–inactivated WGA–HRP labeled with colloidal gold (HG) (Basbaum and Menetrey, 1987), the beta subunit of cholera toxin (CTB) (Luppi et al., 1987), Fluorogold [Schmued](Schmued and Fallon, 1986), Fast Blue [Bentivoglio](Bentivoglio et al., 1980), and tetanus toxin fragment C [Dumas](Dumas et al., 1979). Variables we considered in choosing compatible tracer pairs included cross–reactivity, compatibility of perfusion and histological processing, survival times, typical injection site size, the need for serial versus single–section analysis, and, of course, strength of labeling.

Brains were examined for distribution of the tracers, and for immunohistochemical localization of enkephalin and tyrosine hydroxylase in serial 40 μm coronal sections. Met and CTB, and HG and CTB, could also be analyzed in doubly stained single sections. Anteroposterior levels of sections were assigned according to the atlas of Gergen and McLean (Gergen and MacLean, 1962).

RESULTS

Injection pairs. The results of the stimulation and recording mapping have been described previously (chapters 2, 3). In 13 monkeys, 25 hemispheres

contained one or more pairs of anterograde and retrograde tracer injection sites, in which the anterograde tracer was placed in a electrophysiologically-identified region of motor or somatosensory cortex, and the retrograde tracer was placed in GPe or GPi. Of the many anterograde and retrograde tracers tried, the four that produced the most robust labeling and were most compatible with each other were CTB, HG, Met, and WGA-HRP. We confirmed our previous findings that there was no significant difference in the extent of anterograde labeling by ^{35}S-methionine or WGA-HRP [F/G '90 abstr](Flaherty and Graybiel, 1990), or of retrograde labeling by CTB or HG (chapter 4). The typical injection site size varied with tracer, HG tending to produce the smallest injection sites, and CTB the second smallest.

Most monkeys had, in each hemisphere, injections of ^{35}S-methionine and WGA-HRP in different cortical sites, and CTB and HG in different pallidal sites. Such monkeys had up to 8 separate pairs of anterograde and retrograde labeling to compare per brain. In all, there were 76 independent pairs of anterogradely and retrogradely labeled projection fields in the striatum that could be compared. Anterograde-retrograde tracer pairs are described in Tables 5-1 and 5-2. Anterograde-anterograde and retrograde-retrograde pairs are not listed, but have been previously described (chapters 3 and 4).

Anterograde tracer injection sites, ranging in size from 0.5 mm diameter to 2 mm wide by 10 mm long, were placed in a variety of electrophysiologically-identified sites in either motor cortex (area 4) or somatosensory cortex (areas 3a, 3b, 1, and 2). Most anterograde tracer deposits were relatively small (1-2 mm diameter) and filled a single body part representation in a given cortical map, such as the foot representation in area 3b. In 7 hemispheres, however, much larger injections were made; for instance, in monkey 35, nearly all of the motor cortex was labeled bilaterally.

Retrograde tracer injections were aimed at regions of the pallidum and substantia nigra that in previous experiments had retrogradely labeled cells in the sensorimotor region of the putamen. Retrograde injection sites ranged from 0.3

mm to 2 mm in diameter. All striatal projections labeled anterogradely from the cortex or retrogradely from the pallidum were distinctly patchy, heavily labeling zones with diameters on the order of 0.2 mm to 2 mm, and sparsely labeling regions in between. The most densely-labeled region of the projection -- the "main field" -- was relatively uniformly labeled. Because these zones were predominantly in the extrastriosomal matrix [G&G,F&G1,F&G2](Giménez-Amaya and Graybiel, 1990; Flaherty and Graybiel, 1991a), we will refer to the zones as matrisomes [G,F,G](Graybiel et al., 1991).

Of the 76 anterograde-retrograde tracer pairs, 38 had GPe injection sites, and 38 had GPi injection sites. Some of the pallidal injections missed the desired area in the pallidum, and retrogradely labeled regions of the striatum which do not receive sensorimotor cortex projections. Others, although they retrogradely labeled part of the sensorimotor putamen, did not label a region that happened to be anterogradely labeled in that case -- for instance a retrograde tracer injection in GPi might label what looked to be the hand area of the putamen whereas the only cortical injection in that hemisphere anterogradely labeled the foot area. In all, of the 76 labeled striatal projection fields, 45 were mismatched, and labeled unrelated regions of the striatum (Fig. 5-1). These injection pairs were not analyzed further in this paper. The other 31 pairs labeled the same general region of the striatum.

Of those 31 pairs, relationships between labeled input and output patches ranged from nearly complete overlap to complete interdigitation. We will present evidence that much or perhaps all of this variation can be attributed to the precise injection site locations of the injections in cerebral cortex and striatal target nuclei.

Matrisomes projecting to a given pallidal site receive similar cortical inputs

Motor cortex input matrisomes innervate output matrisomes projecting to both GPe and GPi. In 4 of the tracer pairs, striatal input matrisomes which were anterogradely labeled by injections of tracer in motor or somatosensory

cortex overlapped striatal output matrisomes projecting to the pallidum. Two of these pairs had output matrisomes labeled by tracer injections in GPe; the other 2 were labeled by injections in GPi.

Thus, injections of retrograde tracer in either GPi or GPe could label matrisomes which had a systematic, patch-for-patch overlap with sensorimotor cortex input matrisomes (Figs. 5–2 and 5–3). Not only the location, but also the number, shape, orientation and size of the input and output matrisomes was similar in tissue sections where both types of matrisomes were labeled. However, as noted above, the larger anterograde injection sites tended to label a greater extent of the striatum.

The cortical and pallidal injection sites which labeled overlapping matrisomes are shown in Fig. 5–4, and the stereotaxic coordinates of the pallidal sites are given in Tables 5–1 and 5–2. Both of the GPe injection sites were in roughly the same region of GPi. This was also true of the two GPi injection sites. Moreover, the GPe and GPi injection sites were related to each other: the GPi injection sites were about 1.5 mm posterior, and 1.0 mm ventral, from the GPe injection sites. This is compatible with the two sets of injection sites being along the same radially oriented fibers leaving the putamen. It is also roughly the same stereotaxic relation that has previously been shown to produce overlap of GPe- and GPi-output matrisomes when the regions are doubly labeled in a single brain (chapter 4).

Divergent corticostriatal projections from a known body part representation can reconverge on the pallidum. Most of our anterograde injections were in regions of cortex representing the foot, and all of the 4 injection site pairs in which there was excellent input-output matrisome overlap matrisomes happened to have cortical injections in the foot region of the somatosensory body map. Three pairs had anterograde injection sites in the foot region of area 4, and one in the foot region of area 3b. The precise input-output alignment shown in Figs. 5–2 and 5–3 therefore indicates that the GPe and GPi tissue at the injection sites received convergent inputs from the divergent foot

input patches in the striatum.

There were fewer hemispheres in which we could compare matrisomes outputs to inputs from other cortical body part representations, to see if reconvergence was a general rule. Some evidence that it is comes from one hemisphere with an anterograde tracer injection in the mouth region of area 4. There was a rough correspondence between the inputs labeled by this injection and outputs labeled by an injection in GPi (Fig. 5–5). The patch–for–patch lineup was not as precise as it was in the best foot cases described above (hemispheres 31R, 29R), but was as good as that seen between the foot cortex and GPe projections of hemisphere 39R. The retrograde injection site in this and other hemispheres in which the mouth region of the putamen was retrogradely labeled was somewhat more ventral and caudal in the pallidum than the injection sites that retrogradely labeled the foot region of the putamen.

Adjacent regions of the pallidum receive different corticostriatal inputs.

Of the 31 anterograde–retrograde injection pairs that labeled the same general region of the striatum, 23 labeled striatal matrisomes that predominantly interdigitated with each other. The interdigitation cases did not form a completely discrete category from the "overlap" and "miss" cases; rather, there was a continuum.

In 13 of the 23 injection pairs, the cortical injection sites were in a single body part representation, and we could not rule out the possibility that the output matrisomes, while not overlapping the sensorimotor input matrisomes labeled with that particular injection, might overlap unlabeled sensorimotor cortical inputs from other body part representations. In 10 of the pairs, however, the cortical injection sites were very large, and filled nearly all of either MI or SI. In these cases the output matrisomes did not overlap the MI or SI input matrisomes (Fig. 5–6). This held for both GPi outputs and GPe outputs.

In the hemisphere shown in Fig. 5–6, we could compare output matrisomes

to matrisomes receiving inputs from contralateral MI as well as ipsilateral MI. Fig. 5–6 shows that the set of output matrisomes which did not receive ipsilateral MI inputs did not receive contralateral ones either. However, the fact that ipsilateral and contralateral MI tend to project to different input matrisomes (chapter 3) makes it possible that a given set of output matrisomes does not always receive both ipsilateral and contralateral MI projections. And indeed we found that in a few tracer pairs the output matrisomes had some tendency to preferentially overlap ipsilateral but not contralateral inputs, or vice versa (Fig. 5–7).

The GP injection sites that labeled matrisomes interdigitating with MI or SI input matrisomes were in regions close to those in the overlap pairs (Fig. 5–8). In fact, the average stereotaxic coordinates of the GP injection sites in overlap and interdigitation pairs did not differ significantly. Thus within a given sector of each segment of GP, regions that are near each other can nonetheless receive input from striatal neurons receiving different types of cortical information.

DISCUSSION

These experiments demonstrate that cortical inputs carrying information about single body parts diverge to innervate sets of striatal zones whose outputs show a highly specific reconvergence onto discrete regions in both GPe and GPi. Regions in the pallidum that are very near those receiving the sensorimotor inputs via the striatum do not appear to receive any sensorimotor cortical inputs, suggesting that the pallidum processes at least some cortical information in parallel.

Input matrisomes as output matrisomes

The patch-for-patch line-up of physiologically-identified corticostriatal inputs and striatopallidal outputs can be striking -- but is if fair of us to focus on these cases when there are many in which inputs and outputs interdigitated

or missed each other? The goal of our electrophysiological mapping and tracer injections was to label the same regions of the striatum both anterogradely and retrogradely. As a working hypothesis, we assumed that if we placed an anterograde tracer in the foot region of motor cortex, the appropriate site in GPe or GPi would be the region from which cells responsive to foot movement have been recorded [Crutcher; Mink?](DeLong et al., 1985; Mink and Thach, 1991c). Surgical levels of anesthesia suppress pallidal movement–related activity and stimulation–induced movement, so that we could not make electrophysiologically guided tracer injections in the pallidum as we could in the cortex. We therefore resorted to stereotaxic injections of regions of GPe and GPi that previous experiments showed receive projections from the lateral putamen, the striatal region which receives the bulk of the sensorimotor cortex projections.

Squirrel monkeys are a natural, not an artificially inbred population, and have a normal range of anatomical variation. Stereotaxic coordinates are only a rough guide of location in any particular animal. It is likely that the range of overlap, interdigitation and miss patterns we saw with different tracer pairs is explained by the fact that many of our stereotaxic injections were not perfectly placed. Thus, pallidal injections were to varying degrees in or out of the region corresponding to the cortical injection site in that tracer pair. An alternate explanation, of course, is that the relationship between input and output matrisomes is random, or varies from animal to animal, and that our best cases of overlap were statistical accidents rather than examples of a fundamental principle.

Three pieces of evidence support the former explanation. First, the cases shown in Figs. 5–2 through 5–4 have input–output overlap that is systematic, not random. Even if the overlap between any individual input and output matrisomes could be ascribed to chance, what is remarkable is the precision with which the entire set of labeled input matrisomes overlaps the output set, over nearly the entire mediolateral and rostrocaudal extent of the projection. The precision of the overlap was very similar to that seen between input matrisomes labeled by

different physiologically-guided anterograde tracer injections in homologous body part regions of MI and SI (chapters 2, 3). Second, input-output overlap did not crop up in random hemispheres, but occurred only when the retrograde tracer was injected in a particular region of either GPe or GPi. These pallidal regions were roughly those that the radial orientation of the striatopallidal projection would predict would retrogradely label the sensorimotor region of the putamen. Third, injection sites in GPe and GPi that retrogradely labeled sensorimotor cortical input zones bore a roughly constant relation to each other, as well as to the cortical injection site.

Parallel inputs to the pallidum

Sites in GP which are near the sites receiving input from sensorimotor matrisomes may receive inputs from matrisomes that, although they are also in the lateral putamen, do not get strong sensorimotor cortical input. What inputs might these be, and what might this mean for basal ganglia processing? The overall rostrocaudal topography of the corticostriatal projection makes the premotor cortex and parietal regions such as area 5 likely possibilities. Inputs from contralateral motor cortex are another possibility, because contralateral motor cortex sends inputs to matrisomes which are largely separate from those innervated by ipsilateral area 4 (chapter 3), and because the present experiments provide evidence that pallidal output matrisomes may in some cases receive inputs preferentially from the motor cortex of one hemisphere rather than the other. This suggests that the distinction made in the striatum between information about left and right sides of the body is maintained during basal ganglia processing at least until the pallidum.

The fact that some cortical areas send inputs to matrisomes that innervate the pallidum in parallel rather than convergently does not, of course, rule out the possibility that there is a great deal of convergence in the pallidum. Morphological studies indicate that whereas striatal neurons have relatively

confined terminal arbors [Parent](DiFiglia et al., 1982; Smith and Parent, 1986; Hazrati and Parent, 1992), pallidal neurons have widespread dendritic arbors oriented at right angles to the incoming striatal axons, and consequently integrate many striatal inputs [Percheron](Percheron et al., 1984; Percheron and Filion, 1990). Such a morphology does not, however, rule out the possibility that the basal ganglia's parallel processing of some cortical inputs continues through the pallidum; for instance striatal neurons innervating the most distal pallidal dendrites might have much less effect than those synapsing more proximally.

Relationship between GPe- and GPi-projecting matrisomes

In the present study we focused on the relationship between matrisome inputs and outputs rather than on the relationship between different outputs. Nonetheless, because we injected two differentiable retrograde tracers in most hemispheres, it was also possible to analyze the relationship between matrisome outputs to GPe and GPi. These results have been described separately (chapter 4). They demonstrated that GPe- and GPi-projecting matrisomes can sometimes overlap, and that neurons projecting to the two segments are intimately intermingled, even though very few neurons project to both GPe and GPi. The intermingling of GPe- and GPi-projecting neurons in the striatum is compatible with the present result that sensorimotor matrisomes can overlap matrisomes projecting to both GPe and GPi.

The present results add new information about the relationship of output modules in the striatum. In the cases shown in Figs. 5-2 through 5-4, sensorimotor matrisomes overlapped both GPe and GPi matrisomes. This suggests that if those two pallidal sites had been injected with tracer in the same brain, then the same output matrisomes would have been labeled. It also suggests that if a given set of matrisomes all send outputs to a single site in GPe, they also all send outputs to a single, homologous site in GPi. In the double-retrograde tracer pairs described in chapter 4, the projection overlap seen was never as systematic

as it was in the anterograde–retrograde tracer pairs, leaving open the possibility that GPe and GPi matrisomes were randomly oriented with respect to each other. This may have been due to our having by chance never injected exactly corresponding sites in GPe and GPi -- there were many fewer pairs of retrograde injection sites to compare than there were anterograde–retrograde pairs. Support for the idea of homologous or corresponding regions of GPe and GPi comes from the fact that the stereotaxic relationship between the pallidal sites which retrogradely labeled roughly overlapping matrisomes was about the same as the relationship seen here between the sets of GPe and GPi matrisomes that were both anterogradely labeled from sensorimotor cortex. The hypothesis is also supported by somatotopic mapping in the alert monkey, which demonstrates body maps in roughly the regions we injected [DeLong](DeLong et al., 1985).

The present results suggest, then, that there exist sets of matrisomes which share three properties: they all receive inputs from the same regions of cortex, they all project to a single region in GPe, and they all project to a single region in GPi. Just how precisely these three properties are coextensive is not known; there might be some sloppiness in the system such that of all the matrisomes projecting to a given region in GPi, some of them projected to one region of GPe, and some projected to another. Such sets of matrisomes might act as a functional as well as anatomical units, or different types of processing might occur in each member of a set of matrisomes.

Reconvergence of body part information in the pallidum

"Ipsilateral sensorimotor matrisomes," which receive inputs from homologous body part regions in areas 4, 3a, 3b, and 1, and are near a different set of matrisomes receiving inputs from the same body part regions in contralateral area 4 (chapters 2, 3)
correspond to the discrete zones with movement–responsive cells recorded in the striatum of alert monkeys [Crutcher, Liles](Crutcher and DeLong, 1984; Liles and

Updyke, 1985). Their relation to striatal microexcitable zones [Alex](Alexander and DeLong, 1985a) is not known. The fact that maps of different sensorimotor modalities kept separate in the cortex project to the same matrisomes in the putamen, but that there are nonetheless multiple matrisomes receiving input from a given body part suggests that the striatum is making some new distinction between sensorimotor modules. It has long been hypothesized that output matrisomes selectively projected to different striatal target nuclei [Divac, Feger, JC, GA, Selemon](Divac, 1983; Feger and Crossman, 1984; Jiménez–Castellanos and Graybiel, 1989a; Giménez–Amaya and Graybiel, 1990; Selemon and Goldman–Rakic, 1990). If this were true, then a set of sensorimotor matrisomes might exist to project selectively to only one striatal target nucleus (Fig. 5–9A). A related possibility is that the set of matrisomes might project to both GPe and GPi, but individual matrisomes would project only to one or the other target (Fig. 5–9B). Such channeling would have significant physiological implications, because GPe and GPi have such different effects on basal ganglia processing and movement control.

Three pieces of evidence rule out both these possibilities. First, the present work shows that sets of sensorimotor matrisomes project systematically to both GPe and GPi. Second, individual matrisomes projecting to GPe and GPi are not segregated in the striatum; rather, GPe and GPi–projecting neurons are intermingled (chapter 4). Third, the roughly constant stereotaxic relationship between the GPe and GPi sites labeled by sensorimotor inputs -- the same relationship as that between GPe and GPi sites that retrogradely label the same region of the striatum (chapter 4) -- suggests that GPe- and GPi–projecting matrisomes may be the same.

A third possible function for the multiplicity of matrisomes receiving input from a given sensorimotor cortical body part representation is that different matrisomes channel their outputs to different sites within both GPe and GPi (Fig. 5–9C), sites which might have different physiological roles or connections. Our evidence that all or nearly all of the sensorimotor matrisomes receiving input

about a specific body part can reconverge on a single GP region makes this unlikely.

We therefore propose the model of corticostriatopallidal circuitry shown in Fig. 5-9E, in which divergent inputs concerned with a given body part reconverge on single sites in both GPe and GPi. Of the assumptions on which this model is based, the least certain is the evidence for the claim that if retrograde tracer were placed in somatotopically homologous sites of GPe and GPi, it would label exactly the same matrisomes, i.e. that the GPe and GPi output matrisomes are identical. Our retrograde double-labeling experiments (chapter 4) did not completely rule out the hypothesis that GPe and GPi matrisomes are randomly distributed or offset with respect to each other (Fig. 5-9D). The anterograde-retrograde comparisons provide evidence against it, however: it would be impossible for every input matrisome in a set to overlap every output matrisome converging on one region of GPe, and also to overlap every output matrisome converging on one region of GPi, while still having some output matrisomes project to one of the two pallidal regions and not the other.

To test the precision with which GPe and GPi-projecting matrisomes overlap, it would be useful to have an independent way of identifying homologous regions of GPe and GPi -- for instance, through electrophysiological stimulation or recording. For instance, in alert monkeys one could record or stimulate motor activity in the pallidum, locate regions in GPe and GPi with similar somatotopic responses -- for instance, regions responsive to arm movement, and make small retrograde tracers in exactly those sites. Ideally, it would be good to anterogradely label the arm area of motor cortex in the same brain, because although it is likely that pallidal movement-responsive neurons receive their motor inputs from the cortex via the striatum, they might conceivably get them via the subthalamic nucleus, which also receives a strong motor cortical projection. We are currently studying the relationships of subthalamic projection topography to striatopallidal circuitry.

The evidence in the present work for reconvergence of all the matrisomes that receive inputs from the same cortical body part representations raises again the question of why the corticostriatal projection is divergent, if it does not channel the inputs to multiple outputs. One possibility is that the striatum acts as more than a switching station that merely combines certain inputs into matrisomes (or striosomes) and directs them to certain targets. The intermingled striosomes and matrisomes may also interact with each other, along their borders, within the striatum. Thus the projection from a given body part representation would be broken up in the striatum to maximize its ability to interact with neighboring input–output systems, and the results sent to the pallidum and reintegrated. The fractionation of striatal input–output topography is what would be predicted for a system in which both local (within–compartment) and non–local (across–compartment) interactions are important for processing [Nelson/Bower](Nelson and Bower, 1990).

In such a scenario, the borders of striosomes and matrisomes would be important. And there is evidence that such borders are specialized: rings of especially dense staining for neurotransmitter–related compounds such as enkephalin and acetylcholinesterase, as well as glycoconjugate boundaries and myelin staining are often seen around the borders of striosomes, especially in primates [Chesselet/G?, Ragsdale/G?, Faull, Steindler, Quinn, Cole](Beach and McGeer, 1984; Steindler et al., 1988; Cole and Kowall, 1990). Moreover, while the dendrites of some striatal neurons obey striosomal boundaries, others cross them, and may be the mechanism of integration across compartmental boundaries [Bolam, Penny & other Kitai group, Walker/G](Penny et al., 1984; Bolam et al., 1988; Penny et al., 1988; Walker et al., 1991). Border interactions would explain why, even in the most perfect pairings of input–input or input–output matrisomes, there is some slop in segregation, so that inputs to two different systems faintly innervate each other. The imprecision of the projections might thus have a function, rather than being merely a developmental error.

Our evidence that both GPe and GPi may receive the product of such

striatal sensorimotor processing supports the assumption made by the current model of basal ganglia processing, that pathways through GPe and GPi in the basal ganglia, work in tandem to control movement. Because GPe and GPi have opposite ultimate effects on cortical activity, they are often described as being in opposition, or forming a balance of cortical excitation and inhibition. However, their net effects on the cortex could be complementary rather than antagonistic. It might be, for instance, that the net excitatory activity of the GPi pathway facilitated the intended movement, while the net inhibitory activity of the GPe pathway selectively inhibited competing movements or postures [Mink](Mink and Thach, 1991a).

Does divergence and reconvergence occur in other striatal systems?

Although it is common to study a single body part representation and generalize from that to the rest of a body map, it can be misleading; for instance, the cortical hand areas of primates differ from adjacent trunk and mouth areas in having much sparser callosal connections, and in the striatum inputs from mouth regions of ipsilateral and contralateral motor cortex project to the same matrisomes, whereas those from other regions of motor cortex are segregated (chapter 3). The fact that all four of our best overlap pairs had input matrisomes labeled from foot regions of sensorimotor cortex might reflect a fundamental difference between foot inputs and those representing the rest of the body. Three things suggest, however, that it is merely a selection error. First, we made many more anterograde injections in foot regions than in other parts of the body maps. Second, we saw input–output overlap, although somewhat less precise, in one of the two hemispheres in which the mouth region of cortex was injected. The pallidal injection site was slightly ventral to those which had retrogradely labeled foot matrisomes, mirroring the somatotopy demonstrated by recording in alert monkeys [DeLong](DeLong et al., 1985). Third, in many hemispheres the retrograde injections labeled matrisomes that were situated in the correct part of

the putamen to overlap inputs from trunk, arm, or face regions of sensorimotor cortex, even though the appropriate part of the cortex was not labeled in that hemisphere.

Nonetheless, even if it is permissible to assume the input–output relationships described for projections from the foot region apply to all of the sensorimotor putamen, it might not apply to the rest of the striatum. The sensorimotor putamen is specialized -- sensorimotor cortical inputs appear to be denser than other corticostriatal projections, and the sensorimotor putamen is selectively affected in Parkinson's disease [](Kish et al., 1988). On the other hand, inputs to other regions of the striatum are as patchy as the sensorimotor projection [Goldman '77, Selemon '85](Goldman and Nauta, 1977; Selemon and Goldman–Rakic, 1985). And oculomotor inputs from the frontal and supplementary eye fields show the same functionally–relevant convergence that inputs from motor and somatosensory cortex do [Partha/G](Parthasarathy et al., 1992). Non–cortical inputs to the matrix, such as the centromedian–parafascicular complex of the thalamus, also innervate discrete matrisomes [Ragsdale/G ch, Parent, Francois '91??](Ragsdale and Graybiel, 1988; Sadikot et al., 1990); it will be interesting to see how these input matrisomes are organized with respect to the sensorimotor matrisomes. Not all inputs to the matrix are patchy, however. Inputs from SNc seem to be diffuse [Haber?](Lynd–Balta et al., 1991), although different dopaminergic cell groups do selectively innervate striosomes and matrix [JC/G, LFL/G](Jiménez–Castellanos and Graybiel, 1987; Langer and Graybiel, 1989). There is also evidence that cortical inputs from association areas such as the anterior cingulate cortex may be more diffuse than those from primary sensory or motor areas [St. Cyr](Saint–Cyr et al., 1990).

Pallidal output neurons cluster in matrisomes throughout the striatum, not merely in the sensorimotor putamen, and there is some evidence that SNr output neurons do the same [Jc/G, GA/G, Selemon, Desban](Jiménez–Castellanos and Graybiel, 1989a; Giménez–Amaya and Graybiel, 1990; Selemon and Goldman–Rakic, 1990; Desban et al., 1989). Generalizing our pallidal results

would suggest that sensorimotor matrisomes project to discrete regions in SNr as well as in GPe and GPi. This is compatible with a recent report that SNr contains neurons responsive to body movement [Magarinos](Magarinos-Ascone et al., 1992), as well as the eye-movement responsive neurons for which SNr is better known [Hikosaka](Hikosaka and Wurtz, 1983b). On the other hand, there is initial evidence that SNr- and GP-projecting striatal neurons are segregated into separate matrisomes [Kemel abstr, Selemon](Selemon and Goldman-Rakic, 1990), unlike GPe- and GPi-projecting neurons.

One intriguing possibility, suggested by the anatomical and neurochemical homology of GPi and SNr, is that SNr-projecting matrisomes are segregated from those projecting to GPi but partly or completely overlap those projecting to GPe. This would be compatible with evidence suggesting that the caudate nucleus projects more strongly to SNr, and the putamen more strongly to the pallidum. Thus in pathways carrying oculomotor information through the caudate nucleus to SNr, matrisomes receiving inputs from frontal and supplementary eye fields might overlap those projecting to GPe and SNr the way that, in the putamen, motor and somatosensory cortical inputs overlap projections to GPe and GPi.

Such an hypothesis would explain the cell density data described in chapter 4, in which the maximum cell density of patches retrogradely labeled from GPe, GPi, and SN was about 40% each, adding up to more than 100%. That could only occur if the relative distribution of neurons projecting to the three targets varied across striatal regions. It would be unwise to generalize too much from GPi-SNr homology. There are fundamental differences between GPi and SNr pathways through the basal ganglia -- for instance the intimate relationship SNr neurons have with the dopaminergic dendrites of SNc neurons, the strong projection from SNr to the superior colliculus, and the fact that eye movements are not as impaired as body movements in Parkinson's disease. Nonetheless, the possibility that GPi-SNr homology extends to matrisomal organization is attractive because it would help unify what we know about oculomotor and somatomotor processing in the basal ganglia.

TABLES

Table 5-1. Input-output injection site pairs: GPi. Cases are listed in order of decreasing overlap in the putamen between tracers transported from the cortex and GPi. * = projection from the contralateral hemisphere, ft = foot region, mth = mouth region, hnd = hand region, trk = trunk region, A = anterior, H = horizontal, L = lateral.

	cx.	cx.	cx.	body	GPi	GP coordinates			
Result	Case	tracer	area	part	tracer	A	H	L	Figs.
overlap	31R	HRP	4	ft	CTB	9.0	11.5	6.5	5-1, 5-3A, 5-8A
"	39R	Met	4	ft	CTB	10.0	12.5	6.0	5-3C, 5-4
overlap/interdig.	40L	Met	4	mth	CTB	9.0	11.5	6.0	5-5
"	40L	HRP	4*	mth	CTB	9.0	11.5	6.0	
interdig.	35L	HRP	4	all	HG	9.0	12.5	6.5	5-6, 5-8A
"	31L	HRP	3a	hnd	CTB	10.5	12.5	5.5	
"	34L	Met	4*	leg	HG	9.5	13.0	7.0	
"	34R	HRP	3b	all	HG	9.5	13.0	7.0	
"	34L	HRP	3b	all	HG	9.5	13.0	7.0	
"	34R	Met	4	leg	HG	9.5	13.0	7.0	
"	39R	HRP	4	hnd	CTB	10.0	12.5	6.0	
"	39L	HRP	4	ft	CTB	10.0	12.5	4.5	
"	31L	Met	3a	ft	CTB	10.5	12.5	5.5	
"	35L	Met	4*	all	HG	9.0	12.5	6.5	5-6, 5-8A
interdig/miss	36R	Met	3b	trk	CTB	8.5	12.0	6.5	
"	37R	HRP	4*	ft	CTB	9.0	11.5	6.5	
miss	28R	Met	1	ft	CTB	9.0	12.0	6.5	
"	30R	HRP	3b	hnd	CTB	8.5	13.5	7.0	
"	40R	Met	4*	mth	CTB	9.5	11.5	6.0	
"	40R	HRP	4*	ft	CTB	9.5	11.5	6.0	
"	40L	Met	4*	ft	CTB	9.0	11.5	6.0	
"	33R	Met	3b	all	CTB	8.5	12.5	7.0	
"	40R	HRP	4	mth	CTB	9.5	11.5	6.0	
"	40R	Met	4	ft	CTB	9.5	11.5	6.0	
"	39L	Met	4	hnd	CTB	10.0	12.5	4.5	
"	40L	HRP	4	ft	CTB	9.0	11.5	6.0	
"	36R	HRP	4*	ft	CTB	8.5	12.0	6.5	
"	37L	HRP	4	ft	CTB	9.0	11.0	6.0	
"	37L	Met	3b	trk	CTB	9.0	11.0	6.0	
"	33R	HRP	4	leg	CTB	8.5	12.5	7.0	
"	30L	Met	3b	hnd	CTB	8.5	14.0	7.5	
"	30L	HRP	3b	ft	CTB	8.5	14.0	7.5	
"	33L	HRP	4*	leg	CTB	8.5	11.5	7.0	
"	33L	Met	3b	all	CTB	8.5	11.5	7.0	
"	36L	HRP	4	ft	CTB	8.0	12.0	6.5	
"	36L	Met	3b	trk	CTB	8.0	12.0	6.5	
"	30R	Met	3b	ft	CTB	8.5	13.5	7.0	

Table 5-2. Input-output injection site pairs: GPe. Cases are listed in order of decreasing overlap in the putamen between tracers transported from the cortex and GPe. Abbreviations are as in Table 1.

Putamen relation	Case	cx. tracer	cx. area	body part	GPe tracer	GP coordinates A	H	L	Figs.
overlap	29R	HRP	3b	ft	CTB	10.5	13.0	7.0	5-2, 5-3B, 5-8B
"	39R	Met	4	ft	HG	11.5	13.0	6.5	5-3C, 5-4
overlap/interdig.	39R	HRP	4*	ft	HG	11.5	13.0	6.5	
"	35L	HRP	4	all	CTB	10.5	13.0	7.0	
interdig.	35R	HRP	4*	all	CTB	10.5	13.0	6.5	5-7, 5-8B
"	29L	Met	3b	all	CTB	11.0	13.5	7.0	
"	34R	HRP	3b	all	CTB	10.5	14.0	6.5	5-9
"	35L	Met	4*	all	CTB	10.5	13.0	7.0	
"	29L	HRP	4	all	CTB	11.0	13.5	7.0	
"	34L	Met	4*	leg	CTB	11.0	14.0	7.0	
"	34L	HRP	3b	all	CTB	11.0	14.0	7.0	
"	34R	Met	4	leg	CTB	11.0	14.0	6.5	
"	40L	HRP	4*	mth	HG	9.5	13.5	7.0	
"	39L	Met	4	hnd	HG	11.0	13.0	7.0	
"	39L	HRP	4	ft	HG	11.0	13.0	7.0	
"	36R	HRP	4*	ft	HG	9.0	13.5	6.0	
"	37L	Met	3b	trk	HG	10.5	12.0	7.0	
interdig./miss	35R	Met	4	all	CTB	10.5	13.0	6.5	
"	36L	HRP	4	ft	HG	10.0	13.5	7.0	
miss	37R	Met	3b	trk	CTB	9.0	11.5	6.5	
"	30R	Met	3b	ft	HG	10.0	14.5	7.0	
"	37L	HRP	4	ft	HG	10.5	12.0	7.0	
"	27L	Met	1	ft	CTB	11.0	12.0	5.0	
"	30L	HRP	3b	ft	HG	10.0	13.5	6.5	
"	30R	HRP	3b	hnd	HG	10.0	14.5	7.0	
"	30L	Met	3b	hnd	HG	10.0	13.5	6.5	
"	40R	Met	4	ft	HG	10.0	13.0	7.0	
"	39R	HRP	4	hnd	HG	11.5	13.5	6.5	
"	36L	Met	3b	trk	HG	10.0	13.5	7.0	
"	27R	Met	1	ft	CTB	12.0	13.0	6.0	
"	40L	Met	4	mth	HG	9.5	13.5	7.0	
"	40R	Met	4*	mth	HG	10.0	13.0	7.0	
"	40L	HRP	4	ft	HG	9.5	13.5	7.0	
"	40R	HRP	4	mth	HG	10.0	13.0	7.0	
"	40R	HRP	4*	ft	HG	10.0	13.0	7.0	
"	40L	Met	4*	ft	HG	9.5	13.5	7.0	
"	36R	Met	3b	trk	HG	10.0	13.5	6.0	
"	37R	HRP	4*	ft	HG	10.5	12.0	8.0	
"	37R	Met	3b	trk	HG	10.5	12.0	8.0	

FIGURES

Fig. 5–1. Example of an injection site pair that labeled different regions of the striatum. A. CTB injection site in GPi, and WGA–HRP injection site in the mouth region of motor cortex (hemisphere 40R). The cortical injection site is shown both in coronal section and superimposed on the electrophysiological stimulation map. Straight dotted lines on the surface map = boundaries of Betz cell distribution. Stimulating electrode penetration sites are marked by symbols:
= movement stimulated less than 100 μA, = movement stimulated ≥ 100 μA,
= no stimulated response at 400 μA. B. An overlay drawing of two serial coronal sections through the putamen, in which the input matrisomes labeled from the mouth region are all ventral to the GPi output matrisomes, and never overlap. The GPi output matrisomes label a region approximately corresponding to the hand region of the putamen.

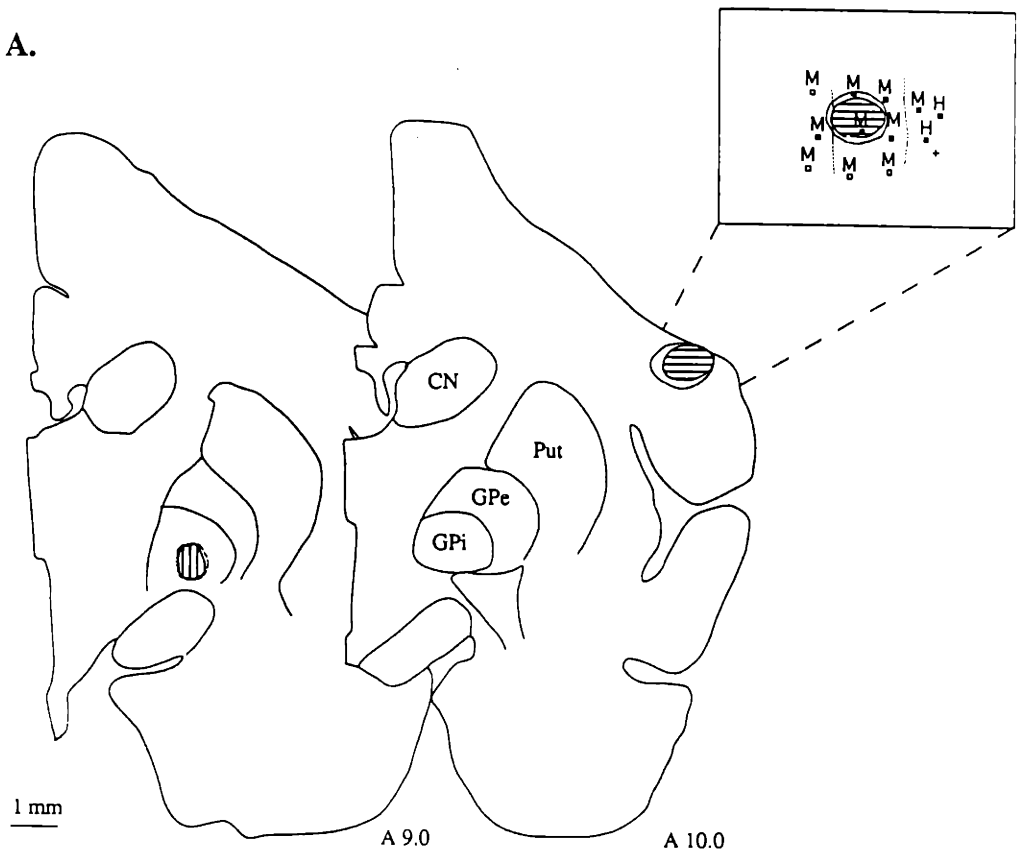
A.
CN
Put
GPe
GPi
1 mm
A 9.0
A 10.0

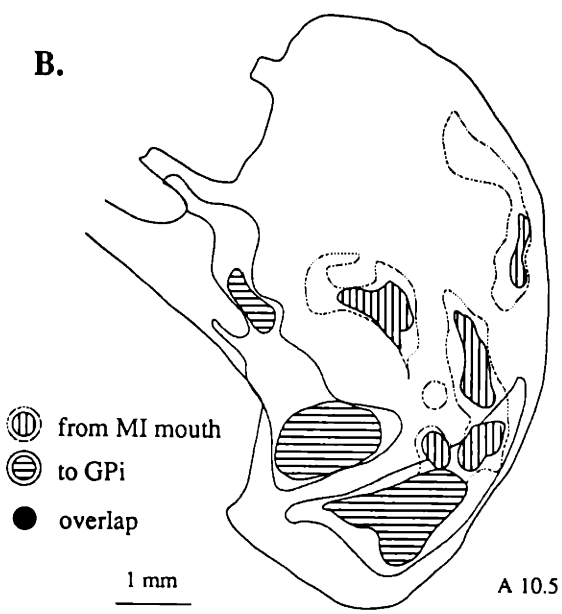
B.
from MI mouth
to GPi
overlap
1 mm
A 10.5

Fig. 5–2. Sets of input matrisomes can be sets of output matrisomes. Tracer injection sites are shown in Fig. 5–3. A. A dark–field photomicrograph of a coronal section (level A 13.0) through the putamen of hemisphere 31R, with input matrisomes anterogradely labeled by an injection of WGA–HRP in the foot region of motor cortex. A'. A serial section with output matrisomes retrogradely labeled by an injection of CTB in GPi. A and A' are also drawn as overlays in Fig. 5–3. B. A coronal section (level A 13.5) through the putamen of hemisphere 29R, with input matrisomes anterogradely labeled by an injection of WGA–HRP in the foot region of somatosensory cortex. B'. A serial section with output matrisomes retrogradely labeled by an injection of CTB in GPe. Borders of the putamen are outlined in white. Scale bar, 1 mm.

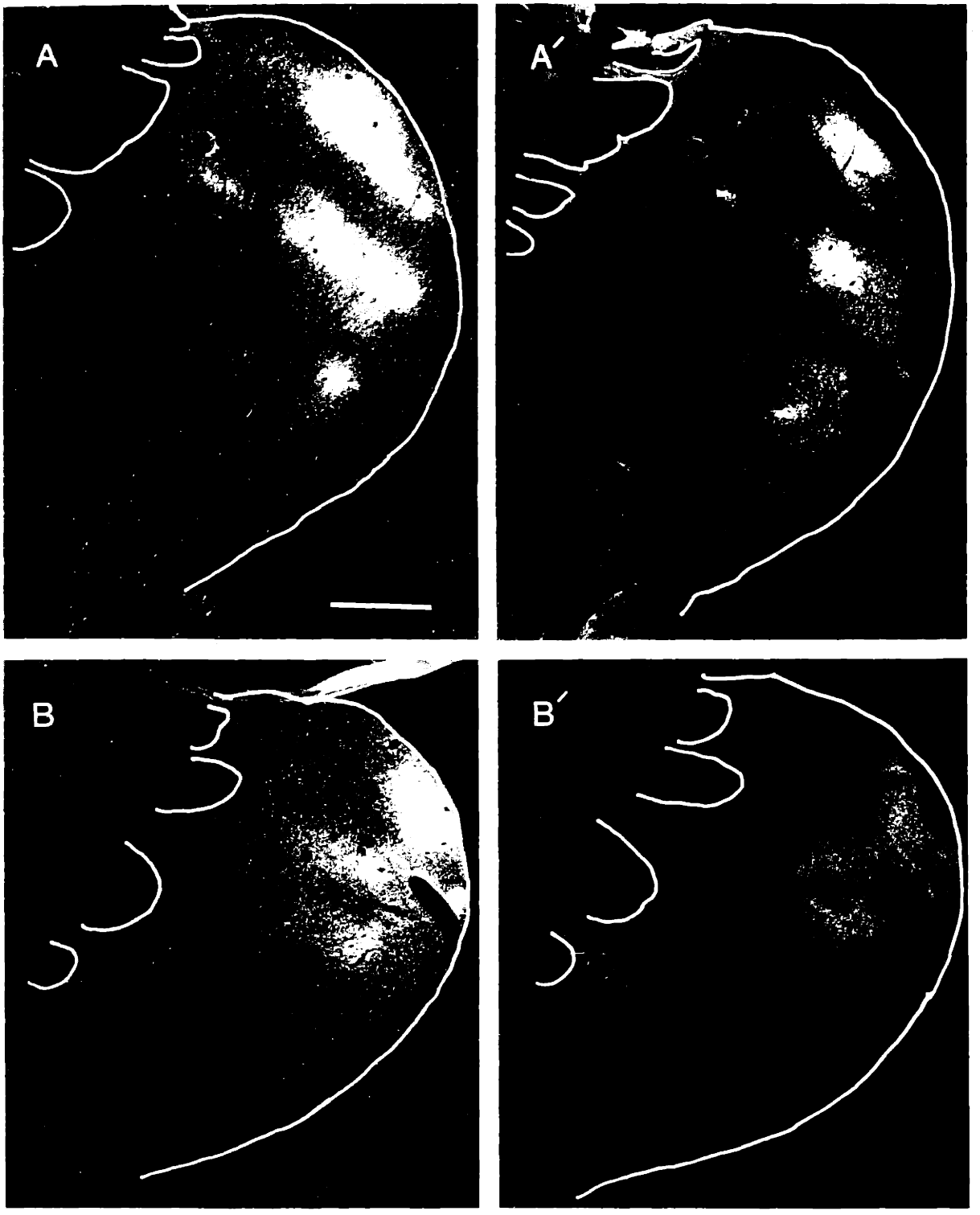
A
A´
B
B´

Fig. 5–3. Sets of input and output matrisomes match over an extended anteroposterior distance. Overlay drawings of pairs of serial sections at intervals through the projection fields in the putamen. Injection sites are shown in Fig. 5–4. A. Foot sensorimotor cortex inputs line up with GPi outputs (hemisphere 31R). The middle pair of sections from which the overlay drawings were made are shown in Fig. 5–2. B. Foot sensorimotor cortex inputs line up with GPe outputs (hemisphere 29R).

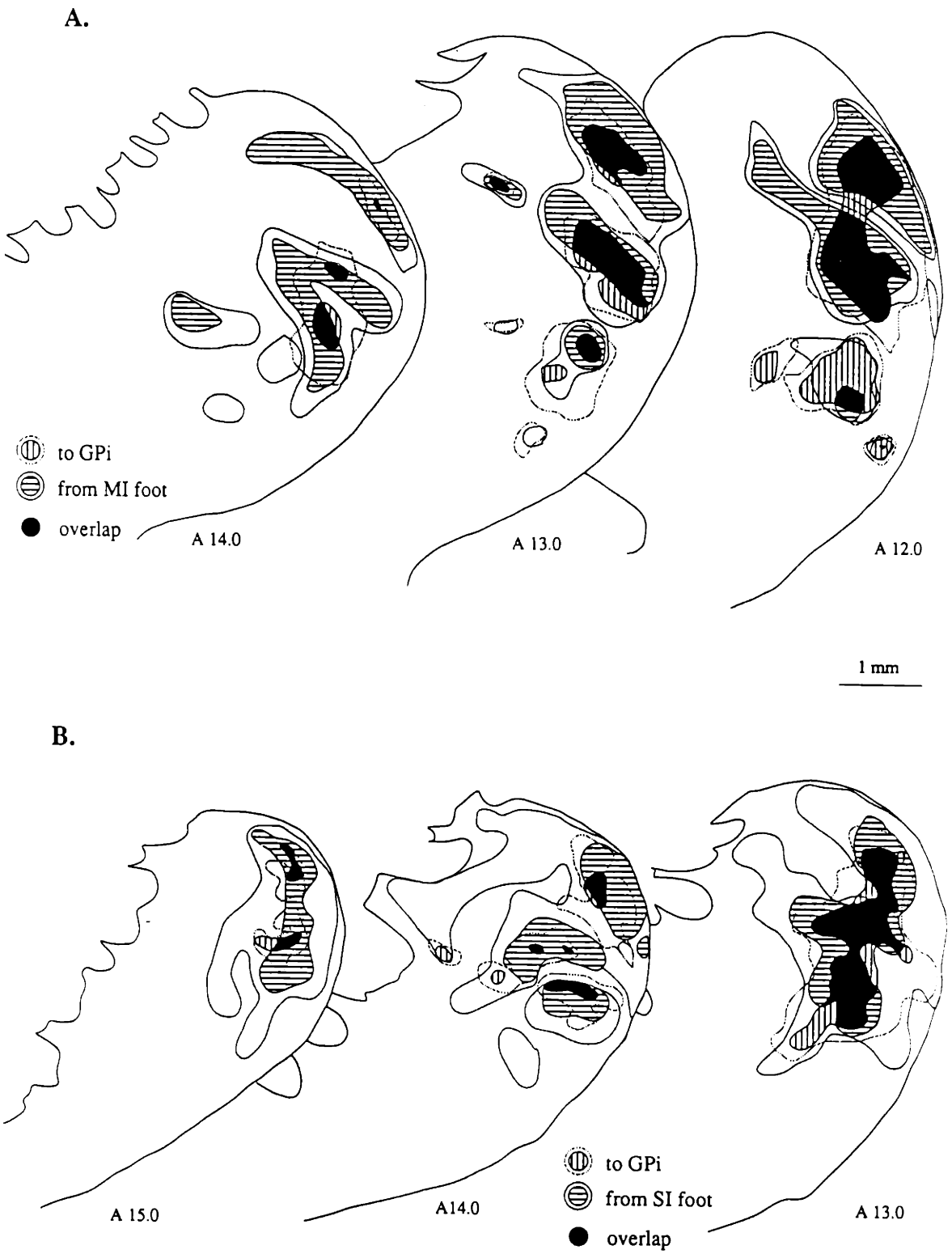
A.
to GPi
from MI foot
overlap
A 14.0
A 13.0
A 12.0
1 mm
B.
A 15.0
A14.0
to GPi
from SI foot
overlap
A 13.0

Fig. 5–4. Two pairs of anterograde and retrograde injection sites that label overlapping input and output matrisomes. Cortical injection sites are shown both in coronal section and superimposed on the electrophysiological stimulation and recording map. Stimulation map conventions are as in Fig. 5–1. Recording penetrations are marked by the following symbols: = area 3a, = area 3b, = area 1, = area 2, = no recorded response. Figs. 5–2 and 5–3 show the corresponding labeling in the putamen.

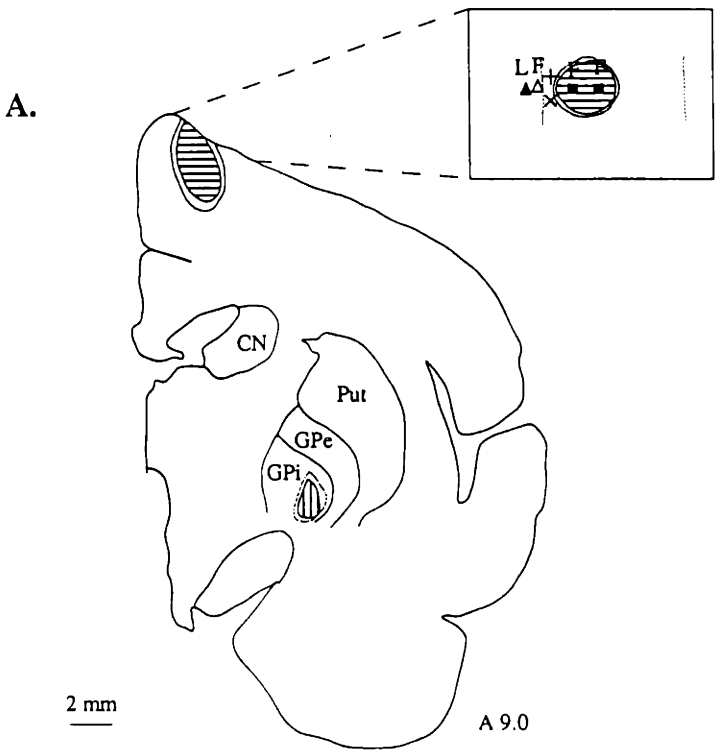
A.
LF
CN
Put
GPe
GPi
2 mm
A 9.0

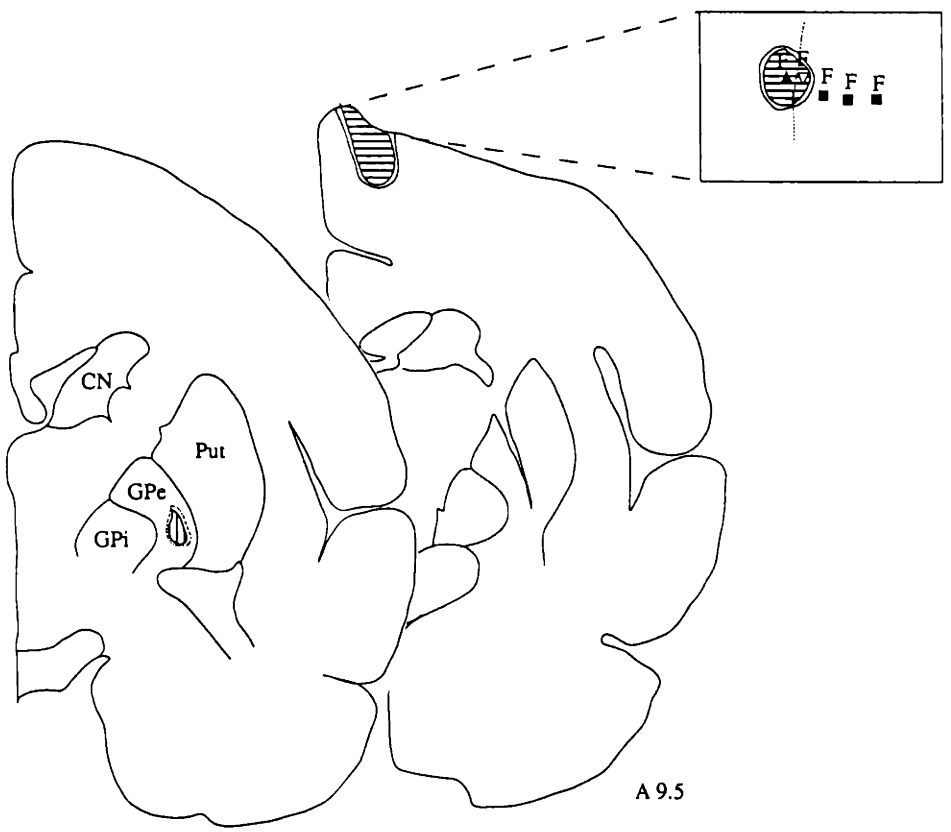
F F F
CN
Put
GPe
GPi
A 9.5

Fig. 5–5. Rough overlap between input matrisomes labeled by an injection in the mouth region of area 4 and output matrisomes labeled by an injection in GPi (hemisphere 40L). A. Anterograde and retrograde injection sites. The cortical injection site is shown both in coronal section and superimposed on the electrophysiological stimulation and recording map. Stimulation and recording map conventions are as in Figs. 5–1 and 5–4. B. Overlay drawings of pairs of serial sections at intervals through the putamen, in which there are increasing amounts of projection field overlap in more caudal sections.

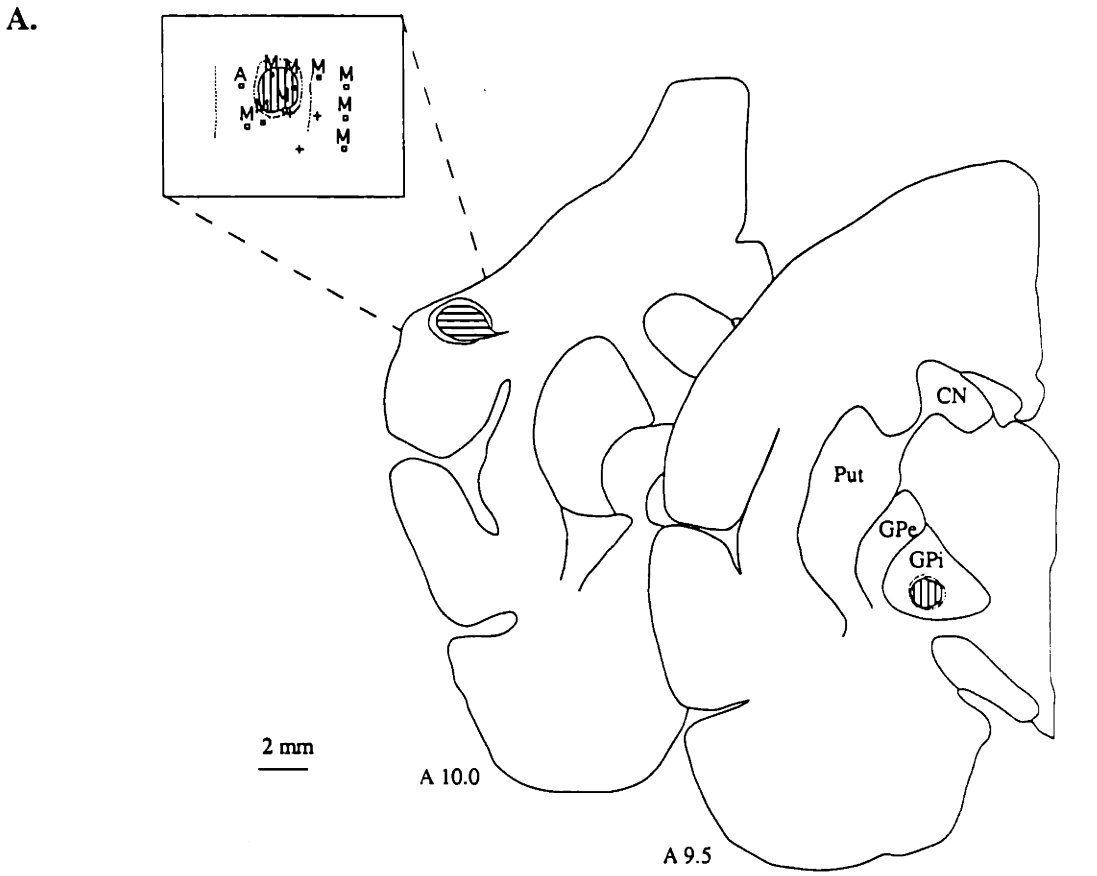
A.
CN
Put
GPe
GPi
2 mm
A 10.0
A 9.5

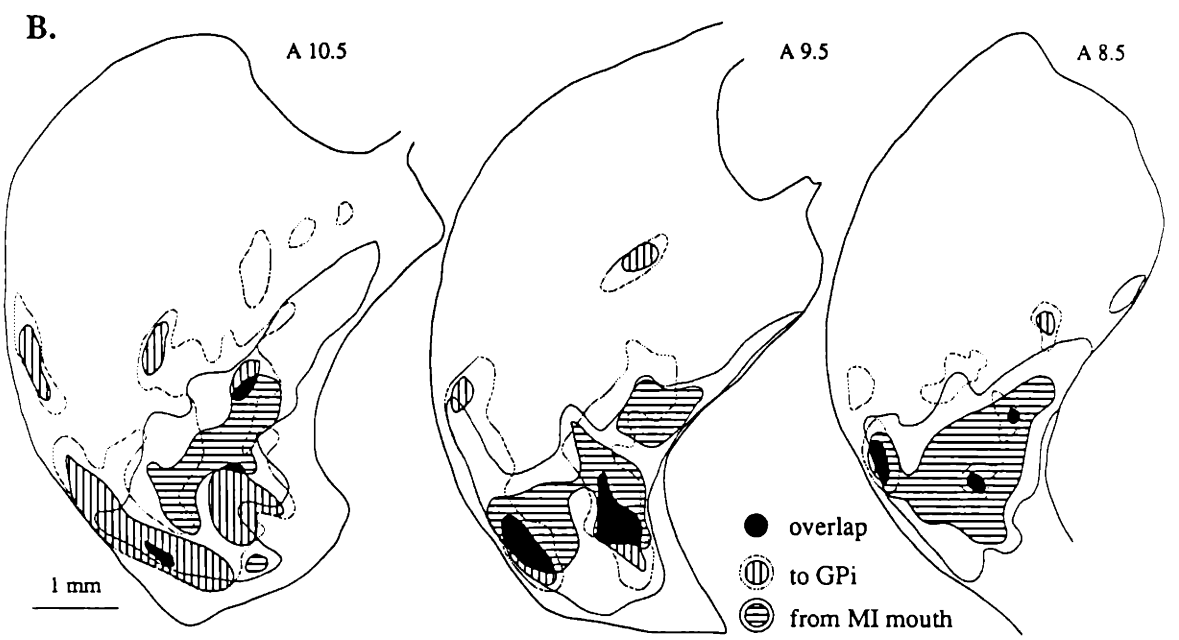
B.
A 10.5
A 9.5
A 8.5
1 mm
overlap
to GPi
from MI mouth

Fig. 5–6. Some GP output matrisomes do not receive motor cortex inputs. A. WGA–HRP injection site filling most of the left motor a Met injection site filling most of the right motor cortex, and and an HG injection site in the left GPi (case 35). Cortical injection sites are shown both in coronal section and superimposed on the electrophysiological stimulation and recording map. Stimulation and recording map conventions are as in Figs. 5–1 and 5– 4. CS = central sulcus. B. Overlay drawings of pairs of serial sections at intervals through the putamen, in which there is predominant interdigitation between labeled input and output patches.

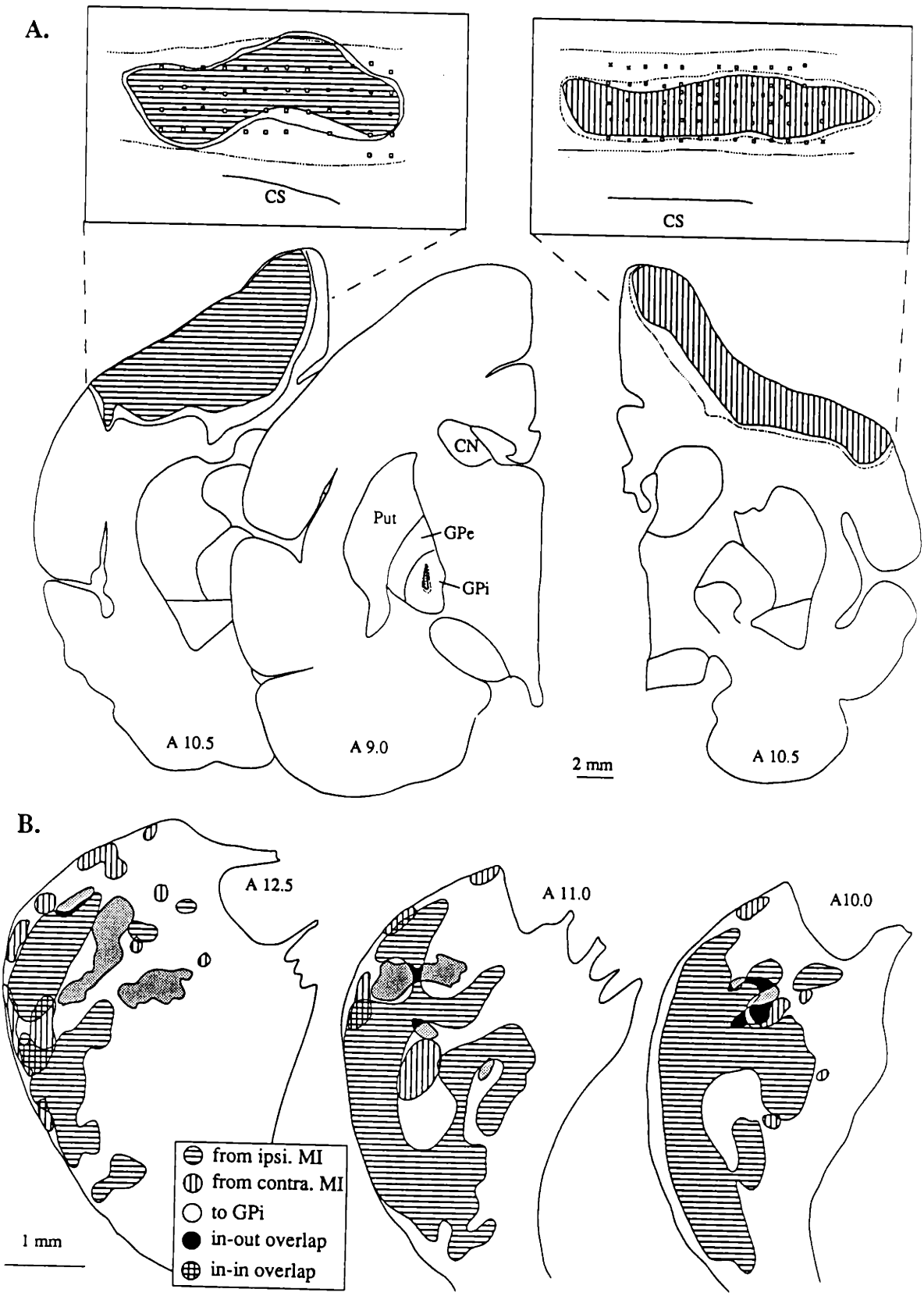
A.
CS
CS
CN
Put
GPe
GPi
A 10.5
A 9.0
2 mm
A 10.5
B.
A 12.5
A 11.0
A10.0
from ipsi. MI
from contra. MI
to GPi
in-out overlap
in-in overlap
1 mm

Fig. 5–7. Some GP output matrisomes receive more input from the motor cortex of one hemisphere than from the other. A. A CTB injection site in GPe (hemisphere 35L). The cortical injection sites are shown in Fig. 5–6. B. An overlay drawing of a pair of serial sections through the putamen, in which the GPe output matrisomes overlap input matrisomes labeled from ipsilateral motor cortex more than those labeled from contralateral motor cortex.

A.

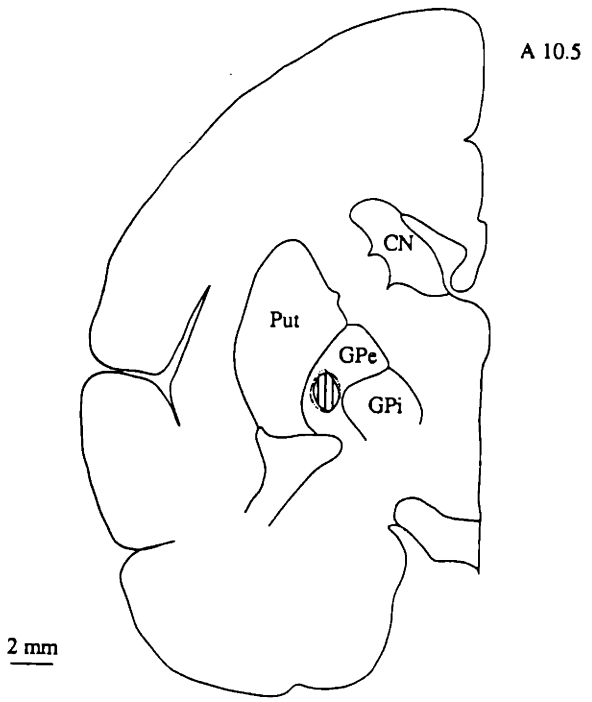
A 10.5
CN
Put
GPe
GPi
2 mm

B.

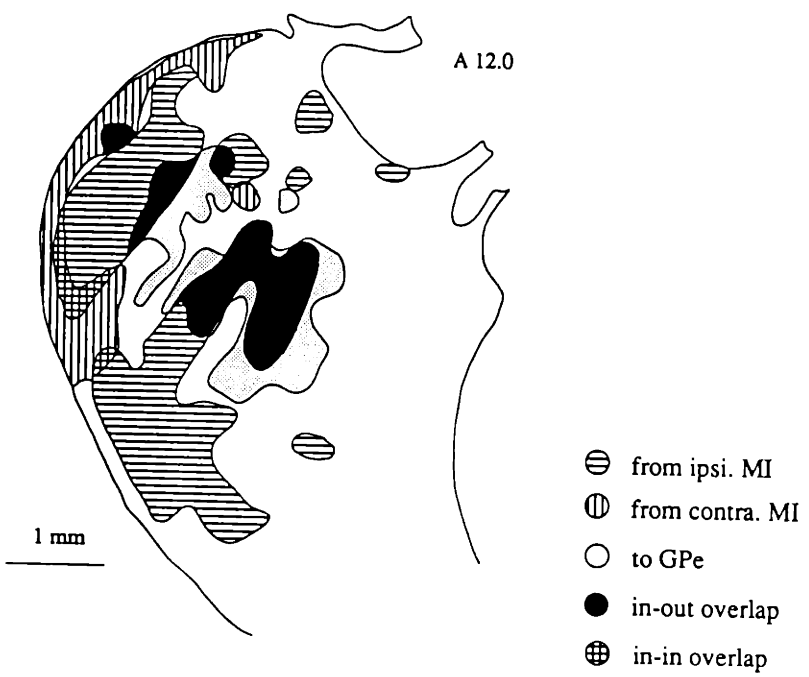
A 12.0
1 mm
from ipsi. MI
from contra. MI
to GPe
in-out overlap
in-in overlap

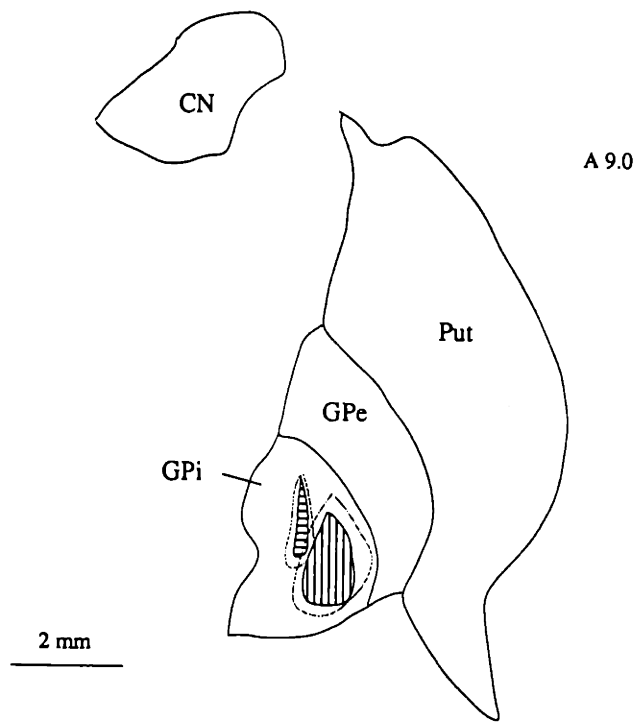

Fig. 5–8 (*above*). Output matrisomes which do not receive sensorimotor inputs project to regions of GP near those which do receive sensorimotor inputs. The injection sites of Figs. 5–3 and 5–6 hemispheres are drawn on standard atlas sections; one has been drawn reversed for ease of comparison. Horizontal hatches mark the HG injection site in hemisphere 35L, which labeled matrisomes receiving little motor cortex input; vertical hatches mark the CTB injection site in hemisphere 31R, which received heavy motor cortex input from the foot region.

Fig. 5–9 (*right*). Five hypotheses about basal ganglia circuitry. See text for descriptions. The evidence in this paper supports hypothesis 5–5E, recovergence in each segment, over the first four hypotheses.

A. Cortical channeling

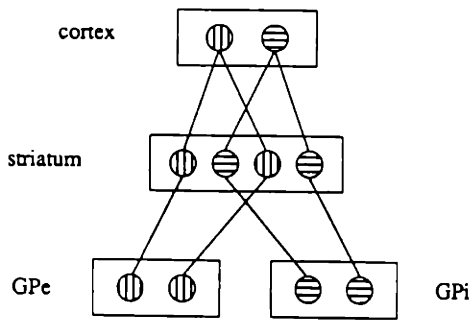

B. Striatal channeling

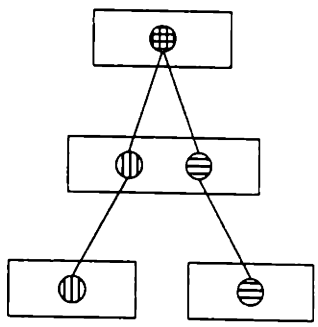

C. Multiple targets in each segment

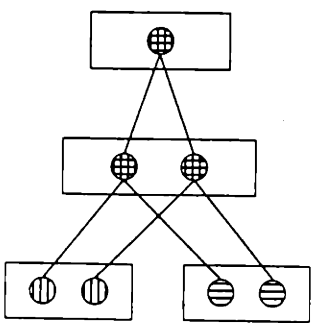

D. Random relation of output matrisomes

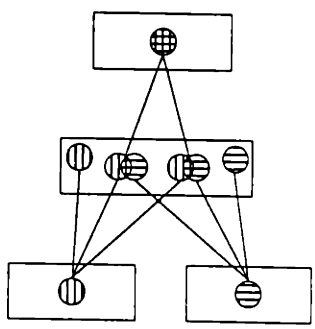

E. RECONVERGENCE IN EACH SEGMENT

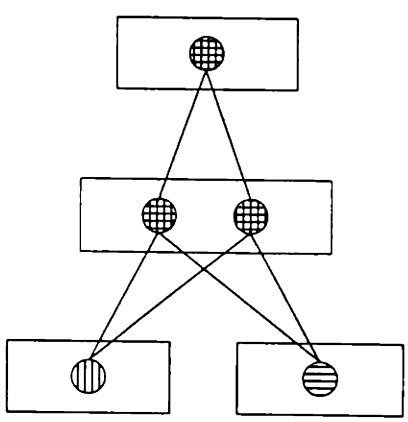

REFERENCES

The ultimate outcome of unrestrained growth, whether of tissues or of references, is death.

- Pathology lecture, Harvard Medical School, 1987

Albin, R.L., A.B. Young and J.B. Penney (1989). The functional anatomy of basal ganglia disorders. Trends Neurosci. *12*:366–375.

Albin, R.L., A.B. Young, J.B. Penney, B. Handelin, R. Balfour, K.D. Anderson, D.S. Markel, W.W. Tourtellotte and A. Reiner (1990). Abnormalities of striatal projection neurons and NMDA receptors in pre–symptomatic Huntington's disease. New Eng.J.Med. *322*:1293–1297.

Alexander, G.E., V.E. Koliatsos, L.J. Martin, J. Hedreen, I. Hamada and M.R. DeLong (1988). Organization of primate basal ganglia "motor circuit": 1. Motor cortex (MC) and supplementary motor area (SMA) project to complementary regions within matrix compartment of putamen. Soc.Neurosci.Abstr. *14*:720.(Abstract)

Alexander, G.E. and M.D. Crutcher (1990). Functional architecture of basal ganglia circuits: neural substrates of parallel processing. Trends Neurosci. *13*:266–272.

Alexander, G.E. and M.R. DeLong (1985a). Microstimulation of the primate neostriatum: II. Somatotopic organization of striatal microexcitable zones and their relation to neuronal response properties. J.Neurophysiol. *53*:1433–1446.

Alexander, G.E. and M.R. DeLong (1985b). Microstimulation of the primate striatum: I. Physiological properties of striatal microexcitable zones. J.Neurophysiol. *53*:1417–1432.

Alheid, G.F. and L. Heimer (1988). New perspectives in basal forebrain organization of special relevance for neuropsychiatric disorders: the striatopallidal, amygdaloid, and corticopetal components of the substantia innominata. Neurosci. *27*:1–39.

Asanuma, C., W.T. Thach and E.G. Jones (1983). Distribution of cerebellar terminations and their relation to other afferent terminations in the ventral lateral thalamic region of the monkey. Brain Res.Rev. *5*:237–265.

Basbaum, A.I. and D. Menetrey (1987). WGA–apoHRP gold: a new retrograde tracer for light– and electron–microscopic single– and double–label studies. J.Comp.Neurol. *261*:306–318.

Bauswein, E., C. Fromm and A. Preuss (1989). Corticostriatal cells in comparison with pyramidal tract neurons: contrasting properties in the behaving monkey. Brain Res. *493*:198–203.

Beach, T.G. and E.G. McGeer (1984). The distribution of substance P in the

primate basal ganglia: an immunohistochemical study of the baboon and human brain. Neuroscience *13*:29–52.

Beckstead, R.M. and C.J. Cruz (1986). Striatal axons to the globus pallidus, entopeduncular nucleus and substantia nigra come mainly from separate cell populations in cat. Neuroscience *19*:147–158.

Beninato, M. and R.F. Spencer (1986). A cholinergic projection to the rat superior colliculus demonstrated by retrograde transport of horseradish peroxidase and choline acetyltransferase immunohistochemistry. J.Comp.Neurol. *253*:525–538.

Bentivoglio, M., H.G.J.M. Kuypers, C.E. Catsman-Berrevoets, H. Lowe and O. Dann (1980). Two new fluorescent retrograde neuronal tracers which are transported over long distances. Neurosci Lett. *18*:25–30.

Bergman, H., T. Wichmann and M.R. DeLong (1990). Reversal of experimental parkinsonism by lesions of the subthalamic nucleus. Science *249*:1436–1438.

Berod, A., B.K. Hartman and J.F. Pujol (1981). Importance of fixation in immunohistochemistry: Use of formaldehyde at variable pH, for the localization of tyrosine hydroxylase. J.Histochem.Cytochem. *29*:844–850.

Besson, M.-J., A.M. Graybiel and B. Quinn (1990). Coexpression of neuropeptides in the cat's striatum: an immunohistochemical study of substance P, dynorphin B and enkephalin. Neuroscience *39*:33–58.

Bolam, J.P., J.F. Powell, S. Totterdell and A.D. Smith (1981). The proportion of neurons in the rat neostriatum that project to the substantia nigra demonstrated using horseradish peroxidase conjugated with wheatgerm agglutinin. Brain Res. *220*:339–343.

Bolam, J.P., P.N. Izzo and A.M. Graybiel (1988). Cellular substrate of the histochemically-defined striosome/matrix system of the caudate nucleus: a combined Golgi and immunocytochemical study in cat and ferret. Neuroscience *24*:853–875.

Brinkman, C. (1984). Supplementary motor area of the monkey's cerebral cortex: short-and long-term deficits after unilateral ablation and the effects of subsequent callosal section. J.Neurosci. *4*:918–929.

Brown, L.L., L.I. Wolfson and S.M. Feldman (1987). Functional neuroanatomic mapping of the rat striatum: regional differences in glucose utilization in normal controls and after treatment with apomorphine. Brain Res. *411*:65–71.

Brown, L.L. (1991). Somatotopic maps in rat striatum: evidence that the striatum plays a role in coordination of the two sides of the body. Soc.Neurosci.Abstr. *17*:453.

Camps, M., R. Cortes, B. Gueye, A. Probst and J.M. Palacios (1989). Dopamine receptors in human brain: autoradiographic distribution of D2 sites. Neurosci. *28*:275–290.

Carlsson, M. and A. Carlsson (1990). Interactions between glutamatergic and monoaminergic systems within the basal ganglia -- implications for schizophrenia and Parkinson's disease. Trends Neurosci. *13*:272–276.

Carpenter, M.B. and A. Jayaraman (1991) Subthalamic nucleus afferents:

anatomical and immunocytochemical features. In G. Bernardi, M.B. Carpenter, G. di Chiara, M. Morelli, and P. Stanzione (eds): The basal ganglia III. New York: Plenum Press, pp. 109–118.

Cenci, M.A., R.J. Mandel, P. Kalen, K. Wictorin and A. Björklund (1990). C–fos induction in intrastriatal grafts of fetal nigral and striatal tissue: functional role of D1 dopamine receptors in graft–host interactions. Soc.Neurosci.Abstr. *16*:469.(Abstract)

Chevalier, G. and J.M. Deniau (1990). Disinhibition as a basic process in the expression of striatal functions. TINS *13*:277–280.

Cole, D.G. and N.W. Kowall (1990). A dyadic patch–matrix scheme does not adequately define the histochemical heterogeneity of the human striatum. Soc.Neurosci.Abstr. *16*:954.(Abstract)

Cowan, W.M., D.I. Gottleib, A.E. Hendrickson, J.L. Price and T.A. Woolsey (1972). The autoradiographic demonstration of axonal connections in the central nervous system. Brain Res. *37*:21–51.

Crutcher, M.D. and G.E. Alexander (1990). Movement–related neuronal activity selectively coding either direction or muscle pattern in three motor areas of the monkey. J.Neurophysiol. *64*:151–163.

Crutcher, M.D. and M.R. DeLong (1984). Single cell studies of the primate putamen. I. Functional organization. Exp.Brain Res. *53*:233–243.

de Keyser, J., A. Claeys, J.P. de Backer, G. Ebinger, F. Roels and G. Vauquelin (1988). Autoradiographic localization of D1 and D2 dopamine receptors in the human brain. Neurosci.Lett. *91*:142–147.

DeLong, M.R., M.D. Crutcher and A.P. Georgopoulos (1985). Primate globus pallidus and subthalamic nucleus: functional organisation. Journal of Neurophysiology *53*:530–543.

DeLong, M.R., I. Hamada, G.E. Alexander, V.E. Koliatsos, L.J. Martin and J. Hedreen (1988). Organization of primate basal ganglia "motor circuit": 3. Relations of striatal microexcitable zones to afferent and efferent projections. Soc.Neurosci.Abstr. *14*:721.(Abstract)

DeLong, M.R. and A.P. Georgopoulos (1981) Motor functions of the basal ganglia. In V.B. Brooks (ed): Handbook of Physiology, sect. 1, v. 2, pt. 2. Baltimore, MD: Williams and Wilkins, pp. 1054.

Deniau, J.M. and G. Chevalier (1985). Disinhibition as a basic process in the expression of striatal functions. II. The striato–nigral influence on thalamocortical cells of the ventromedial thalamic nucleus. Brain Res. *334*:227–233.

Desban, M., C. Gauchy, M.L. Kemel, M.J. Besson and J. Glowinski (1989). Three–dimensional organization of the striosomal compartment and patchy distribution of striatonigral projections in the matrix of the cat caudate nucleus. Neuroscience *29*:551–566.

DiFiglia, M., T. Pasik and P. Pasik (1978). A golgi study of the afferent fibers of the neostriatum in monkey. Brain Res. *152*:341–347.

DiFiglia, M., P. Pasik and T. Pasik (1982). A golgi and ultrastructural study of the monkey globus pallidus. J.Comp.Neurol. *212*:53–75.

DiFiglia, M. (1990). Excitotoxic injury of the neostriatum: a model for Huntington's disease. Trends Neurosci. *13*:286–289.

Divac, I. (1983). Two levels of functional heterogeneity of the neostriatum. Neuroscience *10*:1151–1155.

Divac, I. (1984) The neostriatum viewed orthogonally. In Functions of the Basal Ganglia. Ciba Foundation Symposium. London: Pitman, pp. 201–215.

Donoghue, J.P. (1985). Contrasting properties of neurons in two parts of the primary motor cortex of the awake rat. Brain Res. *333*:173–177.

Donoghue, J.P. and M. Herkenham (1986). Neostriatal projections from indiviual cortical fields conform to histochemically distinct striatal compartments in the rat. Brain Res. *365*:397–403.

Donoghue, J.P. and S.T. Kitai (1981). A collateral pathway to the neostriatum from corticofugal neurons of the rat sensory–motor cortex: an intracellular HRP study. J.Comp.Neurol. *201*:1–13.

Dragunow, M., G.S. Robertson, R.L.M. Faull, H.A. Robertson and K. Jansen (1990a). D2 dopamine receptor antagonists induce fos and related proteins in rat striatal neurons. Neuroscience *37*:287–294.

Dragunow, M., M. Williams and R.L.M. Faull (1990b). Haloperidol induces Fos and related molecules in intrastriatal grafts derived from fetal striatal primordia. Brain Res. *530*:309–311.

Dumas, M., M.E. Schwab, R. Baumann and H. Thoenen (1979). Retrograde transport of tetanus toxin through a chain of two neurons. Brain Res. *165*:354–357.

Dunnett, S.B. and S.D. Iversen (1980). Regulatory impairments following selective kainic acid lesions of the neostriatum. Behav.Brain Res. *1*:497–506.

Dunnett, S.B. and S.D. Iversen (1982). Sensorimotor impairments following localized kainic acid and 6–hydoxydopamine lesions of the neostriatum. Brain Res. *248*:121–127.

Feger, J. and A.R. Crossman (1984). Identification of different subpopulations of neostriatal neurons projecting to globus pallidus or substantia nigra in the monkey: A retrograde fluorescence double–labelling study. Neurosci.Lett. *49*:7–12.

Ferrante, R.J., M.F. Beal, N.W. Kowall, E.P. Richardson,Jr. and J.B. Martin (1987). Sparing of acetylcholinesterase–containing striatal neurons in Huntington's disease. Brain Res. *411*:162–166.

Ferrante, R.J., N.W. Kowall, K. Harrington and E.P. Richardson,Jr. (1990). Terminal striatal substance P– and met–enkephalin–projections in the globus pallidus are equally affected in Huntington's disease. Soc.Neurosci.Abstr. *16*:1120.(Abstract)

Ferrante, R.J. and N.W. Kowall (1987). Tyrosine hydroxylase–like immunoreactivity is distributed in the matrix compartment of normal human and Huntington's disease striatum. Brain Res. *416*:141–146.

Filion, M., L. Tremblay and P.J. Bédard (1988). Abnormal influences of passive limb movement on the activity of globus pallidus neurons in parkinsonian monkeys. Brain Res. *444*:165–176.

Flaherty, A.W., A.M. Graybiel, M. Sur and P.E. Garraghty (1989). Distinctive patterns of projections to striatum from physiologically-mapped somatosensory representations in primate cortex. Soc.Neurosci.Abstr. *15*:659.(Abstract)

Flaherty, A.W. and A.M. Graybiel (1990). Proprioception and the striatum: primate somatosensory cortical area 3a projects more broadly to the striatum than do areas 3b or 1. Soc.Neurosci.Abstr. *16*:1231.(Abstract)

Flaherty, A.W. and A.M. Graybiel (1991a). Corticostriatal transformations in the primate somatosensory system. Projections from physiologically mapped body-part representations. J.Neurophysiol. *66*:1249-1263.

Flaherty, A.W. and A.M. Graybiel (1991b). Corticostriatal transformations in the primate somatosensory system: II. Differential magnifications of areas 3a, 3b, and 1. (in prep.)

Flaherty, A.W. and A.M. Graybiel (1991c). A second input system for body representations in the primate striatal matrix. Soc.Neurosci.Abstr. *17*:1299.(Abstract)

Flaherty, A.W. and A.M. Graybiel (1992). Multiple stages of sensorimotor processing in the primate basal ganglia. IBAGS Abstract

Fotuhi, M., V.E. Koliatsos, G.E. Alexander and M.R. DeLong (1989). Patterns of sensorimotor integration in the primate neostriatum: primary somatosensory cortex (SC) and motor cortex (MC) project to coextensive territories in the putamen. Soc.Neurosci.Abstr. *15*:285.(Abstract)

Freedman, J.E. and F.F. Weight (1988). Single postassium channels activated by D2 dopamine receptors in acutely dissociated neurons from rat corpus striatum. Proc.Natl.Acad.Sci.USA *85*:3618-3622.(Abstract)

Freund, T.F., J.F. Powell and A.D. Smith (1984). Tyrosine hydroxylase immunoreactive boutons in synaptic contact with identified striatonigral neurons, with particular reference to dendritic spines. Neuroscience *13*:1189-1215.

Friedman, D.P., E.G. Jones and H. Burton (1980). Representation pattern in the second somatic sensory area of the monkey cerebral cortex. J.Comp.Neurol. *192*:21-41.

Fuster, J.M. (1989) The prefrontal cortex. New York: Raven Press.

Georgopoulos, A.P., J.T. Lurito, M. Petrides, A.B. Schwartz and J.T. Massey (1989). Mental rotation of the neuronal population vector. Science *243*:234-236.

Gerfen, C.R. (1984). The neostriatal mosaic: compartmentalization of corticostriatal input and striatonigral output systems. Nature *311*:461-464.

Gerfen, C.R. (1985). The neostriatal mosaic. I. Compartmental organization of projections from the striatum to the substantia nigra in the rat. J.Comp.Neurol. *236*:454-476.

Gerfen, C.R. (1989). The neostriatal mosaic: striatal patch-matrix organization is related to cortical lamination. Science *246*:385-388.

Gerfen, C.R., T.M. Engber, L.C. Mahan, Z. Susel, T.N. Chase, F.J. Monsma,Jr. and D.R Sibley (1990). D1 and D2 dopamine receptor-regulated gene expression of striatonigral and striatopallidal neurons. Science

250:1429–1432.

Gerfen, C.R. and P.E. Sawchenko (1984). An anterograde neuroanatomical tracing method that shows the detailed morphology of neurons, their axons and terminals: Immunohistochemical localization of an axonally transported plant lectin, Phaseolous vulgaris leucoagglutinin (PHA–L). Brain Res. *290*:219–238.

Gerfen, C.R. and W.S. Young,III (1988). Distribution of striatonigral and striatopallidal peptidergic neurons in both patch and matrix components: an in situ hybridization histochemistry and fluorescent retrograde tracing study. Brain Res. *460*:161–167.

Gergen, J.A. and P.D. MacLean (1962) A Stereotaxic Atlas of the Squirrel Monkey's Brain (Saimiri sciureus). Bethesda: National Institutes of Health.

Giménez–Amaya, J.–M. and A.M. Graybiel (1990). Compartmental origins of the striatopallidal projection in the primate. Neuroscience *34*:111–126.

Giménez–Amaya, J.–M. and A.M. Graybiel (1991). Modular organization of projection neurons in the matrix compartment of the primate striatum. J.Neurosci. *11*:779–791.

Goldman, P.S. and W.J.H. Nauta (1977). An intricately patterned prefronto–caudate projection in the rhesus monkey. J.Comp.Neurol. *171*:369–386.

Goldman–Rakic, P.S. and L.D. Selemon (1990). New frontiers in basal ganglia research. Trends Neurosci. *13*:241–243.

Gould, H.J., C.G. Cusick, T.P. Pons and J.H. Kaas (1986). The relationship of corpus callosum connections to electrical stimulation maps of motor, supplementary motor, and the frontal eye fields in owl monkeys. J.Comp.Neurol. *247*:297–325.

Graybiel, A.M., C.W. Ragsdale and S. Moon Edley (1979). Compartments in the striatum of the cat observed by retrograde cell–labelling. Exp.Brain Res. *34*:189–195.

Graybiel, A.M. (1984) Neurochemically specified subsystems in the basal ganglia. In D. Evered and M. O'Connor (eds): Functions of the Basal Ganglia. Ciba Foundation Symposium 107. London: Pitman Press, pp. 114–143.

Graybiel, A.M., M.–J. Besson and E. Weber (1989). Neuroleptic–sensitive binding sites in the nigrostriatal system: evidence for a differential distribution of sigma sites in the substantia nigra, pars compacta of the cat. J.Neurosci. *9*:326–338.

Graybiel, A.M. (1990). Neurotransmitters and neuromodulators in the basal ganglia. Trends Neurosci. *13*:244–254.

Graybiel, A.M., R. Moratalla and H.A. Robertson (1990). Amphetamine and cocaine induce drug–specific activation of the c–fos gene in striosome–matrix and limbic subdivisions of the striatum. Proc.Natl.Acad.Sci.USA *87*:6912–6916.

Graybiel, A.M., A.W. Flaherty and J.–M. Giménez–Amaya (1991) Striosomes and matrisomes. In G. Bernardi, M.B. Carpenter, G. di Chiara, M. Morelli, and P. Stanzione (eds): The basal ganglia, III. NY: Plenum Press, pp. 3–12.

P. Stanzione (eds): The basal ganglia, III. NY: Plenum Press, pp. 3-12.
Graybiel, A.M. and M.-F. Chesselet (1984). Compartmental distribution of striatal cell bodies expressing met-enkephalin-like immunoreactivity. Proc.Natl.Acad.Sci.USA *81*:7980-7984.
Graybiel, A.M. and R. Moratalla (1989). Dopamine uptake sites in the striatum are distributed differentially in striosome and matrix compartments. Proc.Natl.Acad.Sci.USA *86*:9020-9024.
Groves, P.M. (1983). A theory of the functional organization of the neostriatum and the neostriatal control of voluntary movement. Brain Res.Rev. *5*:109-132.
Gundlach, A.L., B.L. Largent and S.H. Snyder (1986). Autoradiographic Location of Sigma Receptor Binding Sites in Guinea Pig and Rat Central Nervous System with (+)3H-3-(3-Hydroxyphenyl)-N-(1-propyl)piperidine. J.Neurosci. *6*:1757-1770.
Haber, S. and R. Elde (1982). The distribution of enkephalin immunoreactive fibers and terminals in the monkey central nervous system: An immunohistochemical study. Neuroscience *7*:1049-1095.
Hattori, T., M. Takada, T. Moriizumi and D. van der Kooy (1991). Single dopaminergic nigrostriatal neurons form two chemically distinct synaptic types: possible transmitter segegration within neurons. J.Comp.Neurol. *309*:391-401.
Hazrati, L.-N., A. Parent, S. Mitchell and S.N. Haber (1990). Evidence for interconnections between the two segments of the globus pallidus in primates: a PHA-L anterograde tracing study. Brain Res. *533*:171-175.
Hazrati, L.-N. and A. Parent (1992). Modular organization of the striatopallidal system. Soc.Neurosci.Abstr. *17*:455.(Abstract)
Hedreen, J.C. (1990). Pathological changes in early Huntington's disease. Soc.Neurosci.Abstr. *16*:1121.
Hendrickson, A., L. Moe and B. Nobel (1972). Staining for autoradiography of the central nervous system. Stain Technol. *47*:283-290.
Hicks, T.P. and R.W. Dykes (1983). Receptive field size for certain neurons in primary somatosensory cortex is determined by GABA-mediated intracortical inhibition. Brain Res. *274*:160-164.
Hikosaka, O., M. Sakamoto and S. Usui (1989). Functional properties of monkey caudate neurons. III. Activities related to expectation of target and reward. J.Neurophysiol. *61*:814-832.
Hikosaka, O. and M. Sakamoto (1986). Cell activity in monkey caudate nucleus preceding saccadic eye movements. Exp.Brain.Res. *63*:659-662.
Hikosaka, O. and R.H. Wurtz (1983a). Visual and oculomotor functions of monkey Macaca mulatta substantia nigra pars reticulata. 4. Relation of substantia nigra to superior colliculus. J.Neurophysiol. *49*:1285-1301.
Hikosaka, O. and R.H. Wurtz (1983b). Visual and oculomotor functions of monkey Macaca mulatta substantia nigra pars reticulata. 1. Relation of visual and auditory responses to saccades. J.Neurophysiol. *49*:1230-1253.
Hikosaka, O. and R.H. Wurtz (1985a). Modification of saccadic eye movements

by gamma aminobutyric-acid-related substances. 2. Effects of muscimol in monkey (Macaca mulatta) substantia nigra pars reticulata. J.Neurophysiol. *53*:292-308.

Hikosaka, O. and R.H. Wurtz (1985b). Modification of saccadic eye movements by gamma aminobutyric-acid-related substances. I. Effect of muscimol and bicuculline in monkey Macaca mulatta superior colliculus. J.Neurophysiol. *53*:266-291.

Hirsch, E.C., A.M. Graybiel, C. Duyckaerts and F. Javoy-Agid (1987). Neuronal loss in the pedunculopontine tegmental nucleus in Parkinson disease and in progressive supranuclear palsy. Proc.Natl.Acad.Sci.USA *84*:5976-5980.

Holsapple, J.W., J.B. Preston and P.L. Strick (1991). The origin of thalamic inputs to the 'hand' representation in the primary motor cortex. J.Neurosci. *11*:2644-2654.

Hoover, J.E. and P.L. Strick (1991). Transneuronal transport of HSV-1 from the primary motor cortex and the SMA: evidence for separate "motor" circuits within the basal ganglia. Soc.Neurosci.Abstr. *17*:453.(Abstract)

Huang, C.S., M.A. Sirisko, H. Hiraba, G.M. Murray and B.J. Sessle (1988). Organization of the primate face motor cortex as revealed by intracortical microstimulation and electrophysiological identification of afferent inputs and corticobulbar projections. J.Neurophysiol. *59*:796-818.

Hubel, D.H. and T.N. Wiesel (1962). Receptive fields, binocular interaction, and functional architecture in the cat's visual cortex. J.Physiol. *160*:106-154.

Huerta, M.F. and J.H. Kaas (1990). Supplementary eye fields as defined by intracortical microstimulation: connections in macaques. J.Comp.Neurol. *293*:299-330.

Huerta, M.F. and T.P. Pons (1990). Primary motor cortex receives input from area 3a in macaques. Brain Res. *537*:367-371.

Ilinsky, I.A., M.L. Jouandet and P.S. Goldman-Rakic (1985). Organization of the nigrothalamocortical system in the rhesus monkey. J.Comp.Neurol. *236*:315-330.

Illing, R.B. and A.M. Graybiel (1985). Convergence of afferents frontal cortex and substantia nigra onto acetylcholinesterase patches of the cat's superior colliculus. Neuroscience *14*:455-482.

Illing, R.B. and A.M. Graybiel (1986). Complementary and non-matching afferent compartments in the cat's superior colliculus: innervation of the acetylcholinesterase-poor domain of the intermediate gray layer. Neuroscience. *18*:373-394.

Illing, R.B. and H. Wassle (1979). Visualization of the HRP reaction product using the polarization microscope. Neurosci.Lett. *13*:7-11.

Jacobs, K.M. and J.P. Donoghue (1991). Reshaping the cortical motor map by unmasking latent intracortical connections. Science *251*:944-947.

Jenkins, W.M., M.M. Merzenich, M.T. Ochs, T. Allard and E. Guic-Robles (1990). Functional reorganization of primary somatosensory cortex in adult owl monkeys after behaviorally-controlled tactile stimuli. J.Neurophysiol. *63*:82-104.

Jiménez-Castellanos, J. and A.M. Graybiel (1987). Subdivisions of the dopamine-containing A8-A9-A10 complex identified by their differential mesostriatal innervation of striosomes and extrastriosomal matrix. Neuroscience *23*:223-242.

Jiménez-Castellanos, J. and A.M. Graybiel (1989a). Compartmental origins of striatal efferent projections in the cat. Neuroscience *32*:297-321.

Jiménez-Castellanos, J. and A.M. Graybiel (1989b). Evidence that histochemically distinct zones of the primate substantia nigra pars compacta are related to patterned distributions of nigrostriatal projection neurons and striatonigral fibers. Exp.Brain Res. *74*:227-238.

Jiménez-Castellanos, J. and A.M. Graybiel (1989c). Compartmental origins of striatal efferent projections in the cat. Neuroscience *32*:297-321.

Jones, E.G., J.D. Coulter, H. Burton and R. Porter (1977). Cells of origin and terminal distribution of corticostriatal fibers arising in the sensory-motor cortex of monkeys. J.Comp.Neurol. *173*:53-80.

Jones, E.G., J.D. Coulter and S.H.C. Hendry (1978). Intracortical connectivity of architectonic fields in the somatic sensory, motor and parietal cortex of monkeys. J.Comp.Neurol. *181*:291-347.

Joyce, J.N., D.W. Sapp and J.F. Marshall (1986). Human striatal dopamine receptors are organized in compartments. Proc.Natl.Acad.Sci.USA *83*:8002-8006.

Kassel, J., G.M. Shambes and W. Welker (1984). Fractured cutaneous projections to the granule cell layer of the posterior cerebellar hemisphere of the domestic cat. J.Comp.Neurol. *225*:458-468.

Katz, L.C., A. Burkhalter and W.J. Dryer (1984). Fluorescent latex microspheres as a retrograde neuronal marker for in vivo and in vitro studies of visual cortex. Nature *310*:498-499.

Kawaguchi, Y., C.J. Wilson and P.C. Emson (1990). Projection subtypes of rat neostriatal matrix cells revealed by intracellular injection of biocytin. J.Neurosci. *10*:3421-3438.

Kemel, M.-L., M. Desban, J. Glowinski and C. Gauchy (1989). Distinct presynaptic control of dopamine release in striosomal and matrix areas of the cat caudate nucleus. Proc.Natl.Acad.Sci.USA *86*:9006-9010.

Kennard, C. and C.J. Lueck (1989). Oculomotor abnormalities in diseases of the basal ganglia. Rev.Neurol. *145*:587-595.

Kincaid, A.E., S.W. Newman, A.B. Young and J.B. Penney (1990). Evidence for a projection from the globus pallidus to the entopeduncular nucleus in the rat. Soc.Neurosci.Abstr. *16*:427.(Abstract)

King, M.A., P.M. Louis, B.E. Hunter and D.W. Walker (1989). Biocytin: a versatile anterograde neuroanatomical tract-tracing alternative. Brain Res. *497*:361-367.

Kish, S.J., K. Shannak and O. Hornykiewicz (1988). Uneven patterns of dopamine loss in the striatum of patients with idiopathic Parkinson's disease - pathophysiologic and clinical implications. New Eng.J.Med. *318*:876-880.

Kitai, S.T., D.J. Surmeier and A. Stefani (1990). Dopaminergic modulation of

Kitai, S.T., D.J. Surmeier and A. Stefani (1990). Dopaminergic modulation of voltage-dependent potassium conductances in rat neostriatal neurons. Soc.Neurosci.Abstr. *16*:418.(Abstract)

Koliatsos, V.E., L.J. Martin, J. Hedreen, G.E. Alexander, I. Hamada, D.L. Price and M.R. DeLong (1988). Organization of primate basal ganglia "motor circuit": 2. putaminal projections to internal (GPi) and external (GPe) globus pallidus originate in distinct neuronal populations within the matrix compartment. Soc.Neurosci.Abstr. *14*:720.(Abstract)

Künzle, H. (1975). Bilateral projections from precentral motor cortex to the putamen and other parts of the basal ganglia. An autoradiographic study in Macaca Fascicularis. Brain Res. *88*:195-209.

Künzle, H. (1977). Projections from the primary somatosensory cortex to basal ganglia and thalamus in the monkey. Exp.Brain Res. *30*:481-492.

Künzle, H. (1978). Cortico-cortical efferents of primary motor and somatosensory regions of the cerebral cortex in Macaca fascicularis. Neurosci. *3*:25-39.

Langer, L.F. and A.M. Graybiel (1989). Distinct nigrostriatal projection systems innervate striosomes and matrix in the primate striatum. Brain Res. *498*:344-350.

Langston, J.W., L.S. Forno, C.S. Rebert and I. Irwin (1984). Selective nigral toxicity after systemic administration of 1-methyl-4-phenyl-1,2,3,6-tetrahydro-pyridine (MPTP) in the squirrel monkey. Brain Res. *292*:390-394.

Largent, B.L., A.L. Gundlach and S.H. Snyder (1984). Psychotomimetic opiate receptors labeled and visualized with (+)[3H]3-(3-hydroxyphenyl)-N-(1--propyl)piperidine. Proc.Natl.Acad.Sci.USA *81*:4983-4987.

Liles, S.L. and B.V. Updyke (1985). Projection of the digit and wrist area of precentral gyrus to the putamen: relation between topography and physiological properties of neurons in the putamen. Brain Res. *339*:245-255.

Liu, F.-C., A.M. Graybiel, S.B. Dunnett and H.A. Robertson (1991). Intrastriatal grafts derived from fetal striatal primordia. III. Induction of modular patterns of Fos-like immunoreactivity by cocaine. Exp.Brain Res. *85*:501-506.

Loopuijt, L.D. and D. van der Kooy (1985). Organization of the striatum: collateralization of its efferent axons. Brain Res. *348*:86-99.

Luppi, P.-H., K. Sakai, D. Salvert, P. Fort and M. Jouvet (1987). Peptidergic hypothalamic afferents to the cat nucleus raphe pallidus as revealed by a double immunostaining technique using unconjugated cholera toxin as a retrograde tracer. Brain Res. *402*:339-345.

Lynd-Balta, E.L., S.J. Mitchell and S.N. Haber (1991). Organization of nigrostriatal and striatonigral projections in the primate. Soc.Neurosci.Abstr. *17*:1300.(Abstract)

Magarinos-Ascone, C., W. Buno and E. Garcia-Austt (1992). Activity in monkey substantia nigra neurons related to a simple learned movement. Exp.Brain Res. *88*:283-291.

Mahan, L.C., R.M. Burch, F.J.Jr. Monsma and D.R. Sibley (1990). Expression of striatal D1 dopamine receptors coupled to inositol phosphate production

Mahan, L.C., R.M. Burch, F.J.Jr. Monsma and D.R. Sibley (1990). Expression of striatal D1 dopamine receptors coupled to inositol phosphate production and Ca2+ mobilization in Xenopus oocytes. Proc.Natl.Acad.Sci.USA *87*:2196–2200.

Malach, R. and A.M. Graybiel (1984). Organization of somatosensory corticostriatal projections. Neurosci.Abstr. *10*:513.

Malach, R. and A.M. Graybiel (1986). Mosaic architecture of the somatic sensory–recipient sector of the cat's striatum. J.Neurosci. *6*:3436–3458.

Matsubara, J.A., M.S. Cynader and N.V. Swindale (1987). Anatomical properties and physiological correlates of the intrinsic connections in cat area 18. J.Neurosci. *7*:1428–1446.

McGuire, P.K., J.F. Bates and P.S. Goldman–Rakic (1991). Interhemispheric integration: II. Symmetry and convergence of the corticostriatal projections of the left and the right principal sulcus (PS) and the left and the right supplementary motor area (SMA) of the rhesus monkey. Cerebral Cortex *1*:408–417.

Meador–Woodruff, J.H., A. Mansour, D.J. Healy, R. Kuehn, Q.–Y. Zhou, J.R. Bunzow, H. Akil, O. Civelli and S.J. Watson,Jr. (1991). Comparison of the distributions of D_1 and D_2 dopamine receptor mRNA in rat brain. Neuropsychopharmacology *5*:231–242.

Mesulam, M.–M. (1978). Tetramethyl benzidine for horseradish peroxidase neurohistochemistry: a non–carcinogenic blue reaction product with superior sensitivity for visualizing neural afferents and efferents. J.Histochem.Cytochem. *26*:106–117.

Miller, J.C. (1990). Induction of c–fos mRNA expression in rat striatum by neuroleptic drugs. J.Neurochem. *54*:1453–1455.

Miller, W.C. and M.R. DeLong (1987) Altered tonic activity of neurons in the globus pallidus and subthalamic nucleus in the primate MPTP model of parkinsonism. In M.B. Carpenter and A. Jayaraman (eds): The basal ganglia: structure and function. New York: Plenum Press, pp. 415–429.

Mink, J.W. and W.T. Thach (1991a). Basal ganglia motor control. III. Pallidal ablation: normal reaction time, muscle cocontraction, and slow movement. J.Neurophysiol. *65*:330–351.

Mink, J.W. and W.T. Thach (1991b). Basal ganglia motor control. II. Late pallidal timing relative to movement onset and inconsistent pallidal coding of movement parameters. J.Neurophysiol. *65*:301–329.

Mink, J.W. and W.T. Thach (1991c). Basal ganglia motor control. I. Nonexclusive relation of pallidal discharge to five movement modes. J.Neurophysiol. *65*:273–300.

Mori, A., R.S. Waters and H. Asanuma (1989). Physiological properties and patterns of projection in the cortico–cortical connections from the second somatosensory cortex to the motor cortex, area 4 gamma, in the cat. Brain Res. *504*:206–210.

Nakanishi, H., H. Kita and S.T. Kitai (1987). Intracellular study of rat substantia nigra pars reticulata neurons in an in vitro slice preparation: electrical

membrane properties and response characteristics to subthalamic stimulation. Brain Res. *437*:45–55.

Narabayashi, H. (1989). Stereotaxic Vim thalamotomy for treatment of tremor. European Neurology *29 Suppl. 1*:29–32.

Nastuk, M.A. and A.M. Graybiel (1988). Autoradiographic localization and biochemical characteristics of M1 and M2 muscarinic binding sites in the striatum of the cat, monkey, and human. J.Neurosci. *8*:1052–1062.

Nelson, M.E. and J.M. Bower (1990). Brain maps and parallel computers. Trends Neurosci. *13*:403–408.

Nemeroff, C.B., W.W. Youngblood, P.J. Manberg, J.r. Prange AJ and J.S. Kizer (1983). Regional brain concentrations of neuropeptides in Huntington's chorea and schizophrenia. Science *221*:972–975.

Parent, A., C. Bouchard and Y. Smith (1984). The striatopallidal and striatonigral projections: two distinct fiber systems in primate. Brain Res. *303*:385–390.

Parent, A., Y. Smith, M. Filion and J. Dumas (1989). Distinct afferents to internal and external pallidal segments in the squirrel monkey. Neurosci Lett. *96*:140–144.

Parent, A. and Y. Smith (1987). Differential dopaminergic innervation of the two pallidal segments in the squirrel monkey (Saimiri sciureus). Brain Res. *426*:397–400.

Parthasarathy, H.B., J.D. Schall and A.M. Graybiel (1990). Dual–tracer comparison of the corticostriatal projections of the frontal eye field and the supplementary eye field in the primate. Soc.Neurosci.Abstr. *16*:1231.(Abstract)

Parthasarathy, H.B., J.D. Schall and A.M. Graybiel (1992). Distributed but convergent ordering of striatal projections: the frontal eye field and the supplementary eye field in the monkey. J.Neurosci. (in press)

Penny, G.R., C.J. Wilson and S.T. Kitai (1984). The influence of neostriatal patch and matrix compartments on the dendritic geometry of spiny projection neurons in the rat as revealed by intracellular labeling with HRP combined with immunocytochemistry. Soc.Neurosci.Abstr. *10*:514.

Penny, G.R., S. Afsharpour and S.T. Kitai (1986). The glutamate decarboxylase–, leucine enkephalin–, methionine enkephalin– and substance P–immunoreactive neurons in the neostriatum of the rat and cat: evidence for partial population overlap. Neuroscience *17*:1011–1045.

Penny, G.R., C.J. Wilson and S.T. Kitai (1988). Relationship of the axonal and dendritic geometry of spiny projection neurons to the compartmental organization of the neostriatum. J.Comp.Neurol. *269*:275–289.

Percheron, G., J. Yelnik and C. Francois (1984). A Golgi analysis of the primate globus pallidus. III. Spatial organization of the striatopallidal complex. J.Comp.Neurol. *227*:214–227.

Percheron, G. and M. Filion (1990). Parallel processing in the basal ganglia: up to a point. Trends Neurosci. *14*:55–56.

Pizzi, M., M. Da Prada, A. Valerio, M. Memo, P.F. Spano and W.E. Haefely (1988). Dopamine D_2 receptor stimulation inhibits inositol phosphate

generating system in rat striatal slices. Brain Res. *456*:235–240.
Ragsdale, C.W. and A.M. Graybiel (1981). The fronto-striatal projection in the cat and monkey and its relationship to inhomogeneities established by acetylcholinesterase histochemistry. Brain Res. *208*:259–266.
Ragsdale, C.W. and A.M. Graybiel (1988) Multiple patterns of thalamostriatal innervation in the cat. In M. Bentivoglio and R. Spreafico (eds): Cellular Thalamic Mechanisms. Amsterdam: Elsevier, pp. 261–267.
Ragsdale, C.W. and A.M. Graybiel (1990). A simple ordering of neocortical areas established by the compartmental organization of their striatal projections. Proc.Natl.Acad.Sci.USA *87*:6196–6199.
Reiner, A., R.L. Albin, K.D. Anderson, C.J. D'Amato, J.B. Penney and A.B. Young (1988). Differential loss of striatal projection neurons in Huntington disease. Proc.Natl.Acad.Sci.USA *85*:5733–5737.
Richfield, E.K., A.B. Young and J.B. Penney (1987). Comparative distribution of dopamine D-1 and D-2 receptors in the basal ganglia of turtles, pigeons, rats, cats, and monkeys. J.Comp.Neurol. *262*:446–463.
Rutherford, A., M. Garcia-Munoz and G.W. Arbuthnott (1988). An afterhyperpolarization recorded in striatal cells 'in vitro': effect of dopamine administration. Exp.Brain Res. *71*:399–405.
Sadikot, A.F., A. Parent and C. Francois (1990). The centre median and parafascicular thalamic nuclei project respectively to the sensorimotor and associative-limbic striatal territories in the squirrel monkey. Brain Res. *510*:161–165.(Abstract)
Sadikot, A.F. and A. Parent (1989). Differential projections of centre median and parafascicular nuclei in squirrel monkey. Soc.Neurosci.Abstr. *15*:288.(Abstract)
Saint-Cyr, J.A., L.G. Ungerleider and R. Desimone (1990). Organization of visual cortical inputs to the striatum and subsequent outputs to the pallido-nigral complex in the monkey. J.Comp.Neurol. *298*:129–156.
Salin, P., L. Kerkerian-Le Goff, V. Heidet, J. Epelbaum and A. Nieoullon (1990). Somatostatin-immunoreactive neurons in the rat striatum: effects of corticostriatal and nigrostriatal dopaminergic lesions. Brain Res. *521*:23–32.
Schell, G.R. and P.L. Strick (1984). The origin of thalamic inputs to the arcuate premotor and supplementary motor areas. J.Neurosci. *4*:539–560.
Schmued, L.C., K. Kyriakidis and L. Heimer (1991). In vivo anterograde and retrograde axonal transport of the fluorescent rhodamine-dextran-amine, fluoro-ruby, within the CNS. Brain Res. *526*:127–134.
Schmued, L.C. and J.H. Fallon (1986). Fluoro-Gold: a new fluorescent retrograde axonal tracer with numerous unique properties. Brain Res. *377*:147–154.
Schneider, J.S. and T.I. Lidsky (1981). Processing of somatosensory information in the striatum of behaving cats. J.Neurophysiol. *45*:841–851.
Schultz, W. and R. Romo (1990). Dopamine neurons of the monkey midbrain: contingencies of responses to stimuli eliciting immediate behavioral reactions. J.Neurophysiol. *63*:607–624.
Sedvall, G. (1990). PET imaging of dopamine receptors in human basal ganglia:

relevance to mental illness. TINS *13*:302–307.
Selemon, L.D. and P.S. Goldman-Rakic (1985). Longitudinal topography and interdigitation of corticostriatal projections in the rhesus monkey. J.Neurosci. *5*:776–794.
Selemon, L.D. and P.S. Goldman-Rakic (1990). Topographical intermingling of striatonigral and striatopallidal neurons in the rhesus monkey. J.Comp.Neurol. *297*:359–376.
Sessle, B.J. and M. Wiesendanger (1982). Structural and functional definition of the motor cortex in the monkey (Macaca fascicularis). J.Physiol. *323*:245–265.
Seto-Ohshima, A., P.C. Emson, E. Lawson, C.Q. Mountjoy and L.H. carrasco (1988). Loss of matrix calcium-binding protein-containing neurons in Huntington's disease. Lancet *1(8597)*:1252–1255.
Smith, Y. and J.P. Bolam (1990). Convergence of pallidal and striatal inputs to neurones in the entopeduncular nucleus and substantia nigra of the rat: application of a new double anterograde labeling method at electron microscopic level. Soc.Neurosci.Abstr. *16*:236.(Abstract)
Smith, Y. and A. Parent (1986). Differential connections of caudate nucleus and putamen in the squirrel monkey (Saimiri sciureus). Neuroscience *18*:347–371.
Smith, Y. and A. Parent (1988). Neurons of the subthalamic nucleus in primates display glutamate but not GABA immunoreactivity. Brain Res. *453*:353–356.
Sokoloff, P., B. Giros, M.-P. Martres, M.-L. Bouthenet and J.-C. Schwartz (1990). Molecular cloning and characterization of a novel dopamine receptor (D_3) as a target for neuroleptics. Nature *347*:146–151.
Sonnenberg, J.L., F.J.III. Rauscher, J.I. Morgan and T. Curran (1989). Regulation of proenkephalin by fos and jun. Science *246*:1622–1625.
Staines, W.A. and H.C. Fibiger (1984). Collateral projections of neurons of the rat globus pallidus to the striatum and substantia nigra. Exp.Brain Res. *56*:217–220.
Stanton, G.B., M.E. Goldberg and C.J. Bruce (1988). Frontal eye field efferents in the macaque monkey: I. subcortical pathways and topography of striatal and thalamic terminal fields. J.Comp.Neurol. *271*:473–492.
Steindler, D.A., T.F. O'Brien and N.G.F. Cooper (1988). Glycoconjugate boundaries during early postnatal development of the neostriatal mosaic. J.Comp.Neurol. *267*:357–369.
Sternberger, L.A. (1979) Immunocytochemistry. New York: Wiley.
Stoof, J.C. and J.W. Kebabian (1981). Opposing roles for D-1 and D-2 dopamine receptors in efflux of cyclic AMP from rat neostriatum. Nature *294*:366–368.
Strick, P.L. and J.B. Preston (1978a). Sorting of somatosensory afferent information in primate motor cortex. Brain Res. *156*:364–368.
Strick, P.L. and J.B. Preston (1978b). Multiple representations in the primate motor cortex. Brain Res. *154*:366–370.

Sunahara, R.K., H.-C. Guan, B.F. O'Dowd, P. Seeman, L.G. Laurier, G. Ng, S.R. George, J. Torchia, H.H.M. Van Tol and H.B. Niznik (1991). Cloning of the gene for a human dopamine D_5 receptor with higher affinity for dopamine than D_1. Nature *350*:614-619.

Sur, M., R.J. Nelson and J.H. Kaas (1982). Representations of the body surface in cortical areas 3b and 1 of squirrel monkeys: comparisons with other primates. J.Comp.Neurol. *211*:177-192.

Surmeier, D.J., C.J. Wilson, A. Stefani and S.T. Kitai (1991). Dopaminergic modulation of sodium currents in retrogradely-identified rat striatonigral neurons. Soc.Neurosci.Abstr. *17*:851.(Abstract)

Tanji, J., K. Okano and K.C. Sato (1988). Neuronal activity in cortical motor areas related to ipsilateral, contralateral, and bilateral digit movements of the monkey. J.Neurophysiol. *60*:325-343.

Tanji, J. and S.P. Wise (1981). Submodality distribution in sensorimotor cortex of the unanesthetized monkey. J.Neurophysiol. *45*:467-481.

Turski, L., K. Bressler, K.-J. Rettig, P.-A. Löschmann and H. Wachtel (1991). Protection of substantia nigra from MPP^+ neurotoxicity by N-methyl-D-aspartate antagonists. Nature *349*:414-418.

Van Tol, H.H.M., J.R. Bunzow, H.-C. Guan, R.K. Sunahara, P. Seeman, H.B. Niznik and O. Civelli (1991). Cloning of the gene for a human dopamine D_4 receptor with high affinity for the antipsychotic clozapine. Nature *350*:610-614.

Vonsattel, J.-P., R.H. Myers, T.J. Stevens, R.J. Ferrante, E.D. Bird and E.P. Richardson,Jr. (1985). Neuropathological classification of Huntington's Disease. J.Neuropath.& Exp.Neurol. *44*:559-577.

Walker, R.H., G.W. Arbuthnott and A.M. Graybiel (1991). Intracellular labelling of medium spiny neurons in the primate caudate nucleus: anatomical relationship of dendrites to striosomal borders. Soc.Neurosci.Abstr. *17*:456.

West, M.O., R.M. Carelli, M. Pomerantz, S.M. Cohen, J.P. Gardner, J.K. Chapin and D.J. Woodward (1990). A region in the dorsolateral striatum of the rat exhibiting single-unit correlations with specific locomotor limb movements. J.Neurophysiol. *64*:1233-1246.

Woolf, N.J. and L.L. Butcher (1986). Cholinergic systems in the rat brain. III. Projection from the pontomesencephalic tegmentum to the thalamus, tectum, basal ganglia and basal forebrain. Brain Res.Bull. *16*:603-637.

Yeterian, E.H. and D.N. Pandya (1991). Topography and laminar origin of corticocaudate projections in rhesus monkeys. Soc.Neurosci.Abstr. *17*:454.(Abstract)

Yeterian, E.H. and G.W. Van Hoesen (1978). Cortico-striate projections in the rhesus monkey: the organization of certain cortico-caudate connections. Brain Res. *139*:43-63.

Young, S.T., L.J. Porrino and M.J. Iadarola (1991). Cocaine induces striatal c-Fos-immunoreactive proteins via dopaminergic D1 receptors. Proc.Natl.Acad.Sci.USA *88*:1291-1295.

Yumiya, H. and C. Ghez (1984). Specialized subregions in the cat motor cortex:

anatomical demonstration of differential projections to rostral and caudal sectors. Exp.Brain Res. 53:259–276.

Zweig, R.M., P.J. Whitehouse, M.F. Casanova, L.C. Walker, W.R. Jankel and D.L. Price (1987). Loss of pedunculopontine neurons in progressive supranuclear palsy. Ann.Neurol. 22:18–25.

Thus I ended this month with the greatest joy that ever I did any in my life, because I have spent the greatest part of it with abundance of joy..., and pleasant journeys, and brave entertainments, and without cost of money; and at last live to see the business ended with great contentment on all sides.

– Samuel Pepys, *Diary*, July 31, 1665

3/14-11